S
625.84
M41p
1966

PLEASE RETURN

PRESTRESSED CONCRETE DURABILITY & CORROSION

A Research Study performed for
The Montana State Highway Commission
Planning Survey Section
and
The U. S. Bureau of Commerce
Bureau of Public Roads

STATE DOCUMENTS COLLECTION

MAY 24 1978

MONTANA STATE LIBRARY
930 E Lyndale Ave.
Helena, Montana 59601

ENGINEERING

Research Laboratories

MONTANA STATE UNIVERSITY, BOZEMAN

MONTANA STATE LIBRARY
S 625.84 M41p c.1 Moss
Prestressed concrete durability & corros
3 0864 00016542 6

PRESTRESSED CONCRETE DURABILITY & CORROSION

A Research Study performed for
The Montana State Highway Commission
Planning Survey Section
and
The U. S. Bureau of Commerce
Bureau of Public Roads

by

Martin E. Moss

Associate Professor in Civil Engineering and Engineering Mechanics at

Montana State University

Bozeman, Montana

1966

ACKNOWLEDGMENT

Thanks are given to Dr. Eldon R. Dodge and the Department of Civil Engineering and Engineering Mechanics for encouragement and very real help in support of the project.

The investigation was sponsored by the Planning and Survey Section of the Montana Highway Commission in cooperation with the U. S. Department of Commerce, Bureau of Public Roads. Their interest and willing assistance was much appreciated.

Special acknowledgement and recognition is given to Mr. Michael J. Gonsior, now with the U. S. Forestry Sciences Laboratory, who as a graduate fellow developed the computer programs and carried out a major portion of the laboratory work.

TABLE OF CONTENTS

		Page
CHAPTER I	INTRODUCTION	
	Background	3
	Research Approach	6
CHAPTER II	INVESTIGATIONAL METHODS, EQUIPMENT, MATERIALS	
	DURABILITY AND SCALING	
	Slab Specimens	10
	Materials	12
	Fabrication	14
	Curing	15
	EXPOSURE CONDITIONS AND TESTING PROCEDURES	16
	Scaling and Durability	18
	Wet and Wet-Dry	20
	Primary Permeability - Slabs	21
	Secondary Permeability and Corrosion	21
	Mortar Bars	21
	Strands	22
CHAPTER III	DURABILITY AND SCALING - TEST RESULTS AND DISCUSSION	
	TEST RESULTS	24
	DISCUSSION	63
	Statistical Comments	63

CONTENTS

CHAPTER III (continued)		Page
	SCALING	
	Effect of Prestress	63
	Effect of Curing	63
	Effect of Salt Solution	63
	Relation between Scaling and Durability	66
	DURABILITY	
	Effect of Prestress	66
	Effect of Cure	67
	Effect of Salt Solution	68
	Effect of Permeability	68
	Miscellaneous	69
CHAPTER IV	PERMEABILITY AND CORROSION-TEST RESULTS AND DISCUSSION	
	PERMEABILITY	
	TEST RESULTS	71
	Standpipe Slabs	71
	DISCUSSION	93
	Effect of Prestress	93
	Effect of Curing	93
	Effect of Solution	94
	Miscellaneous Tests	95

CONTENTS

CHAPTER IV (continued)		Page
	CORROSION	
	TEST RESULTS	96
	DISCUSSION	103
	Encased Strands	103
	Exposed Strands	104
CHAPTER V	CONCLUSIONS	
	DURABILITY	105
	SCALING	106
	MISCELLANEOUS	106
	STRAND CORROSION	106
APPENDIX A	SLAB PRESTRESSING OPERATIONS	108
APPENDIX B	MATERIALS	123
APPENDIX C	INDIVIDUAL DATA RECORDS	142
APPENDIX D	STATISTICAL METHODS	209
LITERATURE CITED		216

LIST OF FIGURES

Figure		Page
1	Specimens, Tests, and Environments	7
2	Pretensioned Slabs	10
3	Slab Prepared for Permeability Study	13
4	Refined Slab Series	18
5	Complete Slab Specimen Program	19
6	Freeze-Thaw Treatments & Comparisons	25
7-15	Results of Duncan tests of mean transformed relative dynamic moduli	36-53
16	Results of Duncan tests of mean adjusted weight changes	55-56
17	Results of Duncan tests of mean length changes	58-59
18	Results of Duncan tests of mean scaling weight losses.	61-62
19	Fluid Flow Treatments & Comparisons	72
20-28	Results of Duncan tests of mean net absorptions	75-92
29	Reclaimed Strands	98
30	Salt Clogged Specimen	100
31	Wire Tensile Strength vs Solution Exposure Time	102
32	Slab Specimens	109
33	Pretensioning equipment	110
34	Pretensioning operations	113
35	Pretensioning Casting Beds	121
36	Fine aggregate gradation	126
37	Coarse aggregate gradation	127

LIST OF FIGURES (continued)

Figure		Page
38	Combined aggregate gradation	128
39	Gilson testing screen	131
40	Lancaster mixer and apparatus	131
41	Vibration table with casting bed in place	134
42	Load Cell description	139
43	Bridge arrangement for load cells	140
44	Calibration curves for load cells	141
45-56	Relative dynamic moduli of elasticity vs number of freeze-thaw cycles	143-154
57-68	Adjusted weight changes vs number of freeze-thaw cycles	155-166
69-80	Length changes vs number of freeze-thaw cycles	179-184
87-98	Net absorptions vs number of days	185-208
99	Example of Bartlett and Duncan tests results	210

LIST OF TABLES

Table		Page
I	Typical Slab Durability & Scaling Study Data	24
II	Computed Slab Results	29
III	Results of Bartlett Tests of Transformed Relative Dynamic Moduli	35
IV	Results of Bartlett Tests of Adjusted Weight Changes	54
V	Results of Bartlett Tests of Length Changes	57
VI	Results of Bartlett Tests of Scaling Weight Losses	60
VII	Results of Bartlett Tests of Net Absorptions	74
VIII	Identification of Items in Figure 33	111
IX	Summary of Strand Loading Procedures	118
X	Cement Chemical Analysis	125
XI	Material Quantities for each 2 cu ft Batch	132
XII	Individual Concrete Batch Properties	132
XIII	Concrete Cylinder Compressive Test Results	136
XIV	Casting Schedules	137

ABSTRACT

Two series of small prestressed slabs were tested for freeze-thaw durability, scaling, and for ingressing salt ion corrosion of the encased strands. The stress levels used were: zero psi, 500 psi, and 1200 psi. Tap water, calcium chloride solution, and magnesium sulfate solution were the study solutions for both normally cured and steam cured specimens. It was found that durability is moderately stress dependent, that steam curing reduces durability, and that magnesium sulfate solution has no durability effects while calcium chloride solution slightly reduces durability. Scaling was not related to compressive prestress load nor was it aggravated by magnesium sulfate solution, as compared with water. Calcium chloride solution caused extreme scaling when it was continuously ponded on the slabs; a more severe exposure than thawing ice with the solid salt. Early scaling was reduced by steam curing but late scaling was increased. No evidence of ion penetration corrosion of the encased strands was found even though the fluids had been in contact with the strands for various lengths of time.

Mortar bar specimens, with varying cover over the strands, were submerged in salt solutions to investigate penetration corrosion. The strands were reached by the solutions but no corrosion resulted.

Clean strand wires were exposed to the three solutions by towel wicks. Calcium chloride solution was the most corrosive. Magnesium sulfate solution and water followed in that order of relative corrosion.

CHAPTER I

INTRODUCTION

Nondurability of concrete in selected environments and exposures is the most pressing problem in the field today. When it is realized that concrete repair material may cost $330 per cubic yard (1) and that the volume of concrete used is rising exponentially along with public insistence for ever smoother, larger, and attractive road facilities and structures, its importance is apparent.

The scope of the problem is extremely wide, varying from all possible detrimental physical and chemical actions on the concrete proper to incompatibility with or nonprotection of embedded fixtures and structural elements. Yet, trouble is encountered in a very small percentage of the concrete in service. Unfortunately when it is encountered it is often magnified by being glaringly obvious to the public users. Scaling of concrete roads and structures due to de-icing salts is an example of this. More serious damage may not be so apparent. Corrosion of prestressing strands hidden from view by the covering concrete but leading to structural unsoundness illustrates this.

All phases of nondurability are under intense study. The aspects having to do with the suitability of the components of the concrete constitute one broad area of research. Another area deals with the damage to basically sound concrete by exterior agents. While there is an overlap between these areas and information from one is often transferable to the other, this report is primarily concerned with the attack

by some external agents upon high quality concrete.

To damage the concrete the harmful agent must contact and progressively penetrate the concrete. Prevention of contact by using barrier materials such as linseed oil, silicones, and epoxies is of varying effectiveness. Some success has resulted from devising methods of reducing the harmful effects, after contact, by altering the physical or chemical character of the concrete. One method of altering the physical structure of the concrete matrix is by entraining air, which provides protection against freezing and thawing damage. Variations in the chemical constituents of cement may partially protect the concrete against damage by sulfate ground waters.

Any method of reducing the ingress of harmful solutions should be helpful to the degree by which the penetration is impeded. After penetration any method of prolonging the integrity of the mortar matrix should also be beneficial.

The present program was undertaken to test the hypothesis that prestressing might restrict the penetration of harmful salt solutions into concrete and that it might also increase the durability of concrete in a freeze-thaw environment. Secondary information was sought on the detrimental effect of corrosive ions after they had penetrated the concrete and contacted the prestressing strands, and the relative degree of corrosion resulting from chloride and sulfate salt solutions. Some of these concepts have been partially reported or implied in recent investigations. Often the results are in conflict.

Background

It is substantiated that air entrainment in the proper amount protects concrete against freezing and thawing damage. It has also been proven effective in reducing surface scaling from freezing and thawing of de-icing salt solutions (2,3). The role of prestressing forces is not so clear. Gutzwiller & Musleh (4) found a definite increase in freeze-thaw durability due to precompression loading of 2000 psi. Reib (5) reported no difference with stresses varying by 500 psi increments up to 2000 psi. These sources have been cited as indicating precompression either effective or ineffective in increasing concrete durability. One of the essential differences between the studies was the level of entrained air. Reib's concrete contained from 3.4 to 4.8% air while Gutzwiller and Musleh used less than 3%. The effect of prestress could have been overshadowed by the air entrainment so buttressing the durability that it would require very long exposures to evaluate any durability contribution of precompression. This relationship is indicated in results by Klieger (2) who noted small but insignificant durability increase due to a 370 psi compressive stress.

Calcium chloride, when used as an accelerator in fresh concrete, is known to be harmfully corrosive to prestressing strands (6)(7)(8). The threshold amount is undefined but present practice forbids its use in all prestressed work. The possibility of chloride ions coming from exterior sources, penetrating the concrete cover, and attacking the

encased strand has not been reported for solution concentrations stronger than sea water* Whether or not harmful chloride ions could contact and corrode the strand should be of prime importance. Obscure references in the literature to "aggressive ground waters" and unidentified soils in contact with failed prestressed concrete elements leave doubt as to the damaging agent. These may have been chlorides or sulfates. Sulfates in sea water and soils are corrosive according to some reports (9)(10)(11) while sea water and sulfate gasses are reported innocuous in others (12). Sulfide bearing slag cements are in themselves noncorrosive (11). The relative corrosive capacities of sulfates and chlorides have not been reported but presumably much less trouble has been encountered with sulfates, at least in prestressing work.

Scaling of concrete surfaces due to de-icing salts is related to corrosion in that the primary agent used is usually some form of chloride. Much research has been done on this problem in recent years. The basic mechanism of surface destruction is still in doubt. It has been suggested that cement compounds become more soluble as the ionic strength of the surrounding solution increases due to the soluble salts; the salts apparently not reacting directly with the compounds (13). Damaging osmotic pressures are envisioned as another probable cause. This entirely physical explanation by Hansen (14) and others (15), states that ice or salt crystals will begin to form in the larger voids when the conditions for nucleation are reached, these crystals will

*See late Ref. (22)

draw saturated solutions by diffusion from adjacent regions incompatible with nucleation, the crystals growth then produces disruptive pressures. Another proposal is that large crystal growth is not necessary for damaging pressures to develop. As the "pure" water is frozen out of a solution the remainder becomes more concentrated and an osmotic pressure cell is formed with the cement matrix acting as the membrane separating zones of lesser concentrations. Both physical systems would be more severe with the presence of de-icing salts. The most recent theory (21) attributes scaling damage to excessive pressures developed in the surface of a slab. These pressures develop because a salt concentration gradient in the concrete has allowed the interior regions to freeze first, thus forming a barrier against water movement which normally relieves the high hydraulic pressure that leads the inward advance of ice.

Most of the scaling research has been directed toward barrier treatments or integral additives (16). The effect of physical restraint is unreported, as is the importance of the penetration of the salt ions into the concrete and the possible corrosive effects of such penetration.

For physical methods to be effective they must augment some property of the concrete to the extent that a significant advantage is realized. Presumably prestressing would increase the concrete tensile capacity in the direction of the force while decreasing it laterally to some extent by a poisson effect. Should a net gain be realized,

prestressing would increase the freeze-thaw durability of the concrete. In a like fashion, should the micro structure be altered by the superimposed force a net decrease in permeability could result. Lower penetration volumes and rates could enhance the resistance to permeability related modes of destruction such as freeze-thaw, scaling, sulfate attack, and leaching.

The permeability-creep relationships are unknown. Aggregates restrain creep (17)(18) apparently by restricting the free response of the gel to the imposed load but the exact mechanism of creep is disputed. Glucklich and Ishai (19) consider only two theories to have merit; the viscous theory and the seepage theory. They present evidence that creep is solid body deformation due to water seepage migration under differential pressures. The viscous theory holds that creep is due to viscous deformation of the gel proper. More pore deformation might result from a gel flow rather than an elastic solid distortion, but in either event it is not unlikely that some permeability change could result from the loads applied by prestressing.

No studies have attempted to evaluate the effect of prestress on scaling, permeability, and late corrosion of the strands. Conflicting results have come from freeze-thaw studies. The present study is an attempt to furnish more information on these factors.

Research Approach

Three basic laboratory specimens were used. The primary specimen was a small slab which was either nonstressed, prestressed to 500 psi,

or prestressed to 1200 psi. The two secondary specimens were mortar prisms with variable cover over nonstressed strands and clean, short pieces of the prestressing strand.

The slabs were used to evaluate the effect of precompression on: (a) freeze-thaw scaling due to water, chloride solution, and sulfate solution, (b) freeze-thaw durability due to the same solutions, (c) fluid penetration or absorption, (d) wet-dry deterioration with chloride and sulfate solutions, (e) specimens continuously submerged in chloride and sulfate solutions.

The mortar prisms were used to attempt an evaluation of the rate of chloride and sulfate penetration into the bar and the relative corrosion of the encased strand after penetration.

The strand specimens were used to judge the relative corrosive capacities of the chloride and sulfate solutions.

Attempts were made to determine the inter-relationships between variables in a given specimen and between specimens. These multiple objectives are illustrated by Figure 1, where for example the same slab might be used to measure scaling, durability, and possible corrosion in freezing and thawing exposure. Similarly a permeability sample could also be used for a corrosion measurement under room conditions. These corrosion determinations could then be compared and related to the results from the prisms and strands.

For convenience the main phases of the research were divided according to the specimen used and the general test categories were designated as: Scaling, Durability, Permeability, and Corrosion.

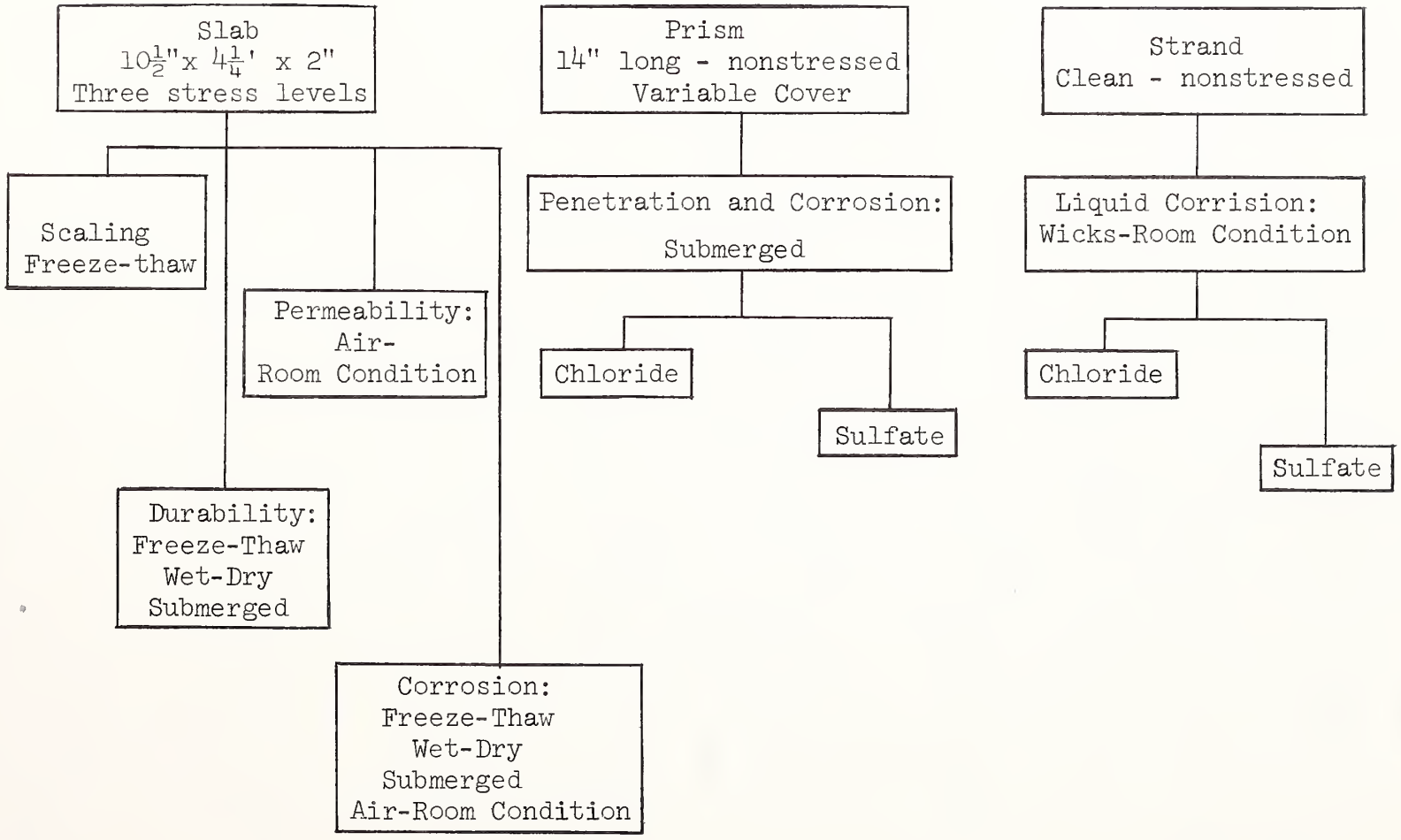

Figure 1. Specimens, Tests, & Environments

The test names and terms used are intended to convey the following meanings:

Durability - deep structural integrity of the whole concrete or mortar specimen.

Scaling - flaking of the paste or mortar, progressing from the surface inward, finally resulting in exposing and dislodging large aggregate particles.

Permeability - unidirectional moisture absorption and passage through unsaturated slabs, induced by gravity and a small pressure head.

Corrosion - pitting and rusting of the prestress strand.

CHAPTER II

INVESTIGATIONAL METHODS, EQUIPMENT, MATERIALS

DURABILITY AND SCALING

Slab Specimens

The basic slab specimen had concrete dimensions of $10\frac{1}{2}$" x $4\frac{1}{2}$" x 2". The overall length varied with the stress level because of the strand chucks and end plates. This slab size was dictated by the available facilities and the number of slabs to be tested at a given time. The small size posed unique stressing problems and demanded rather exceptional procedures and control, which are given in Appendix A.

All specimens contained one 3/8 inch ASTM Grade seven wire cable. The nonstressed slab contained a cable which had been loaded only enough to straighten it. The stressed slabs required a hybrid pretension scheme since bond transfer of the load was impossible. The chucks were spot welded to the end plates and the strand grips were preseated on the cable, thus load was applied to the concrete through the anchorage and plates while allowing intimate bonding contact between the concrete and cable. The 500 psi stress level, which was arbitrarily chosen, was applied through $\frac{1}{2}$ inch thick end plates. The 1200 psi stress level, which was dictated by the maximum cable capacity minus losses, was applied through 3/4 inch thick end plates. Typical slabs are shown in Figure 2.

Fig. 2. Pretensioned Slabs. (from left: zero, 500, and 1200 psi)

Except for the surface treatment the same fabrication procedures were used for all of the slab test series. The wet-dry series used a standard flat wood-floated finish. The permeability slabs had circular depressions formed on their surfaces for the later positioning of the fluid standpipes. The scaling and durability specimens had mortar dams attached to the finished surface peripheries to retain ponded solutions. Details of these procedures are covered in the section on fabrication.

Two curing methods were used in the slab sequence: a normal moist room cure and an atmospheric pressure steam cure.

The entire slab program consisted of 192 slabs from 8 batches of concrete. The initial development series was based on one-half of the total and the remaining 96 slabs were used for final evaluation of durability, scaling, and permeability.

Materials

A single concrete mix was used for all slabs. This was a nominal 4,000 psi mix (28 day), non air-entrained, 3/4 inch maximum size aggregate, with Type II cement and a 2 inch slump. The mix was purposely non air-entrained and cast on steel beds since both of these practices are known to adversely affect durability (16) and the intent was to accentuate and accelerate non-durable results, to magnify any effect of precompression, and to shorten the testing time.

The aggregate was well rounded, stream-graded, sound, granitic material. All fractions of both the fine and coarse material were oven-dried and stored separately. They were recombined at the time of batching. Good performance histories exist for the aggregates in the study exposures and they are not in themselves thought to add any extraneous variables.

The cement analysis, aggregate gradations, concrete mix design data, and mortar dam materials are detailed in Appendix B.

The two salt solutions used in all phases of the investigation were calcium chloride ($CaCl_2$) and magnesium sulfate ($MgSO_4 \cdot 7H_2O$), both

in concentrations of 20,000 parts of chloride or sulfate per million parts of water. Expressed as a percentage this concentration is 3.1 percent of calcium chloride and 5.1 percent magnesium sulfate. This concentration of sulfate, while high, is not an unreasonable concentration for some western region ground waters. The chloride concentration, not to be expected in natural ground waters, is well within reasonably common ranges found where deicing salts have accumulated. (1)

The standpipes used to create the pressure head for the permeability study are shown in Figure 3. Each was made of a glass milk bottle, a drilled rubber stopper, and length of 12 mm glass tubing.

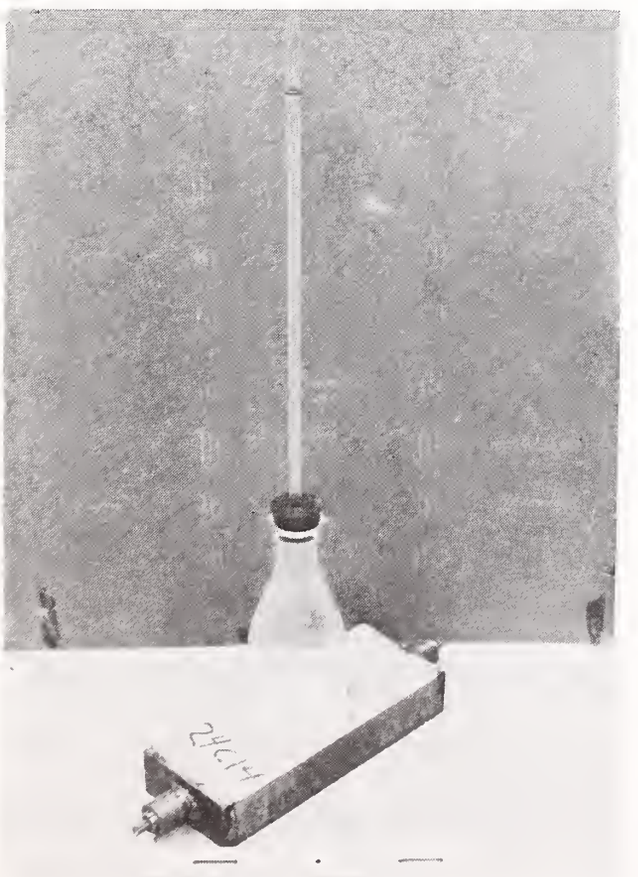

Fig. 3. Slab Prepared for Permeability Study.

Fabrication

The casting beds used for all the slab specimens were 7 [9.8 channel sections $33\frac{1}{2}$ inches long. The end jacking plates were 7" x 2" x $\frac{1}{2}$" for the zero and 500 psi samples and 7" x 2" x 1" for the 1200 psi units. One 7/16" diameter center hole through the plates was provided for the strand passage. The 1200 psi beds were stiffened with 1" x 1" x $\frac{1}{4}$" angles. The channel web was used as the mold floor, 2" x 3/8" bars were placed longitudinally to form the sides, and the end forms for the slabs were the loading plates that became part of the final stressed specimen but were removed from the nonstressed slabs. The assembled side forms and end plates were held in position by 1" x 1/8" spring clips. Two slabs were cast in each bed.

The stressing operation is detailed in Appendix A; the main elements being the determination of the stress level and the elimination of all possible losses. Levels of stress were determined by experimental procedures using external and internal load cells. Losses were diminished by preseating all chucks with overloads and by welding the chucks to the slab loading plates.

Two cubic feet of concrete were mixed per batch in a laboratory pan-type mixer. This quantity yielded 24 slab specimens. A vibrating table was used for compacting the concrete in the molds. Those slabs which were to be used in the continuously wet, wet-dry, and freeze-thaw environments were finished with three passes of a wood float. The freeze-thaw specimens were provided with mortar dams at a later time.

The permeability specimens were finished with the float and then indented to receive the stand pipes after a curing period.

After stress transfer and partial curing the mortar dams were cast on the freeze-thaw slabs. These highly air-entrained dams were 3/4 inch high and tapered from 1/2 inch wide at the base to 5/16 inch at the top. The periphery of the top surface of the slab was wire brushed and the dam was cast on and bonded to this surface with an air-entrained slurry.

Appendix B contains detailed procedures for mixing, vibrating and casting the concrete. It also presents the material and procedural information for fabricating the mortar dams.

The standpipes for the permeability study were made by sawing the bottom from glass milk bottles, wire brushing the preformed annular ring in the slab surface, treating this area with Dow Corning Surface Conditioner A and 780 Building Sealant, positioning the bottle on the sealant, fitting the drilled rubber stopper, and inserting the 12 mm glass tube. After the sealant had cured, three coats of liquid plastic were applied to all exposed concrete surfaces except the bottom. This was done to force unidirectional fluid flow and evaporation through the thickness of the slab.

Curing

Two standard curing procedures were used to evaluate the influence of curing method on the performance of the slabs.

Normal curing for this study began with the placing of the pretensioned slabs, in their casting beds, into a high humidity moist-room for

seven days. They were then loaded by cutting the anchoring strand and removed from the beds. After the mortar dams were applied, moist curing was continued for a total of 14 days. An additional 14 days at "dry" room conditions completed the cure period of 28 days and the specimens were then started in the various environmental tests.

After casting, the specimens to be steam cured remained undisturbed at room conditions for an approximate 5 hour presteam period. They were then placed in the steam chambers and the temperature was manually controlled to permit a rise of 40°F per hour until a temperature of 150°F had been attained. Automatic controls maintained this temperature for 13½ hours after which manual reduction at 40°F per hour returned the samples to room temperature. The total steam time was approximately 18 hours. Following steaming the casting beds were placed in the moist-room and they were then processed the same as the normal cure slabs for the rest of the 28-day period.

Both the curtailed moist curing and the short room drying were again specifically selected to magnify the anticipated damage. Short term curing and only partial drying have adverse durability potential, especially under scaling conditions (16).

EXPOSURE CONDITIONS AND TESTING PROCEDURES

Of the two 96 slab series of specimens which were made, the first was mainly a development series wherein the fabrication procedures were refined and the direction of most of the promising testing was determined. As in most other phases of the program multiple objectives were sought

from the specimens. The number of specimens per environment varied: 18 each in the freeze-thaw ponded with chloride and sulfate solutions; 12 freeze with water-thaw with chloride salt, normal cure, and 6 steam cure; 9 each in the wet-dry and wet for both salt solutions; and 6 in the fluid flow trials. Stress levels were occasionally erratic in this series but still probably sufficient to show differentials of stress if not exact magnitudes. Also, the continuously submerged and the wet-dry tests were found to be of limited promise. For these reasons the last two tests were not reproduced with more refinement but were continued with these first specimens.

Other tests were modified on the basis of the results from this series. The process of freezing water on the slabs and thawing the ice with calcium chloride salt was found to be 5 to 10 times less harsh in scaling than the treatment using continuously ponded salt solutions, so ponding was used for the continuing study. It was also found that magnesium sulfate either ponded or used for thawing was practically innocuous and so sulfate was rejected for further testing of thistype.

Based on these observations the second series was designed to yield more information on the variables of steam curing, ponded water, ponded calcium chloride solution, and water and chloride solution fluid flow. There were four replicas for each variable, again producing a series of 96 slabs. Schematically, the second series is shown in Figure 4. Figure 5 shows the total two series slab program.

Scaling and Durability

The slabs subjected to the freezing and thawing test were all fitted with mortar dams and all were started in test at 28 days of age. The general test routine was to place approximately 170 ml of water or solution on the slabs, freeze them for 16 hours at 5° ± 3° F and then thaw them for 8 hours at room conditions. The slabs assigned to the salt solutions were either frozen while ponded with tap water and thawed with the salt, or ponded with salt solution throughout the cycle. The salt thawed slabs were flushed every day and the solution ponded slabs were flushed every 10 cycles. This was also the schedule for the continuously ponded tap water slabs.

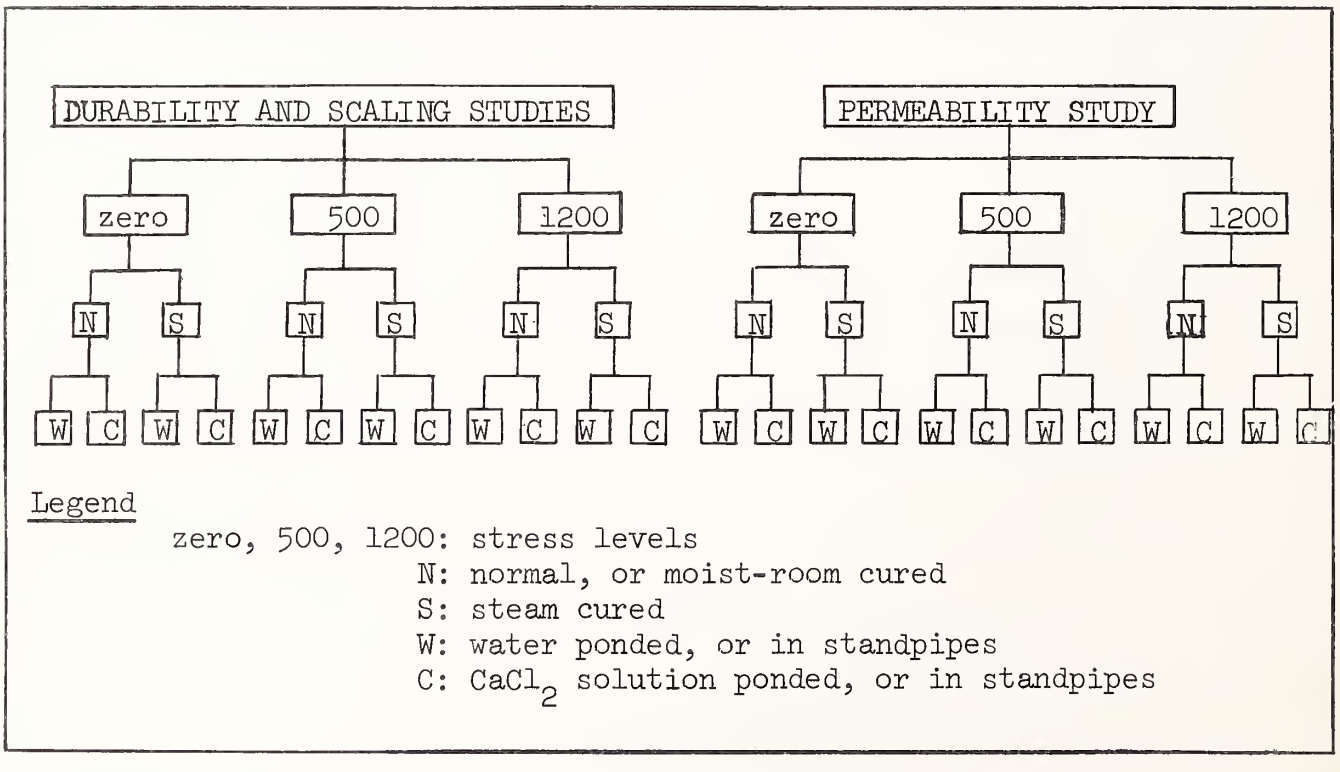

Figure 4. Refined Slab Series

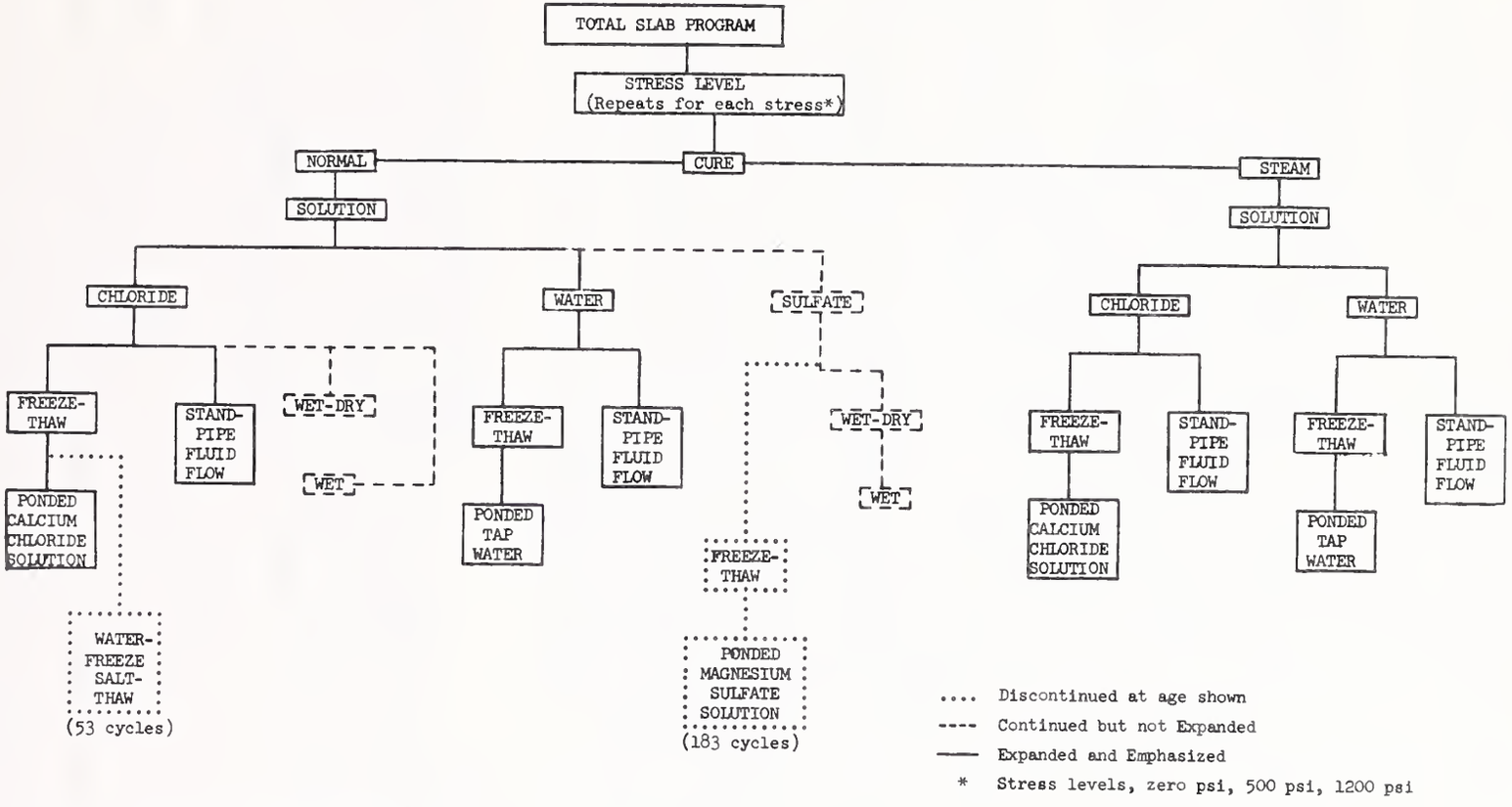

Fig. 5. Complete Slab Specimen Program

The data collected at the end of each 10 cycles were: specimen length and surface-dry weight, the natural transverse vibration frequency, and the scaling value.

The scaling value was initially determined according to a visual reference of 20, which was fairly effective until deep scaling had eroded the entire slab surface. After deep scaling the visual system, either natural or photographic, became meaningless and the oven-dry weight of material flushed from the slabs and retained on a #200 mesh sieve proved to be an excellent scaling indicator.

The length was measured to 0.001 inches and the surface-dry weight was read to 0.01 pounds.

The natural frequency of transverse flexural vibration was determined by standard sonic methods, except that weight was not assumed to remain constant. No conversion to the dynamic modulus of elasticity was made since the frequency was the prime durability indicator and no limiting durability factor was set.

Wet and Wet-Dry

The specimens assigned to wet-dry and continuously wet testing received no special appurtances and started in test just as they had been cast. The wet-dry sequence consisted of submerging the slabs in chloride or sulfate solutions for 24 hours at room temperature and then drying them for 24 hours at 120°F in a hot air enclosure. The samples continuously submerged in the same two solutions were at the prevailing room temperature. Both of these series were examined every 10

cycles or days for evidence of scaling or cracking. The natural frequency weight, and length were recorded. After 100 cycles these readings were taken sporadically because more frequent data collection was not justified by the performance.

Primary Permeability - Slabs

While slabs from all environments were examined for fluid penetration effects, the primary study was made on those slabs using the standpipes. The pipes were marked at the two-foot level and the solutions were added at 10-day intervals to re-establish the level. The fluid added was measured to within 0.1 ml. Every 20 days evaporation losses from reference bottles were determined. These bottles were spaced across the test stand to reflect the room conditions. Since differential absorption was the main concern no data were collected on room temperature, pressure, or humidity. In any event these were uncontrollable. Visual examination was made at the time of fluid addition to determine if any evidence of fluid passage existed.

Secondary Permeability and Corrosion

The specimens used in this work were mortar bars with variable cover over non-stressed strand and lengths of bare, clean, individual wires from the prestressing strands.

Mortar Bars

The mortar bars varied in cross-section: 1" x 1", $1\frac{1}{2}$" x $1\frac{1}{2}$", 2" x 2", and $2\frac{1}{2}$" x $2\frac{1}{2}$". All were 10 inches long and contained one

non-stressed strand. This produced bars with the mortar cover varying from approximately 1/4 inch to 1-1/8 inch. An attempt was made to use two degrees of mortar compaction against the strand. One set of specimens was densely compacted throughout the bar by using the vibration table. The second set was compacted to the mid-strand depth and then a small cord was passed under the strand and along its length using a sawing motion. Before final set, the remainder of the mold was filled and compacted. This was successful in creating small voids along the lower half of the strand, as desired, since it had been shown that such voids were detrimental in corrosive situations (6).

The mortar bar series consisted of three bars of each cover thickness and compaction in each solution. They were continuously submerged in the chloride and sulfate solutions. This constant immersion was not thought to be as rigorous a condition as wetting by draped cloth wicks would have been (6) but a check of a still more severe condition was available from the standpipe slab tests.

Visual checks were made to observe any apparent damage to the bars and for evidence of rust build-up splitting along the strand. Final analysis was made by sawing the sample longitudinally and examining the mortar and the strands.

Strands

The strands were cut into approximately 12 inch lengths and then separated. After cleaning with acetone the wires were spaced across the edges of trays containing water, chloride, and sulfate solutions.

Linen toweling was draped over each individual wire and into the solution (6). Every 10 days 5 wires were removed from each solution for tensile tests and for visual examination.

CHAPTER III

DURABILITY AND SCALING - TEST RESULTS AND DISCUSSION

TEST RESULTS

Referring to Figure 5 showing the total slab program it is evident that the main emphasis was placed on the second and more refined series of slabs and that the most complete analysis was made on this part of the work. Figure 6 is a portion of Figure 4 modified to aid in describing the particular slab solution exposure in ponded freezing and thawing and the comparisons to be studied. The portion of the program detailed in this section used four replicates for each treatment, one from each of four batches of concrete.

TABLE I

TYPICAL SLAB DURABILITY AND SCALING STUDY DATA,

No. of F/T cycles	Length (in)	Weight (lbs.)	Natural frequency (cps.)	Scaling weight loss (gms.)	Remarks
0	11.697	12.64	2840	---	
5	11.697	12.80	2820	6.1	
11	11.697	12.88	2850	13.4	
20	11.697	12.78	2830	38.0	
20	11.698	12.75	2890	---	New dike
30	11.697	12.77	2890	3.5	
40	11.697	12.78	2880	6.7	
50	11.698	12.78	2880	8.6	
50	11.699	12.80	2940	---	New dike
60	11.700	12.77	2900	12.8	
70	11.702	12.77	2910	12.1	
80	11.702	12.73	2890	6.7	
80	11.703	12.74	2960	---	New dike
90	11.703	12.72	2940	3.9	
100	11.703	12.70	2950	3.6	
110	11.703	12.69	2960	5.1	
120	11.704	12.71	2950	4.8	
130	11.705	12.70	2950	6.0	
. . . .	. . . .				

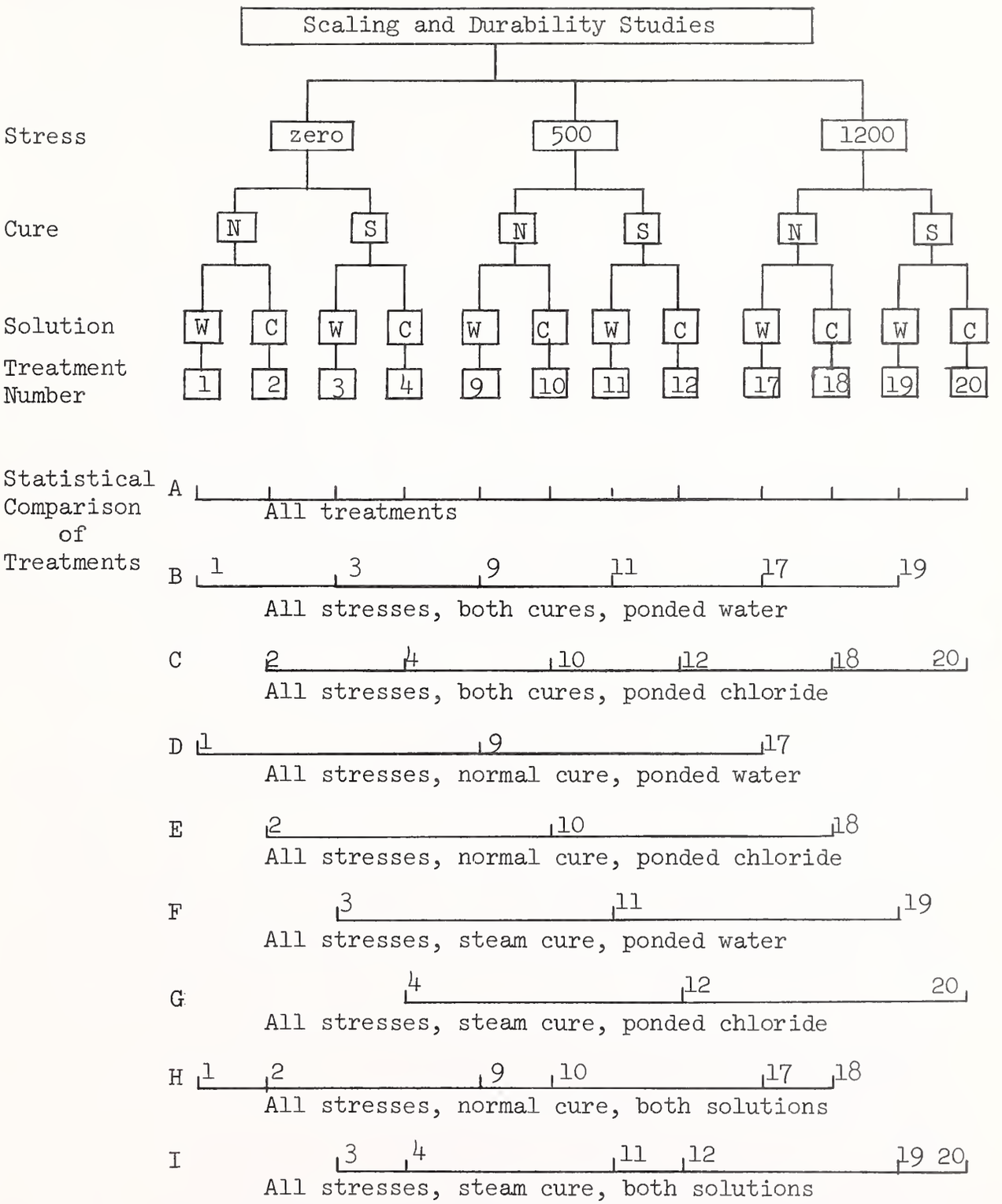

Figure 6. Freeze-Thaw Treatments & Comparisons

Table I is typical of the data collected. This particular data is for a slab exposed to the calcium chloride solution and illustrates one of the problems associated with the scaling investigation. The mortar dams become ineffective in 20 to 30 cycles of freezing and thawing. Most often this was due to undermining of the dam rather than actual destruction of the dam. No method of repair proved successful and the dams had to be replaced. When this was required all slabs of a given batch were removed from test and repaired at the same time to avoid in-batch variations as much as possible. After the dams were all replaced, the slabs were stored in the moist room for seven days to cure the dams. This moist storage resulting in a "healing" of the slabs and the natural transverse frequency usually increased. This can be noted in the table by the repetition of data at 20, 50, and 80 cycles. The repeat readings were taken after the seven day moist cure.

To determine if the natural frequency increase was due to any additional rigidity of the new dams or to the self healing effect, or a combination of these, a comparison was made between the slabs of one batch requiring repair and the slabs of another batch not requiring repair. Both sets were stored in the moist room at the same time. The average frequency increase for slabs not needing repair was 2.49% after seven days moist cure while the increase for the repaired slabs was 2.69%. Also, during normal testing, there was noticeable decrease in the rate of deterioration after the curing periods. These observations indicate that the major cause of the frequency increase is the "self-healing" of the slabs.

The dam replacement was necessary on all slabs ponding calcium chloride solution. The replacement did not take place at the same time for all slab groups but the total number of new dams was approximately the same for all groups. No adjustment of the frequency changes was deemed valid or even necessary for comparisons within the chloride group. However, cross-group frequency comparisons with those slabs ponding water may be suspect since these slabs required little dam repair with only one dam replacement being necessary on the slabs from one batch.

The individual slab graphs in Appendix C Figures 45 to 50 show the mortar dam replacements by vertical dashed line discontinuities. The figures also show the four replicates assigned to a specific treatment.

Due to rusting of the end bearing plates on the stressed specimens and the deterioration of the concrete on the non-stressed specimens, little use was derived from the length measurements.

The weights were adjusted to account for the change between old and new dams. A very small increment of weight due to moisture absorption during dam renewal was ignored. These weight adjustments were made only for comparisons of the effects of various treatment upon weight changes of the concrete slabs. In computing the relative dynamic modulus of elasticity the actual unadjusted weight at any given number of cycles was used. This was done because relatively large weight changes did occur in individual slabs and there were significant weight change differences between the water ponded series and the chloride solution

ponded series. The magnitude of these changes did not allow the common assumption of essentially constant weight when computing the modulus and the equation used was:

$$P_c = \frac{W_c \, n_c^2}{W_o \, n_o^2} \times 100$$

where P_c is the percent relative dynamic modulus

W_c and n_c are the unadjusted weight and the natural frequency at "c" test cycles

W_o and n_c are the original weight and natural frequency at zero test cycles.

All test results and measurements were entered on data processing cards and a Fortran program was developed for the IBM 1620II computer (Montana State University Computing Center). From data such as those in Table I computations were made for the relative dynamic moduli, scaling weight loss conversions from grams to pounds, adjusted weight changes, length changes, and cumulative scaling weight losses. These results were punched on cards and listed for subsequent plotting. Typical of this operation is Table II which is derived from the data of Table I.

TABLE II

COMPUTED SLAB RESULTS

No. of F/T cycles	Relative dynamic modulus (%)	Adjusted weight change (lbs.)	Length change (in.)	Cumulative scaling loss (lbs.)	Comment
0	100.00	0.00	0.000	0.00	
5	99.84	0.16	0.000	0.01	
11	102.61	0.24	0.000	0.04	
20	100.39	0.14	0.000	0.12	
20	104.45	0.14	0.001	0.12	New dike
30	104.61	0.16	0.000	0.13	
40	103.97	0.17	0.000	0.14	
50	103.97	0.17	0.002	0.16	
50	108.52	0.17	0.002	0.16	New dike
60	105.34	0.14	0.003	0.19	
70	106.07	0.14	0.005	0.22	
80	104.28	0.10	0.005	0.23	
80	109.48	0.10	0.006	0.23	New dike
90	107.84	0.08	0.006	0.24	
100	108.40	0.06	0.006	0.25	
110	109.05	0.05	0.006	0.26	
120	108.49	0.07	0.007	0.27	
130	108.40	0.06	0.008	0.28	
. . . .	. . . . .				

No distinct relationship between durability, nor scaling resistance, and number of freeze-thaw cycles was desired in this study. Rather, a comparison of the effects of various treatments, after any given number of freeze-thaw cyles, upon the characteristics of the concrete slabs was intended. Therefore, the statistical method chosen for making these comparisons was Duncan's new multiple-range test (20). This test is designed to test for the significance of differences between any number of mean values, under the assumption of homogeneity of variances (i.e., equal data dispersion about the means, regardless of treatment).

Despite the careful control exercised throughout the study, inherent variability existed between the characteristics of the replicate slabs and a blanket application of the Duncan test, disregarding the magnitude of the variances, would be incorrect. To test for homogeneity of the variances Bartlett's test (20) was used. When diverse treatments are to be analyzed with a given statistical tool, a rigid application of the tool can in some instances cause as much uncertainty as an invalid application. Differing hypotheses may be supported or refuted by the tool.

It will be recalled that the primary purpose of this portion of the investigation was to determine the effect of prestress upon the durability of concrete. In addition, comparisons of the effects of steam curing and normal curing, and of the effects of ponded water and $CaCl_2$ solution upon durability were desired. Also sought were comparisons of the effects of prestress and of the types of curing upon the scaling resistance of concrete. It was anticipated that the Bartlett test would probably show non-homogeneity of variances. To assure, where possible, a valid application of Duncan's test it was decided to make nine comparisons of various treatment combinations. These treatment comparisons were shown in Fig. 6.

For Bartlett's test, the 1 percent significance level was chosen for declaration of homogeneity or non-homogeneity of variances, while the 5 percent level was chosen for decisions regarding the significance or non-significance of differences between treatment mean values in the Duncan test.

Fortran computer programs were written which took the results for each slab, and performed the nine treatment comparisons at intervals of 10 freeze-thaw cycles for the relative dynamic modulus values, and at intervals of 20 cycles, beginning at 10 cycles, for the adjusted weight change, length change, and cumulative scaling loss values.

The detailed results presented in Appendix C show that some data were not taken on the days at which these statistical tests were applied. Here, the computer program supplied intermediate values by linear interpolation between actual days of record.

Also, two slabs became so severely damaged after 70 freeze-thaw cycles that their mortar dikes could not be replaced and they were removed from the cycling and testing program. To include these slabs in the statistical tests, the program assigned their final values of relative scaling losses for the remaining cycles at which statistical tests were desired. This decision was the most conservative possible, but no other method for assigning these non-existent values could be reasonably justified. The omission of these replicates after 70 cycles would have made the statistical tests difficult at best, and would have seriously distorted the average effects of treatment 4, (zero stress, steam cured, chloride ponded).

This same averaging procedure, using the last data of record, was used again for other specimens at later ages whenever slabs were withdrawn from the program. These terminations are shown on the individual specimen

records in Appendix C. The statistical combinations involving these specimens are marked at the time when averaging began so the reader may set his own level of credence on the continuing portion of the summaries.

A brief presentation of the statistical computations and methods used is given in Appendix D. It illustrates the reduction and interpretation of the data in Tables I and II. The data were transformed to bring all values within a given range. Bartlett's test, using the chi-squared statistic at the 1 percent significance level (computed v.s. standard tabulations), was then performed for the statement of homogeneity or non-homogeneity of variance. The Duncan test, at the 5 percent level, for statistically significant difference in performance was then conducted.

The usual method of presenting Duncan results is to rank the treatments in an ascending mean order and then graphically show insignificance of difference at a particular protection level by a common underlining. For example:

17 19 11 9 1 3

This would be interpreted as stating that, at the 5 percent level of significance, treatments 17, 19, 11, 9, 1 are insignificantly different and that 1 and 3 are also insignificantly different but 3 is significantly different from 17, 19, 11 and 9.

The method of reporting Duncan results in this study is the same except that the relationships are shown vertically and repeated as a function of data comparison time. This serves two purposes (1) all of

the Duncan multiple-range results are condensed for ready interpretation, and (2) a qualitative interpretation of the relative magnitudes and directions of change can be made. Figures 7-15 show these results for the durability and scaling series. Also shown on these figures are the homogeneity ranges, where in a strict statistical sense the Duncan tests are valid or invalid. These ranges were taken from Tables III and IV which also show, according to the Bartlett test, which Duncan tests are to be considered statistically valid. The symbols "n.s." and "*" indicate homogeneous variances and "**" means non-homogeneity.

Because of the greater relative importance of the dynamic modulus of elasticity as an index of deterioration in any freeze-thaw durability study, all of the treatment comparisons described in Figure 6 for the mean relative dynamic moduli are presented in Figures 7-15. For comparisons of mean adjusted weight changes, the conclusions to be drawn from treatment comparisons B through I are not different from those related by comparison A. Therefore, only Figure 16 is presented to summarize the results of the average adjusted weight change comparisons. The same reasoning applies to comparisons of the mean length changes, the results of which appear in Figure 17.

For the average scaling weight loss comparisons, only treatment comparisons C, E, and G are appropriate, since data for this study were not obtained from slabs assigned to treatments 1, 3, 9, 11, 17, and 19, that is from slabs which were ponded with water. Further, the conclusions to be drawn from comparisons E and G are not different from those to be

drawn from comparison C for the scaling resistance study; nor can they be more clearly illustrated than in Figure 18 so only this figure is presented.

It may aid the reader in interpreting Figures 7 through 18 if the information in Figure 6 is reviewed. The following will be noted:

(a) The major subdivision is stress. Treatments 1-4 are on non-stressed slabs, 9-12 are on 500 psi slabs, and 17-20 are on 1200 psi slabs.

(b) The next subdivision is cure. Treatments 1, 2, 9, 10, 17, 18 are normally cured while 3, 4, 11, 12, 19, 12 are treatment numbers of steam cured slabs.

(c) The final subdivision is solution. The odd numbers applying to ponded water and the even numbers referring to ponded calcium chloride solution.

Also the Figures 7 through 18 show the mean relationship of the four replicates in each treatment and the Duncan comparisons are shown by the vertical bars intercepting those treatments of insignificant difference.

On the summary curves it will be noted for some treatments the plots are marked at the time some specimens were removed from test. The notation records the average of the four replicates in test until the particular day, after which the upper numeral is the number of specimens in actual test and the lower number, in parenthesis, is the number of specimens for which the last test values are carried. These two separate sources yield the plotted average.

TABLE III

RESULTS OF BARTLETT TESTS OF
TRANSFORMED RELATIVE DYNAMIC MODULI

No. of F/T cycles	Comparison								
	A	B	C	D	E	F	G	H	I
10	**	n.s.	**	n.s.	n.s.	n.s.	n.s.	n.s.	**
20	**	n.s.	**	n.s.	n.s.	n.s.	*	n.s.	**
30	**	n.s.	**	n.s.	n.s.	n.s.	*	n.s.	*
40	**	n.s.	**	n.s.	n.s.	n.s.	n.s.	n.s.	**
50	**	n.s.	**	n.s.	n.s.	*	*	n.s.	**
60	**	*	**	n.s.	n.s.	*	n.s.	n.s.	**
70	**	**	**	n.s.	n.s.	**	*	n.s.	**
80	**	**	**	n.s.	n.s.	**	*	n.s.	**
90	**	**	**	n.s.	n.s.	**	*	n.s.	**
100	**	**	*	n.s.	n.s.	**	*	n.s.	**
110	**	**	*	n.s.	n.s.	**	n.s.	n.s.	**
120	**	**	n.s.	n.s.	n.s.	**	n.s.	n.s.	**
130	**	**	n.s.	n.s.	n.s.	**	n.s.	n.s.	**
140	**	*	n.s.	n.s.	n.s.	*	n.s.	n.s.	*
150	**	**	n.s.	*	n.s.	**	n.s.	n.s.	**
160	*	**	n.s.	*	n.s.	*	n.s.	n.s.	*
170	*	**	n.s.	n.s.	n.s.	**	n.s.	n.s.	**
180	**	**	n.s.	n.s.	n.s.	**	n.s.	n.s.	**
190	*	*	n.s.	n.s.	n.s.	**	n.s.	n.s.	**
200	*	*	n.s.	n.s.	n.s.	**	n.s.	n.s.	**
210	n.s.	*	n.s.	n.s.	n.s.	**	n.s.	n.s.	*
220	*	**	n.s.	n.s.	n.s.	**	n.s.	n.s.	*
230	*	**	n.s.	n.s.	n.s.	**	n.s.	n.s.	**
240	n.s.	n.s.	n.s.	n.s.	n.s.	*	n.s.	n.s.	*
250	n.s.	*	n.s.	n.s.	n.s.	*	n.s.	n.s.	*

Note: n.s. and * homogeneous variance

** variance non-homogeneous

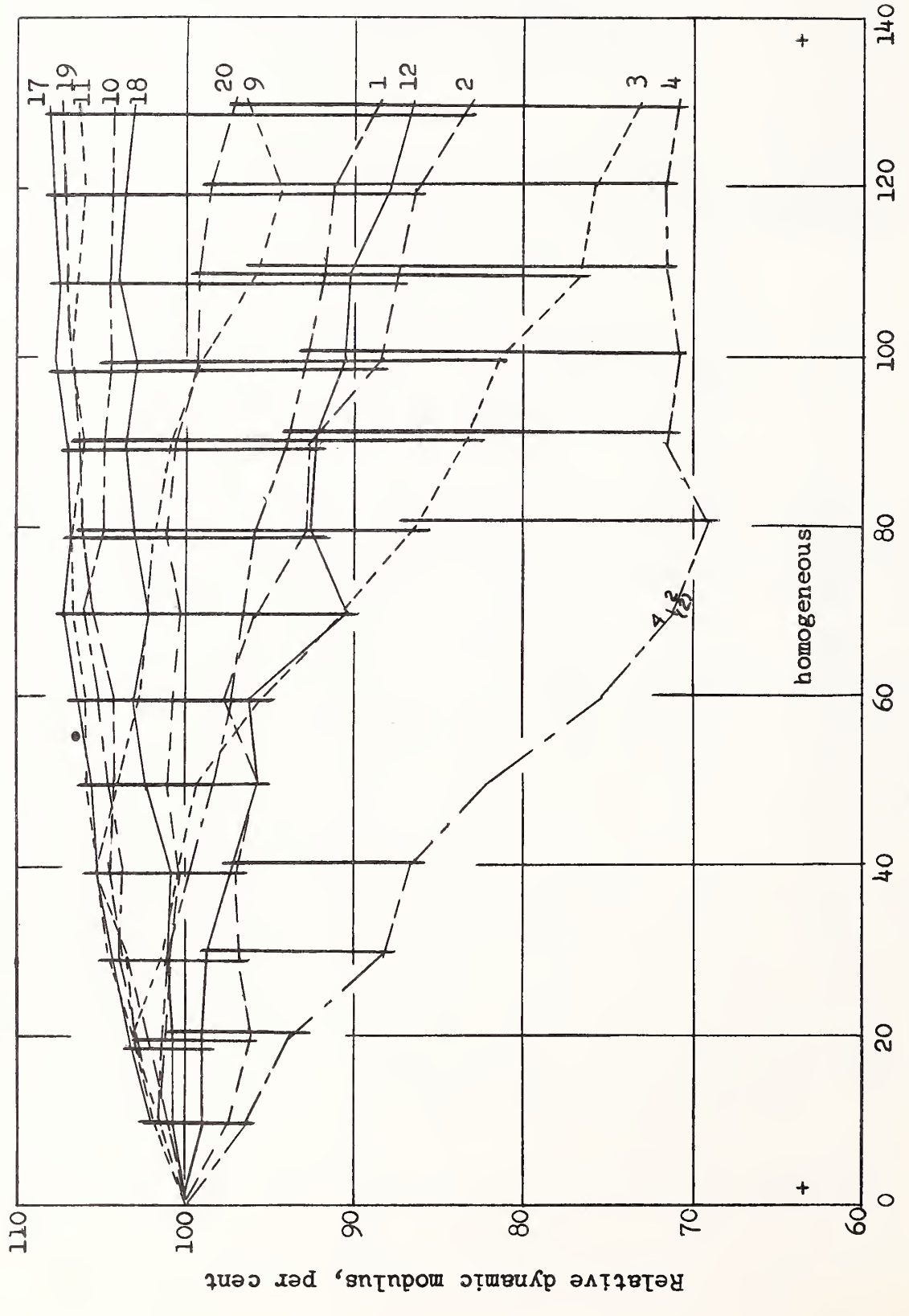

Fig. 7. Results of Duncan tests of mean transformed relative dynamic moduli for treatment comparison A. (All treatments)

Fig. 7 (Cont.) Results of Duncan Test of mean transformed relative dynamic moduli for treatment comparison A. (All treatments)

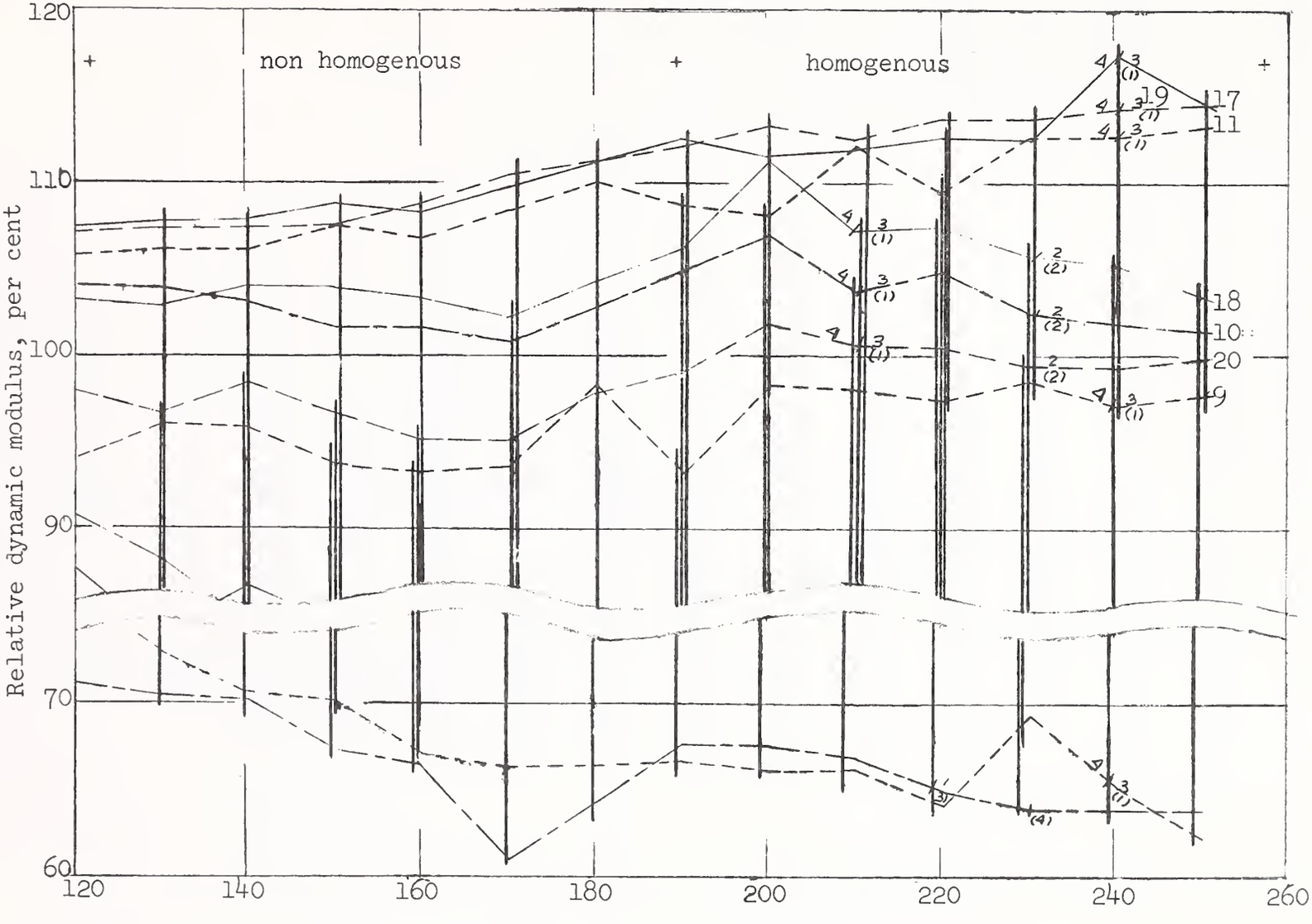

Fig. 8. Results of Duncan tests of mean transformed relative dynamic moduli for treatment comparison B. (All stresses, both cures, water)

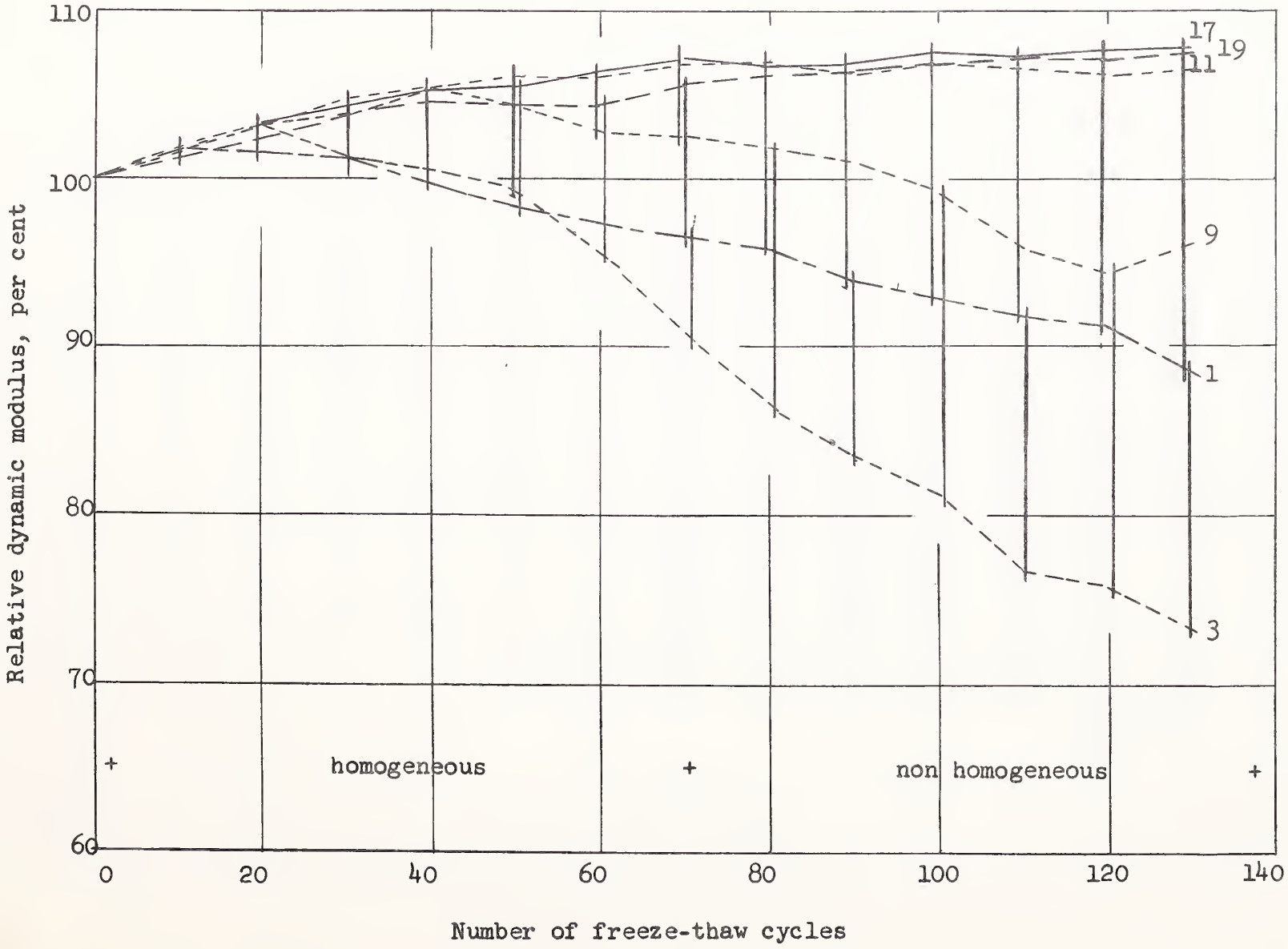

Fig. 8.(Cont.) Results of Duncan tests of mean transformed relative dynamic moduli for treatment comparison B. (All stresses, both cures, water)

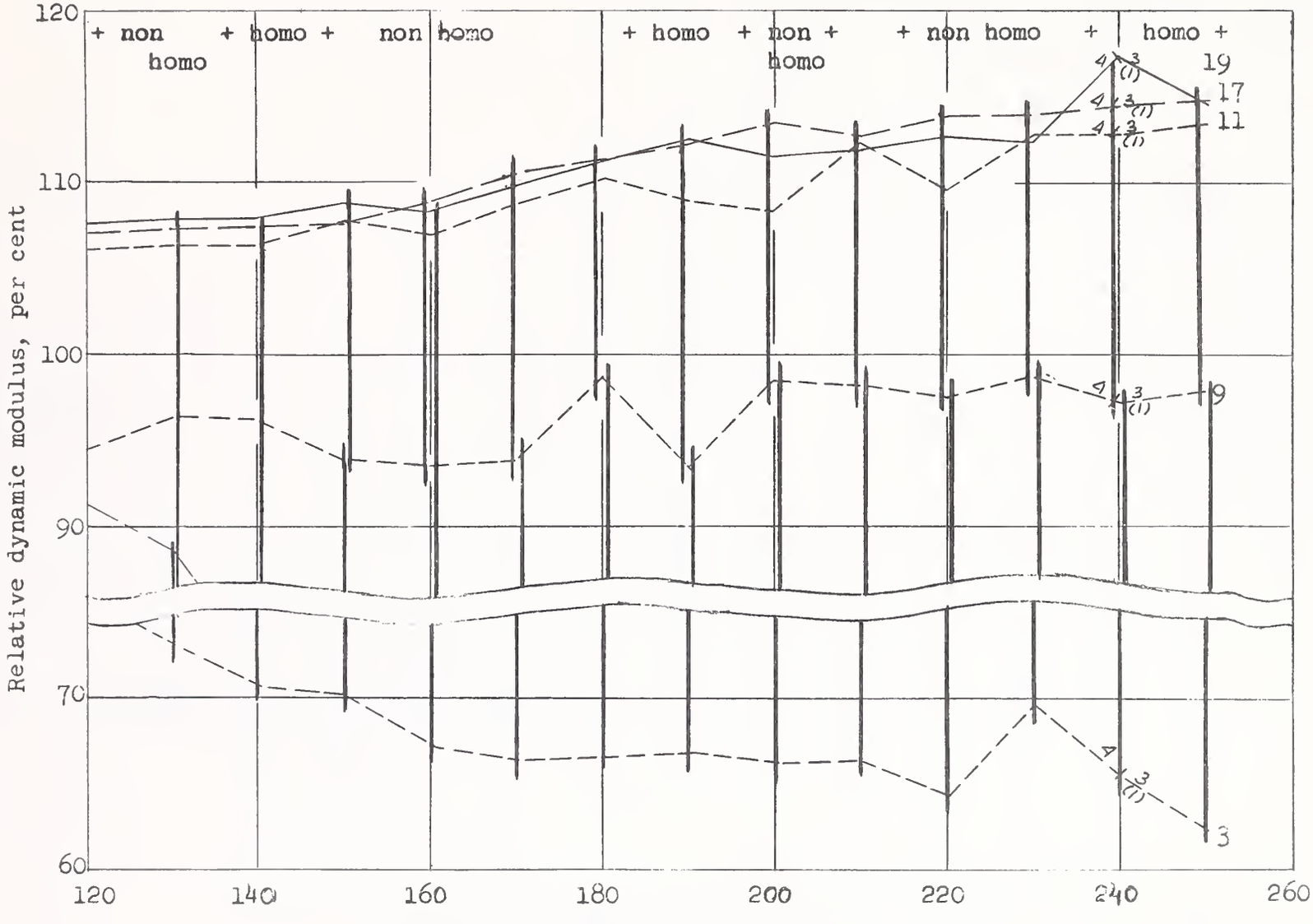

Fig. 9. Results of Duncan tests of mean transformed relative dynamic moduli for treatment comparison C. (All stresses, both cures, chloride)

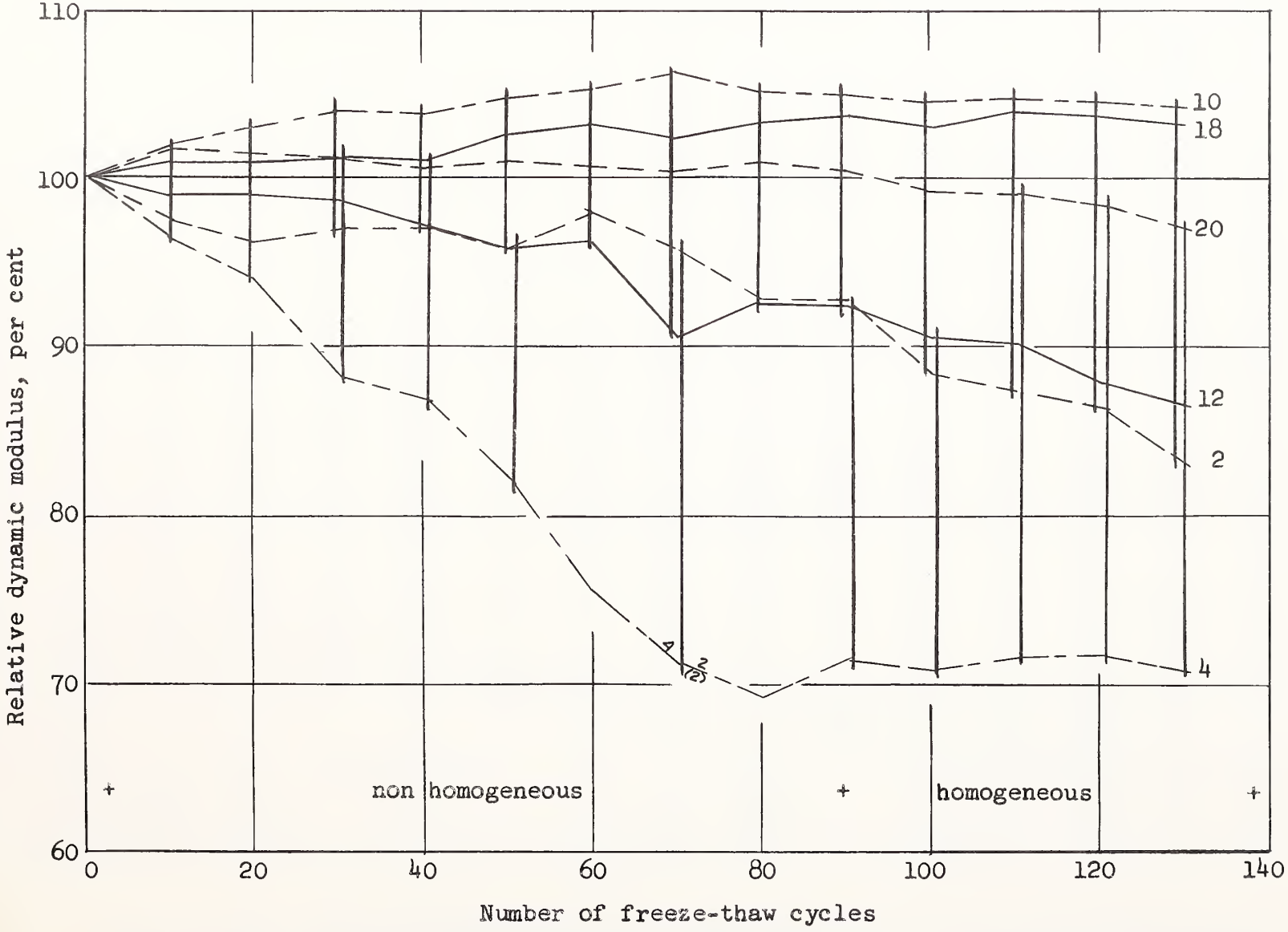

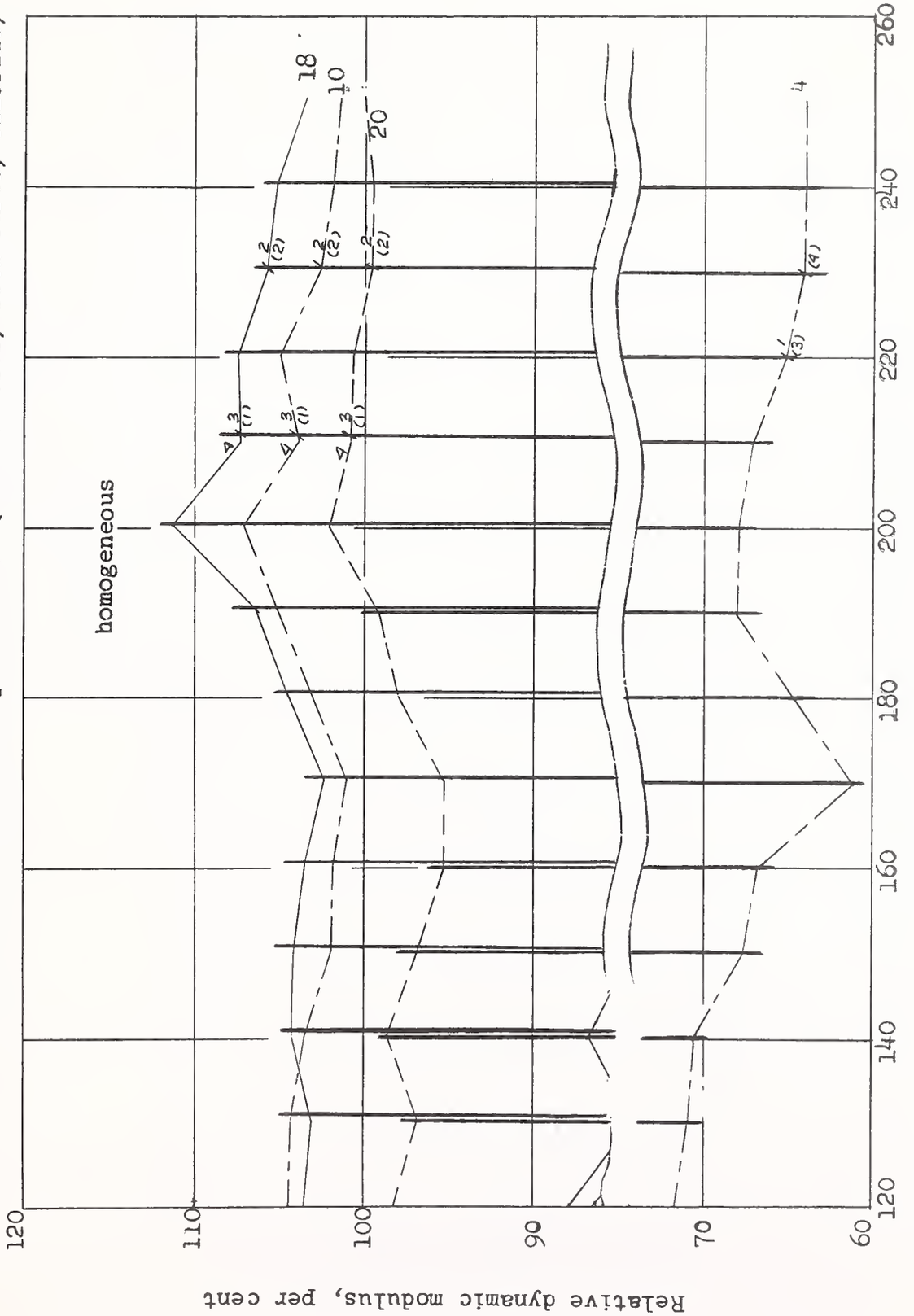

Fig. 9. (Cont.) Results of Duncan tests of mean transformed relative dynamic moduli for treatment comparison C. (All stresses, both cures, chloride)

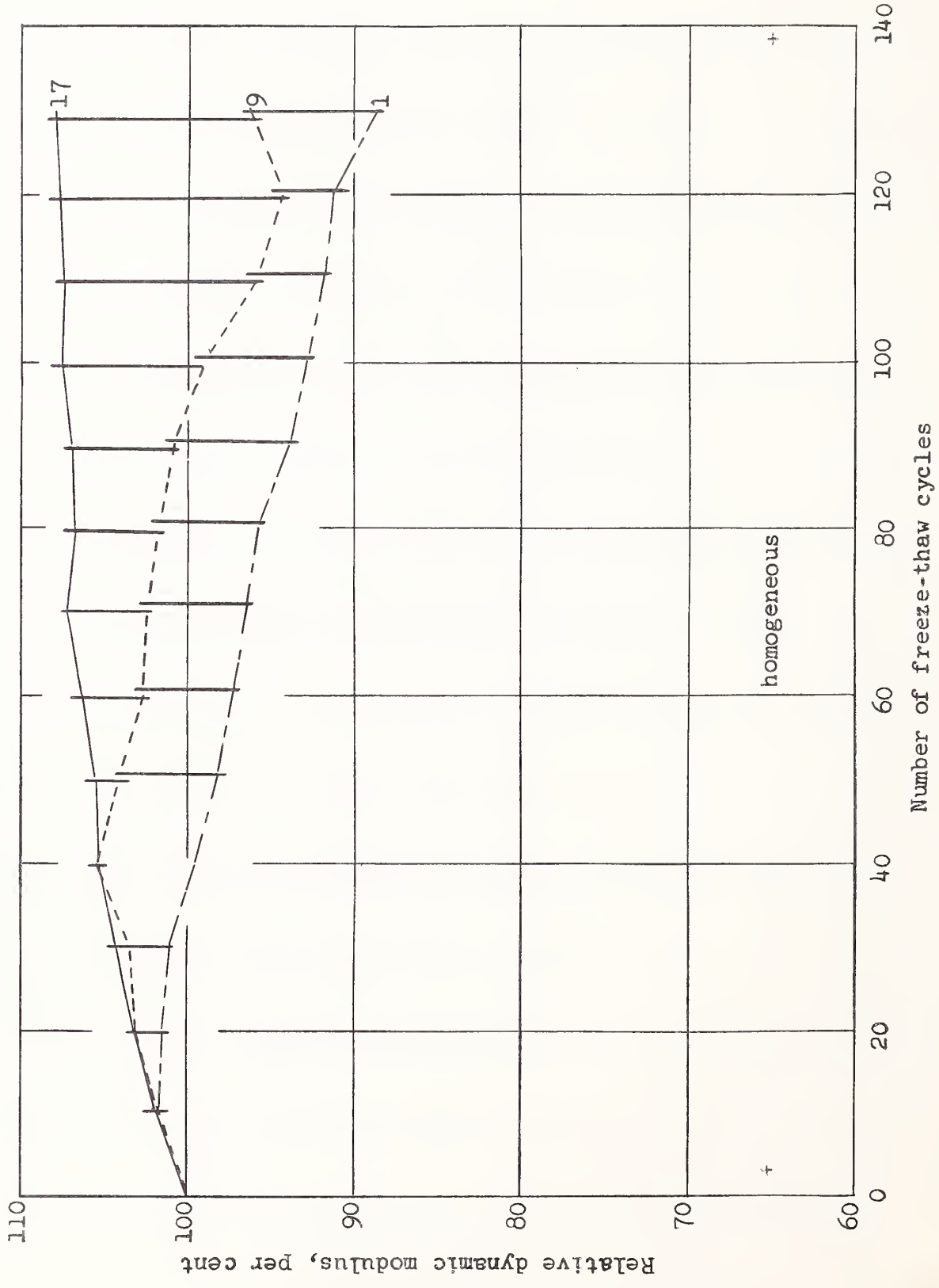

Fig. 10. Results of Duncan tests of mean transformed relative dynamic moduli for treatment comparison D. (All stresses, normal cure, water)

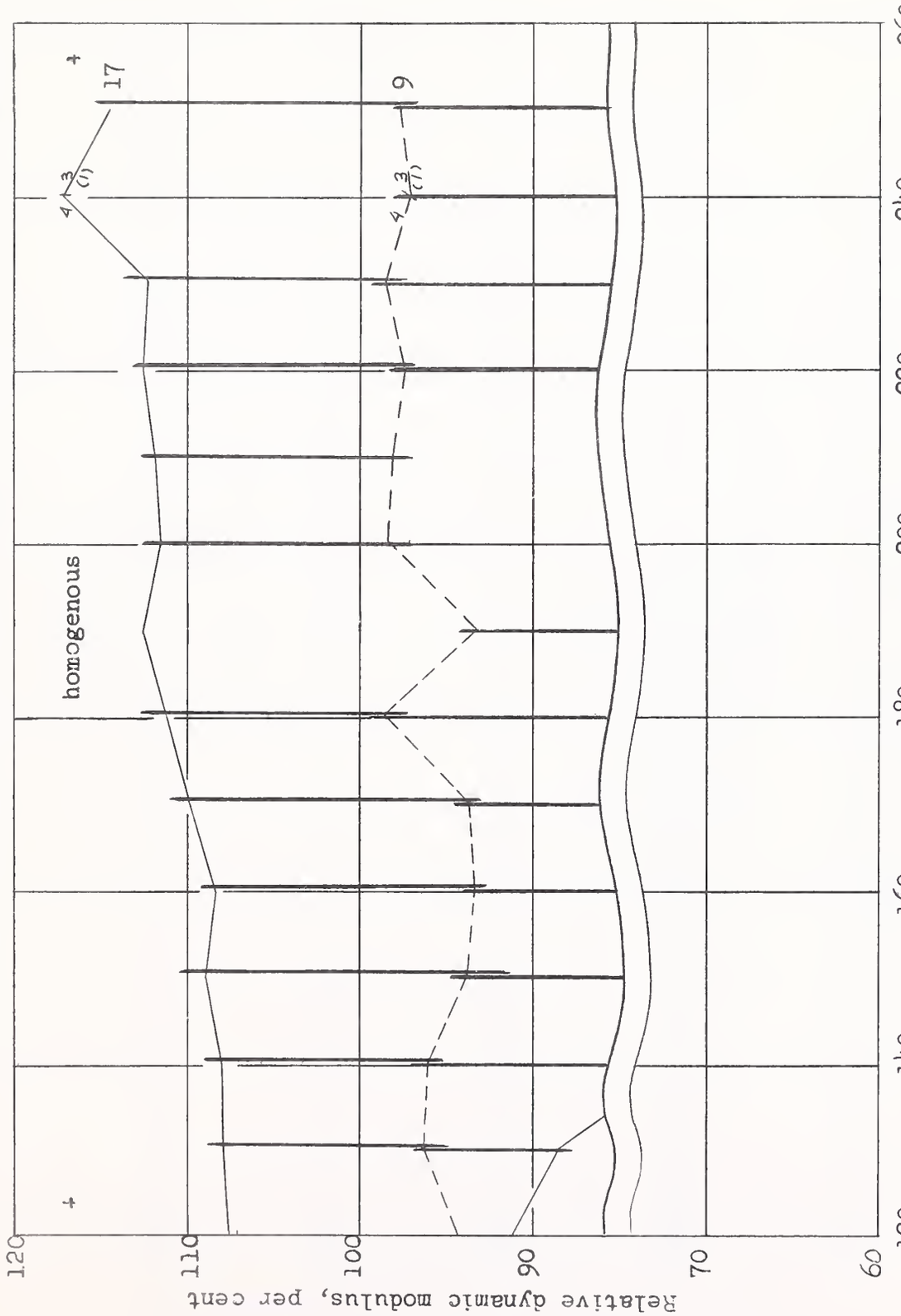

Fig. 10. (Cont.) Results of Duncan tests of mean transformed relative dynamic moduli for treatment comparison D. (All stresses, normal cure, water)

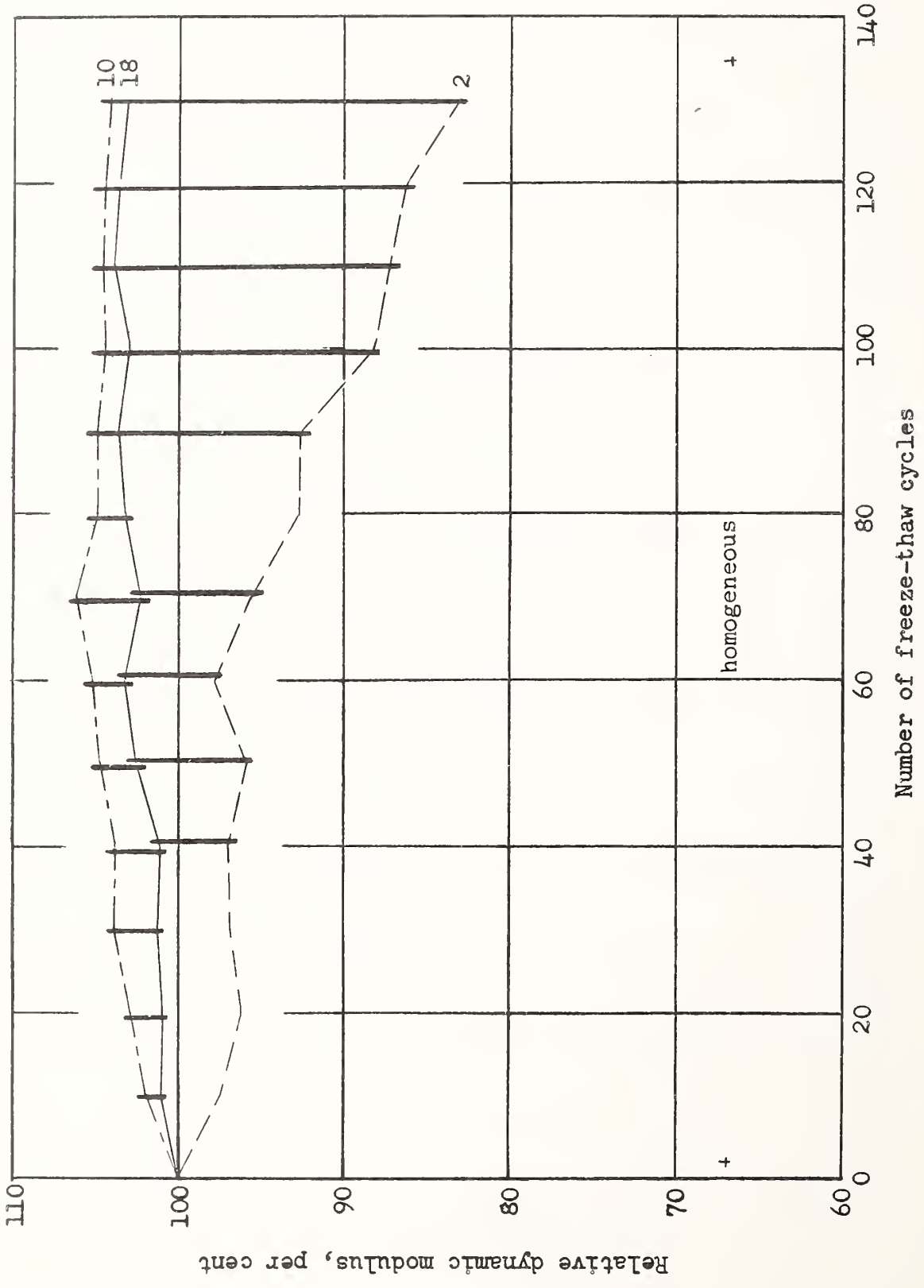

Fig. 11. Results of Duncan tests of mean transformed relative dynamic moduli for treatment comparison E. (All stresses, normal cure, chloride)

Fig. 11. (Cont.) Results of Duncan tests of mean transformed relative dynamic moduli for treatment comparison E. (All stresses, normal cure, chloride)

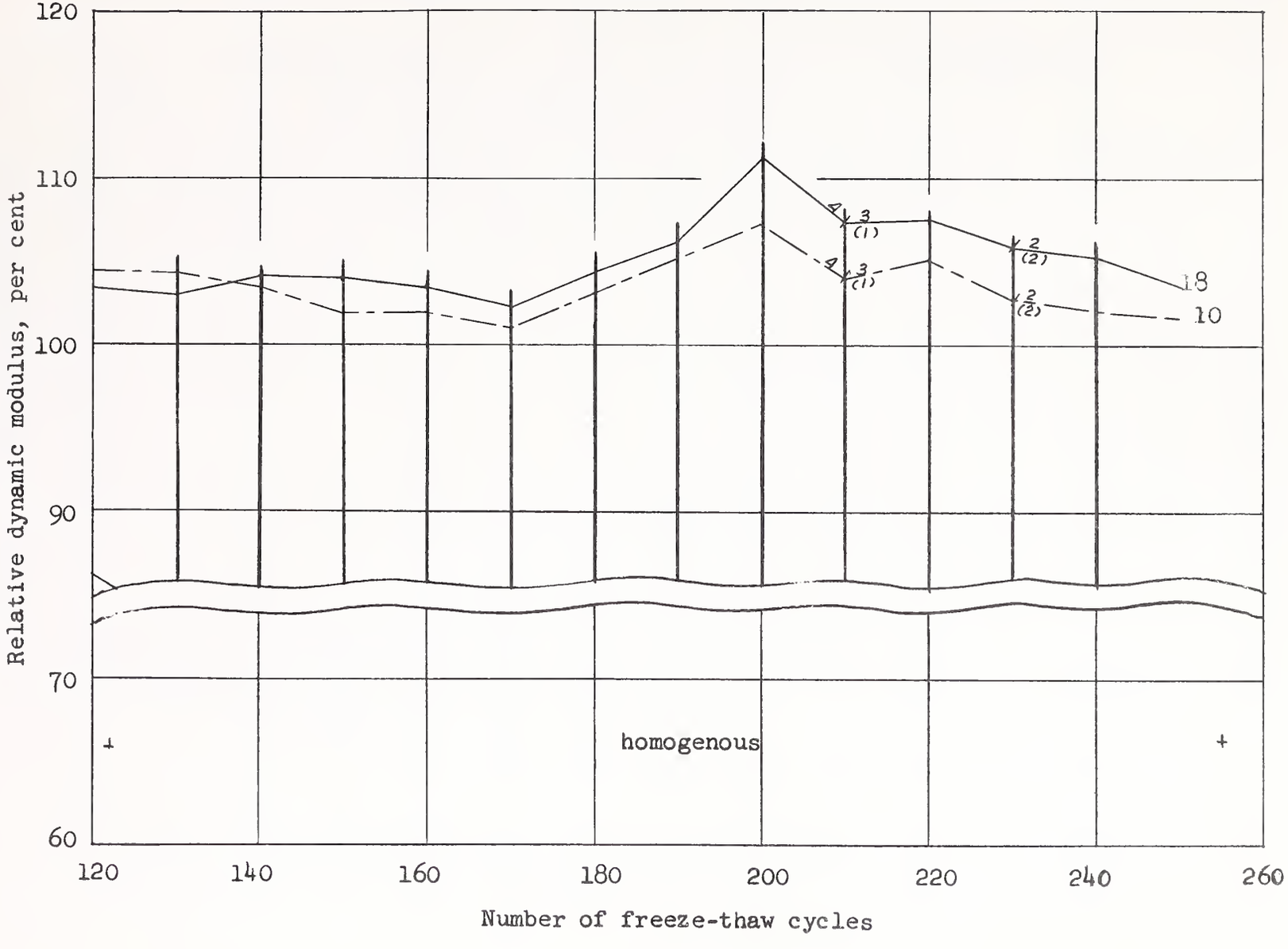

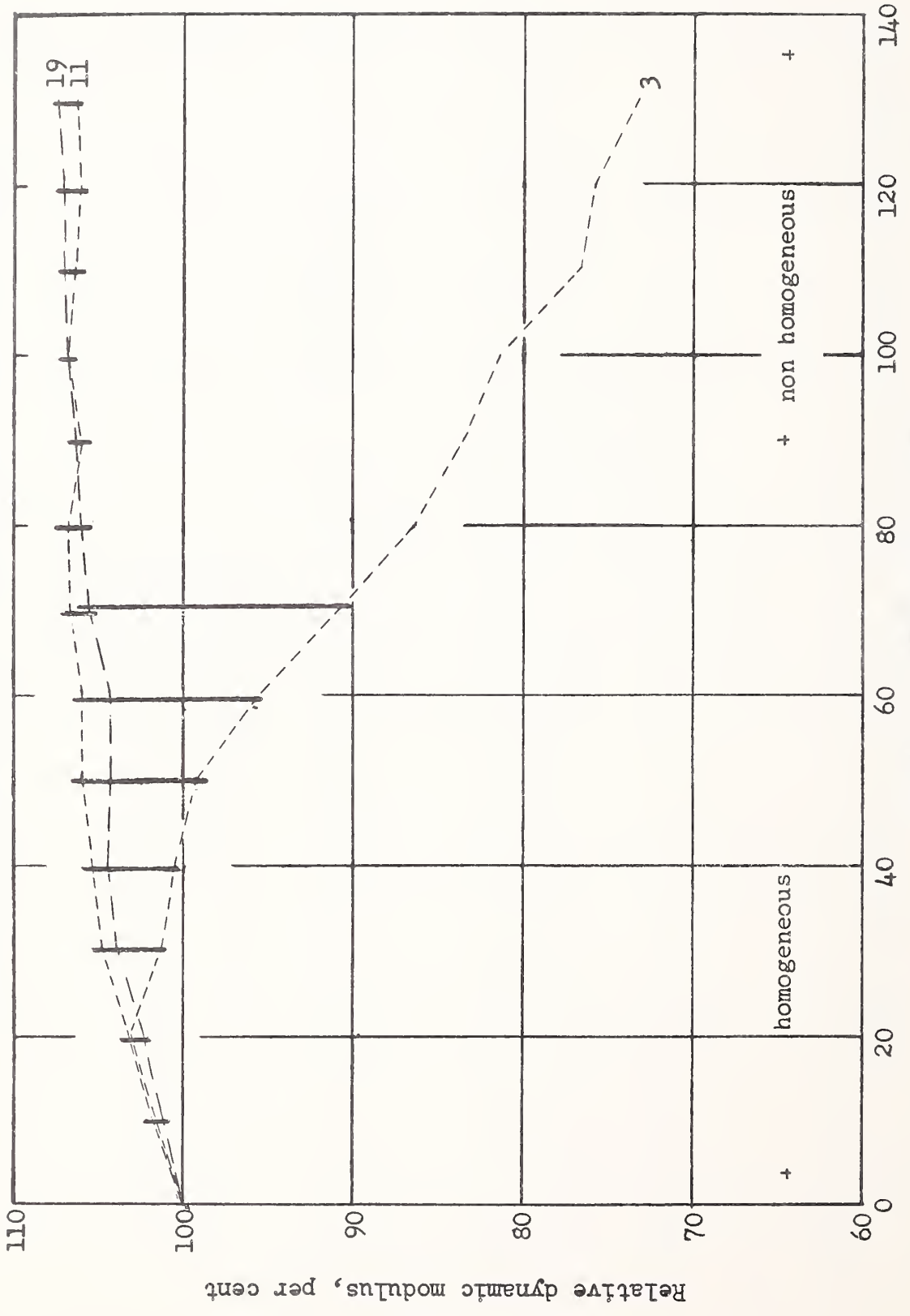

Fig. 12. Results of Duncan tests of mean transformed relative dynamic moduli for treatment comparison F. (All stresses, steam cure, water)

Fig. 12. (Cont.) Results of Duncan tests of mean transformed relative dynamic moduli for treatment comparison F. (All stresses, steam cure, water)

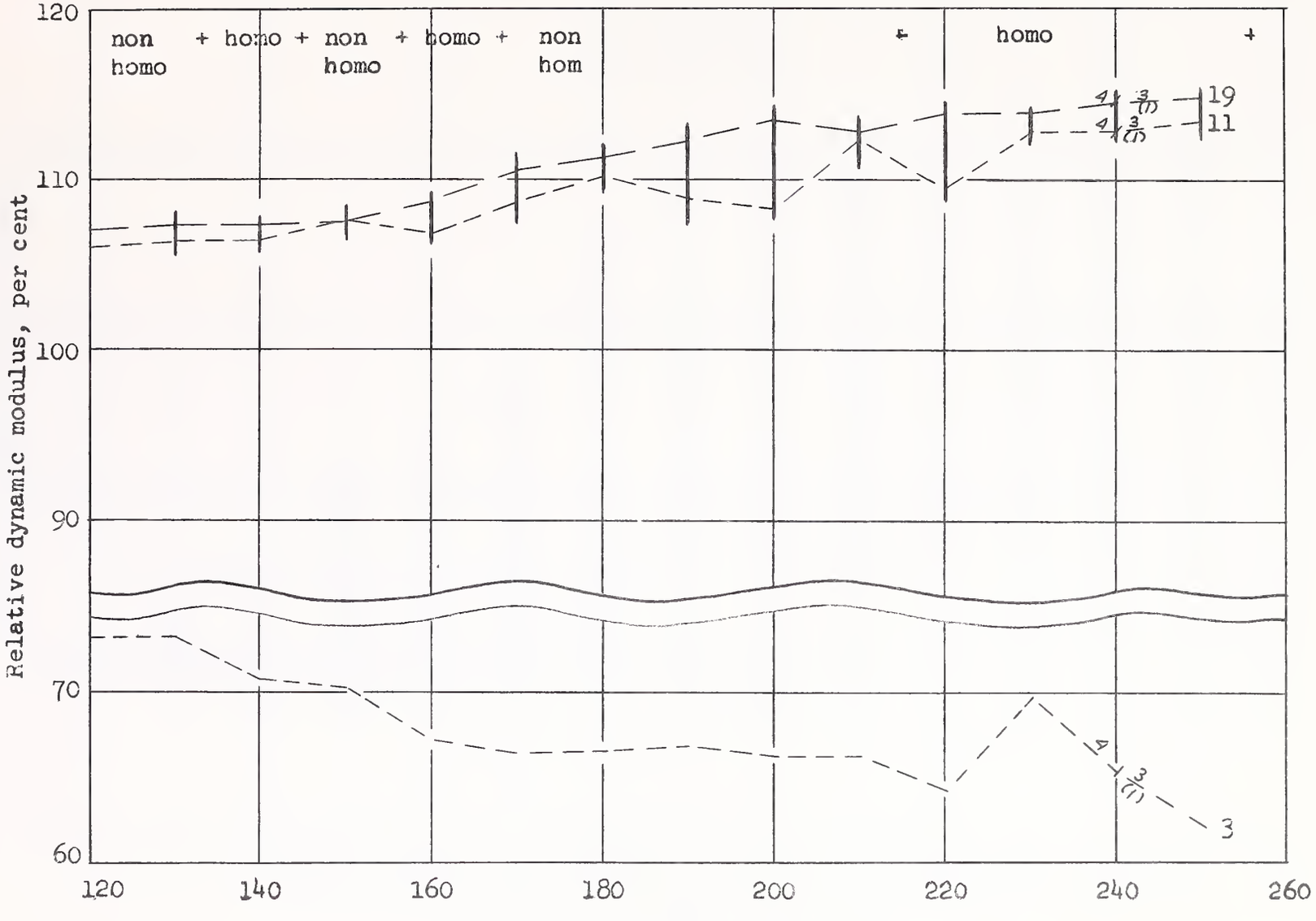

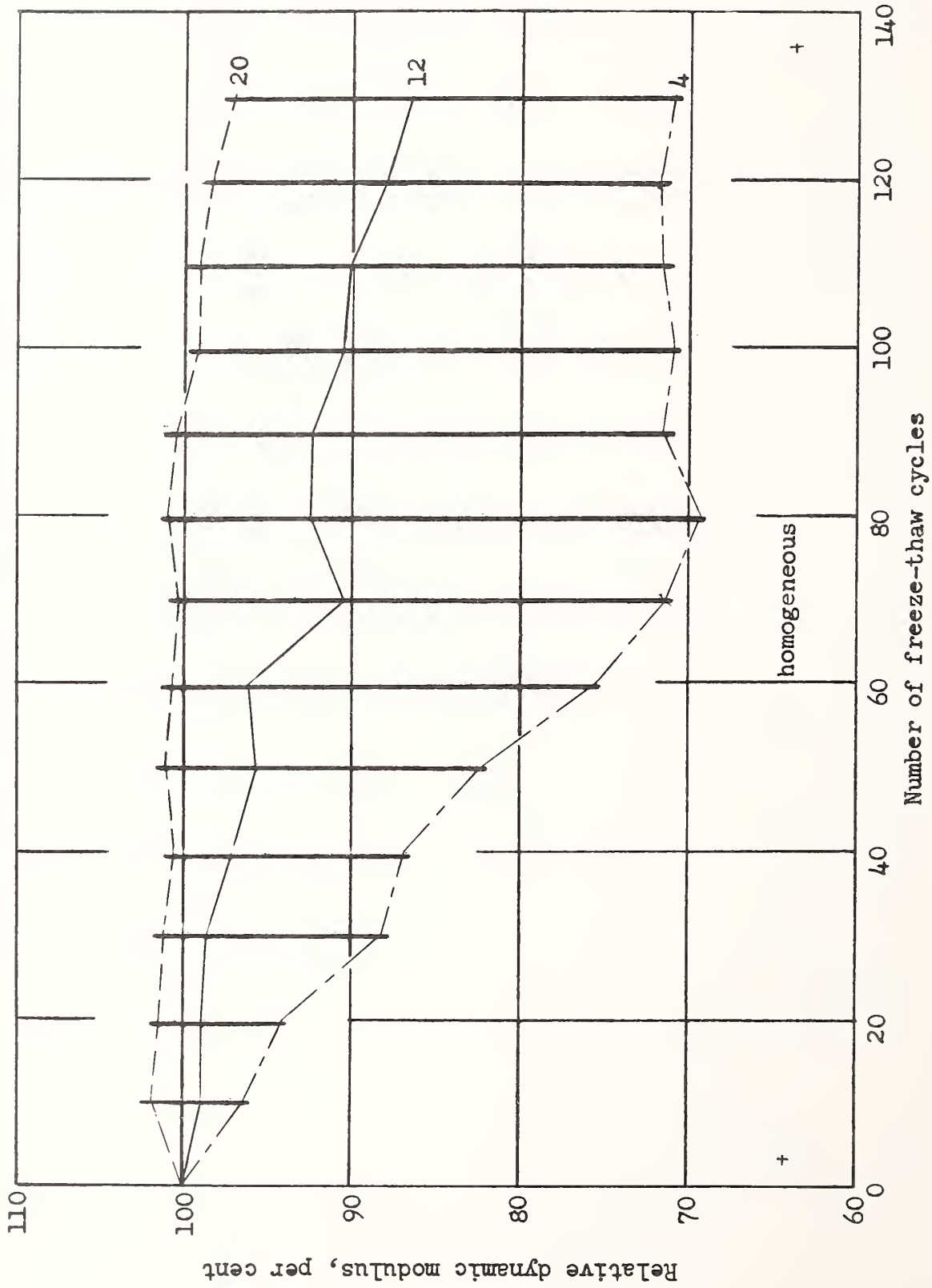

Fig. 13. Results of Duncan tests of mean transformed relative dynamic moduli for treatment comparison G. (All stresses, steam cure, chloride)

Fig. 13. (Cont.) Results of Duncan tests of mean transformed relative dynamic moduli for treatment comparison G. (All stresses, steam cure, chloride)

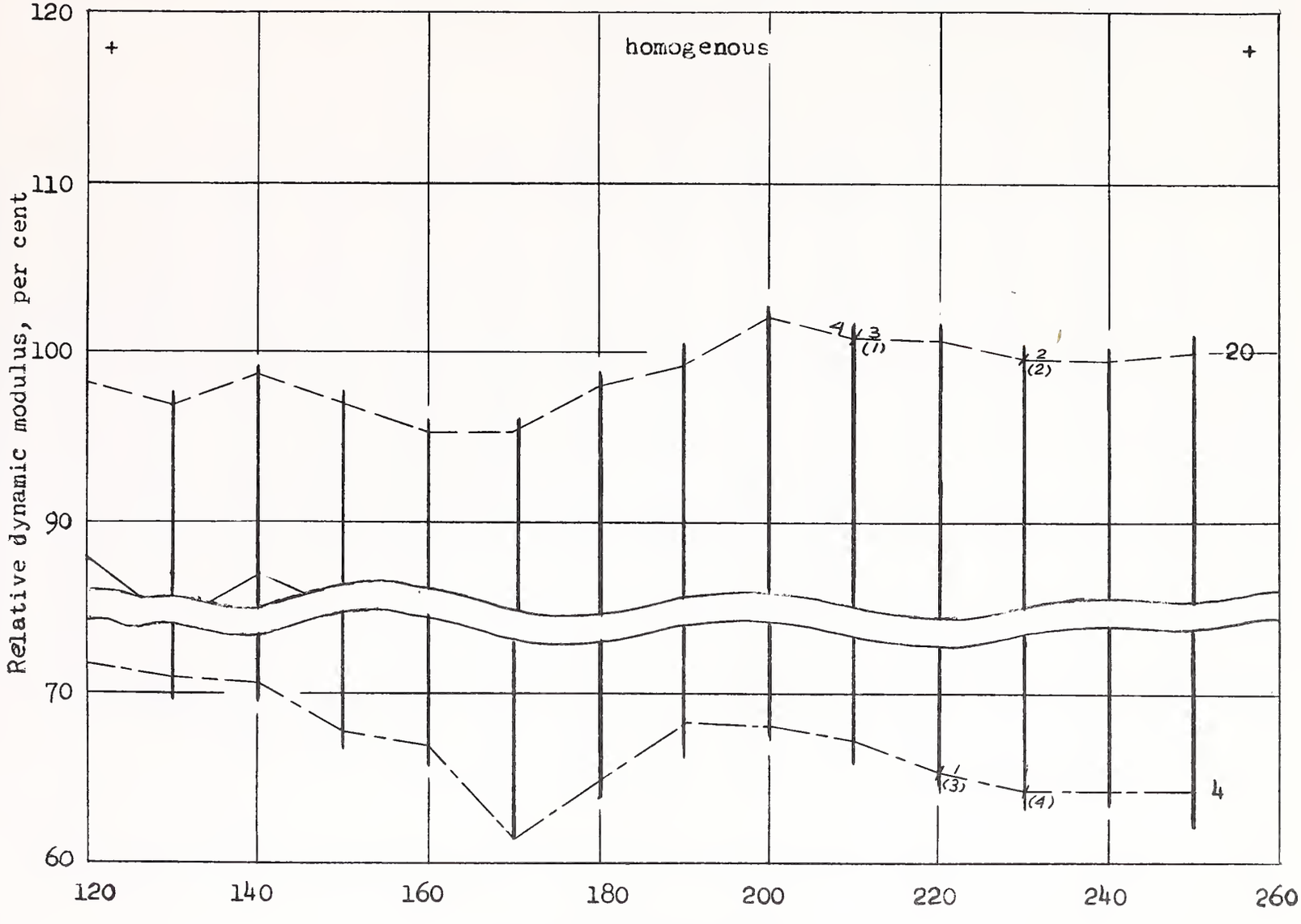

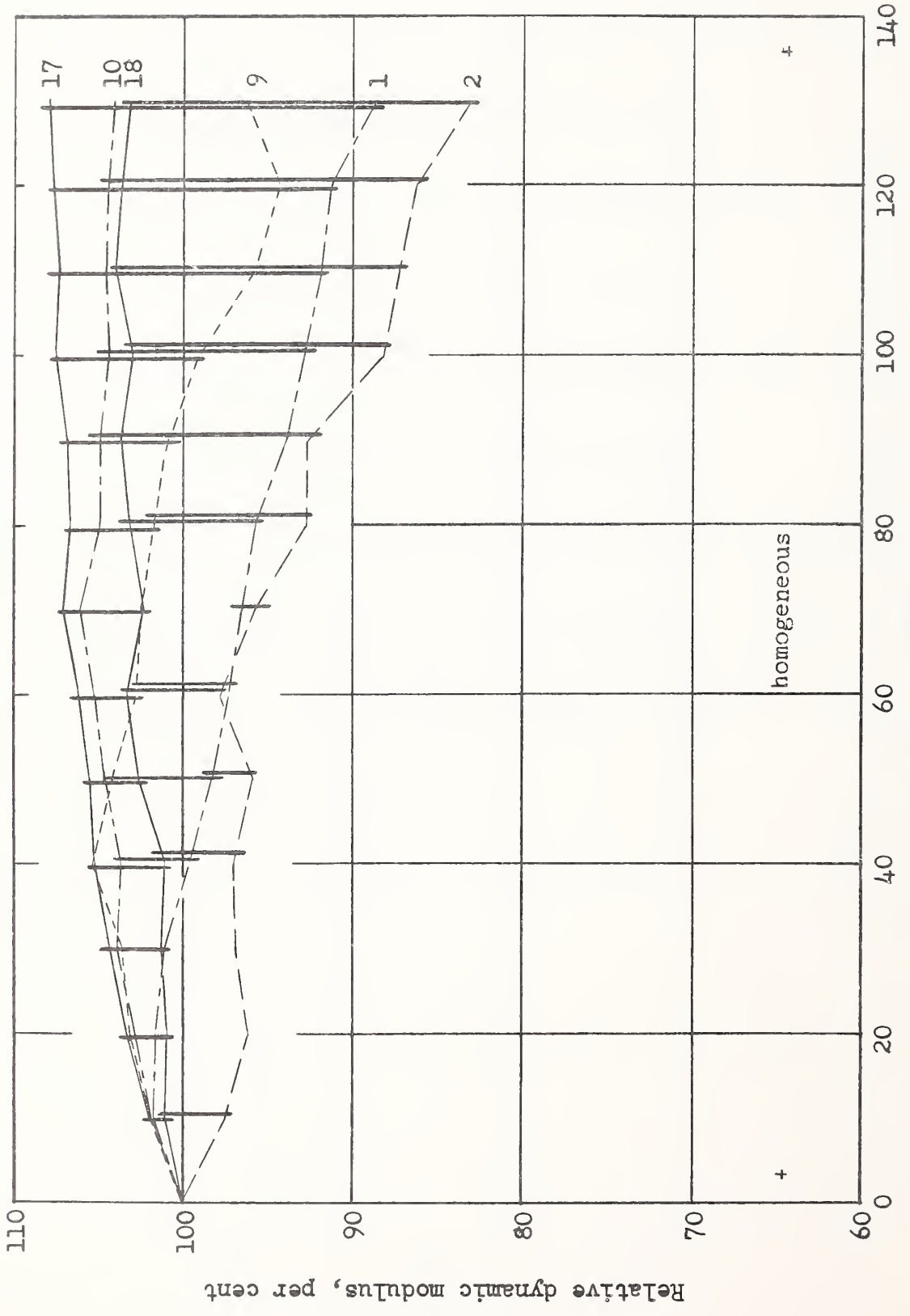

Fig. 14. Results of Duncan tests of mean transformed relative dynamic moduli for treatment comparison H. (All stresses, normal cure, both W & C)

Fig. 14. (Cont.) Results of Duncan tests of mean transformed relative dynamic moduli for treatment comparison H. (All stresses, normal cure, both W&C)

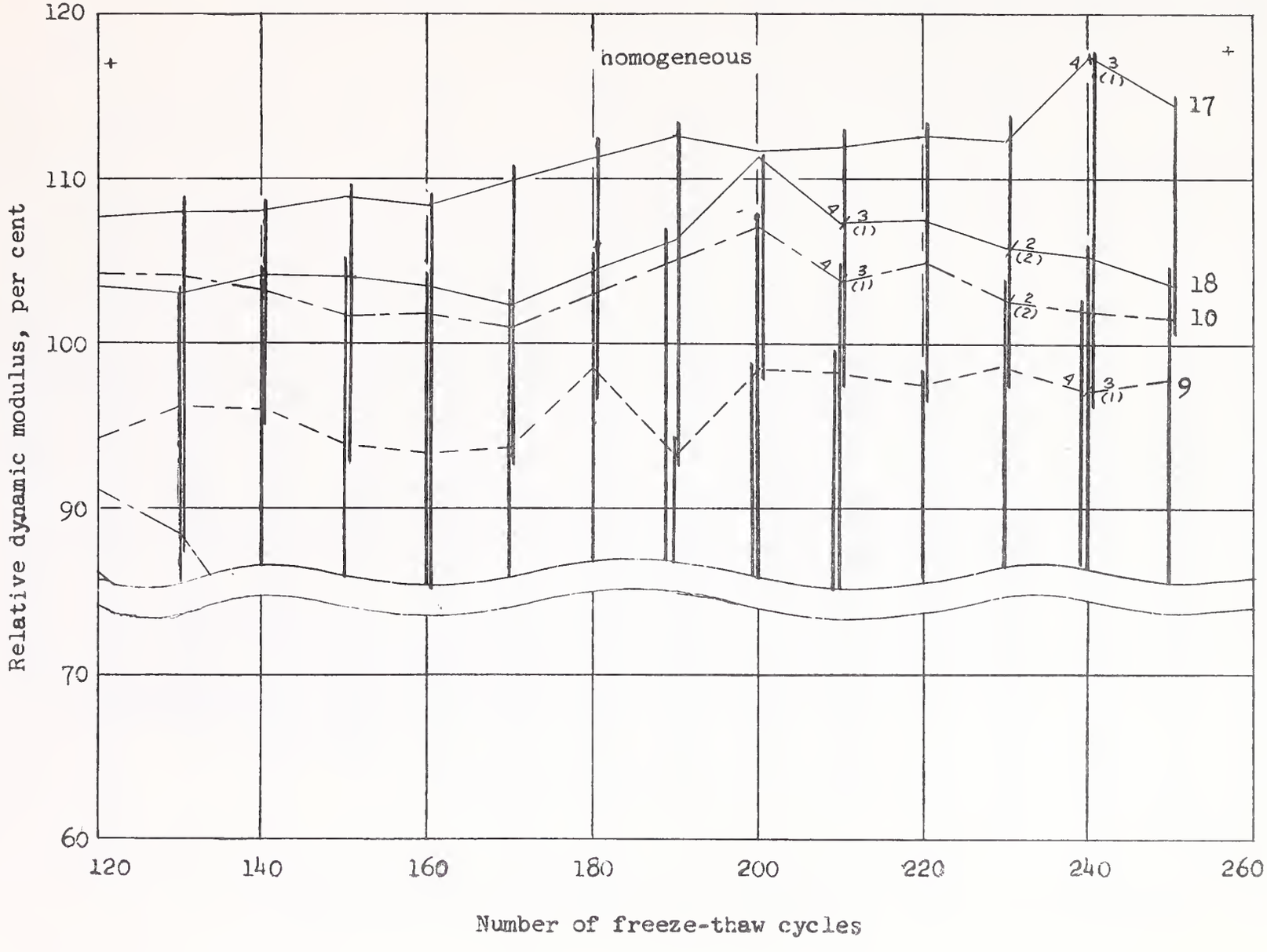

Fig. 15. Results of Duncan tests of mean transformed relative dynamic moduli for treatment comparison I. (All stresses, steam cure, both W & C)

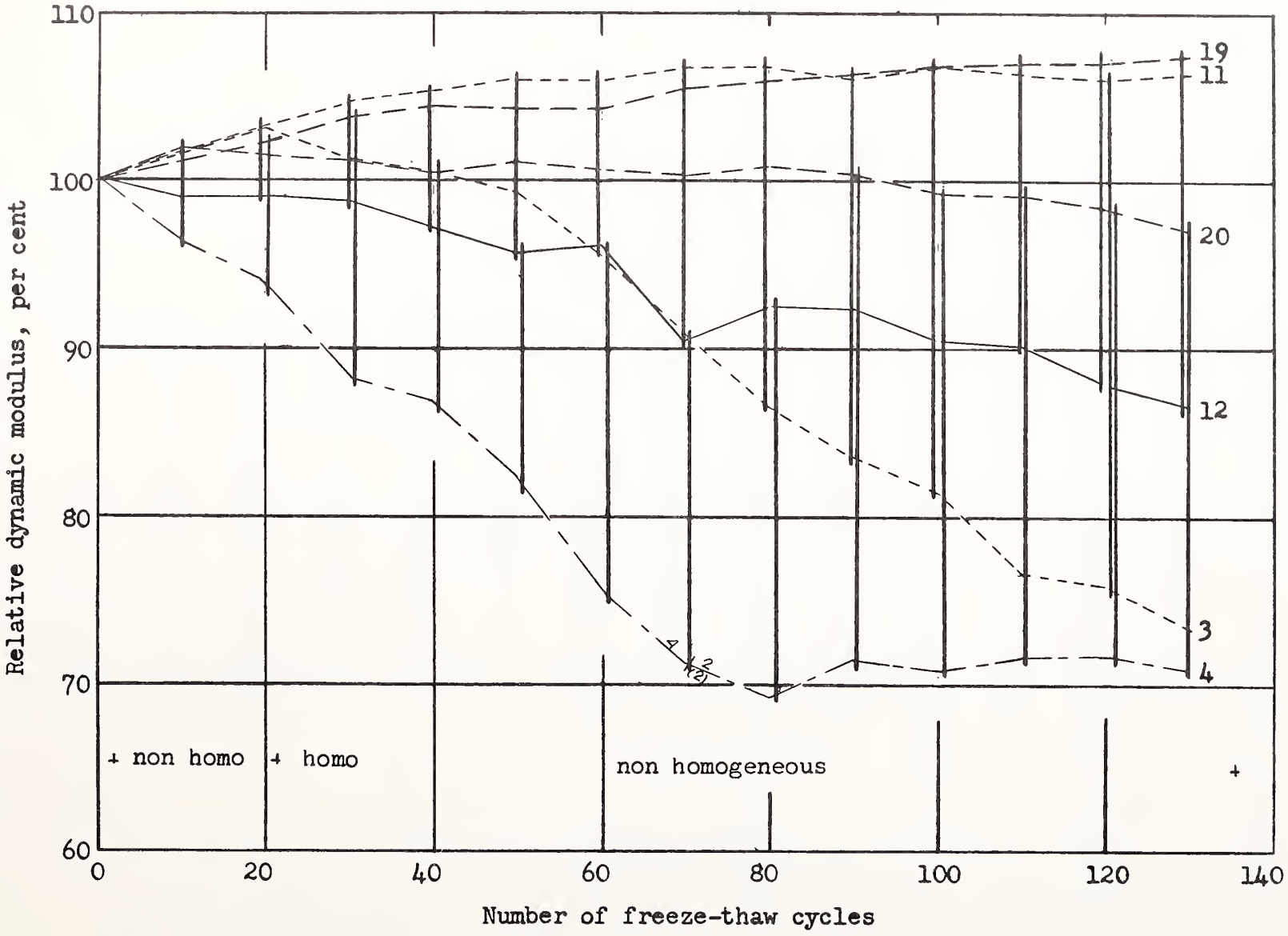

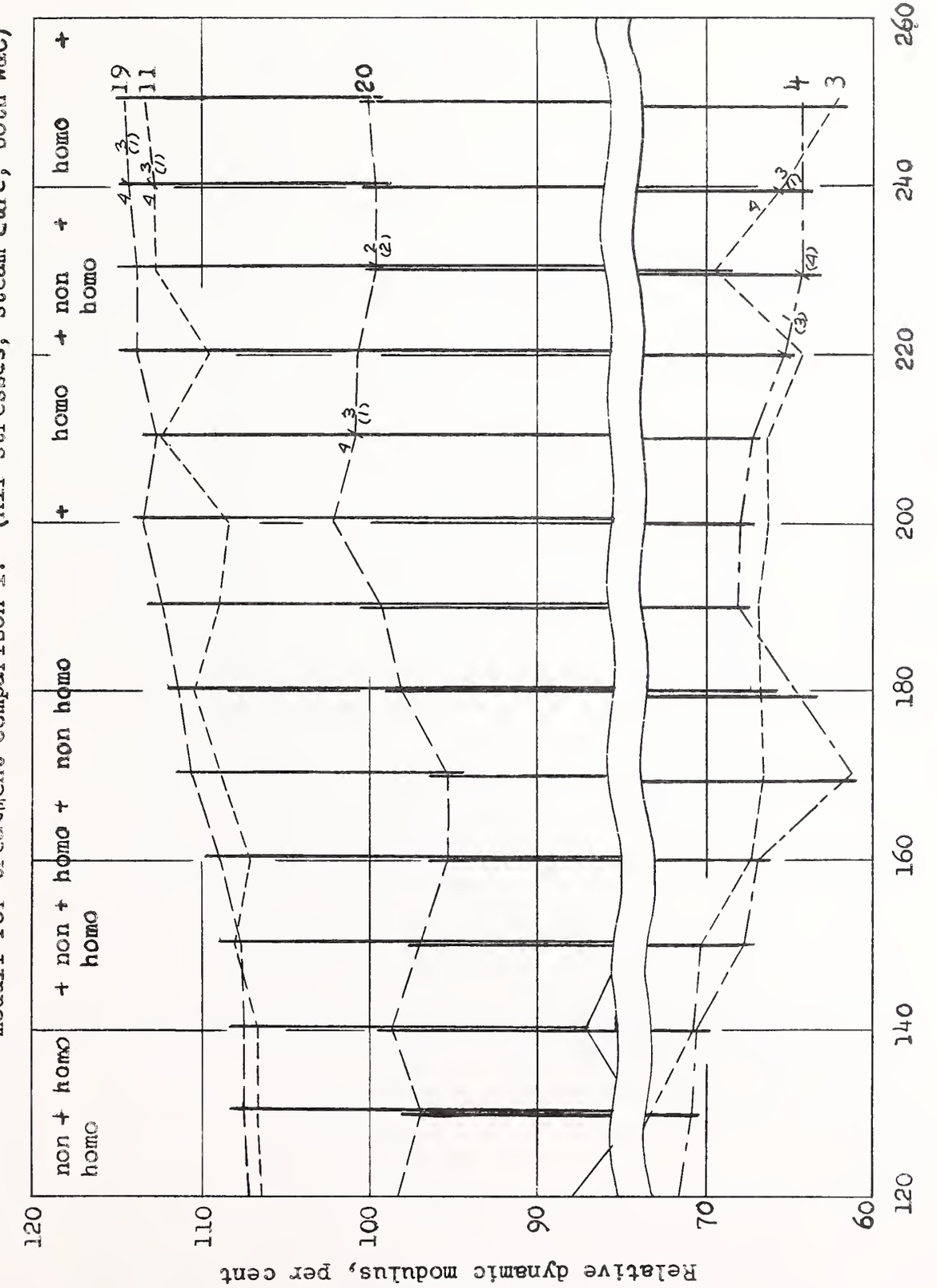

Fig. 15. (Cont.) Results of Duncan tests of mean transformed relative dynamic moduli for treatment comparison I. (All stresses, steam cure, both W&C)

TABLE IV

RESULTS OF BARTLETT TESTS OF
ADJUSTED WEIGHT CHANGES

No. of F/T cycles	Comparison								
	A	B	C	D	E	F	G	H	I
10	n.s.	n.s.	n.s.	n.s.	n.s.	n.s.	n.s.	n.s.	n.s.
30	n.s.	n.s.	n.s.	n.s.	n.s.	n.s.	n.s.	n.s.	n.s.
50	n.s.	n.s.	n.s.	n.s.	n.s.	n.s.	n.s.	n.s.	n.s.
70	n.s.	n.s.	n.s.	n.s.	n.s.	n.s.	n.s.	n.s.	n.s.
90	n.s.	n.s.	n.s.	n.s.	n.s.	n.s.	n.s.	n.s.	n.s.
110	n.s.	n.s.	n.s.	n.s.	n.s.	n.s.	n.s.	n.s.	n.s.
130	n.s.	n.s.	n.s.	n.s.	n.s.	n.s.	n.s.	n.s.	n.s.
150	n.s.	n.s.	n.s.	n.s.	n.s.	n.s.	n.s.	n.s.	n.s.
170	n.s.	n.s.	n.s.	n.s.	n.s.	n.s.	n.s.	n.s.	n.s.
190	n.s.	n.s.	n.s.	n.s.	n.s.	n.s.	n.s.	n.s.	n.s.
210	n.s.	n.s.	n.s.	n.s.	n.s.	n.s.	n.s.	n.s.	n.s.
230	n.s.	n.s.	n.s.	n.s.	n.s.	n.s.	n.s.	n.s.	n.s.
250	*	n.s.	n.s.	n.s.	n.s.	n.s.	n.s.	n.s.	n.s.

Note: n.s. and * homogeneous variance
* * variance non-homogeneous

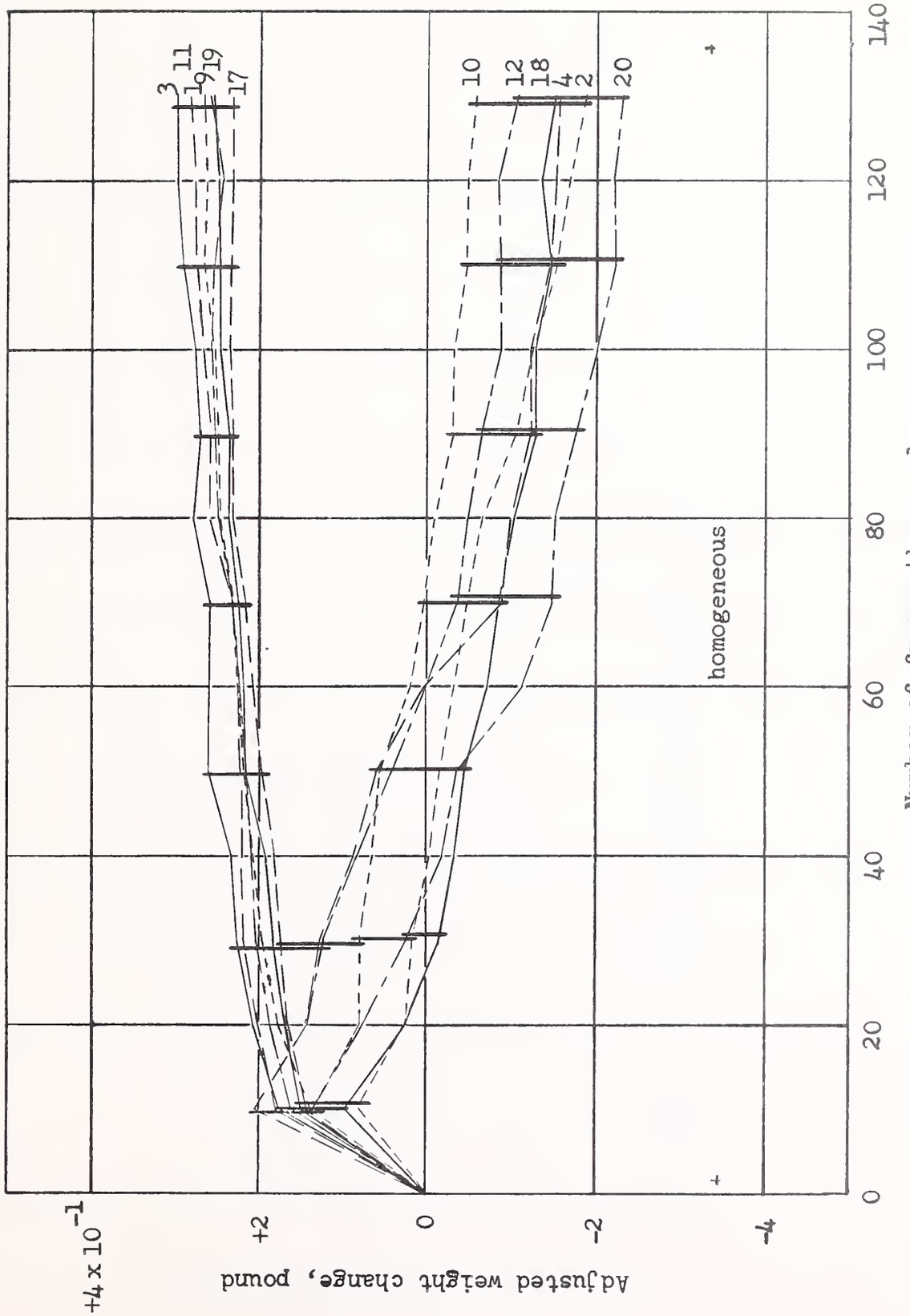

Fig. 16. Results of Duncan tests of mean adjusted weight changes for treatment comparison A. (All treatments)

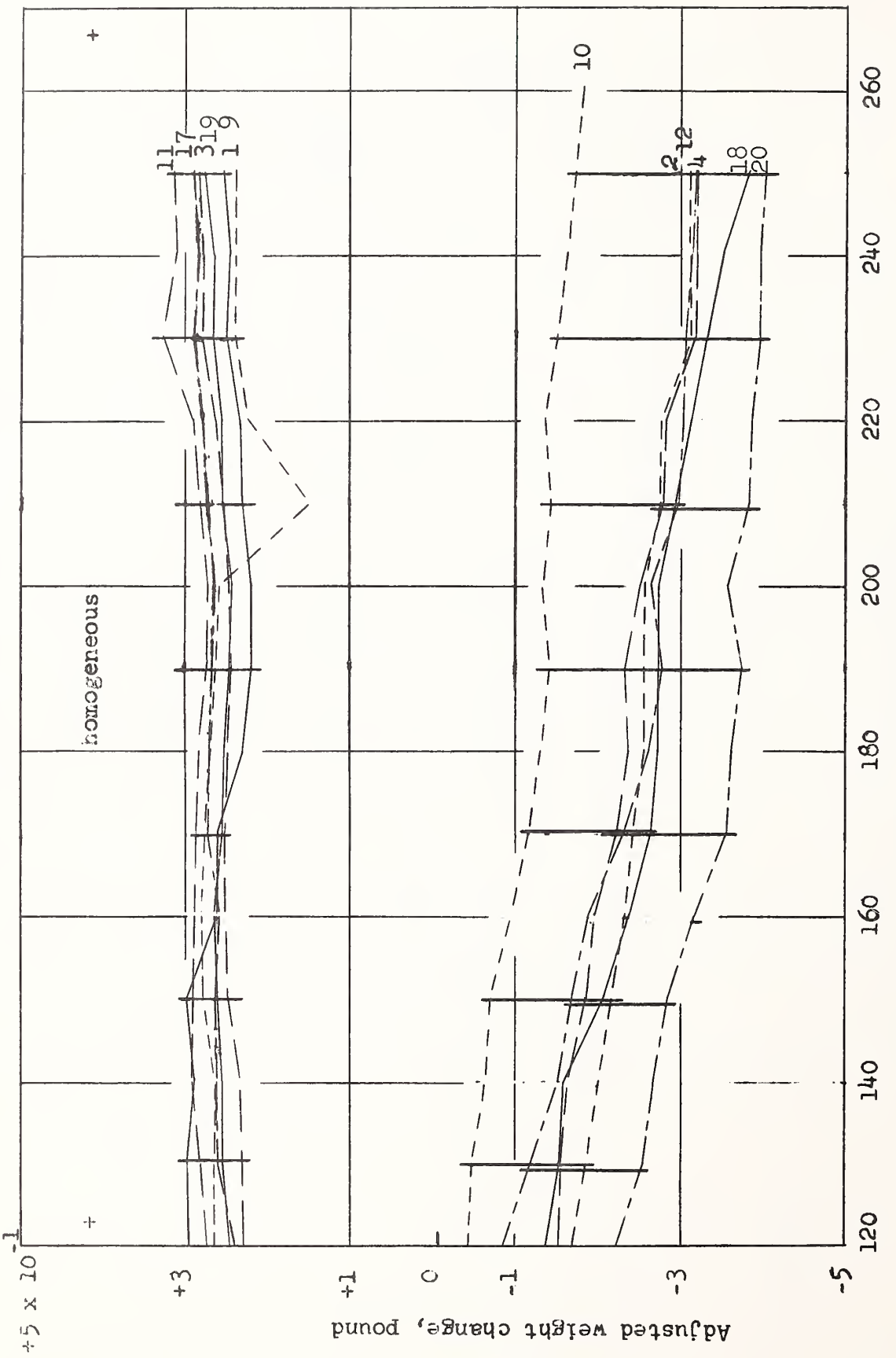

Fig. 16. (Cont.) Results of Duncan tests of mean adjusted weight changes for treatment comparison A. (All treatments)

TABLE V

RESULTS OF BARTLETT TESTS
OF LENGTH CHANGES

No. of F/T cycles	Comparison								
	A	B	C	D	E	F	G	H	I
10	n.s.	n.s.	n.s.	n.s.	n.s.	n.s.	n.s.	n.s.	n.s.
30	**	n.s.	**	n.s.	n.s.	n.s.	**	n.s.	**
50	**	n.s.	**	n.s.	n.s.	n.s.	**	n.s.	**
70	**	*	**	*	n.s.	*	**	**	**
90	**	*	**	n.s.	*	n.s.	**	**	**
110	**	**	**	*	*	*	**	**	**
130	**	**	**	*	*	*	*	**	**
150	*	**	**	*	**	**	n.s.	**	**
170	n.s.	n.s.	n.s.	n.s.	n.s.	n.s.	n.s.	n.s.	*
190	**	*	**	n.s.	**	*	*	**	**
210	**	*	**	n.s.	**	**	**	**	**
230	**	**	**	*	**	**	*	**	*
250	**	**	**	**	**	**	*	**	**

Note: n.s. and * homogeneous variance

** variance non-homogeneous

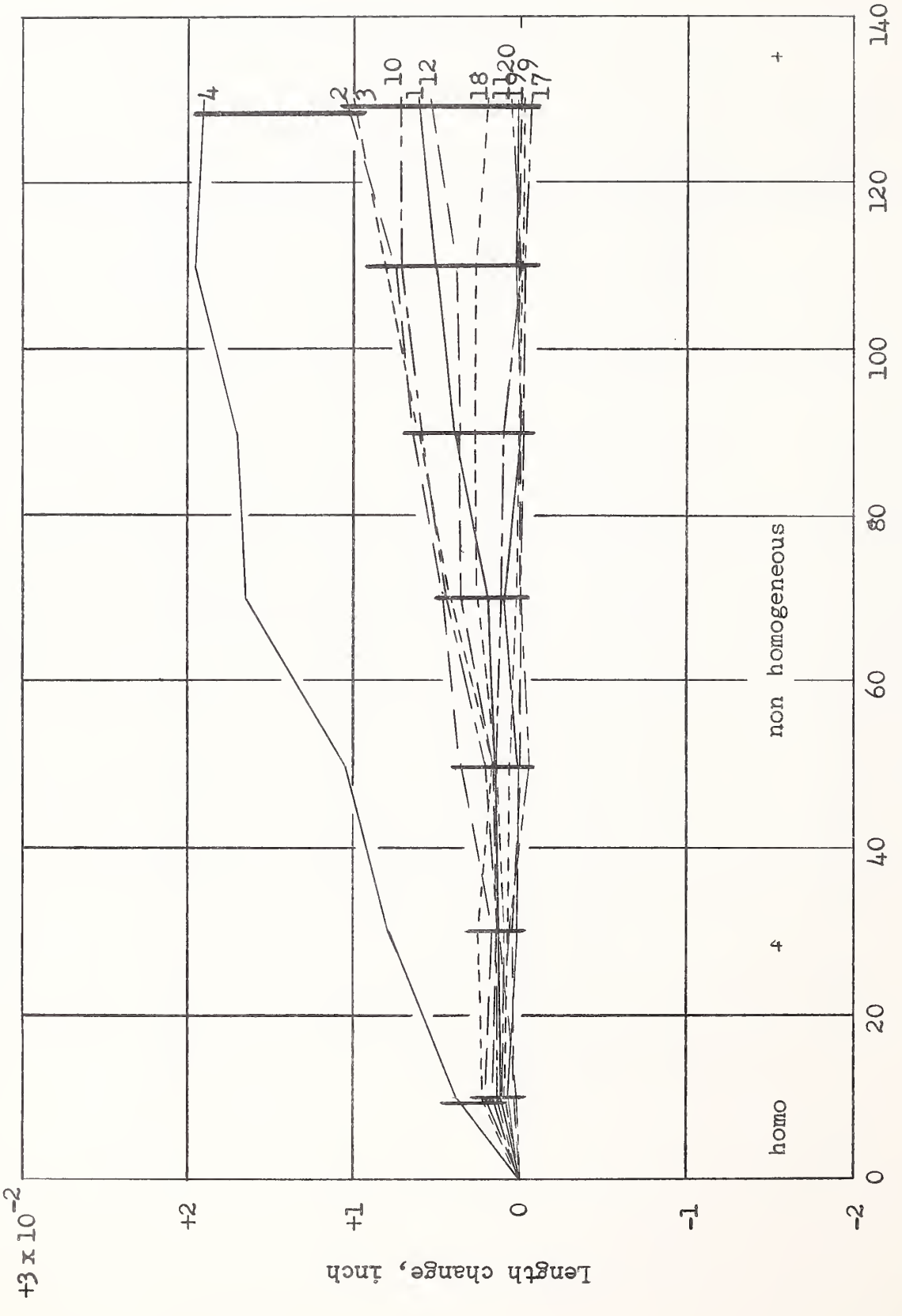

Fig. 17. Results of Duncan tests of mean length changes for treatment comparison A. (All treatments)

Fig. 17. (Cont.) Results of Duncan tests of mean length changes for treatment comparison A. (All treatments)

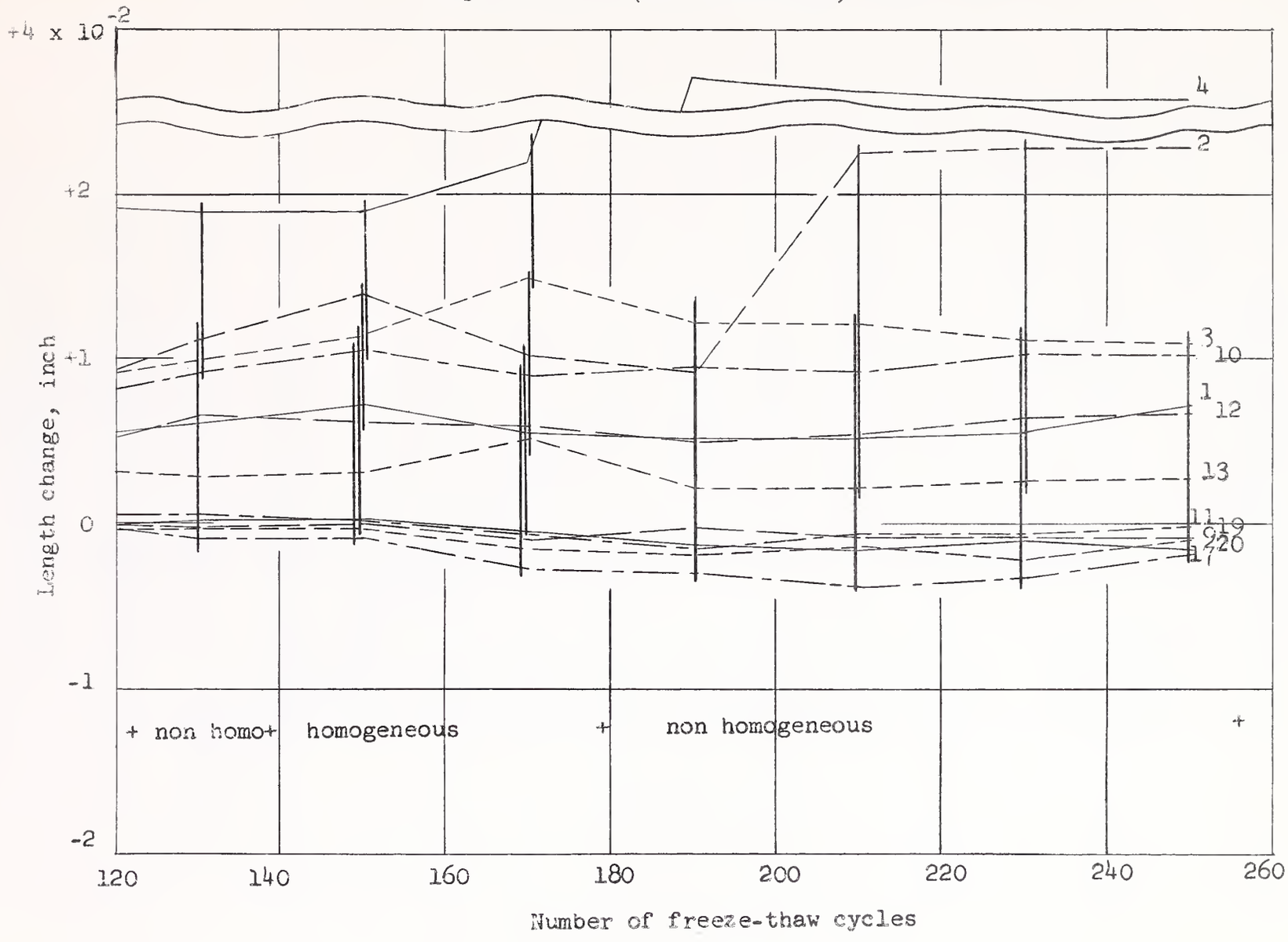

TABLE VI

RESULTS OF BARTLETT TESTS OF
SCALING WEIGHT LOSSES

No. of F/T cycles	Comparison		
	C	E	G
10	n.s.	n.s.	n.s.
30	n.s.	n.s.	n.s.
50	n.s.	n.s.	n.s.
70	n.s.	n.s.	n.s.
90	n.s.	n.s.	n.s.
110	n.s.	n.s.	n.s.
130	n.s.	n.s.	n.s.
150	n.s.	n.s.	n.s.
170	n.s.	n.s.	n.s.
190	n.s.	n.s.	n.s.
210	n.s.	n.s.	n.s.
230	n.s.	n.s.	n.s.
250	n.s.	n.s.	n.s.

Note: n.s. and * homogeneous variance

** variance non-homogeneous

Fig. 18. Results of Duncan tests of mean scaling weight losses for treatment comparison C. (All stresses, both cures, chloride)

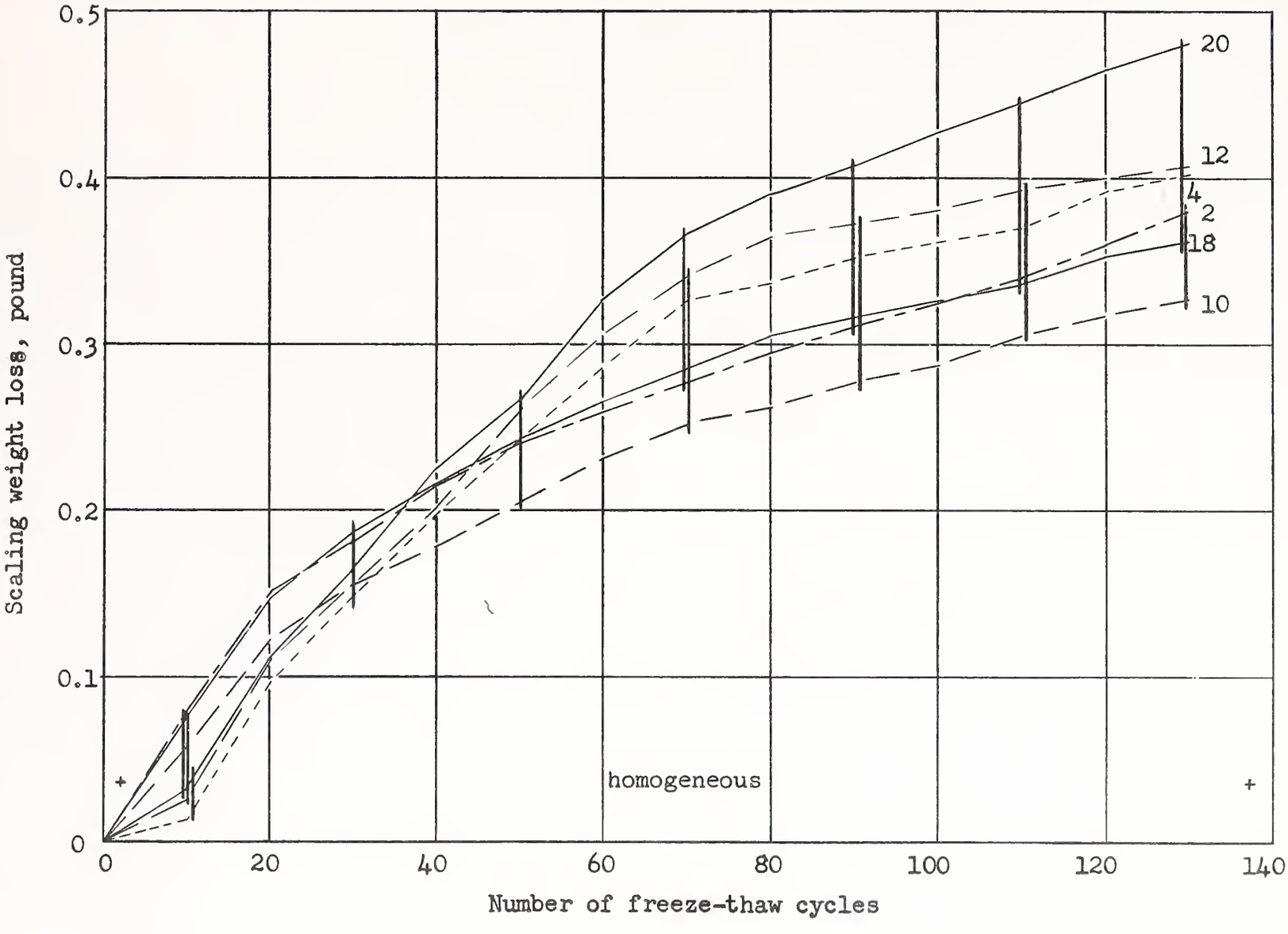

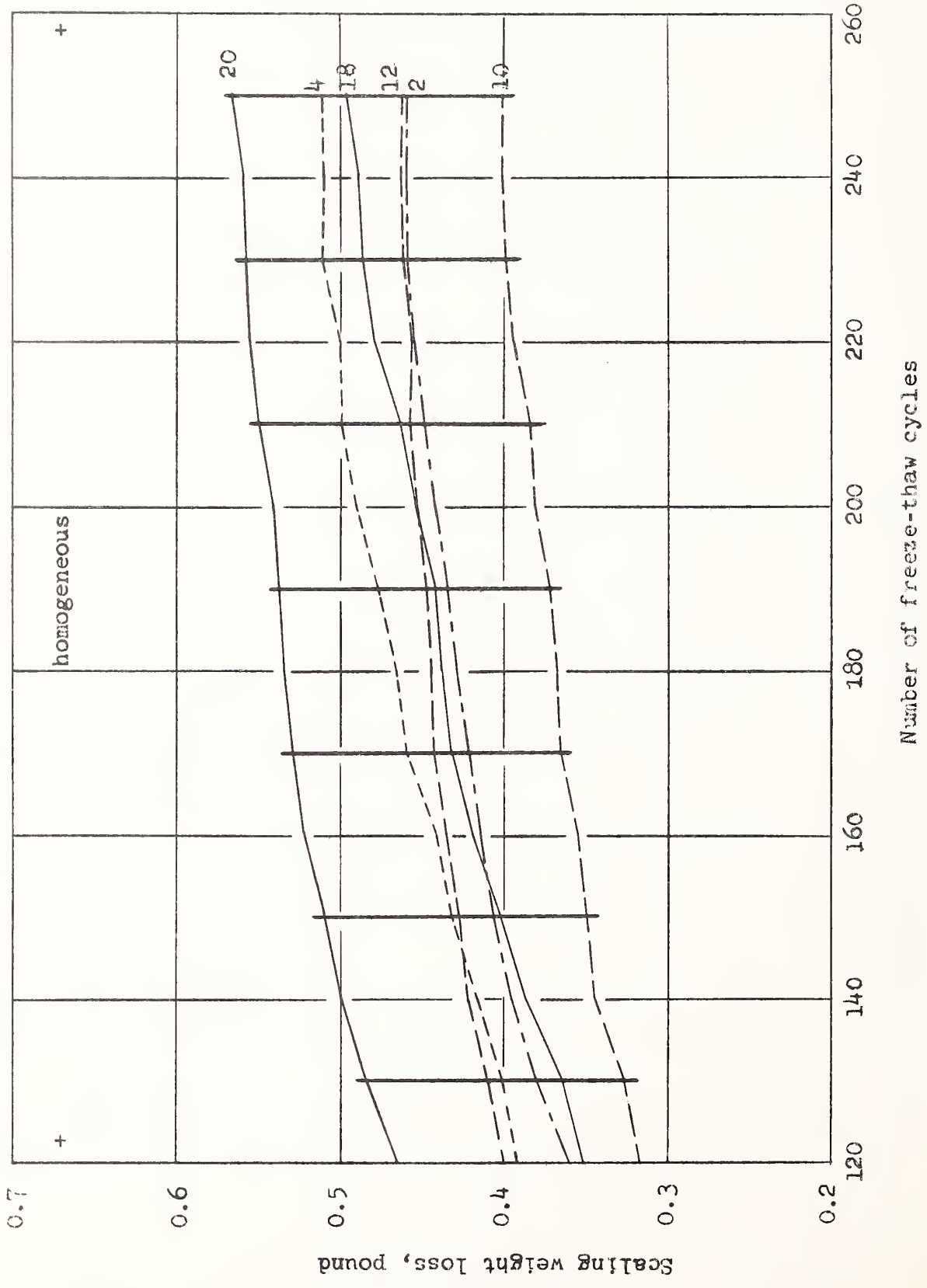

Fig. 18. (Cont.) Results of Duncan tests of mean scaling weight losses for treatment comparison C. (All stresses, both cures, chloride)

DISCUSSION

Statistical Comments

Statistical methods applied to experimental results are useful in the interpretation of those results; they are not an end in themselves. They furnish a frame of reference for judging the validity of a hypothesis, the limits of valid relationship according to a preconceived range of the statistical tool used or the effects allowed by the researcher, the overlapping experimental or response ranges of several similar effects, and simultaneous multiple comparisons. They allow some mode of measuring a comparison on a mathematical rather than an intuitive basis. However, this measurement is a function of how stringent were the originally chosen tolerances of acceptability. A knowledge of the tolerances and a common sense understanding of the physical tests performed are the real basis for interpreting statistical analyses.

The Bartlett test for homogeneity of variance is in essence a collective measure of the uniformity of data spread about the individual test means - in other words, the spread about the individual test mean values must be the same for all compared tests, within limits selected by the investigator, if the collective data is to be termed homogeneous. It is apparent that almost any population can be shown to be homogeneous if the acceptance level is set low enough or if the comparison samples are very few in number, and conversely, the higher the acceptance level or the greater the number of comparisons the greater will be the likelihood of non-homogeneity.

In relation to actual physical tests, scaling weight loss in water or chlorides for example, some tests might have more meaning if the uniformity of spread about the individual means is assured by a test such as Bartlett's. It would show that all samples were responding in nearly the same degree to water or to the chloride and thus a valid significance test could be applied. However, it might also imply non-dependence on stress level. Where stress level is being compared to the relative dynamic modulus, the homogeneity test might be of questionable value since a differential spread about the individual means is inherent in the notion that prestress level should affect the dynamic modulus and non-homogeneity supports the hypothesis.

Other interpretations are possible, such as laboratory control below the one percent significance level for mixing, casting, and curing or an insufficient number of replicates. These functions are undoubtedly reflected in a variance test, but given the samples and very closely controlled testing procedures, Figure 8 is an extreme example of variance designation alternating as the tests progressed. Presumably this reflects fluctuating individual mean dispersions and the sensitivity of the statistical tool which are not necessarily related to the preparatory work.

In any case the Duncan test requires homogeneous variance to be a valid test and the Bartlett ranges of homogeneity at least show where more reliance may be placed on the Duncan representations.

Both are shown in Figures 7 through 18 so qualitative interpretation can be made by the reader.

SCALING

Effect of Prestress

No statistical nor inferential evidence was found to show a relationship between scaling and level of compressive stress. This is most clearly shown by Figure 16 (mean adjusted weight) and Figure 18 (mean scaling weight loss) where the compression stress levels are randomly scattered.

Effect of Curing

Figure 18 illustrates a noticeable trend for steam curing to produce an improved initial scaling resistance. After 20 to 30 cycles this advantage disappeared, and at 130 cycles the trend had been completely inverted. On Figure 18 (continued) the relative treatment orders change, somewhat obscuring the trend and diminishing its importance.

Effect of Salt Solution

The effect of freezing and thawing ponded calcium chloride solution on non-air-entrained concrete is dramatic. As stated earlier, ponding was found to produce 5 to 10 times as much scaling as simply thawing ice with the solid salt. A relative measure between ponded chloride solution and water would be 100-200 to 1, as seen in the individual curves in Appendix C. The earlier preliminary

work also showed the sulfate solution to be practically harmless in scaling tests and thus responding similar to water, where the weight losses were negligible.

Relation between Scaling and Durability

From this study no apparent relationship between scaling and durability was found, except for the inferences that steam cured samples tended to be less durable and more susceptible to late scaling, and that chloride solutions were most severe in both usages: a minuscule amount in durability and tremendous amount in scaling.

DURABILITY

Effect of Prestress

The main relationship derived from the relative dynamic modulus vs freeze-thaw cycle comparison is that durability is stress dependent. This is statistically and qualitatively shown for the zero stress specimens and qualitatively implied for the other stress levels even though the level of stress is not definitive for the intensities used. A general ordering according to stress level is noticeable throughout the test period until at 250 cycles only two of the higher stresses are disordered.

Figure 7 (continued) for comparison A is the only figure losing useful detail in the hiatus. Here the order at 250 cycles is 3, 4, 1, 2, 12, 9, 20, 10, 18, showing that three of the four zero stress groups are significantly different from the higher stress groups.

No association between weight change and durability as a function of stress level is apparent in Figure 16. The pronounced difference in the effect of water and chloride solution will be discussed under scaling. However, it is noteworthy that magnitudes of weight change shown in this figure were the reason for using the modified equation when computing the relative dynamic moduli. The common assumption of constant weight would have distorted upward all moduli for treatments 2, 4, 10, 12, 18 and 20 as well as for those with increasing weights, and all figures reporting these treatments would have been unrealistically moderated.

Figure 17 (mean length changes) at 250 cycles shows an ordering tendency which supports durability as stress dependent function even though it cannot be proved so by this relationship.

Examination of the tested specimens and their mortar dams indicated that expansion restraint was probably one of the major durability contributions of prestressing and that the highly air-entrained dams were much more durable than non-air-entrained prestressed concrete.

Effect of Cure

While statistically unsupported, some other minor relationships or indications might be observed in Figures 7-15. Figures 8 and 9 (relative dynamic moduli) show an apparent tendency for the steam cured specimens to be less durable than the normally cured specimens. In Figure 16, (mean adjusted weight) there appears only a slight tendency for the chloride ponded specimens to show steam curing less durable than normal curing. In the water ponded portion of the

figure this is not confirmed.

Effect of Salt Solution

Comparison of the magnitudes of the relative dynamic modulus between Figures 10 and 11 and between Figures 12 and 13 show the chloride ponding to result in slightly lowered durability. Figures 14 and 15 support this bias and show it to better advantage since like cures are grouped and the solution effect order is more apparent.

No graphical comparison was made for the effect of sulfate solution. It will be recalled that the pilot study showed an increase of approximately 10% in relative dynamic modulus in 200 freeze-thaw cycles with ponded sulfate solution. On this basis it can be concluded that the sulfate solution was not materially different from water in its durability effects.

Effect of Permeability

No direct evidence of a permeability-durability relationship can be developed from the freeze-thaw series alone. Anticipating some of the results from the later section on permeability, an indirect inference can be shown. It has been stated that there exists an implication that steam curing lessens the durability. The permeability results also show trends for steam cured specimens to absorb more water than do normally cured specimens. Thus the argument can be made that higher permeability decreases durability.

Miscellaneous

The main study of scaling and durability was centered on the slab specimens and variations of the freeze-thaw environment. Specimens from other exposures were also examined for evidence of scaling and durability damage.

The wet-dry slab series produced some fine pattern-cracking after approximately 30 cycles but they never progressed beyond an initial stage. After 551 cycles of wetting and drying, the natural frequencies had increased slightly, an average of a few hundred cycles per minute, with no consistent stress relationship being apparent. The scaling value remained zero throughout the test.

The continuously submerged slab series gave no visible evidence of non-durability and the natural frequency increases varied approximately 200 cps, apparently inversely related to stress but the relationship was non-significant. During the entire 551 days of test no scaling developed.

While the mortar bars were primarily intended for the permeability investigation it is noteworthy that those bars submerged in the chloride solution showed no evidence of damage. There was no bar splitting due to rust products developing inward from the exposed ends of the strands; not even for those having 1/4 inch of mortar cover. The bars immersed in the sulfate solution differed from the chloride solution specimens only in that the corners of the bars were slightly eroded and rounded.

The permeability slabs showed no evidence of adverse durability or scaling effects. All solution penetration considerations will be covered in the following section.

CHAPTER IV

PERMEABILITY AND CORROSION - TEST RESULTS AND DISCUSSION

PERMEABILITY

TEST RESULTS

The primary tool for the permeability or fluid passage investigation was the prestressed slab series using a two-foot solution head in standpipes. The final program for this series is shown in the top portion of Figure 19. It will be noted that this diagram is similar to the durability and scaling program diagram and contains replicate slabs from the same four batches of concrete as were used in the previous program. The main difference is the treatment numbers assigned to the slabs and the prime marking of the particular comparisons made. Secondary studies sought evidence of fluid penetration from all other sources such as freeze-thaw, wet-dry, wet, and mortar bar specimens.

Standpipe Slabs

The data collected for this study were the periodic volumes of water added to the standpipes to maintain the two-foot solution head. The solutions were tap water and a 20,000 ppm calcium chloride solution. Evaporation losses were determined from uncut bottle standpipes interspersed among the test specimens. Computer processing of these data yielded the cumulative moisture additions, corrections for evaporation losses, and the net cumulative absorptions. These net absorptions were punched on data cards for the

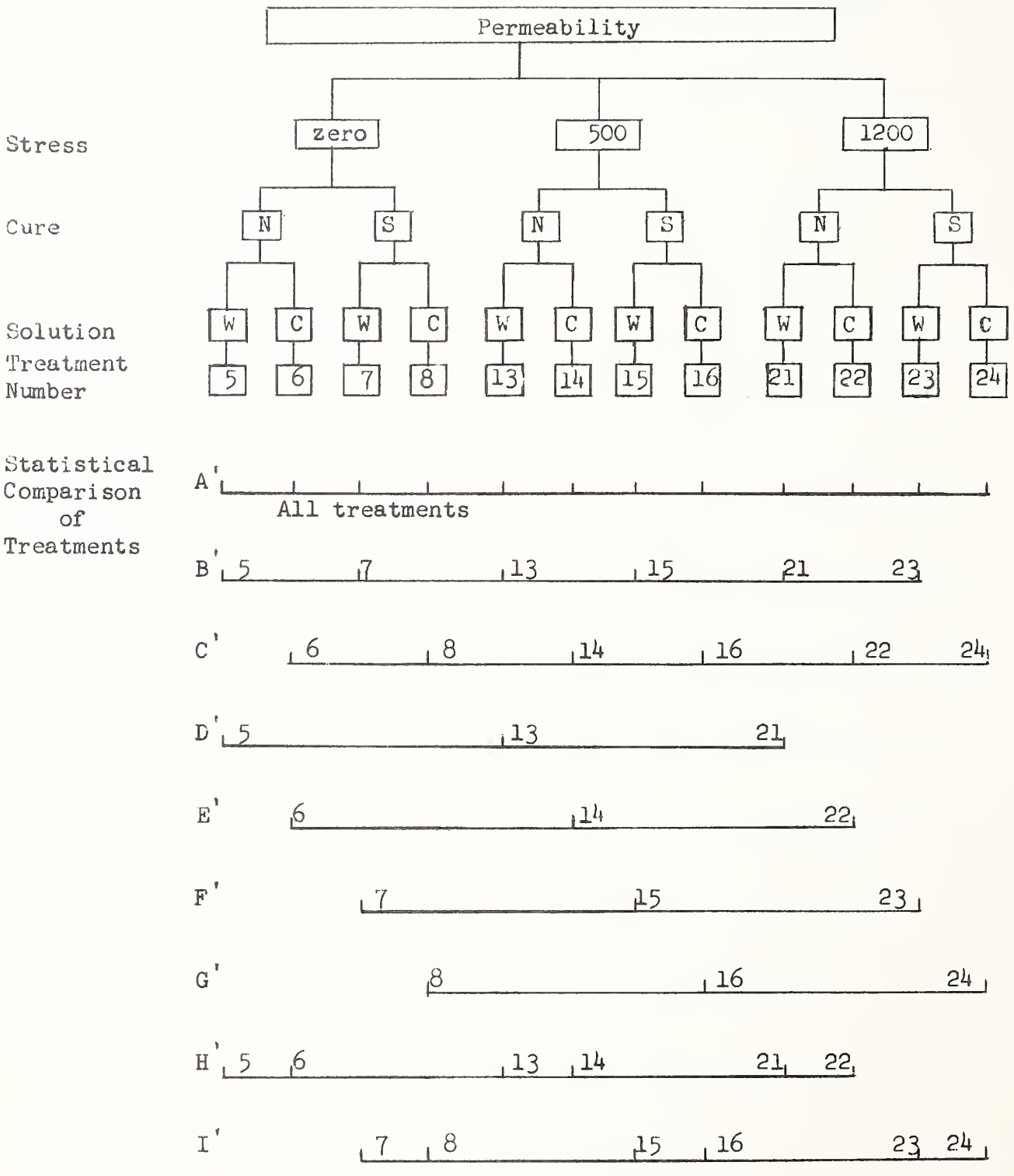

Fig. 19. Fluid Flow Treatments & Comparisons

individual slabs. Preliminary plotting of these data showed a marked linearity after an initial 40 day period for all slabs. For this reason the graphical comparisons, Figures 20 through 28, for the series uses the original data for the first 40 days and for the linear portions use two plots of the equations determined by linear regression analysis, one for 40 to 200 days and another from 200 to 400 days. The individual slab data are given in Appendix C Figures 87 through 98 and shows actual data points with the straight line dashes being the regression lines.

Only three replicates were used for treatments 5, 6, 7, 14, and 22 throughout the test, and for treatment 8 after 200 days. This was due to standpipe leakage in two slabs at the beginning of the test and the reserving of three slabs for a non-productive attempt to measure vapor pressure with a modified Bureau of Reclamation permeability apparatus, and the cutting of one slab for inspection.

An examination of the Appendix C figures indicated that the net absorptions at successive 40-day intervals would be a basis for comparing the treatments of Figure 19. Bartlett's and Duncan's tests were applied to the net absorption data and the results are shown in Table 7 and Figures 20 through 28.

TABLE VII

RESULTS OF BARTLETT TESTS
OF NET ABSORPTIONS

No. of days	Comparison								
	A'	B'	C'	D'	E'	F'	G'	H'	I'
40	**	ns	*	*	ns	ns	ns	*	ns
80	*	ns	*	*	*	ns	ns	**	ns
120	*	ns	ns	*	*	ns	ns	**	ns
160	*	ns	ns	*	*	ns	ns	**	ns
200	*	*	ns	*	*	ns	ns	**	ns
240	ns	ns	ns	ns	*	ns	ns	*	ns
280	ns	ns	ns	ns	ns	ns	ns	ns	ns
320	ns	ns	ns	ns	ns	ns	ns	ns	ns
360	ns	ns	ns	ns	ns	ns	ns	ns	ns
400	ns	ns	ns	ns	ns	ns	ns	ns	ns
440	ns	ns	ns	ns	ns	ns	ns	ns	ns

Note: n.s. and * homogeneous variance

** variance non-homogeneous

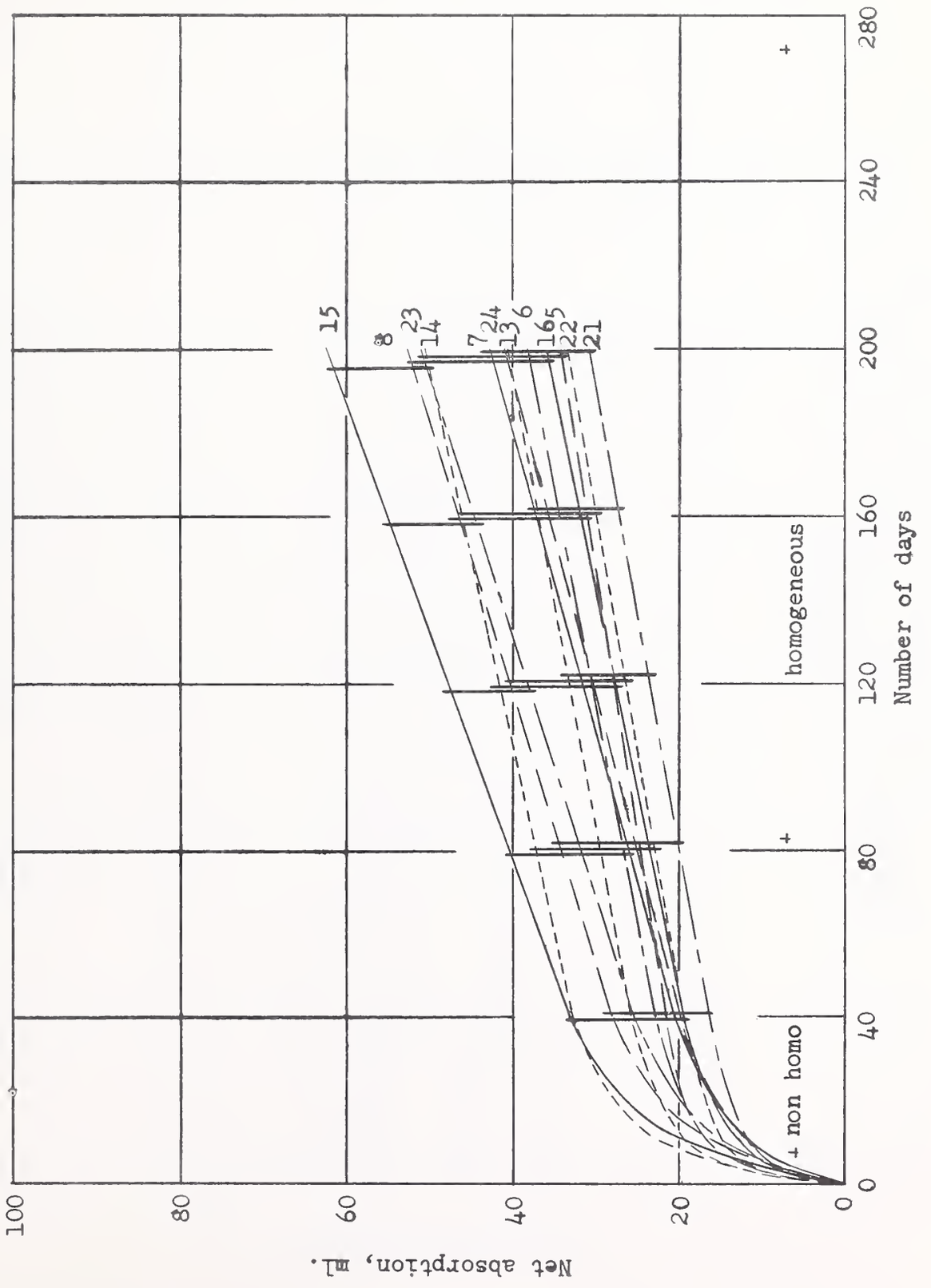

Fig. 20. Results of Duncan tests of mean net absorptions for treatment comparison A'. (All treatments)

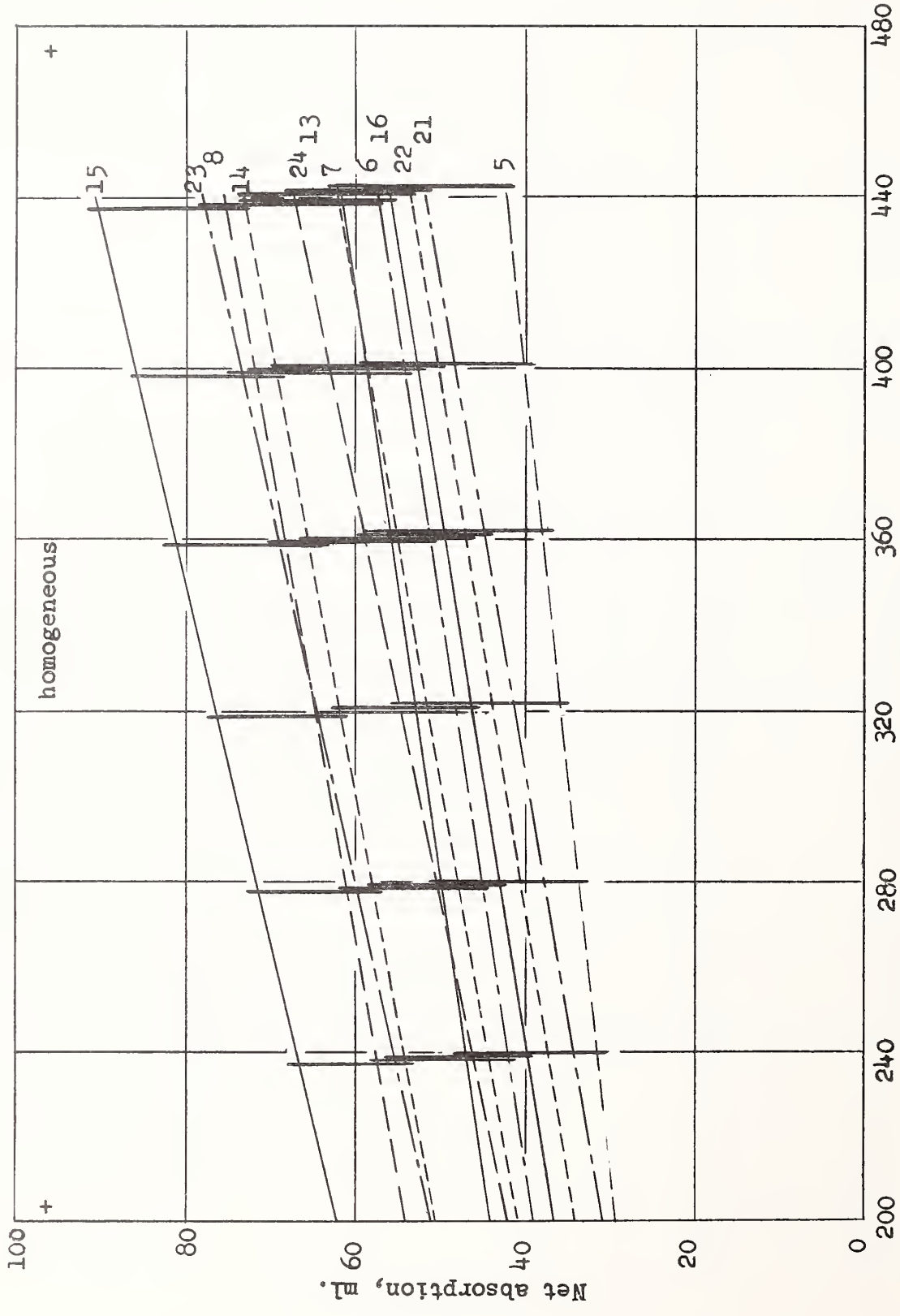

Fig. 20. (Cont.) Results of Duncan tests of mean net absorptions for treatment comparison A'. (All treatments)

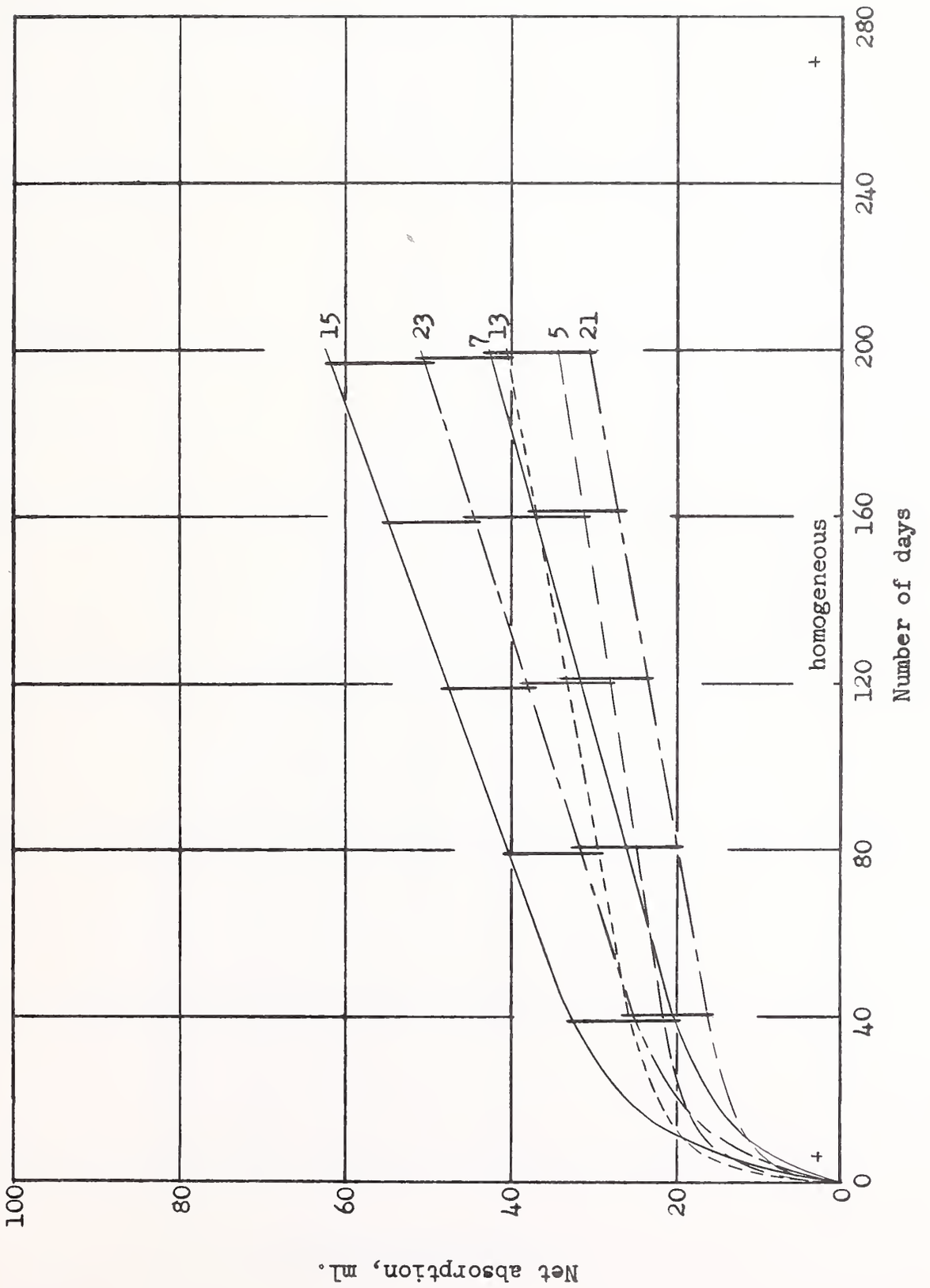

Fig. 21. Results of Duncan tests of mean net absorptions for treatment comparison B'. (All stresses, both cures, water)

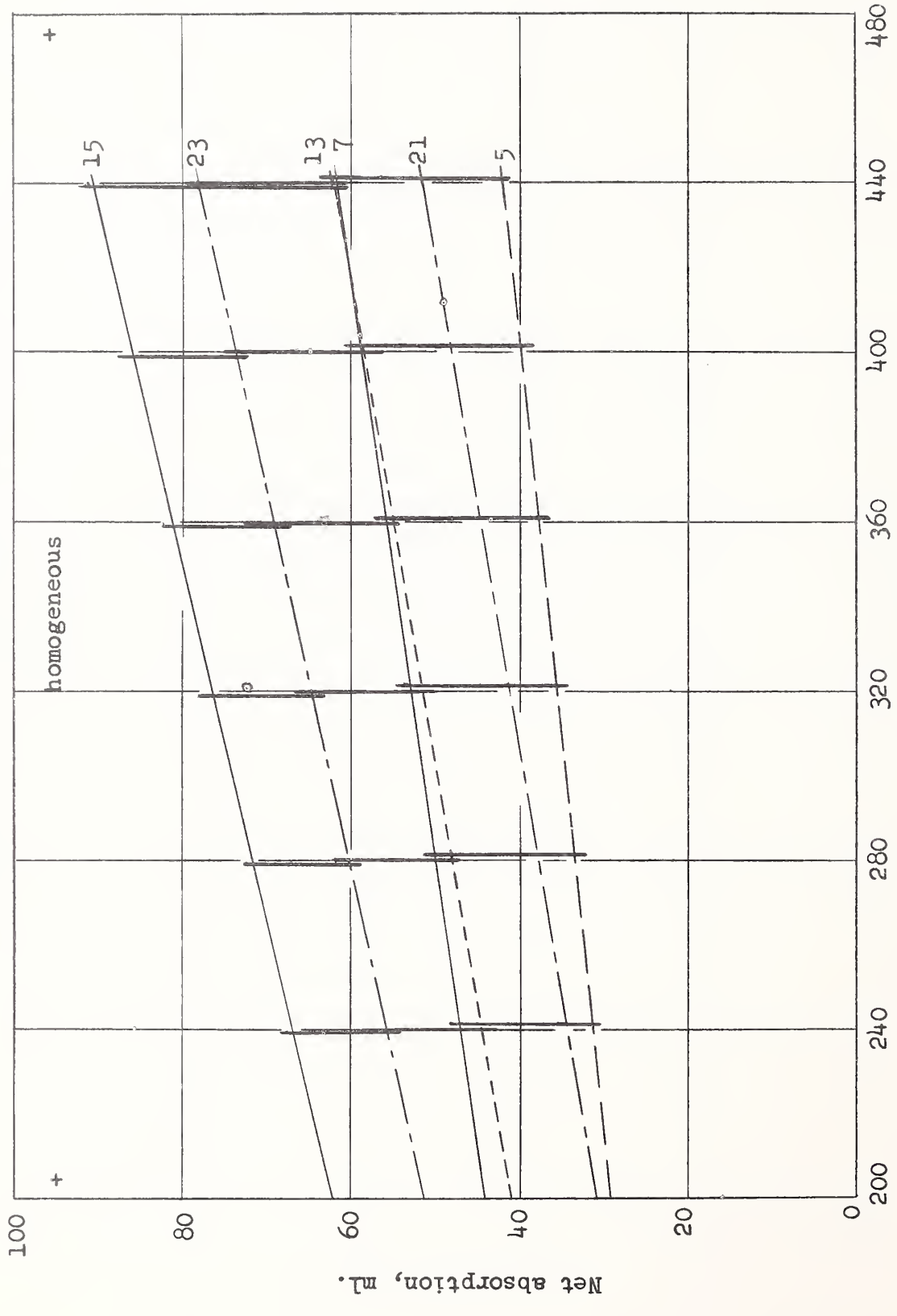

Fig. 21. (Cont.) Results of Duncan tests of mean net absorptions for treatment comparison B'. (All stresses, both cures, water)

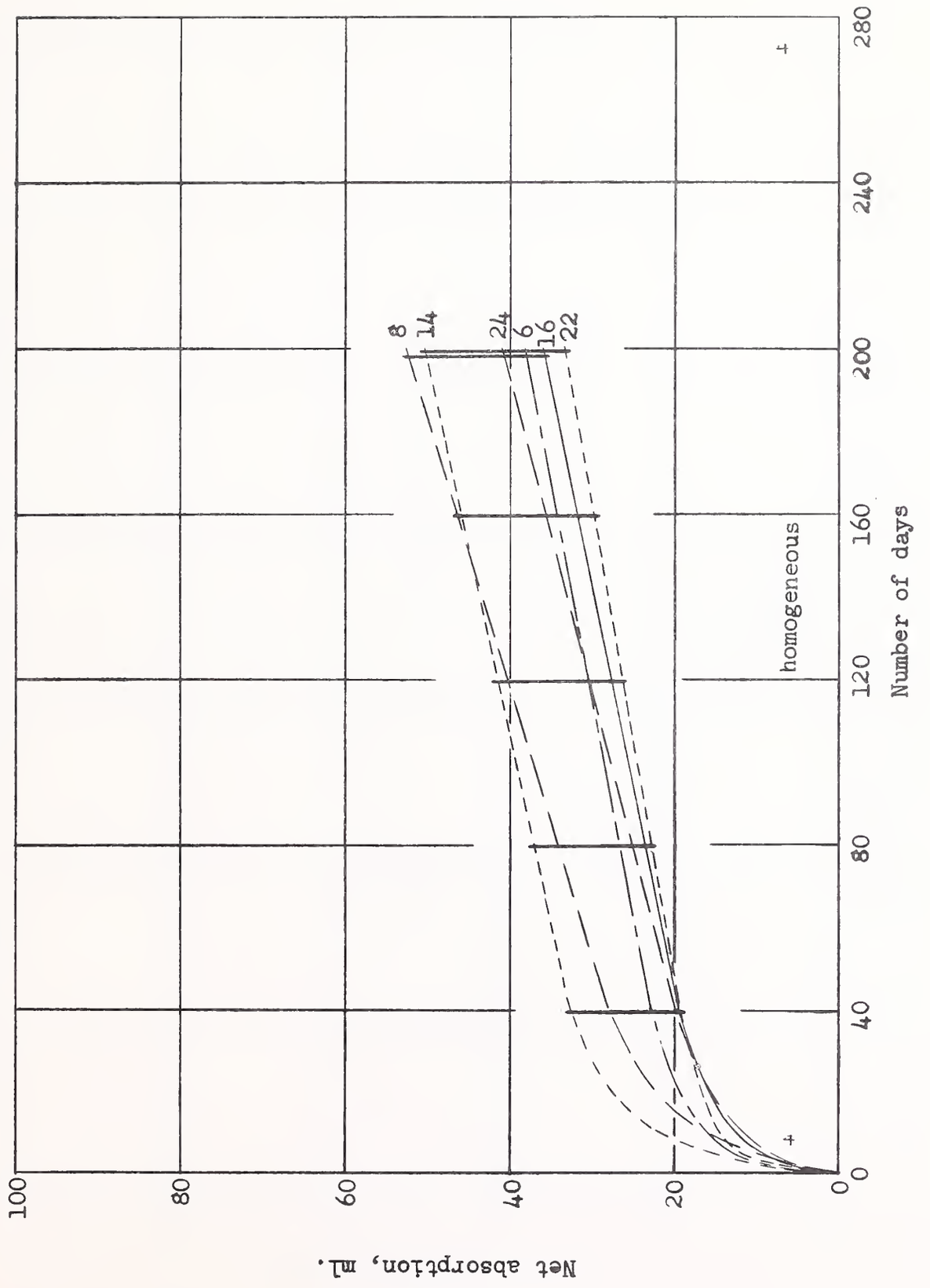

Fig. 22. Results of Duncan tests of mean net absorptions for treatment comparison C'. (All stresses, both cures, chloride)

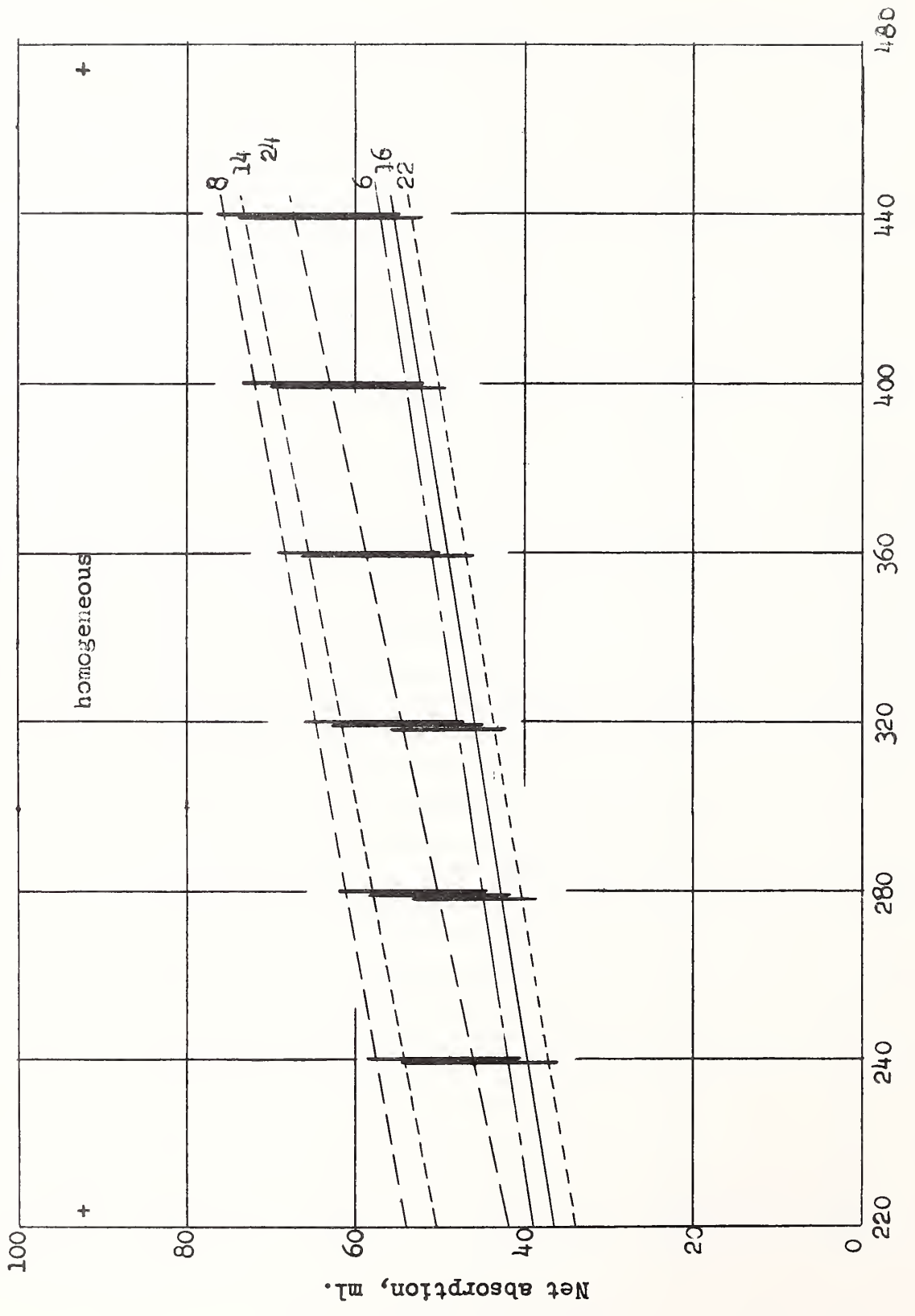

Fig. 22 (Cont.) Results of Duncan tests of mean net absorptions for treatment comparison C'. (All stresses, both cures, chloride)

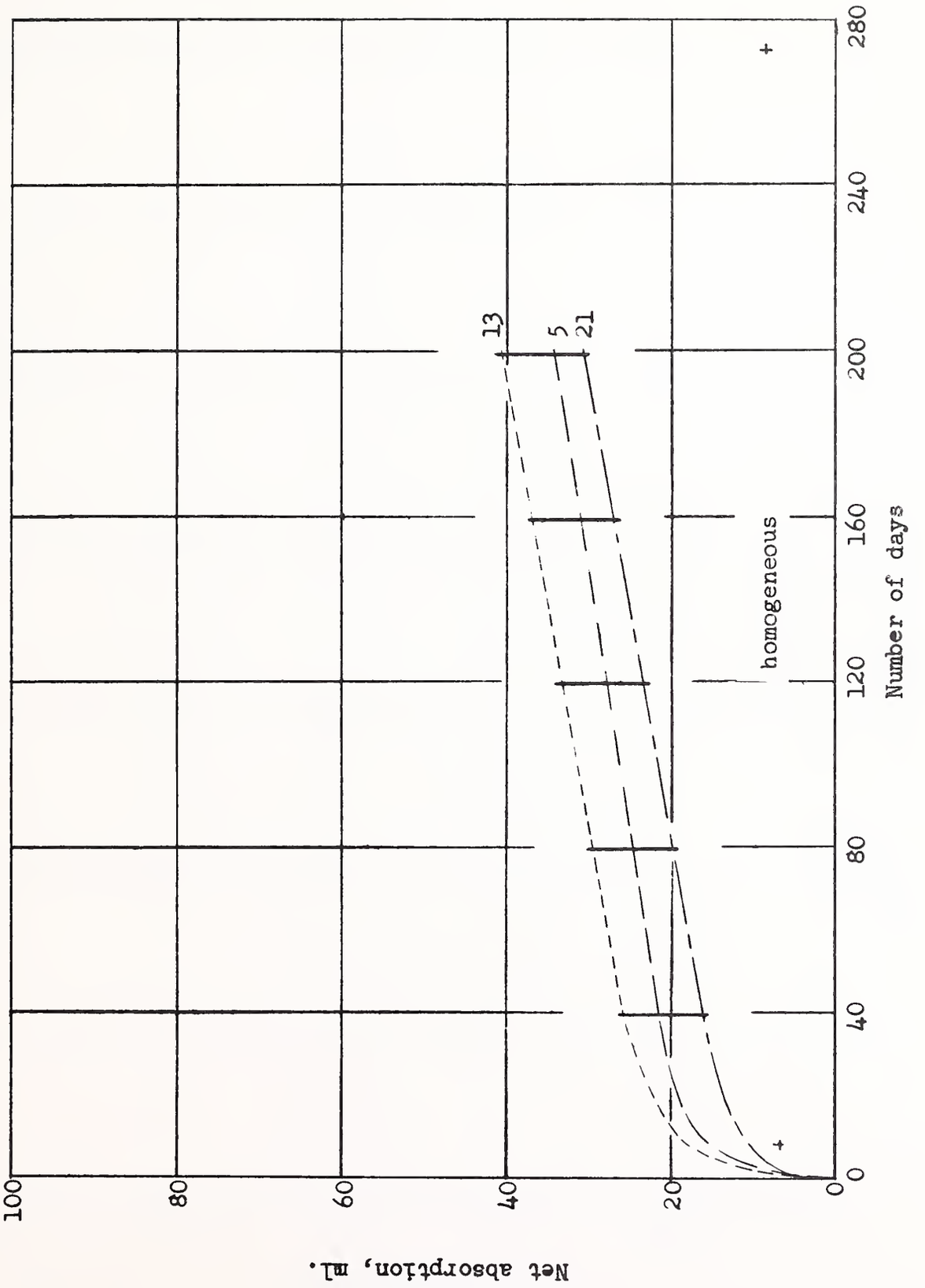

Fig. 23. Results of Duncan tests of mean net absorptions for treatment comparison D'. (All stresses, normal cure, water)

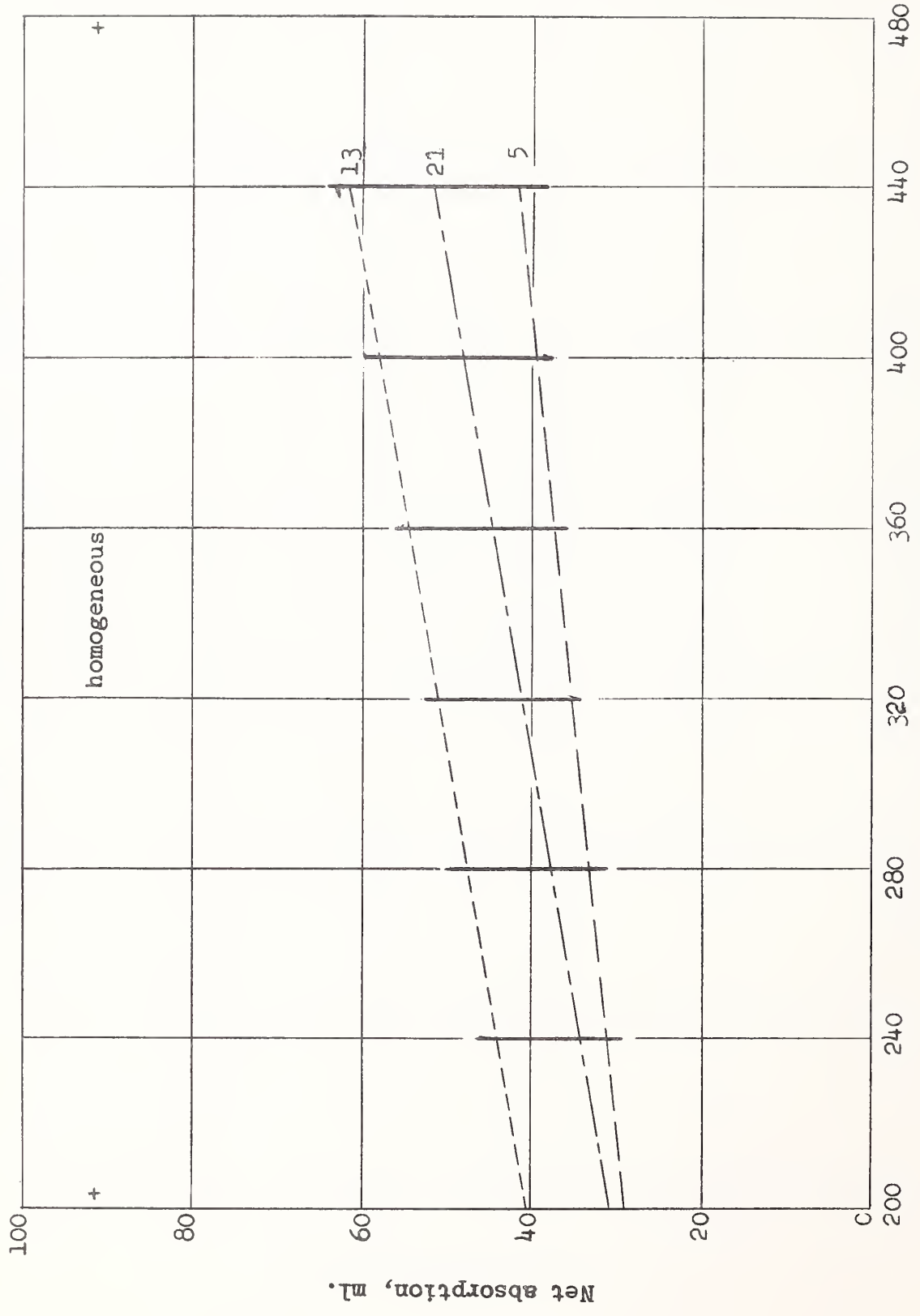

Fig. 23 (Cont.) Results of Duncan tests of mean net absorptions for treatment comparison D'. (All stresses, normal cure, water)

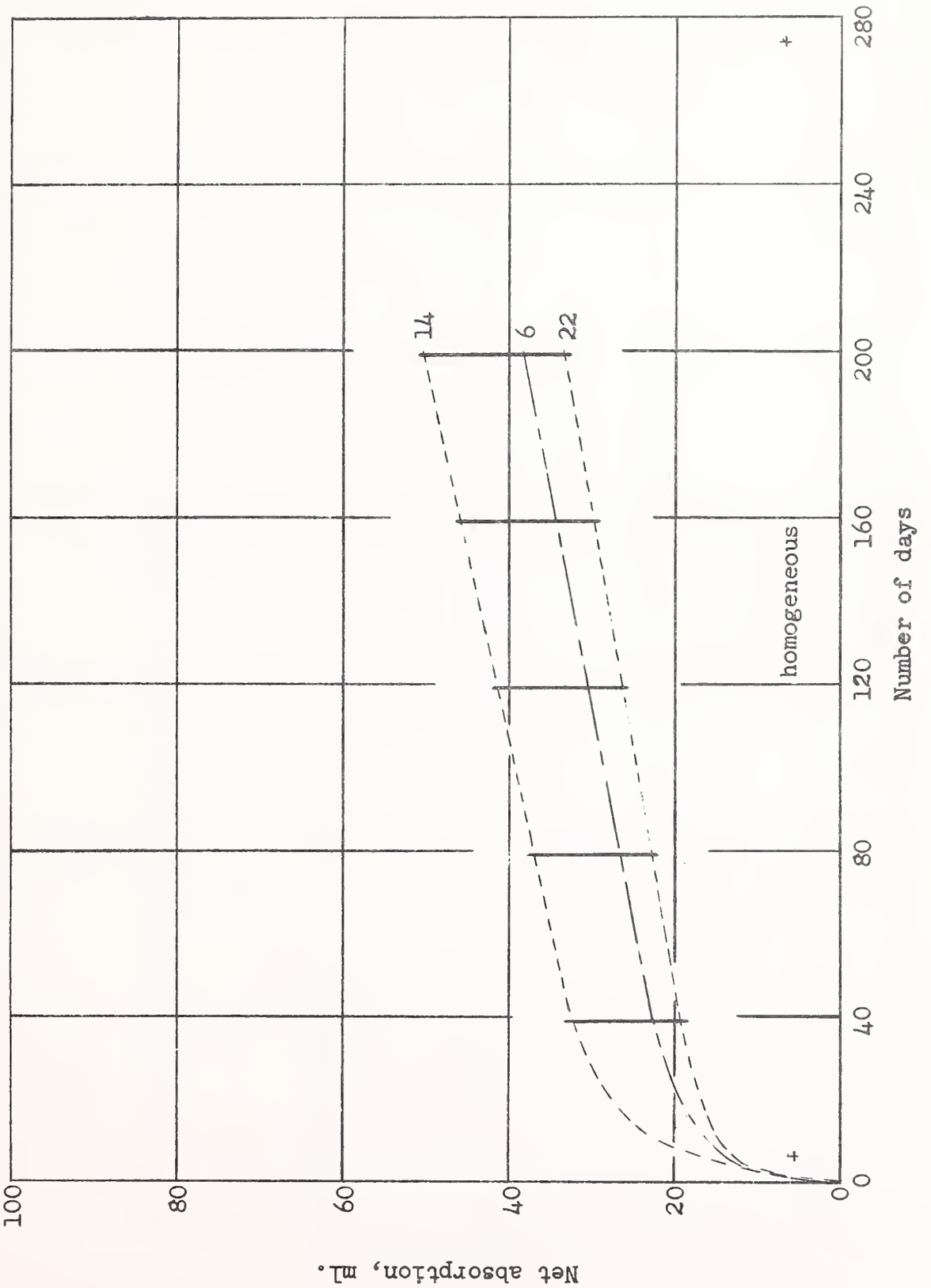

Fig. 24. Results of Duncan tests of mean net absorptions for treatment comparison E'. (All stresses, normal cure, chloride)

Fig. 24. (Cont.) Results of Duncan tests of mean net absorptions for treatment comparison E'. (All stresses, normal cure, chloride)

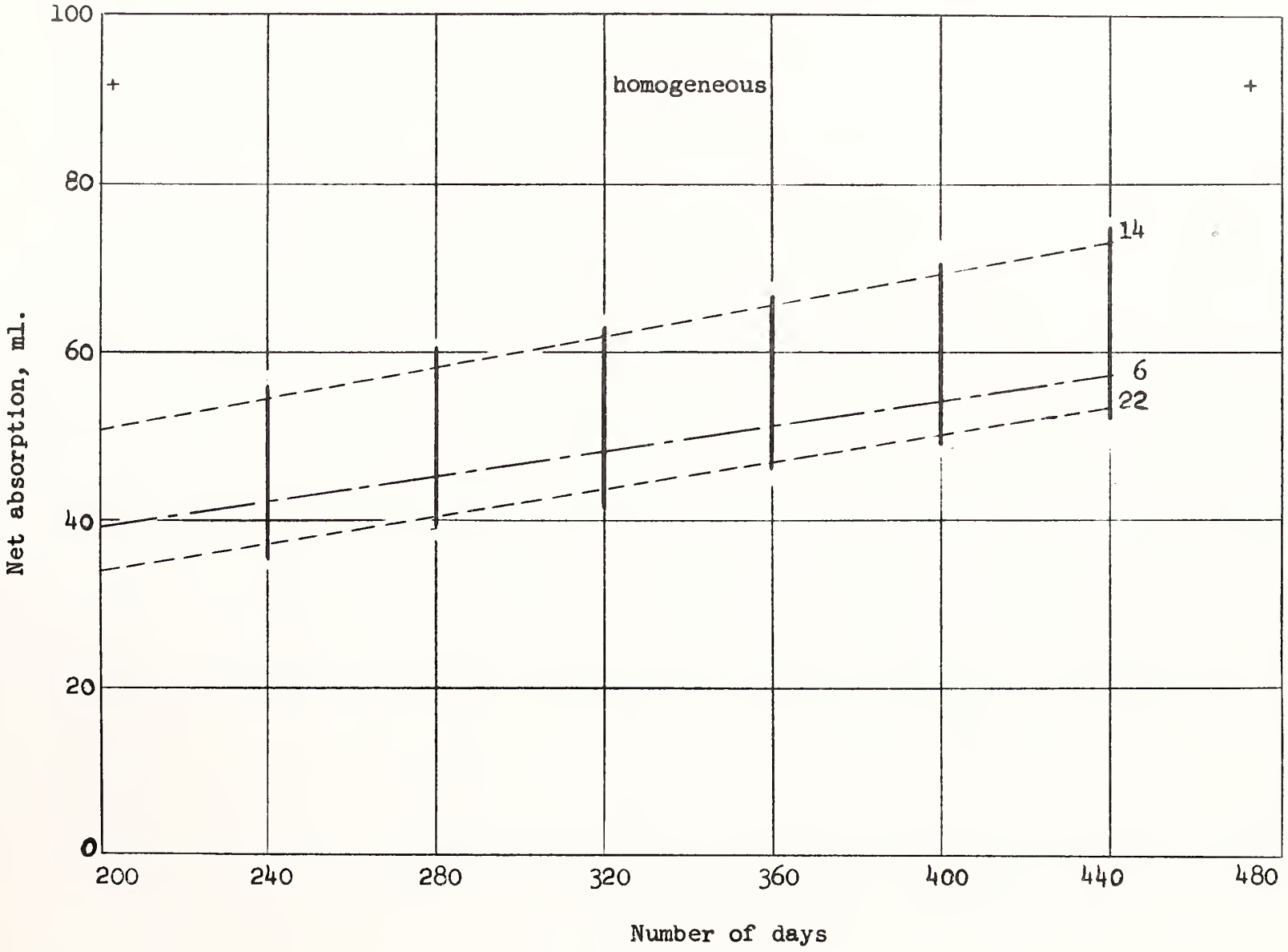

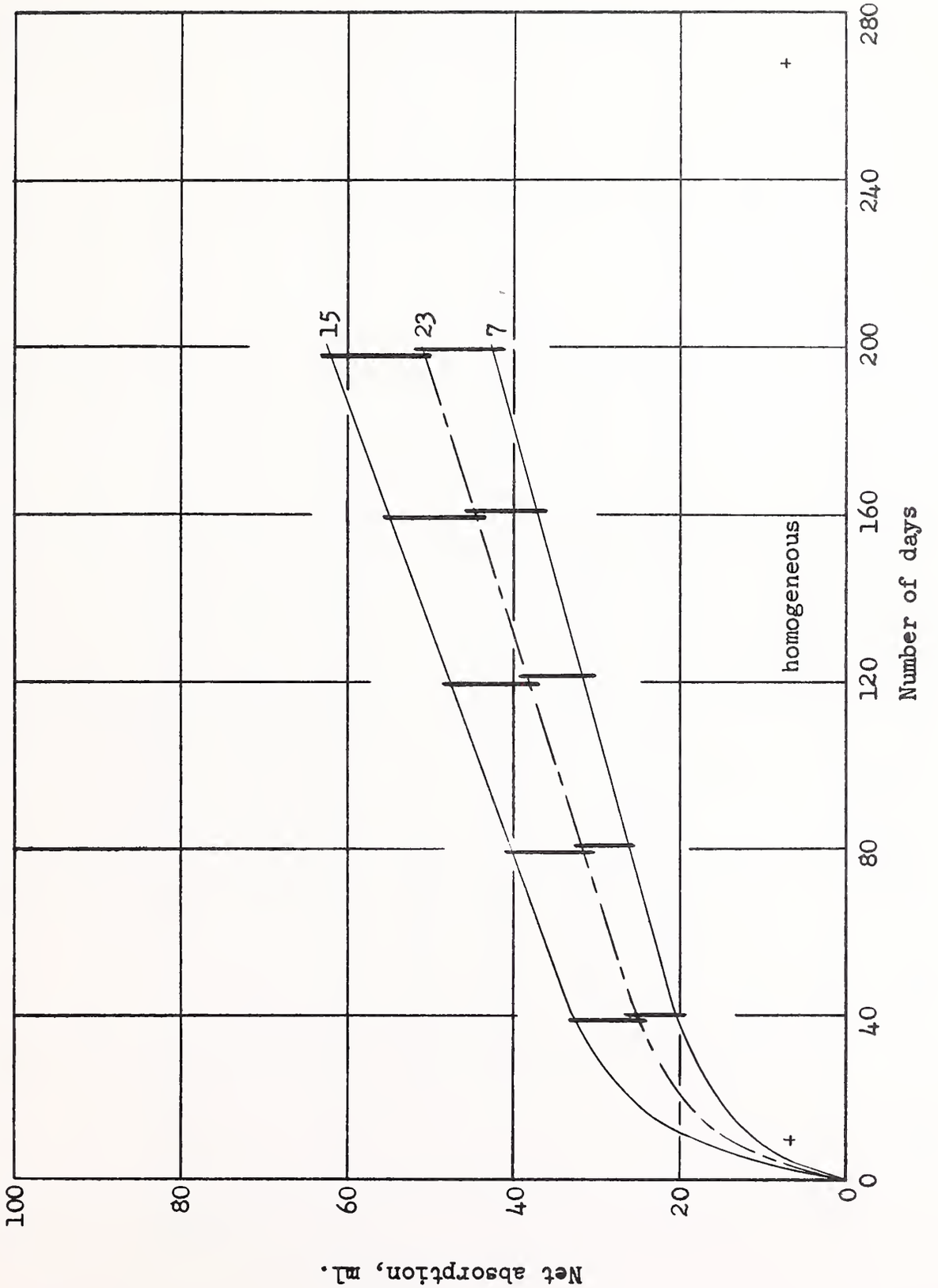

Fig. 25. Results of Duncan tests of mean net absorptions for treatment comparison F'. (All stresses, steam cure, water)

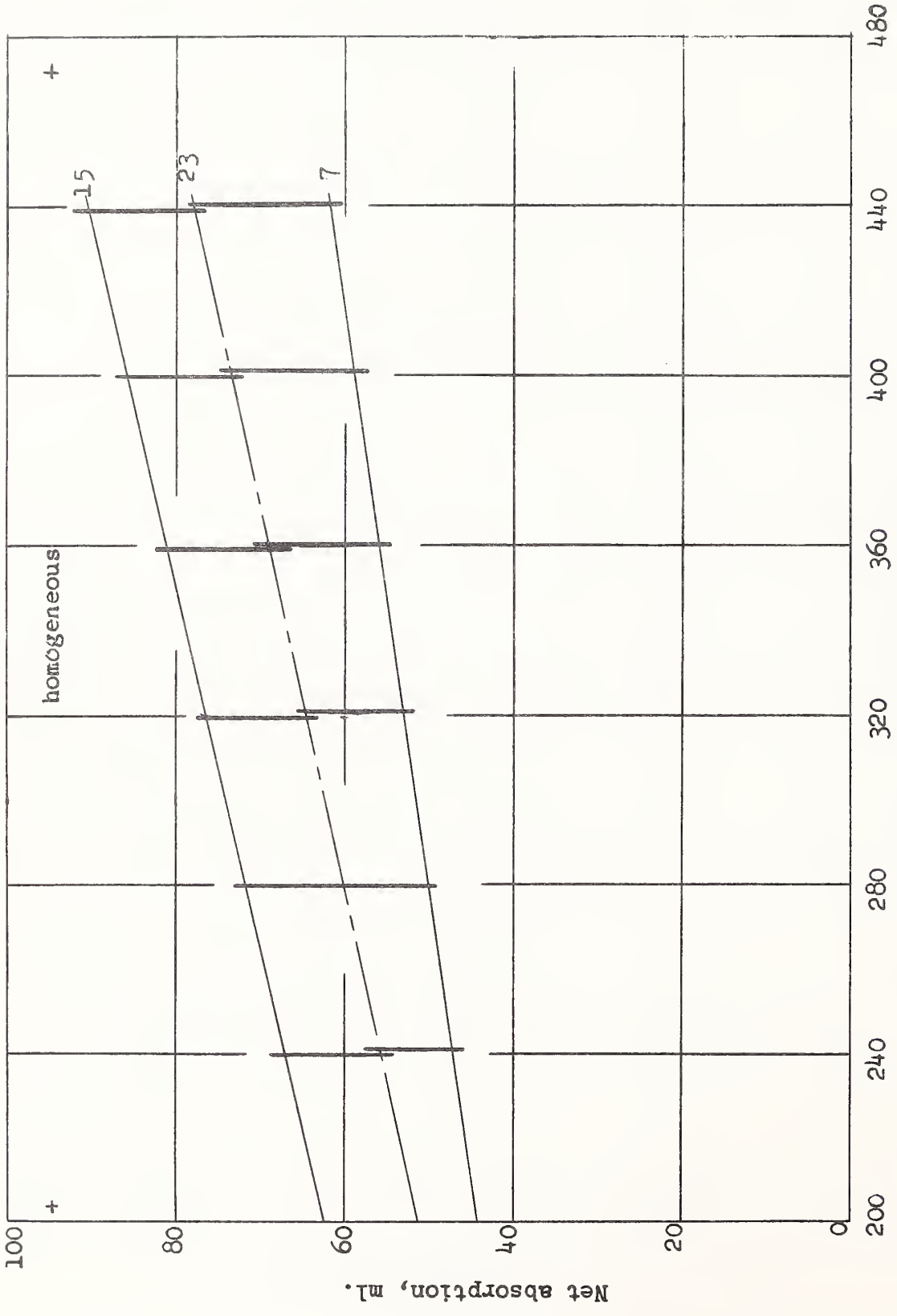

Fig. 25. (Cont.) Results of Duncan tests of mean net absorptions for treatment comparison F'. (All stresses, steam cure, water)

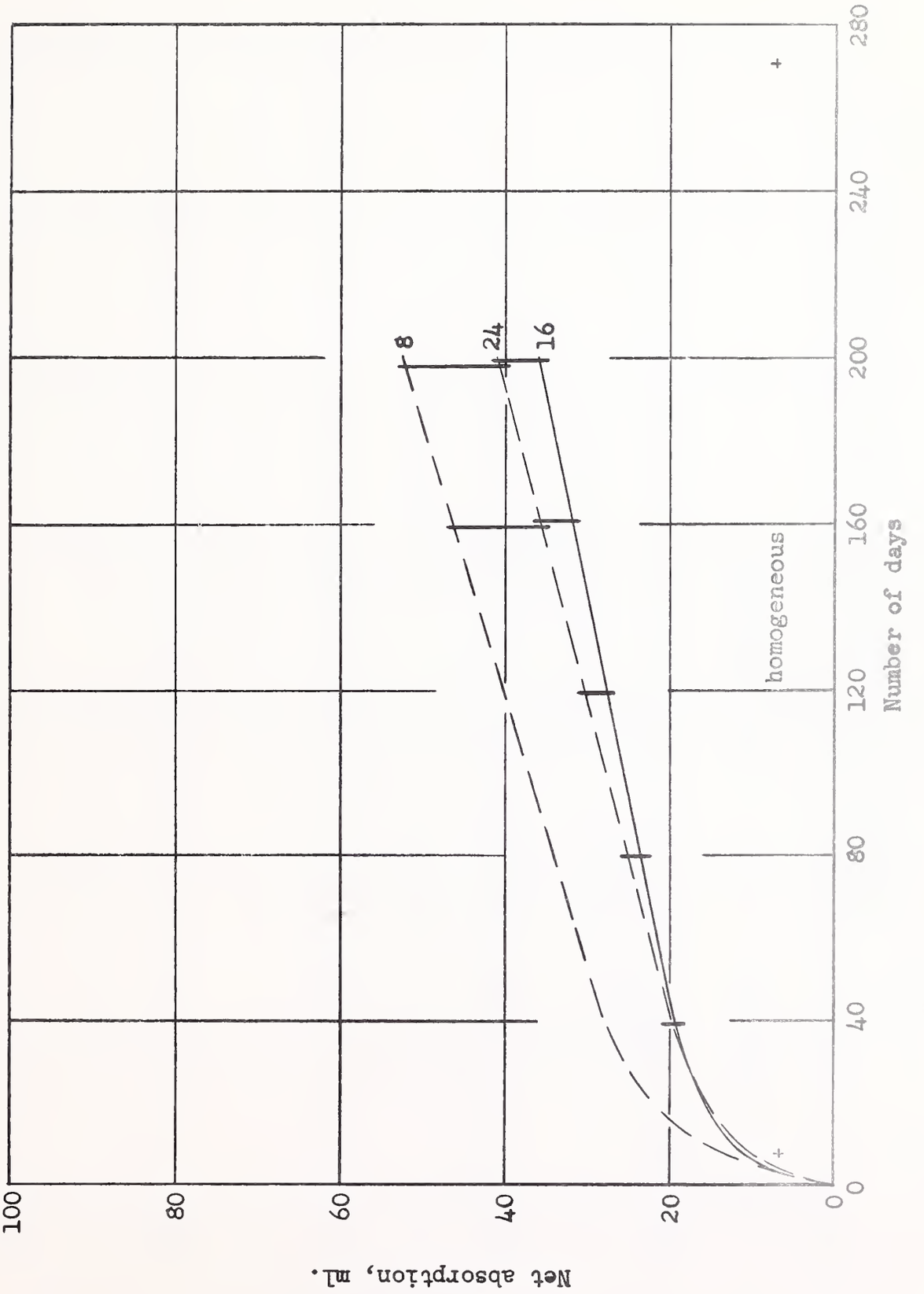

Fig. 26. Results of Duncan tests of mean net absorptions for treatment comparison G'. (All stresses, steam cure, chloride)

Fig. 26. (Cont.) Results of Duncan tests of mean net absorptions for treatment comparison G'. (All stresses, steam cure, chloride)

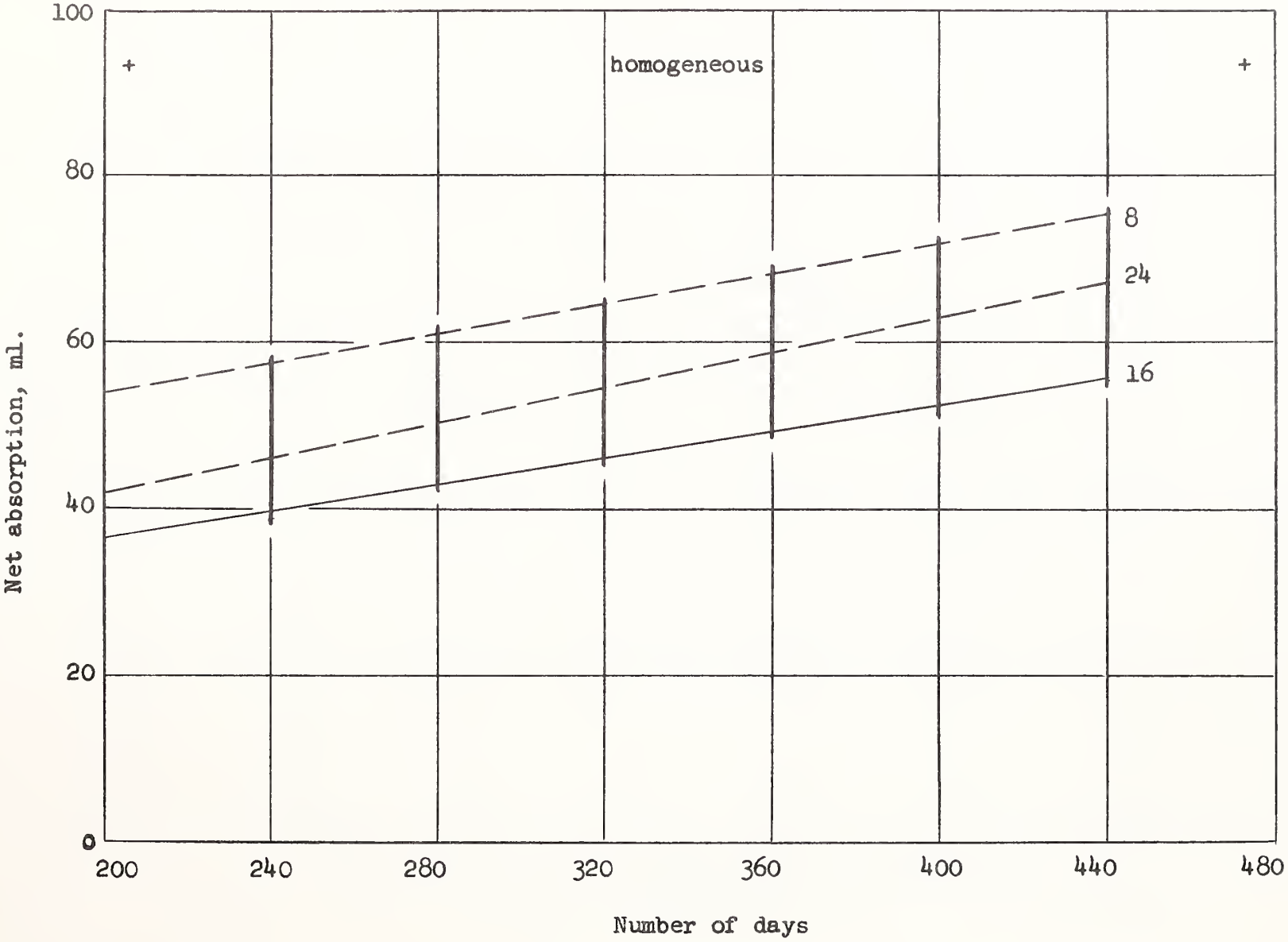

Fig. 27. Results of Duncan tests of mean net absorptions for treatment comparison H'. (All stresses, normal cure, water & chloride)

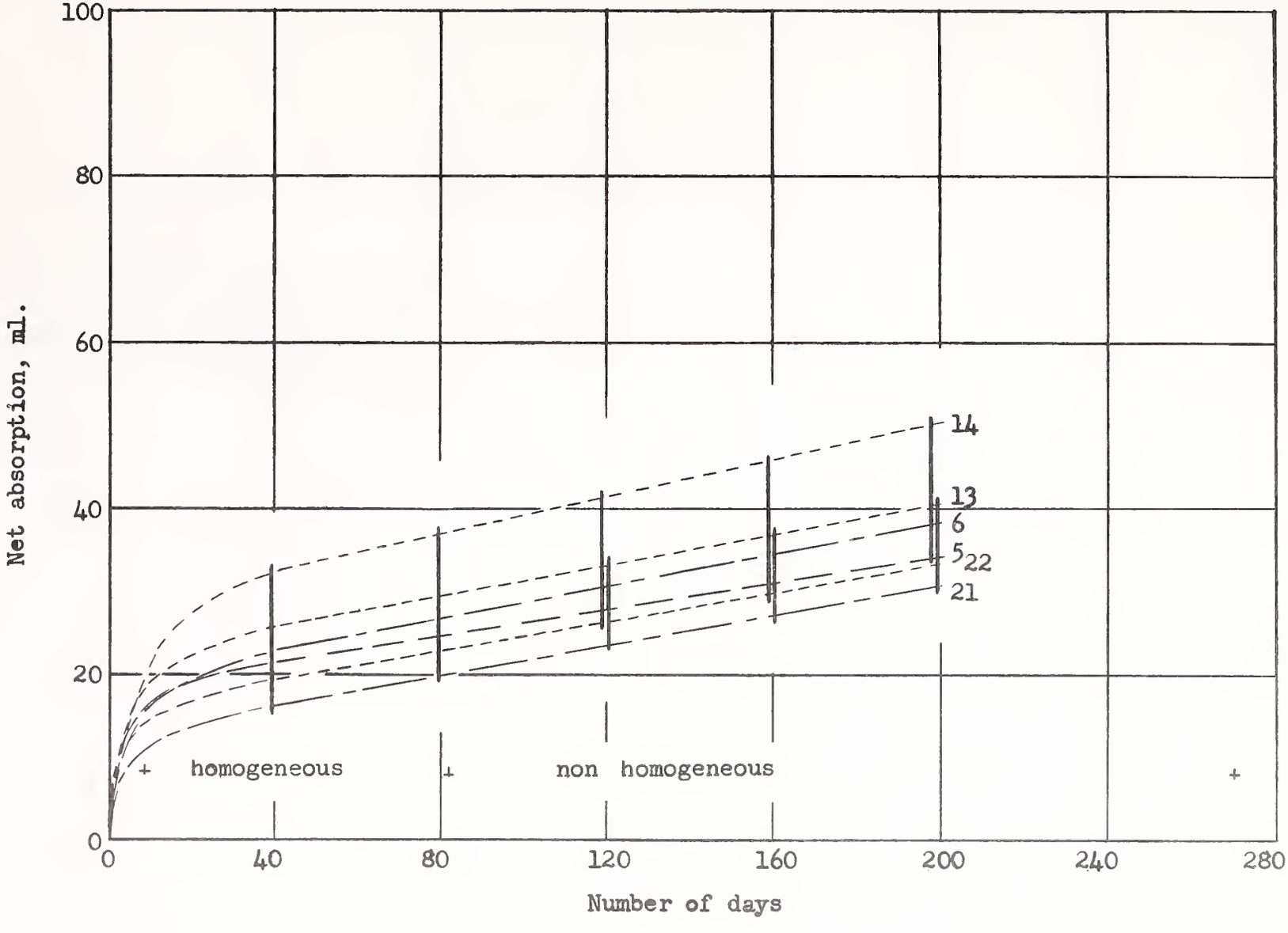

Fig. 27. (Cont.) Results of Duncan tests of mean net absorptions for treatment comparison H'. (All stresses, normal cure, water & chloride)

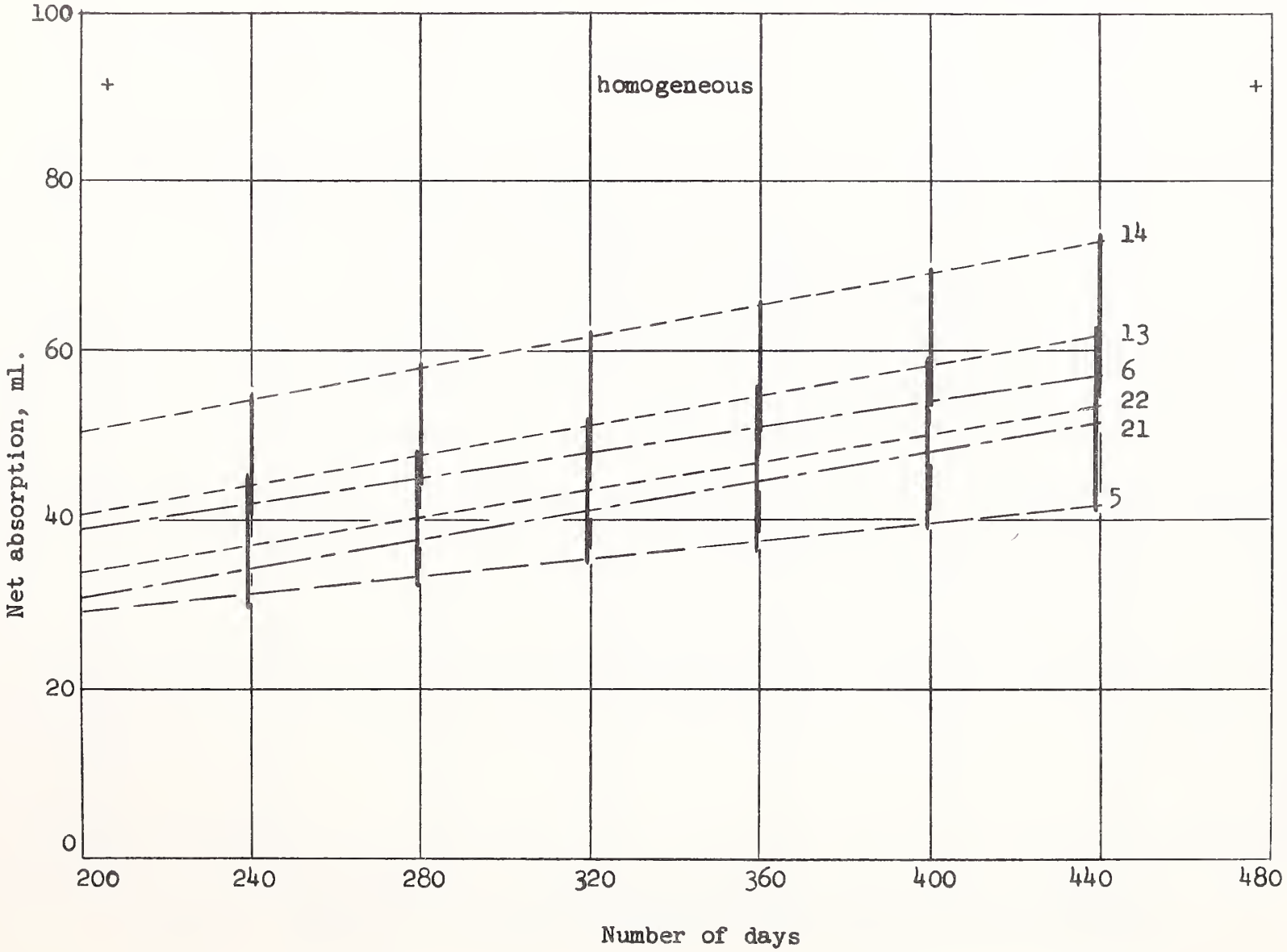

Fig. 28. Results of Duncan tests of mean net absorptions for treatment comparison I'. (All stresses, steam cure, water and chloride)

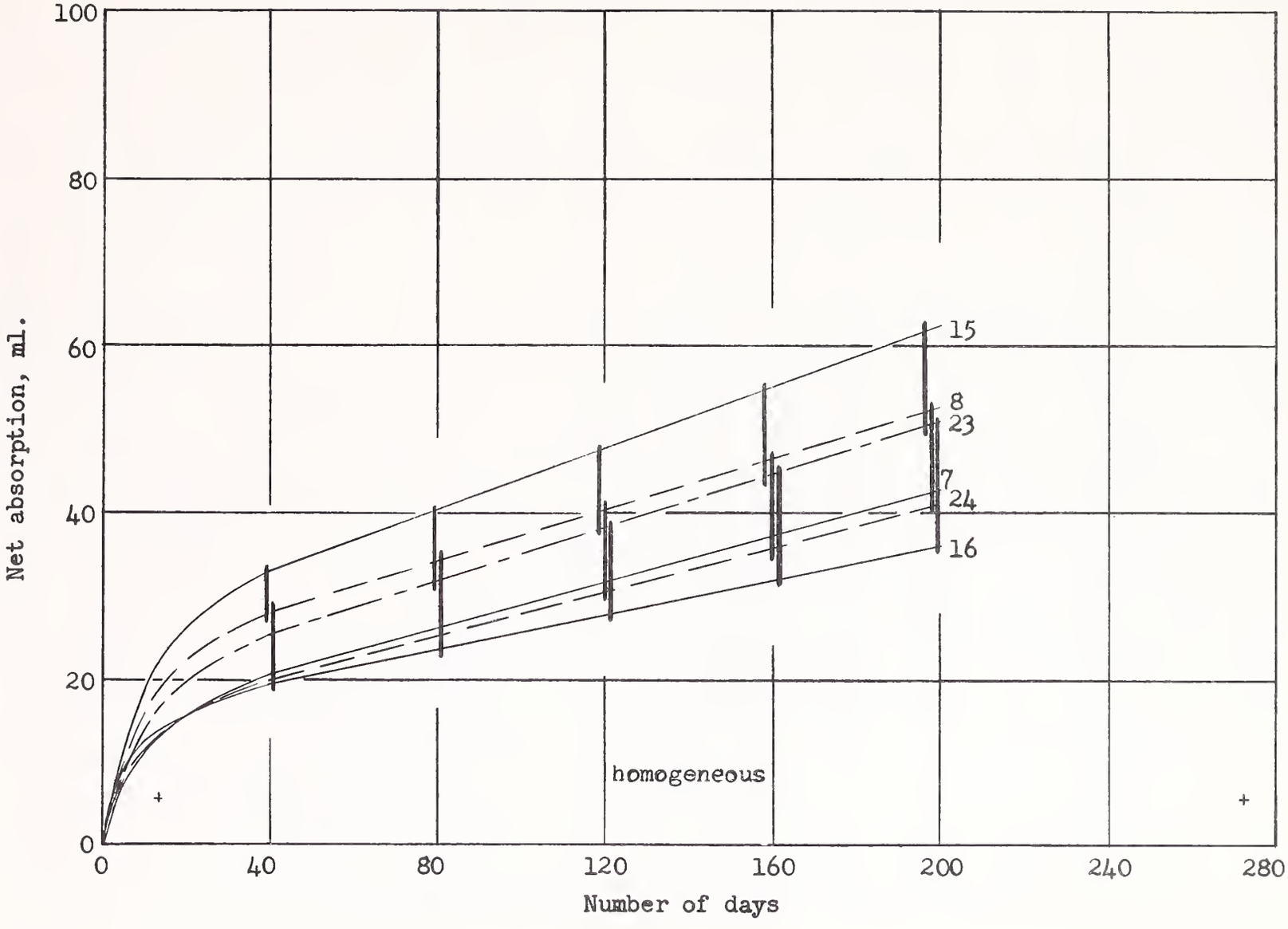

Fig. 28. (Cont.) Results of Duncan tests of mean net absorptions for treatment comparison I'. (All stresses, steam cure, water & chloride)

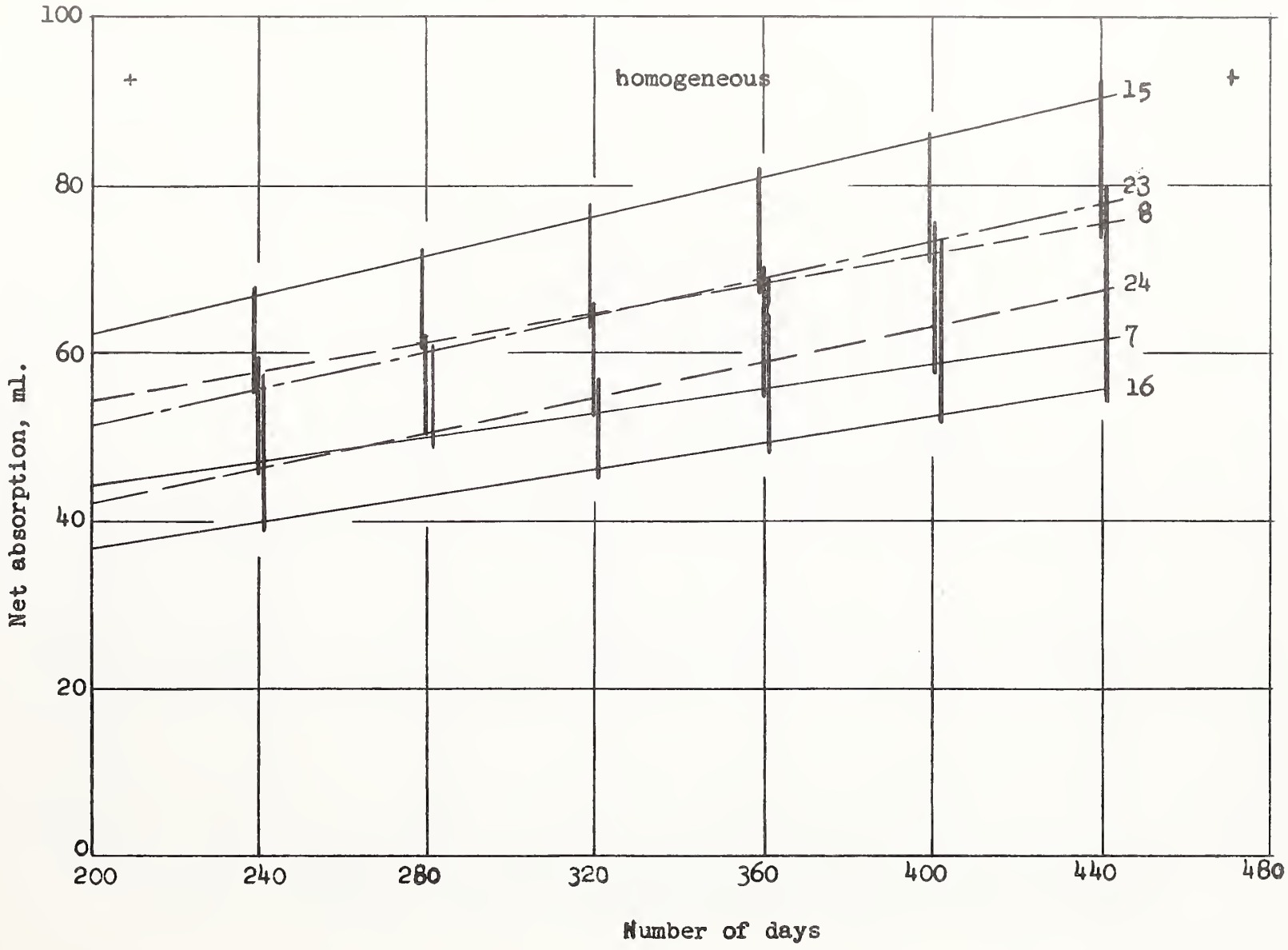

DISCUSSION

Permeability

Because of the rather limited usefulness of this series of tests the graphical summaries are presented as two linear regions. They are truly continuous curves but no additional clarity or purpose would be served by so showing them, nor by further linear segmenting.

Effect of Prestress

Permeability as defined and tested for in this study is unrelated to compressive prestressing. An examination of Figures 20 through 28 shows random order of stress level in nearly all of the comparisons. Figures 25 and 26 typify the lack of coherence even though significant differences are declared.

Effect of Curing

Figures 21 and 22 show some significant differences between the absorptions of steam and normal cured concrete; the steam cured being the most permeable. Treatment 15 (500, steam, water) is different from treatment 21 (1200, normal, water) and treatment 5 (zero, normal, water), the last two are also different than treatment 23 (1200, steam, water). Also treatment 8 (zero, steam, chloride) is different than treatment 22 (1200, normal, chloride). Other relationships, while not declared different, are generally grouped to support the relationship. Another confirmation can be

seen by comparing the magnitudes of total absorption between Figures 23 and 25 where the water gain of the steam cured samples is approximately two times that of normal. Figures 27 and 28 again show steam curing accepting more total fluid than normal curing. But, interestingly, a magnitude comparison between Figures 24 and 26 show steam and normal cured concrete to absorb nearly equal volumes of chloride solution. The conclusion is that steam cured concrete absorbs more water than does normally cured concrete but that it does not absorb more chloride solution.

Effect of Solution

The preceding conclusion can be supported by other comparisons. Figures 21-22 show a total magnitude of water gain greater than the chloride solution gain. Figures 23-24 show normal cure taking more water than chloride and Figures 25-26 show the same relative effect with steam curing.

The decreased chloride intake as compared to water is not unusual. Others have shown this effect and generally ascribe it to a clogging of the pore system.

The apparent equal clogging rate of two dissimilar pore systems was unexpected. That the systems are dissimilar, either in pore size or continuity, is evident from their water acceptance rates and possibly their relative durabilities. It is likely that the test method of measuring absorption was insensitive to magnitudes of difference that presumably should have

existed between the two systems. Should this be correct, then it is quite understandable that no stress dependent relationship could be detected since the stress deformed system, if it exists, would have varied from a non-stressed system much less than would the steamed from the normal system.

Miscellaneous Tests

Because of the specimen surface sealing to force unidirectional flow, the total volume of fluids passing into the slabs, and the evidence of deep chloride solution penetration as shown in Figure 30 in the following section, it is evident that considerable amounts of solution passed completely through the specimens. This resulted in no visible efflorenscence or surface effects. The conical volume of concrete immediately underlying the standpipes containing the calcium chloride solution were obviously less permeable than other portions of the slabs and clearly were not due to progressive hydration since the companion slabs under water heads did not show this zoning. Clogging of the pore system is clearly evident.

From the condition of many of the freeze-thaw specimens and from mineral deposits in interior voids of some mortar bars, solutions must have penetrated deeply into many test specimens. Visual, photographic, and x-ray examinations disclosed nothing of value for better understanding of solution penetration into concrete.

CORROSION

Test Results

The anticipated evidence of ion penetration into the concrete and the subsequent corrosion of the prestressing strand did not develop. Sample wires from all tests and exposure environments were obtained by diamond-sawing specimens and removing the strand. The strand was separated and the wires cleaned and examined. All such wires were found to be undamaged except those encased in mortar bars having 1/4 inch cover, which displayed neglible corrosion.

Since the strand damage was practically non-existent, weight change and corrosion area or volume could not be used as an index of wire corrosion. Tensile tests were run on extracted sample wires from all exposures as a check for non-visual damage. These results were then compared with an undamaged parent sample. No statistical nor even inferential difference was found in any of the comparisons, for example: the mean strength of the parent 50 wires was 2999 lbs. with a standard deviation of 27 lbs.; 12 wires from 1/4 inch mortar covered specimens soaked 551 days had a mean value of 2997 lbs.; 12 wires from ponded calcium chloride freeze-thaw slabs had a mean of 2988 lbs.; all other means were within one deviation of the parent mean.

The wires removed from the mortar bars, giving approximately 1/4 inch of cover, had clearly been reached by the solution in 475 days. Those in the chloride solution were rusted over only a

fractional percentage of the encased surface area and the tensile tests failed to show any damage. At 551 days no additional corrosion was noted. Sulfate solution had also reached the strand as evidenced by small needle-like sulfate crystals which had occasionally formed in the small voids contacting the strand. No evident corrosion was noted with the sulfate solution test.

The mortar bars were completely and continuously submerged throughout the testing period. This was presumed to be not as harsh a test as could have been obtained by using saturated wicks in contact with only part of the bar surface (6). However, the stand-pipe slabs with the two-foot pressure head should have resulted in an even more critical test situation but here again no corrosion resulted. The strand cover on the standard slab was approximately 3/4 inch of concrete. The solution penetration into the mortar bars was presumably slightly more than 1/4 inch in 475 days of submergence since at the same age no evidence of strand contact by the solutions was displayed by bars having 1/2 inch of mortar cover. At 551 days these relative conditions remained unchanged.

It is of interest to note the limited solution penetration longitudinally along the strand. This distance was never more than 1/2 inch and had no apparent relationship to the type of exposure. The concrete mortar produced an effective seal to end ingress of fluids. No material difference existed between

the effects of water, chloride or sulfate solutions. Figure 29 shows typical reclaimed strands and details of the strand ends, which were deeply corroded.

Fig. 29. Reclaimed Strands

In an attempt to determine the relative surface-inward penetration of the salt solutions, thin plate sections were sliced from various specimens and examined. Evidence of penetration was sought from visual inspection, dying the specimens to show regions of damage or absorption change, and x-raying for altered matrix integrity.

None of these methods were definitive. Crystal violet dye was found to be best for delineating regions of intense damage but it was not suitable as a penetration measuring tool. X-ray photographs did not distinguish between porous and non-porous regions of the mortar matrix either for untreated slices or those soaked briefly in barium solution.

One distinctive feature was found in the chloride solution standpipe specimens. When first sawed, at 200 days, the region immediately under the stand pipe was noticeably darker due to solution retention. After drying, a brief rewetting of the sample resulted in a lesser absorption in this same region with a resulting more rapid drying of the region. Presumably the salts had clogged a conical portion of the concrete and decreased the permeability of the concrete. Figure 30 shows a partially dry view of this effect. No external evidence of fluid passage was found on any of the standpipe slabs. Yet, it obviously did pass through considering the volumes of fluid absorbed and from cut sections showing the salt clogging of concrete extending beyond the encased strand. No corrosion of the strand resulted.

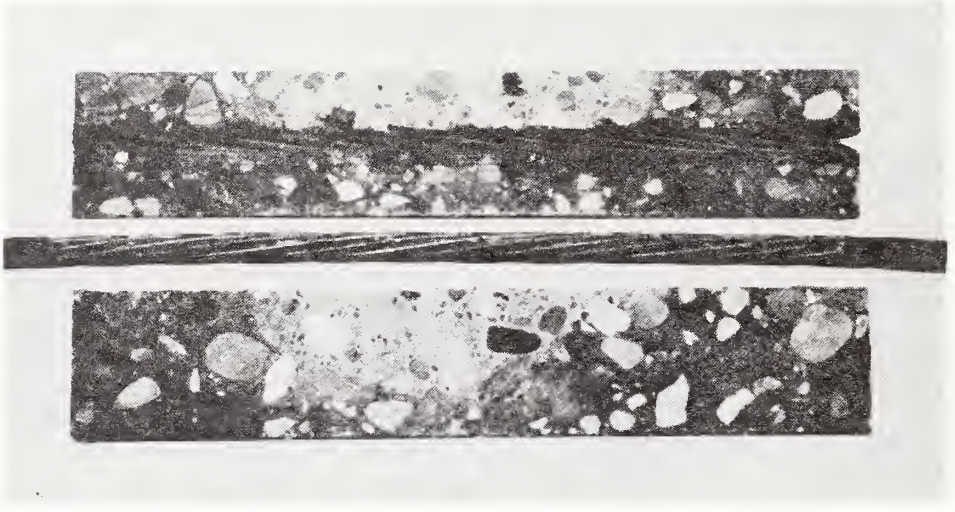

Fig. 30. Salt Clogged Specimens

The relative degrees of wire corrosion by water, chloride solution and sulfate solution were compared by using clean wires exposed to the fluids over a period of time. Exposure to the solutions was by draped, saturated cloth wicks. The basis of comparison was the tensile strength of the wires. Groups of five wires from each solution were tested every ten days until 100 days exposure had been reached by the last group.

The results of this test series is shown in regression line form in Figure 31. Co-variance analysis proved the homogeneity of the regression coefficients at the one percent level. For the individual treatments, the correlation coefficients (indicating a tensile strength vs corrosion time relationship) were: water, non-significant; magnesium sulfate solution, significant; calcium chloride solution, highly significant; and for the "pooled" regression, highly significant. The 95 percent protection level was set for these declarations. The separate means were adjusted to the pooled regression line and a student "t" test was used for the statement of differences between pairings of the adjusted means, again at the 95 percent level. Water and sulfate solution were not significantly different in their corrosive capacities up to 100 days, water and chloride solution were significantly different after 37 days, and chloride and sulfate solutions were significantly different after 31 days.

Fig. 31. Wire Tensile Strength v.s. Solution Exposure Time

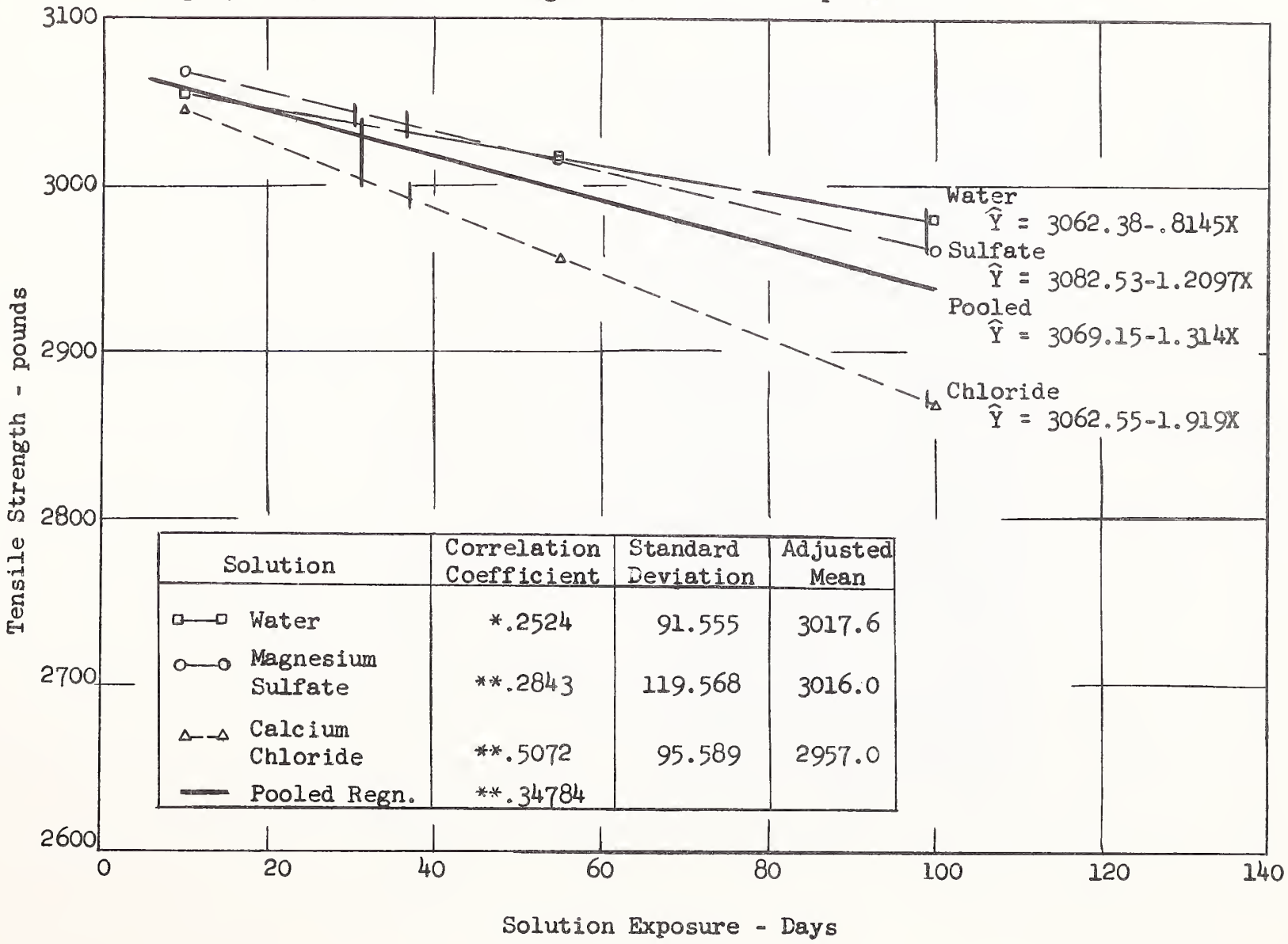

Solution	Correlation Coefficient	Standard Deviation	Adjusted Mean
Water	*.2524	91.555	3017.6
Magnesium Sulfate	**.2843	119.568	3016.0
Calcium Chloride	**.5072	95.589	2957.0
Pooled Regn.	**.34784		

DISCUSSION

Encased Strands

The concrete used in this investigation was quite durable, dense, and of high quality, but it was penetrated readily by the study solutions. Yet, within the time allowed, no significant damage to the encased strands resulted from the penetration of externally supplied ions. For completely submerged specimens both chloride and sulfate salts penetrated more than 1/4 inch of mortar cover in 475 days but less than 1/2 inch in 551 days. There was no evidence that either solution had penetrated 3/4 inch of concrete cover in 440 days. There was no reduction in wire tensile strength and no discernable evidence of corrosion except for very minor surface rust spotting of the wires reclaimed from the 1/4 inch cover mortar bars which had been submerged in chloride solution.

All freeze-thaw slabs furnished 3/4 inch concrete cover over the strands. Water and sulfate solutions gave no physical indication of having reached the strands. The concrete exposed to the chloride solution were so damaged and deeply eroded that it is probable that the chloride contacted the wires. None of the wires were visibly corroded and there were no reductions in tensile strength.

The permeability slabs had both water and chloride solution passing completely through them in less than 200 days. No effect was registered by this passage and wire contact.

In a recent study by Ost and Monfore (22) chloride concentrations at various depths in concrete and paste were determined by chemical analysis. Interpolation of their data indicates that in one year the

permeability slabs (6.73 sacks per cubic yard and a water-cement ratio of 5.64 gallons per sack) could have attained a chloride content of near 8 percent at the strand level and 1 percent at the exposed bottoms surface. The percentages are by weight of cement. This should be a very corrosive concentration at the wire location. In a parallel study, using towel wicks to wet small bars of the same quality of concrete, they report "some" corrosion after two years. This occurred only in the bars having one-half inch of concrete covering the wire. The chloride content at the wire level was not determined but was presumably high.

One conclusion which could be made is that a harmful ion content is a necessary but not sufficient condition for corrosion to develop since other factors such as the availability of oxygen and its distribution along the wires are also involved in the corrosion process. High chloride concentrations must be considered potentially dangerous and it is apparent that in time such concentrations may be expected when deicing salts are used on common concretes with average water-cement ratios. Whether or not corrosion develops is dependent upon the particular situation.

Exposed Strands

The relative corrosive capacities of the solutions can be judged from Figure 31. The differences between these capacities is the important factor when attempting to predict the solution effects in service situations. Since the development of corrosion is problematical even with high chloride concentrations, it would be much less likely in sulfate exposures because the sulfate induced corrosion was not significantly different than that of water in 100 days of exposure.

CHAPTER V

CONCLUSIONS

Within the scope of the investigation, restricted definitions, test methods, and materials used the following conclusions are made. They may be statistically significant or only inferential as explained in the separate discussions.

Durability

1. Deep structural integrity or durability of prestressed concrete is moderately compressive stress dependent. It is likely that the increased durability is due to expansion restraint rather than any significant force-induced structural alteration. The durability advantage to be gained by stressing is much less than would be realized by air entrainment.
2. Steam cured concrete tends to be less durable than normally cured concrete.
3. Ponded magnesium sulfate solution (20,000 ppm) has no freeze-thaw durability effect.
4. Ponded calcium chloride solution (20,000 ppm) may reduce the durability of concrete.
5. The higher the permeability of a concrete the more probable is a reduction of durability.

Scaling

1. No relationship exists between freeze-thaw scaling and compressive prestress loading.
2. Ponded calcium chloride solution (20,000 ppm) causes extreme scaling under freeze-thaw conditions. It is 5 to 10 times as severe as solid salt thawing of ice and over 100 times more harsh than temperature rise ice thawing.
3. Steam curing, as compared to normal curing, improves scaling resistance for a brief initial period after which the resistance decreases and remains lower.
4. Ponded magnesium solution (20,000 ppm) is no more detrimental in freeze-thaw scaling than is ponded water.
5. There is no apparent relationship between scaling and durability except that the more permeable concrete is slightly less serviceable by both measures.

Miscellaneous

1. No scaling or durability effects were registered by the wet-dry, submerged, or fluid passage tests.

Strand Corrosion

1. Strands recovered from concrete exposed to all test environments were undistinguishable from new strands, even after having been contacted by water and chloride solution and being exposed to these solutions for over 100 days.

2. Solution wick-wetted, individual wires tend to corrode in the order: water, magnesium sulfate, and calcium chloride. There was no statistically significant difference between the water and sulfate solutions. The chloride solution was significantly more damaging.

APPENDIX A

SLAB PRESTRESSING OPERATIONS (23)

SLAB PRESTRESSING OPERATIONS

Specimens

The concrete slab specimens were $10\frac{1}{2}$ inches long, $4\frac{1}{2}$ inches wide, and 2 inches deep. The total specimen length varied with the stress level imposed upon the slab. No appurtenances were used on the zero stress slab, a $\frac{1}{2}$ inch thick steel load distributing plate was used on the 500 psi slab, and a 3/4 inch steel plate was used on the 1200 psi slab. Figure 32 shows the three basic specimens.

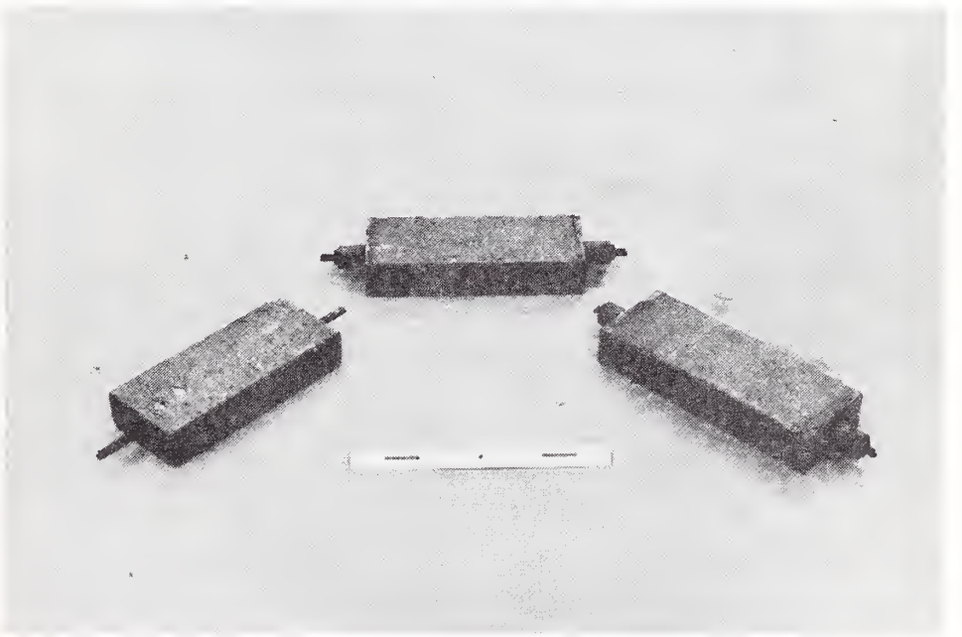

Fig. 32. Slab Specimens, 3000, 500 psi, 1200 psi

Prestressing operation

Figure 33 is a photograph of the equipment necessary for the pretensioning operation; the items shown are described in Table VIII. The

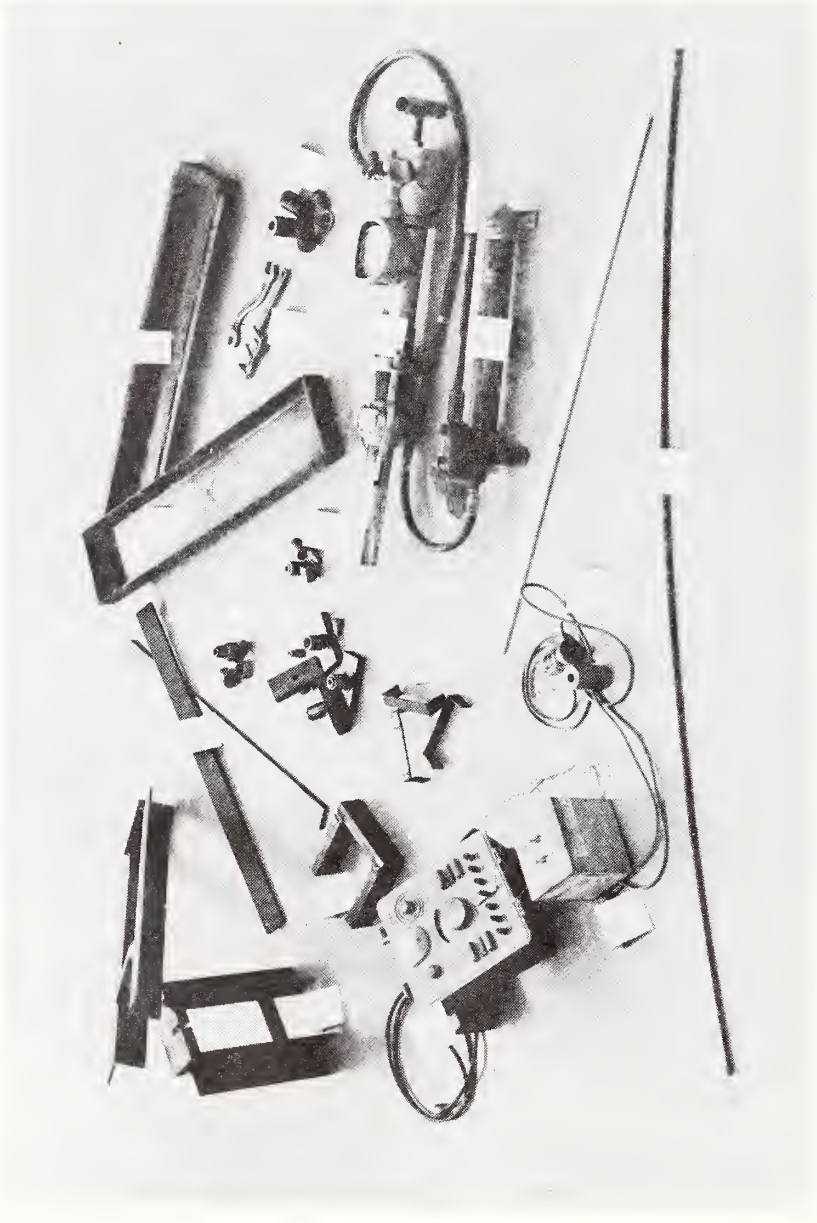

Fig 33. Pretensioning Equipment

TABLE VIII

IDENTIFICATION OF ITEMS IN FIGURE 33

Identification letter	Item	Description
A	zero and 500 psi. casting bed	33½" length of 7 [9.8; 7"x2"x½" end plates, with 7/16" dia. center holes, welded to ends of channel.
B	1200 psi. casting bed	33½" length of 7 [9.8 reinforced with 1"x1"x¼" angles welded to flanges; 7"x2"x1" end plates, with 7/16" dia. center holes, welded to ends of channel.
C	slab side forms	33¼" lengths of 2"x3/8" steel bar.
D	short "seating yoke"	Two 12-3/4" lengths of 2½"x2½"x¼" angles spaced 5" apart; 5"x3"x1" steel bar, with 7/16" wide center notch, welded to one end of angles; angles braced near free end.
E	long "seating yoke"	Same as D, except that angles are 29¼" long.
F	loading "yoke"	Two 6"x2"x1" steel bars spaced 6" c. to c.; 7"x2"x1" steel bar, with 7/16" dia. center hole, welded to one end of the 6" bars.
G	end-bearing chuck-plate combinations	3/8" prestressing strand chucks welded to centers of 4½"x2"x½" steel plates for 500 psi. slabs, and to 4½"x2"x3/4" steel plates for 1200 psi. slabs; 7/16" dia. holes drilled through plates, concentric with chuck axes.
H	hollow bolt and nut	Special truck-wheel nuts (manufactured by Budd Wheel Mfg. Co.); 7/16" hole bored through each "bolt" section.
I	3/8" prestressing strand chucks	Chucks identical to those used for G (made in England, manufacturer unknown).
J	wrenches	One open-end wrench to fit "bolt" section of H, and one pipe-wrench to fit "nut" section of H.
K	3/8" prestressing strand chucks	3/8" strand chucks, No. B610, Supreme Products Corp., Chicago 16, Illinois.
L	clips for holding side forms, C	9" lengths of 1/8"x1" steel strap bent to form 5¼" wide, spring-like clips.
M	strain-gage indicator	Type N, SR-4 strain gage indicator, Baldwin-Lima-Hamilton Corp., Waltham, Mass.
N	load cell switching box	Simple 4-wire, 2-channel switching unit, made with two 2-wire, 2-channel switches.
P	load cells	Refer to Appendix
R	prestressing jack	Gifford-Udall Prestressing Jack, U.S.A.
S	hydraulic pump	Model P76 "Porto-Power" hydraulic hand pump, Blackhawk Mfg. Co., Milwaukee, Wis.
T	3/8" prestressing strand	Supplied by Colorado Fuel and Iron Corp., Denver, Colorado.

utilization of these items is presented in the photographs of Figure 34, and reference to the identification letters of Figure 33 and Table VIII will be made in the following discussion to assist the reader in understanding these procedures.

Figure 34 describes, with photographs, the procedures followed for pretensioning the strands. Each casting bed was prepared for casting two slabs of equal stress.

The shortness of the slabs made it impossible to rely upon the concrete-to-steel bond strength for stress transfer. Thus it was decided to mount end-bearing plates, backed up by strand chucks, on the prestressing strand in the casting beds. These steel plates also served as part of the slab mold. In order to prevent as much prestress loss as possible, the chuck "body", or barrel, was welded to the plate, concentric with the strand hole in the center of the plate. Further, to prevent any losses due to slippage of the chuck "jaws", or grips, on the strand and in the barrel, the chucks were pre-seated on the strand prior to pretensioning the strand. Figure 34a shows the arrangement of the strand (T) and chuck-plate combinations (G) before seating, and Figure 34b illustrates how seating was accomplished. Note that the hydraulic jacking unit (R) is located at the "left" end of the casting bed in Figure 34b. With the jack in this position, the seatings of the chuck-plate combinations at the extreme right and second from the left are effected.

In turn, each "seating yoke" (D,E) was inserted between the appropriate bearing plate and the "left" end-plate of the casting bed.

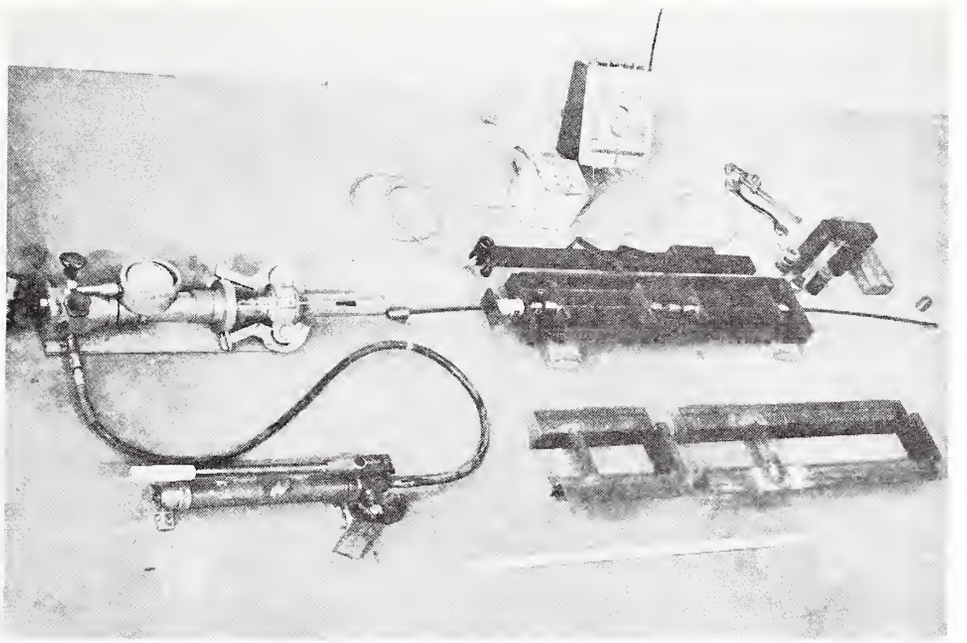

a. Initial arrangement.

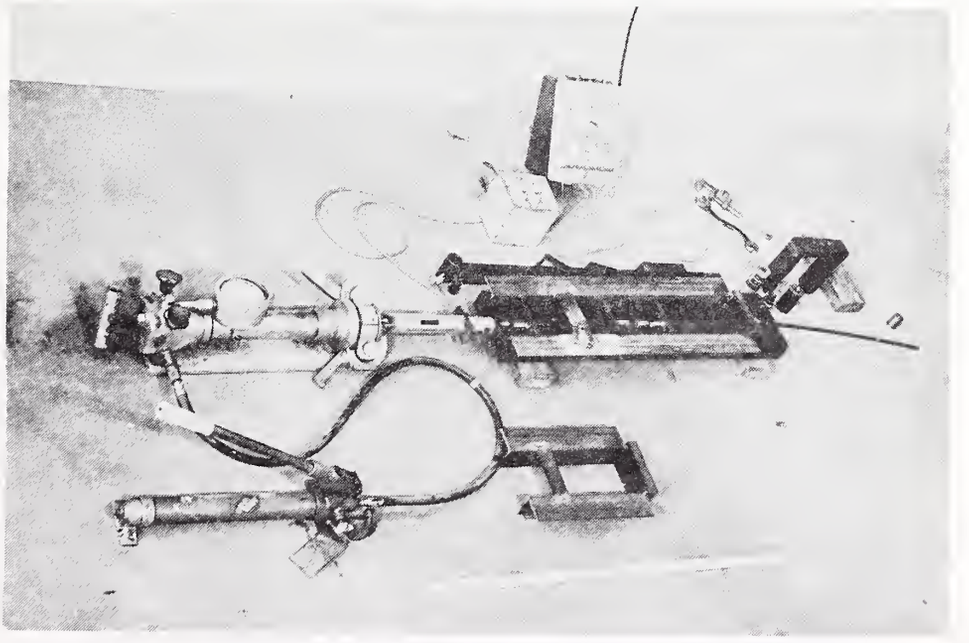

b. Seating of end-bearing plate.

Fig. 34. Pretensioning operations.

In Figure 34b the long "seating yoke" (E) is shown being used to seat the chuck-plate combination (G) at the far right. Each yoke was capable of transmitting the ultimate load capacity of the prestressing strand. All chucks were seated with a load of 14,500 pounds, which exceeded the design load for the slabs, thus reasonably assuring no losses due to slippage.

The load cell shown between the jack and the end plate of the casting bed, in Figure 34b indicated when the correct seating load was attained.

The jack was of the type that seizes a strand chuck (I) identical to those mounted with the end-bearing plates, but located on the strand exterior to the casting bed. Following the seating of the two chuck-plate combinations in Figure 34b, the jack was removed and the strand was severed about six inches from the end plate of the casting bed with an oxy-acetylene torch. This allowed removal of the load cell, and subsequent placement of another chuck (K) on the strand for final pre-tensioning.

The jack was then moved to the opposite, or "right" end of the casting bed. Figure 34c shows the arrangement for seating of the remaining two chuck-plate combinations, and final pretensioning of the strand. Note that the jack and load cell, in Figure 34c, do not bear directly on the end plate of the casting bed, as they did in Figure 34b. Rather, the load is transmitted to the casting bed by another yoke (F), bridging a hollow bolt and nut (H) and a larger chuck (K) mounted loosely on the strand.

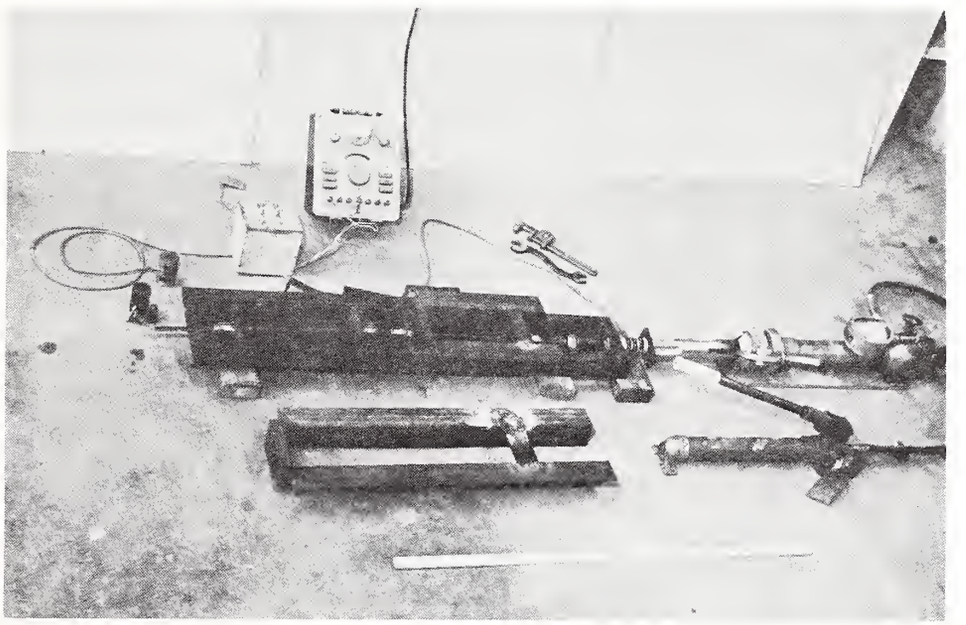

c. Continued seating from opposite end.

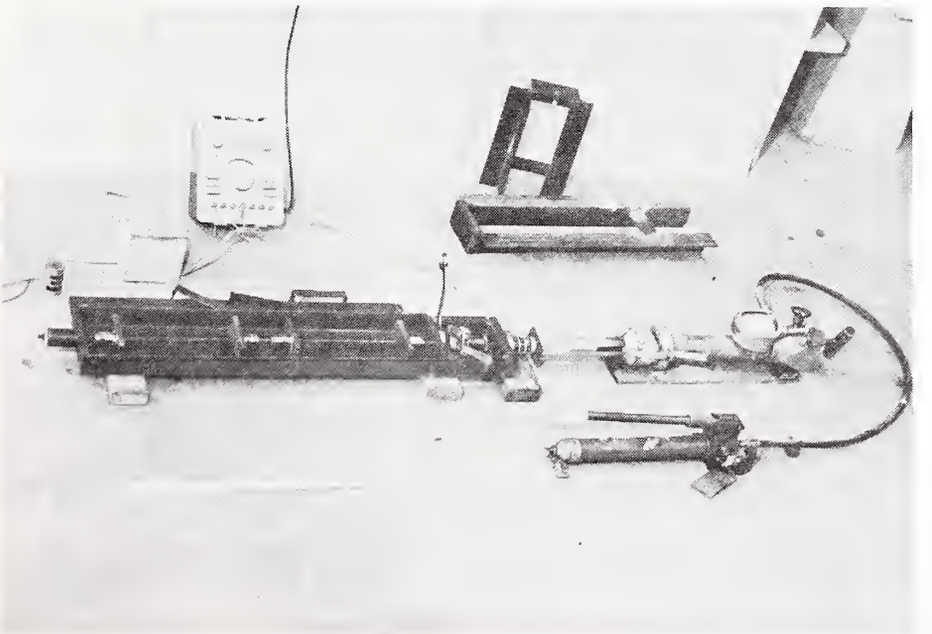

d. Loading and seating of exterior chuck.

Fig. 34. Pretensioning operations, continued.

With the jack located as in Figure 34c, the remaining two chuck-plate combinations (extreme left and second from right) were seated. Care was taken to space the slab end-bearing plates (G) on the strand so that, after seating, the clear distance between plates was about $10\frac{1}{2}$ inches. After seating each of the four chuck-plate combinations, the strand remained unstressed except for probable local stresses near the seated chucks. The steps for final tensioning of the entire strand will now be described. This discussion will be limited to 1200 psi. slab casting beds, and Table IX will summarize the pretensioning operation for both the 500 and 1200 psi. slab casting beds.

A chuck (K), similar to that mounted loosely on the strand in Figure 34c, was assembled and placed on the short length of strand extending out of the "left" end of the casting bed, and mounted in contact with the end plate of the casting bed. The strand was then loaded to 14,000 pounds with the jack, the load being indicated by the load cell. With the load held at 14,000 pounds, the other chuck (K) was assembled within the loading "yoke" (F) and placed snuggly against the hollow bolt and nut combination (H), which in turn was pushed into contact with the end plate of the casting bed. With the nut held fixed against the chuck with one wrench, the bolt was turned with another wrench so that a force was exerted between the end plate of the casting bed and the chuck. The arrangement for this operation is shown in Figure 34d. The bolt was turned until the load indicated by the load cell was decreased by 2000 pounds, that is, decreased to

a load of 12,000 pounds. This seating operation with the nut and bolt combination (H) assured a relatively constant slippage of the "right end chucks (K) for all casting beds which were for 1200 psi. slabs. The jack was then released, causing a seating of the chuck (K) with a load which was determined experimentally to be about 12,000 pounds. Next, the strand was reloaded to 14,000 pounds, followed by a second seating with the bolt and nut (H) until the load indicated by the load cell dropped to 12,500 pounds. The jack was then released, leaving a load in the strand of approximately 13,500 pounds. It should be noted that this procedure was developed by numerous trials with the aid of two load cells, one located as in Figure 34d and the other located between the chuck (K) and end plate at the "left" end of the casting bed.

Table IX summarizes these strand loading procedures, as well as those followed for loading the 500 psi. slab casting beds. In this table, the "Load in load cell" refers to the load measured by the cell located in the position shown in Figure 34d. The "Load in strand" is that load determined experimentally by previous trials with another load cell located between the chuck (K) and end plate at the opposite end of the casting bed.

TABLE IX

SUMMARY OF STRAND LOADING PROCEDURES

Step	Operation	For 500 p.s.i. casting beds		For 1200 p.s.i. casting beds	
		Load in load cell (Lbs.)	Load in strand (Lbs.)	Load in load cell (Lbs.)	Load in strand (Lbs.)
1	Jack	6,100	6,100	14,000	14,000
2	Tighten bolt and nut	5,100	6,700 ± 50	12,000	15,000 ± 100
3	Release jack	0	5,000 ± 200	0	12,000 ± 300
4	Re-jack	6,100	6,100	14,000	14,000
5	Re-tighten bolt & nut	5,300	5,900 ± 50	12,500	15,000 ± 50
6	Release jack	0	5,700 ± 200	0	13,500 ± 200

It should be mentioned that the strand loads immediately after step 6 in Table IX were somewhat higher than those given in the table. However, some slight "settling", or slippage, and perhaps some steel creep occurred for a short period after the final release of the jack. Therefore, the strand loads given in the table after step 6 represent the loads after the system had stabilized; usually these loads were obtained about one-half hour after the final release of the jack.

Note that the loads, 5,700 pounds and 13,500 pounds, result in somewhat higher than the desired stresses, 500 and 1200 psi., respectively, when divided by the slab cross-sectional area of nine square inches.

However, based upon expected values for percentage of prestress loss given by Lin (24) a loss of about 20 per cent was anticipated. Thus, the expected final loads in the stressed slabs were 4,560 and 10,800 pounds, respectively.

After step 6 in Table IX, the jack was removed and the strand was severed with the oxy-acetylene torch, adjacent to the chuck (K) at the "right" end of the casting bed. The stressed casting bed, shortly after the strand had been severed, is shown in Figure 34e. Two long steel bars (C) were then placed in the casting bed to serve as the side forms for the slabs. These were held in place adjacent to the slab end-bearing plates by three "clips" (L), as illustrated in Figure 34f.

Figure 35a is a photograph of the casting bed after the pretensioning operation had been entirely completed. Figure 35b is a photograph of three casting beds prior to casting, one for each of the three stress levels. The casting bed at the extreme left is for non-stressed slabs and, therefore, has no chucks attached to the end-bearing plates. These plates are held in place merely by the force of the small steel clips which hold the form sides against the plates. The strands in the non-stressed casting beds were nominally loaded with the nut and bolt arrangement (H) merely to remove the natural strand curvature which results from being supplied on a "spool". The casting bed in the center is for 500 psi. slabs, and that on the right is for 1200 psi. slabs. Note that the higher stressed casting bed on the right is stiffened with small steel angles welded to the channel flanges. Note

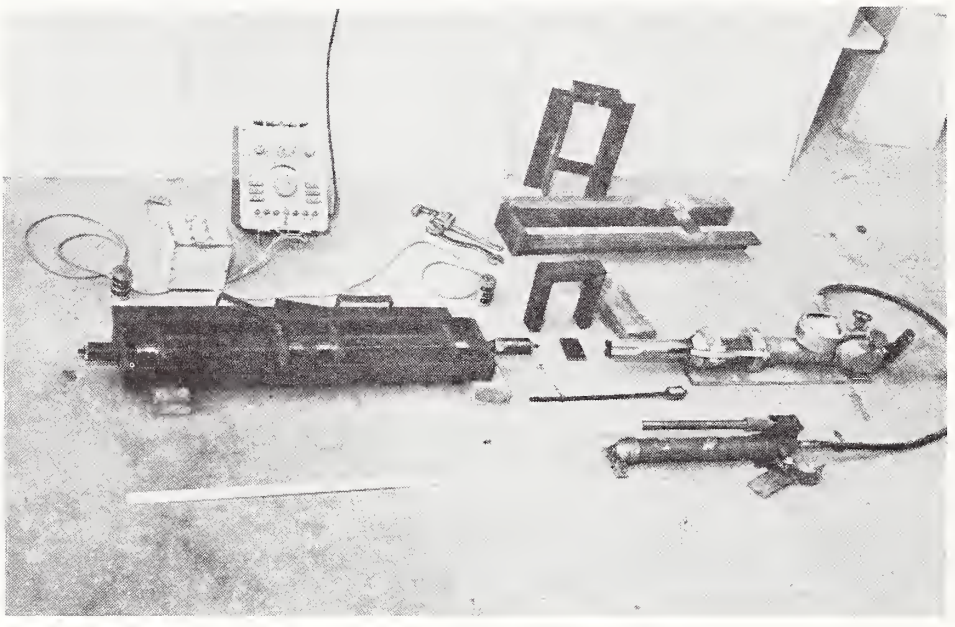

e. Jack removed and exterior strand severed.

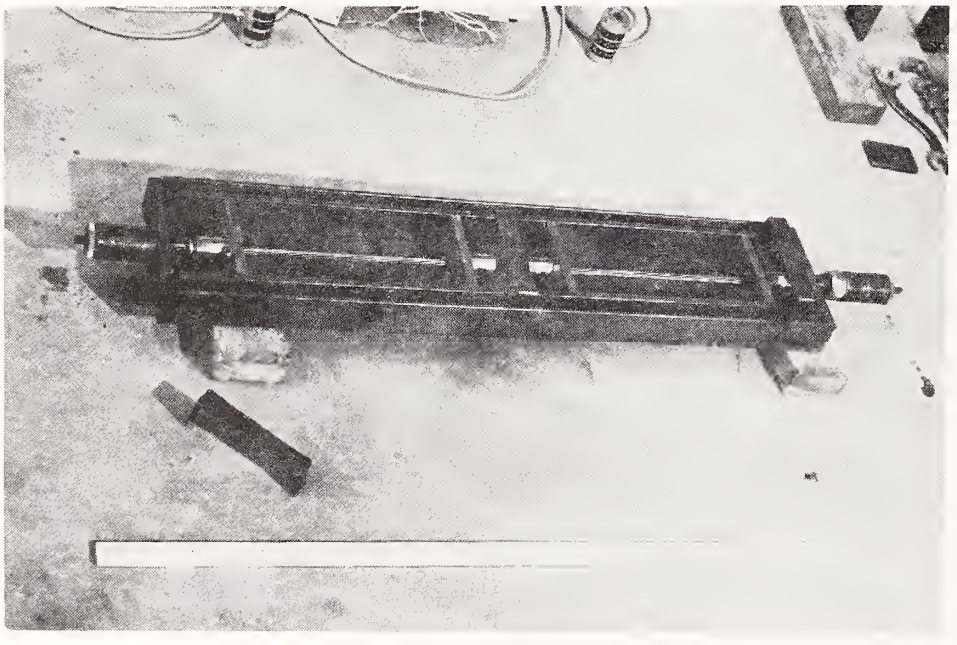

f. Side forms inserted and clipped into position.

Fig. 34. Pretensioning operations, continued.

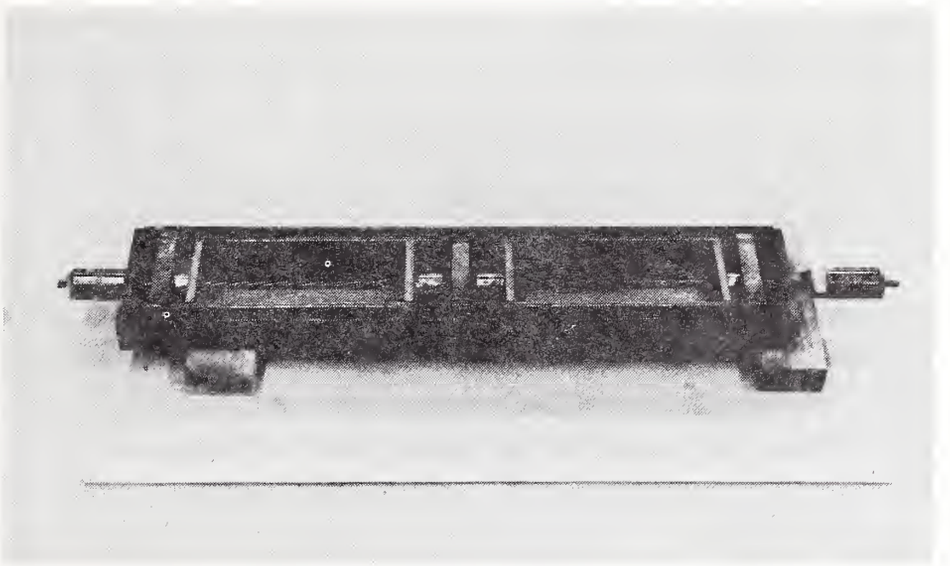

a. Casting bed prepared in Figure 34.

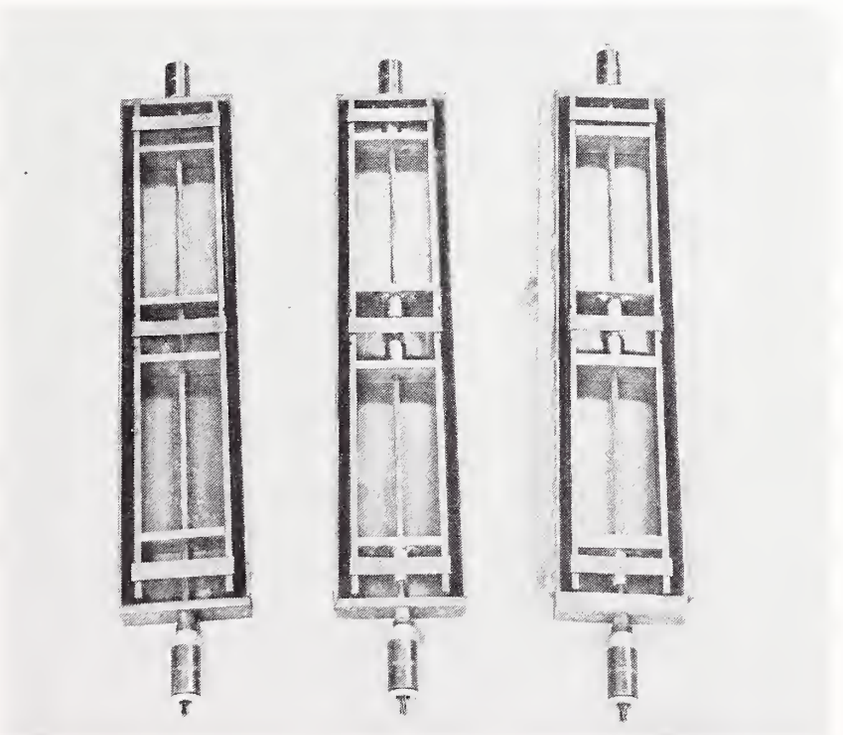

b. Casting beds ready for casting. (from left: for zero, 500, and 1200 psi. slabs)

Fig. 35. Pretensioned casting beds.

also that the end-bearing plates in the higher stressed casting bed are of 3/4 inch thick steel, while those in the center, or 500 psi., casting bed are of 1/2 inch thick steel.

The interior surfaces of the channel section webs served as the floors of the slab molds. All steel mold surfaces, except for the end-bearing plates, were coated with a thin oil film before casting to facilitate removal of the slabs after curing.

APPENDIX B

MATERIALS (23)

CONCRETE MATERIALS

Concrete mix information

The concrete mix was designed by the method prescribed by the Portland Cement Association (25) on the basis of Type I cement for a 28-day compressive strength of 4000 psi. The desired slump was two inches, and no air-entraining admixtures were used since it was desirable to reduce the frost resistance of the concrete as much as possible, and yet retain concrete quality commensurate with good field practice. This mix, for 3/4 inch maximum sized aggregate, called for a sand content of about 42 percent of the total aggregate weight.

Since control of the concrete mixes was most important, it was decided to oven dry all aggregate, separate it into standard sieve sizes, and then recombine for mixing. Thus, based upon the value of 42 percent for the sand content, composite gradation limit curves for the combined coarse and fine aggregate were plotted according to A.S.T.M. Designation: C 33-54T, Tentative Specifications for Concrete Aggregates (25). These limits are shown in Figure 38.

Subsequent trial mixes resulted in slight modifications of the original mix design. Note that the material quantities are given for a two-cubic foot mix, since this was the actual volume mixed for each batch.

All aggregate was dried for 24 hours at 110°C in a small laboratory oven*, and then separated into the sieve sizes indicated.

---

* Laboratory Oven, 1200 watts, American Instrument Co.

TABLE X

CEMENT CHEMICAL ANALYSIS

Oxide	Per cent of total	Phase	Per cent of total
SiO_2	23.26	C_3S	46.3
Al_2O_3	3.97	C_2S	31.0
Fe_2O_3	4.33	C_3A	3.2
CaO	64.10	C_4AF	13.1
SO_3	1.75		
ignition loss	1.09		

Type of cement: Type II

Supplier: Ideal Cement Company
Trident, Montana

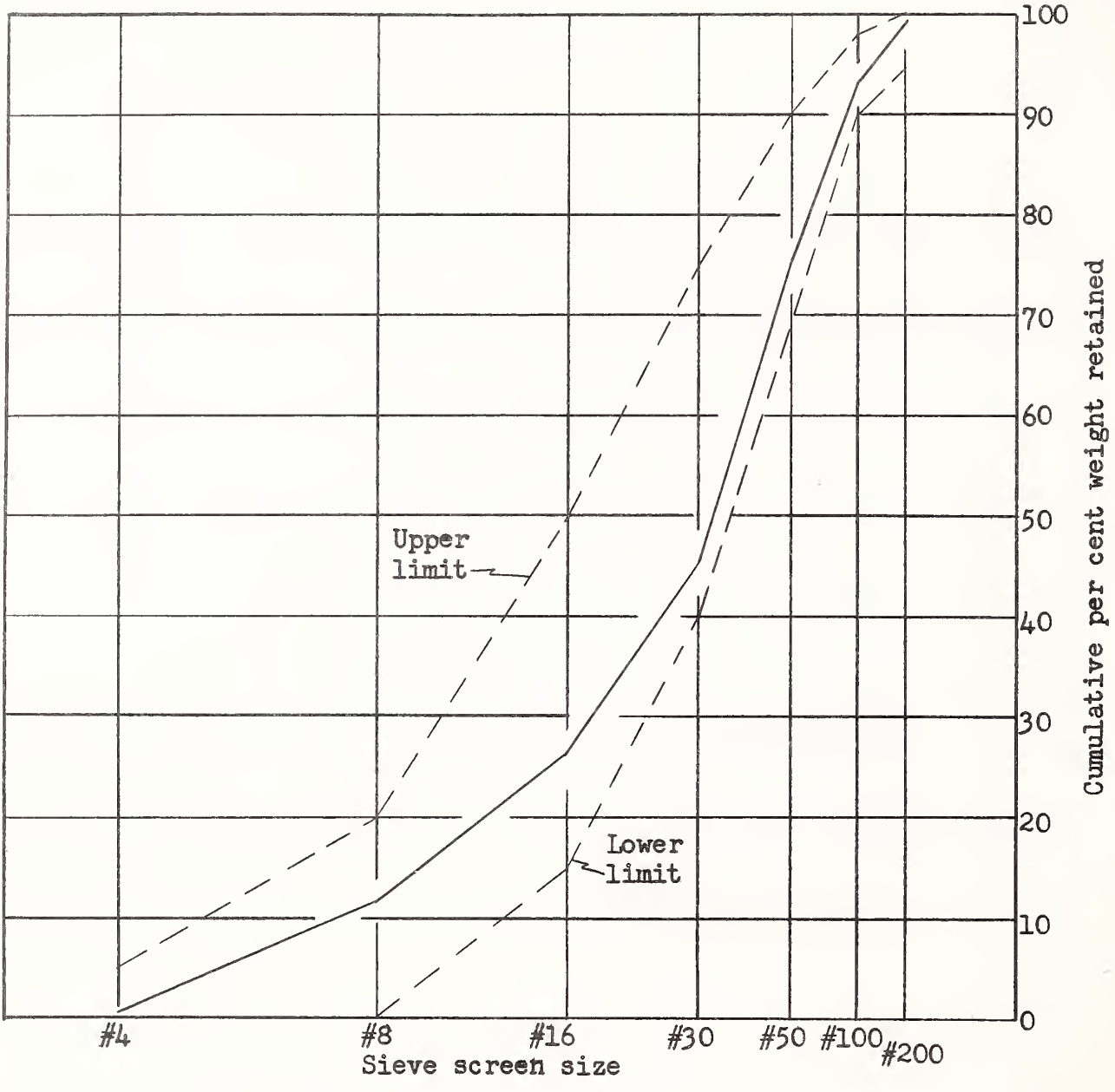

Fig. 36. Fine aggregate gradation.

Fine Aggregate Properties

Unit weight = 101.7 p.c.f.
Bulk specific gravity (A.S.T.M. Des. E12) = 2.572
Bulk specific gravity (saturated surface-dry) = 2.612
Apparent specific gravity (A.S.T.M. Des. E12) = 2.682
Moisture content (saturated surface-dry), by weight = 1.585%
Organic impurities: negligible
Fineness modulus = 2.53

Supplier: Pioneer Ready Mix Co.
Bozeman, Montana

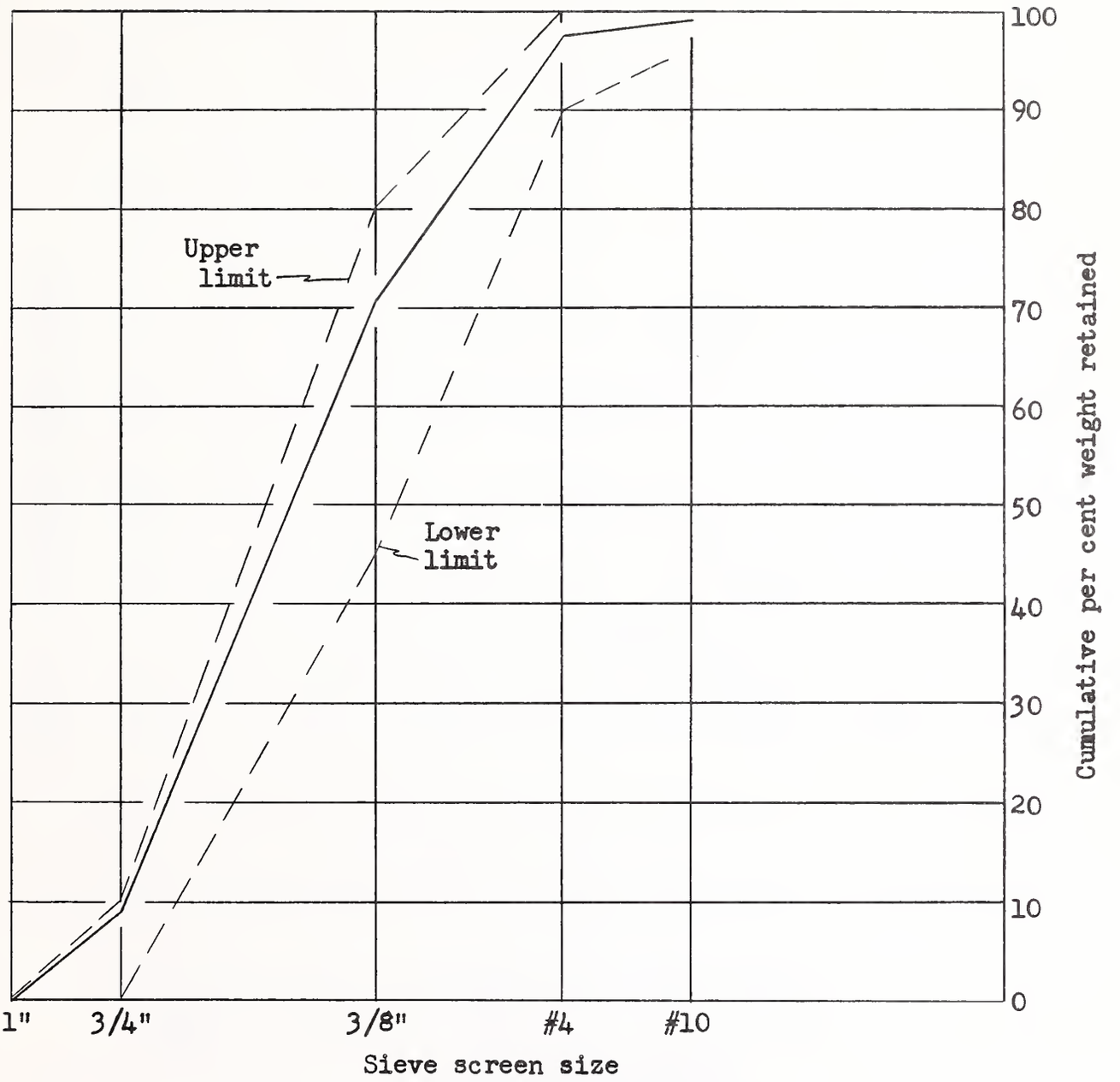

Fig. 37. Coarse aggregate gradation.

Coarse Aggregate Properties

Unit weight = 105.3 p.c.f.
Bulk specific gravity (A.S.T.M. Des. E12) = 2.60
Bulk specific gravity (saturated surface-dry) = 2.635
Apparent specific gravity (A.S.T.M. Des. E12) = 2.695
Moisture content (saturated surface-dry), by weight = 1.354%

Supplier: Pioneer Ready Mix Co.
Bozeman, Montana

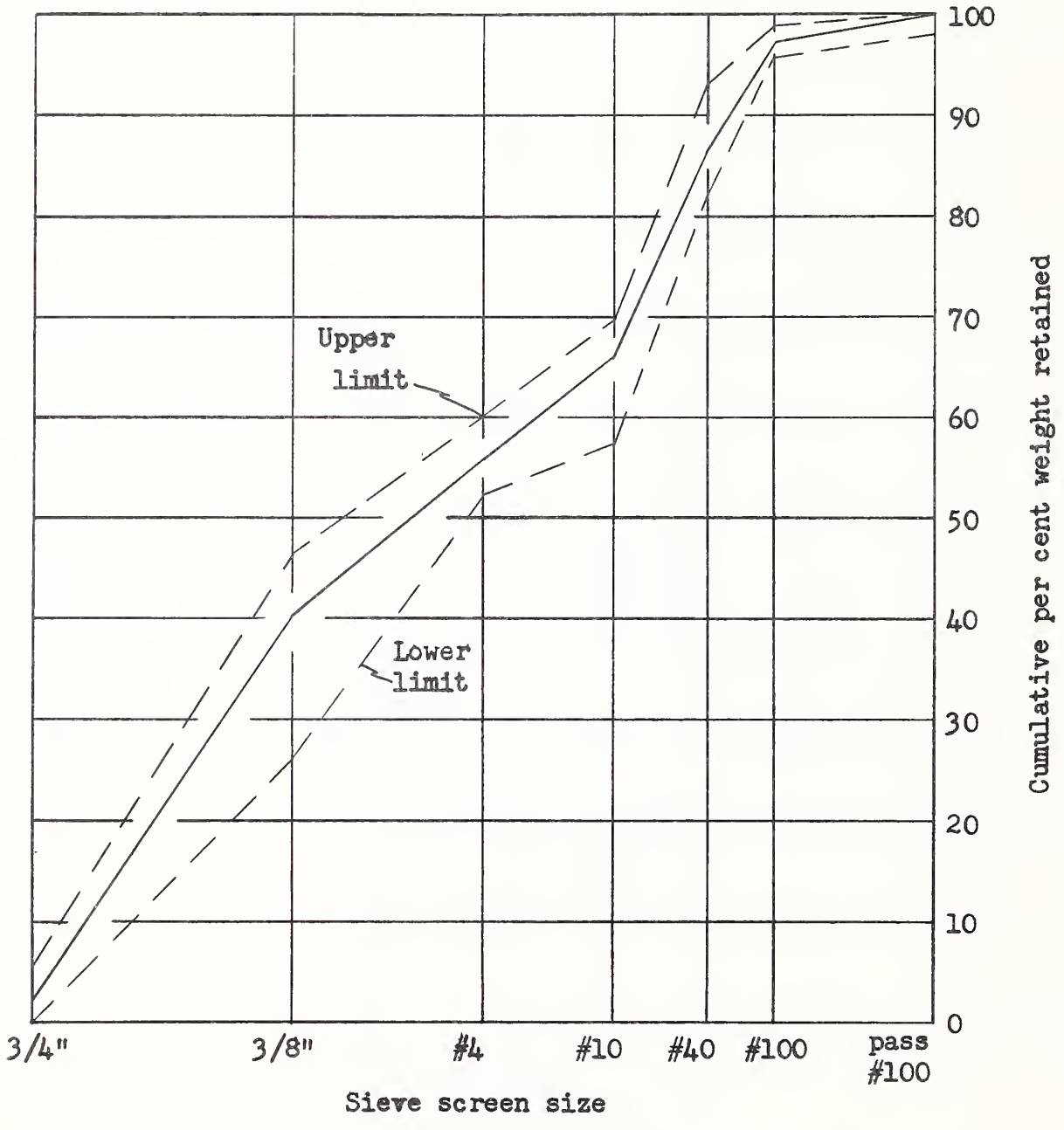

Fig. 38. Combined aggregate gradation for each concrete batch.

Separation was accomplished with a large sieve shaker*. The various sizes of aggregate were then stored in large, covered, cardboard containers, and protected from moisture.

All mixing was done in a large laboratory mixer**, pictured in Figure 40, which has a recommended capacity of about $1\frac{1}{2}$ cubic feet. However, trial mixing showed that two-cubic foot mixes were not excessive. It was desired to obtain one slab for each combination of treatments from each concrete batch, so that the ninety-six required slabs could be made with four concrete batches. A minimum volume of two cubic feet was required for 24 slabs plus enough excess concrete for air content tests or for fabrication of four small cylinders for compressive tests. Larger batches would have been desirable, since removal of enough material for compressive tests cylinders prohibited a measurement of the air content by a pressure method. It was even necessary to return to the mixer all concrete used for slump and unit weight determinations--an inadvisable practice at best.

Therefore, compressive test cylinders were drawn from only half of the batches, while air content determinations by the pressure method were made on the remaining batches. In addition, air content measurements were made on all batches with an AE-55 Air Indicator*.

---

* Gilson Testing Screen, Gilson Screen Company, Malinta, Ohio.

** Lancaster Counter Current Batch Mixer, Type SKG, Posey Iron Works, Inc. Lancaster, Pennsylvania

*** AE-55 Air Indicator, Model CT-158, Soiltest, Inc., Chicago 39, Ill.

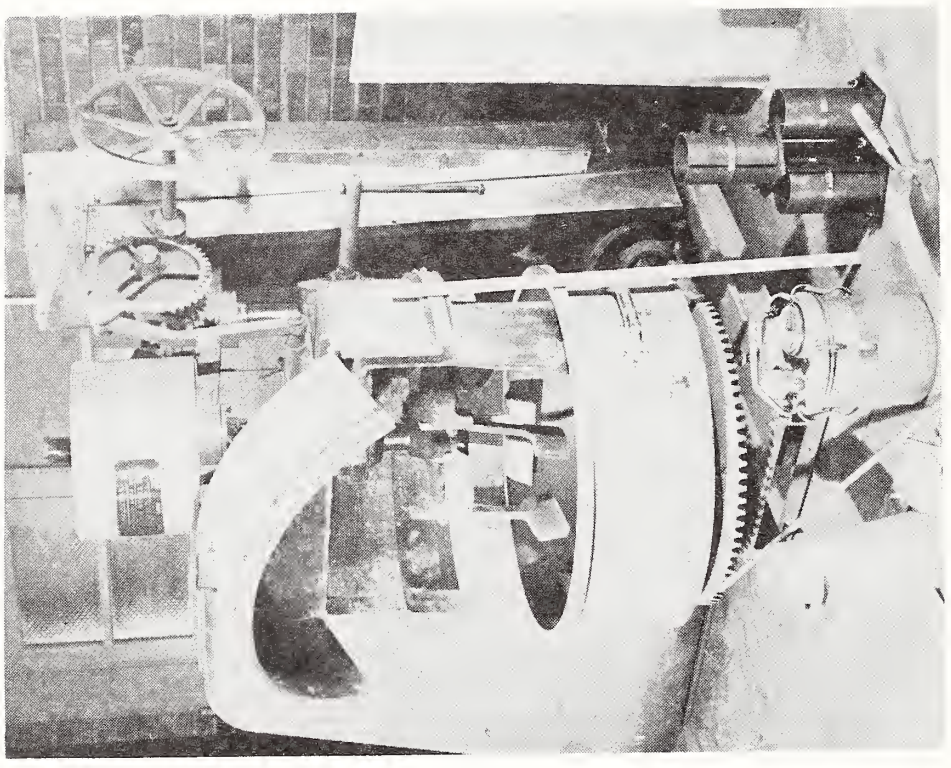

Fig. 40. Lancaster mixer and incidental apparatus.

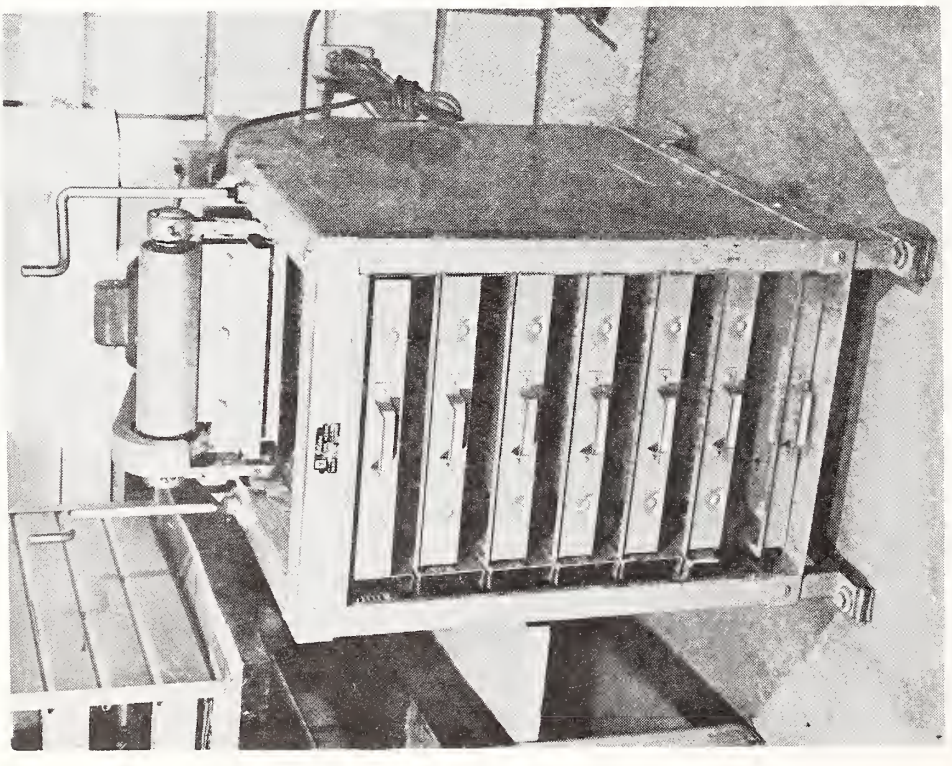

Fig. 39. Gilson testing screen.

This method is not considered to be as reliable as the pressure method, although Newlon (26) has reported that the average air content, as determined by the AE-55 Air Indicator, will be within 1/2 percentage point of air as compared with the pressure method. He also found that the AE-55 Air Indicator tended to give readings which were too high for mortar of low air content, and vice versa.

The procedure followed for mixing each concrete batch was as follows:

1) The appropriate weights of each size of aggregate plus the prescribed weight of cement were added to the mixer tub and dry-mixed for one minute.
2) The proper quantity of water was added to the mixer, and mixing was continued for two minutes.
3) Mixing was stopped and a slump test was performed according to A.S.T.M. Designation C143-52.
4) The slump material was returned to the mixer, and the concrete was remixed for an additional 10 seconds.
5) Mixing was again stopped to perform the unit weight and air content tests. The unit weight was obtained by filling the 1/4 cubic foot container which was part of the pressure method air meter* used in this study. Filling of this container was in accordance with the instructions for molding concrete compression specimens, as contained in A.S.T.M. Designations C31-49 and C192-54.

---

* Techkote White Air Meter, Capacity: 0.25 cu. ft., Presstite Division, American-Marietta Co., El Segundo, California.

TABLE XI

MATERIAL QUANTITIES FOR EACH 2 CU. FT. BATCH

Material	Description	Weight (Lbs.)
Aggregate	passing 1" sieve, but retained on 3/4" sieve	4.5
	" 3/4" " " " " 3/8" "	86.0
	" 3/8" " " " " #4 "	35.1
	" #4 " " " " #10 "	23.0
	" #10 " " " " #40 "	46.1
	" #40 " " " " #100 "	23.8
	passing #100 sieve	6.5
Cement	Type II	46.8
Water	tap water @ approx. 68°F	23.32

TABLE XII

INDIVIDUAL CONCRETE BATCH PROPERTIES

Batch	Slump (in.)	Unit weight (p.c.f.)	Air content (%)	
			Pressure method	AE-55 Air Indicator
21	1-1/2	147.9	2.0	3
22	1-3/4	148.0		3
23	1-3/4	148.3	1.9	3
24	2	147.7		3

Additional data common to each batch

Cement Factor = 6.73

Water/Cement (W/C) Ratio = 0.499 = 5.64 gal./sk.

Following the unit weight determination, the air content was measured either with the AE-55 Air Indicator, or with both the AE-55 Air Indicator and the pressure meter, depending upon whether compressive test cylinders were to be made. For those batches from which test cylinders were to be obtained, the material for the unit weight test was returned to the mixer, and the air content was determined by averaging the results from two tests made with the AE-55 Air Indicator. (See reference 26 for a description of the test procedure.) For those batches from which no cylinders were to be secured, the above procedure for determining the air content was also followed. In addition, a determination of the air content was made by the pressure method on the material used for the unit weight determination, according to the manufacturer's directions. This material was then discarded, since the test method necessitated an addition of water to the test sample.

6) The concrete was then mixed for an additional 10 seconds, prior to casting of the slabs.

Fabrication of slabs

Casting was initiated immediately after the final step of the mixing operation. The fabrication of each pair of slabs was accomplished by the following procedure:

1) The casting bed was secured to the surface of a specially constructed vibration table, shown in Figure 41.

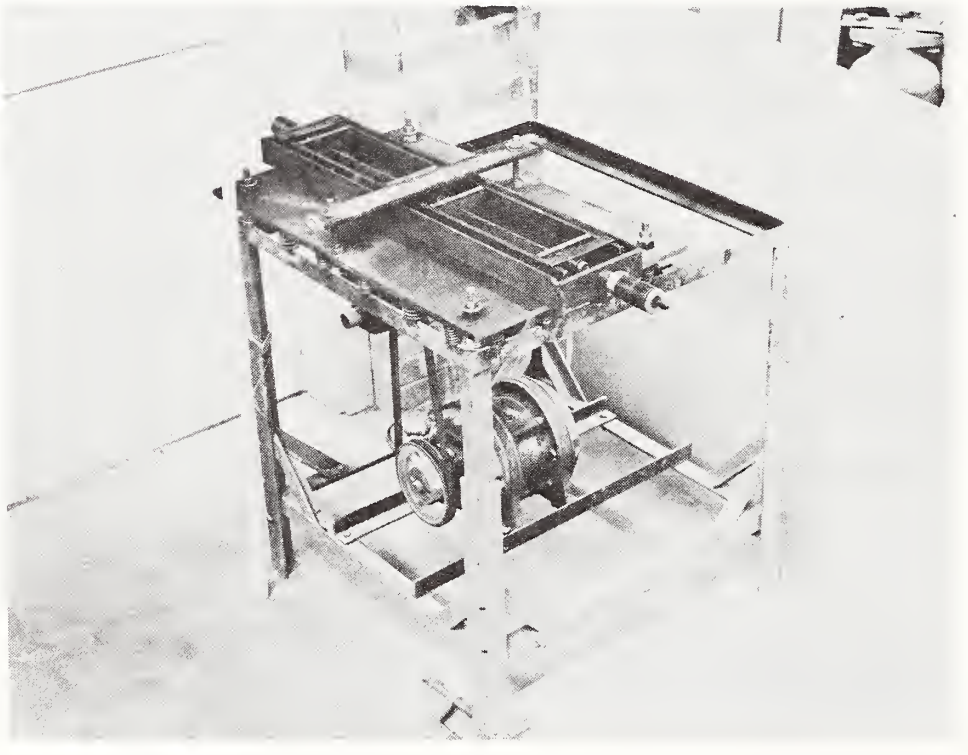

Fig. 41. Vibration table with casting bed in place.

2) Each mold was slightly overfilled with concrete, and the concrete was gently maneuvered into the corners of the mold, and beneath the strand, with a large steel trowel.

3) The casting bed was then vibrated for seven seconds, and the excess concrete was "struck off" with the trowel. The frequency of vibration was approximately 4200 c.p.m.

4) The casting bed was re-vibrated for three seconds, in order to better the compaction and to close surface voids resulting from removal of the excess material in step 3.

5) Following vibration, the surface of each slab was finished by making three passes, with slight circular motion, with a damp-surfaced wooden float, $1\frac{1}{4}$ inch in width.

6) The casting bed was then released from the vibration table, and set aside in the laboratory.

7) After casting each pair of slabs, the remaining concrete was remixed for five seconds, in an attempt to retain workability and homogeneity.

The above steps were followed for each of the twelve casting beds. For those batches from which cylinders were obtained, the procedural cycle was interrupted after half the slabs had been cast (i.e., after the sixth casting bed had been filled) in order to cast four compressive test cylinders. It should also be mentioned that the concrete mixer tub remained covered at all times during the casting procedure, except for removal of concrete. This was done in order to prevent as much variation, due to moisture evaporation loss, as was possible.

Casting began about one-half hour after the addition of water to the mixer. About one hour was required to cast all 24 slabs, and approximately 20 additional minutes were required for those batches from which test cylinders were cast. Thus, an inherent variation was realized due to the length of time required for testing of the fresh

TABLE XIII

CONCRETE CYLINDER COMPRESSIVE TEST RESULTS

Batch	Cylinder	Curing procedure	Age at test (days)	Strength (psi.)
22	1	continuous moist-room	7	3760
	2	18 hours steam cure, remainder in moist-room	7	4970
	3	continuous moist-room	28	4900
	4	18 hours steam cure, remainder in moist-room	28	6240
24	1	continuous moist-room	7	3385
	2	18 hours steam cure, remainder in moist-room	7	4430
	3	continuous moist-room	28	4740
	4	18 hours steam cure, remainder in moist-room	28	6045

Additional compression test information

Nominal cylinder dimensions: Batch 22, 3-1/3" x 6-2/3"
Batch 24, 3-3/4" x 7-1/2"

Casting procedure: All cylinder molds affixed to vibrating table, overfilled in a single lift, and vibrated for six seconds at approximately 4200 cpm.

Capping procedure: All cylinders capped with sulfur capping compound one day before testing.

Testing procedure: All cylinders loaded at 20,000 lbs./min. (approximately 35 psi./sec.) with a Model MCA-300 Riehle Testing Machine, American Machine and Metals, Inc., Riehle Testing Machines Division, East Moline, Illinois.

concrete properties and for casting.

To remove the inherent variability due to the lengthy mixing and casting time, an attempt to randomize the rank in time of casting, for each pair of slabs, was made. Table XIV gives the time of casting, in minutes after addition of water to the mixer, for each pair of slabs from each batch. Thus, for example, slabs 1 and 2 from batch number 21 were cast only one-half hour after mixing began, while the duplicate slabs, 1 and 2, from batch number 24 were cast about $1\frac{1}{2}$ hours after mixing was started. Hopefully this arbitrary scheduling reduced or eliminated the effect of varying fresh concrete age, at time of casting, upon the results of this study.

TABLE XIV

CASTING SCHEDULES

Time after mixing (minutes)	Slab numbers			
	Batch 21	Batch 22	Batch 23	Batch 24
0	add water	add water	add water	add water
30	1, 2	23, 24	21, 22	9, 10
35	15, 16	9, 10	11, 12	7, 8
40	17, 18	1, 2	5, 6	19, 20
45	5, 6	19, 20	17, 18	13, 14
50	11, 12	13, 14	15, 16	3, 4
55	21, 22	3, 4	1, 2	21, 22
60	3, 4	cast cylinders	23, 24	cast cylinders
65	13, 14	" "	9, 10	" "
70	19, 20	" "	7, 8	" "
75	7, 8	21, 22	19, 20	11, 12
80	23, 24	11, 12	13, 14	5, 6
85	9, 10	5, 6	3, 4	17, 18
90		17, 18		15, 16
95		15, 16		1, 2
100		7, 8		23, 24

After all slabs had been cast, a shallow, circular impression was made in the surface mortar of those slabs assigned to the permeability study using one of the "bottomless" milk bottles which served as standpipes. This was done so that bonding of the standpipes after curing could be accomplished more easily and accurately.

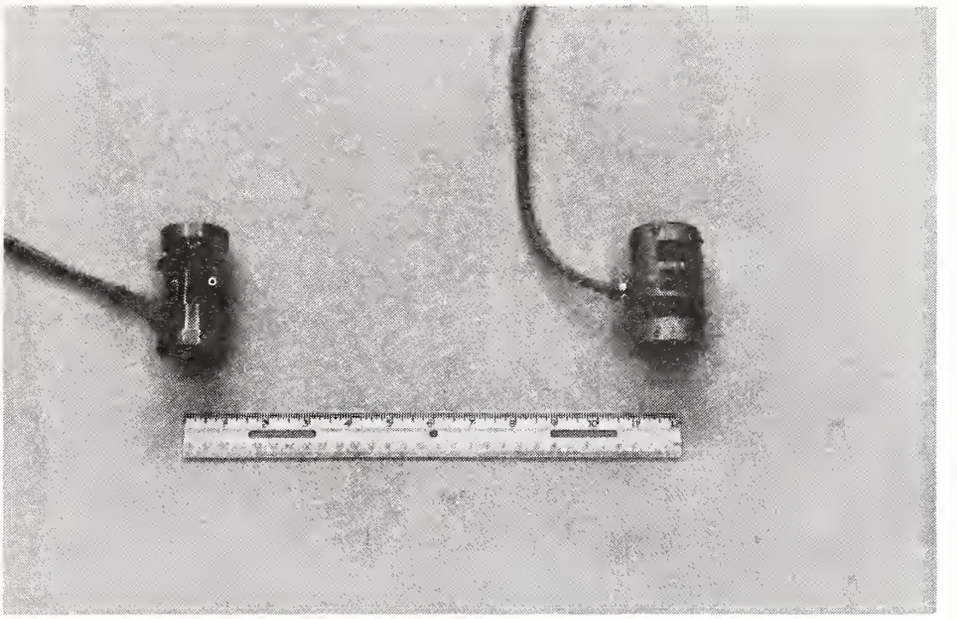

a. Load cells with and without protective shields, showing orientation of strain gages.

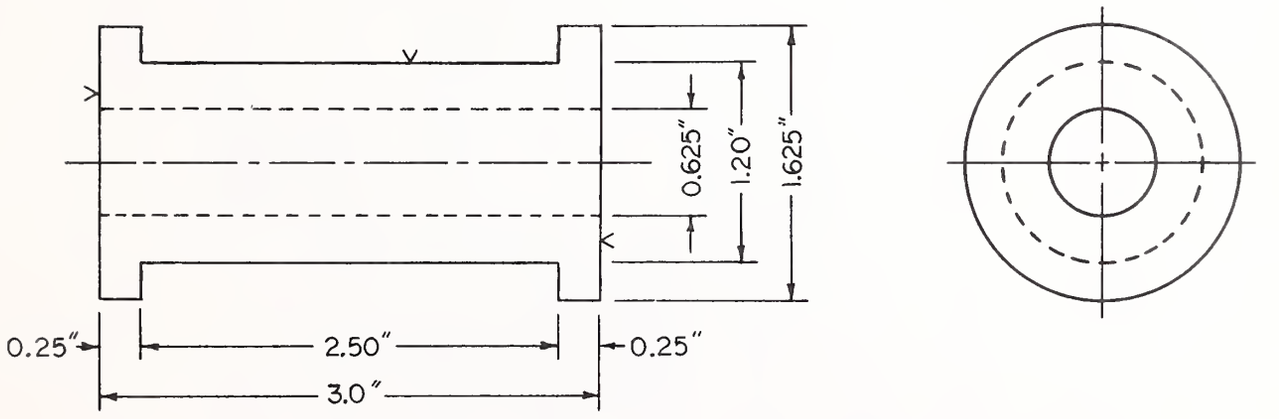

MAT'L.: 1020 C.R. STEEL

b. Load cell dimensions.

Fig. 42. Load cell description.

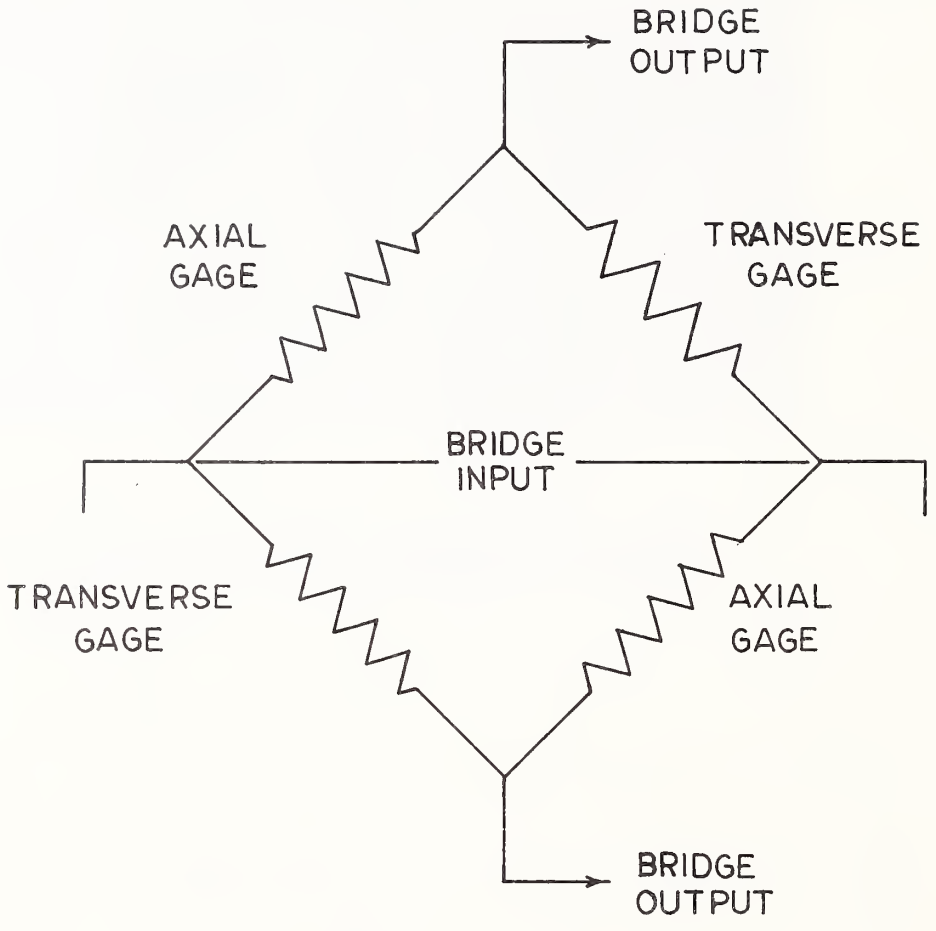

Fig. 43. **Bridge arrangement for load cells (25).**

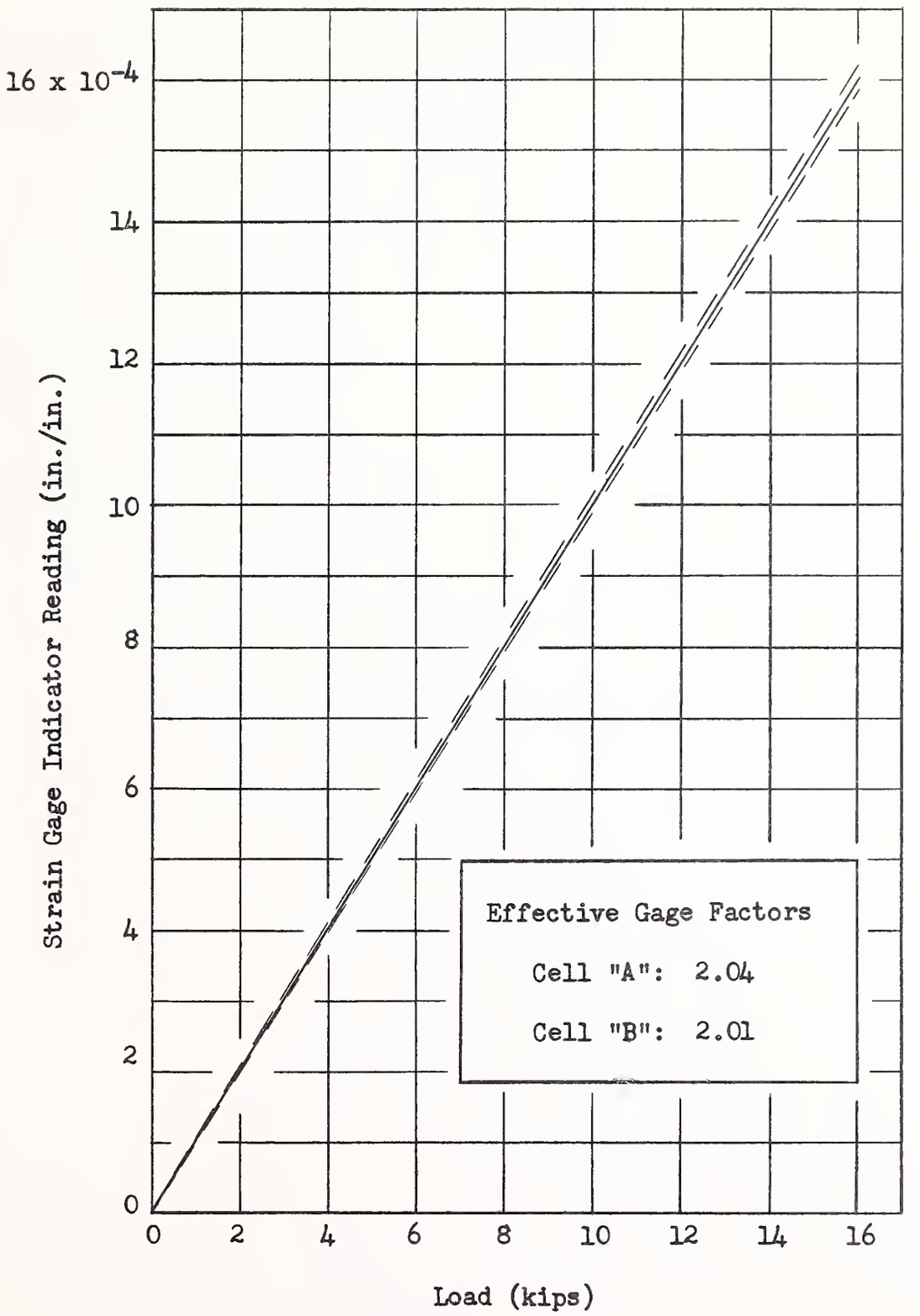

Fig. 44. Calibration curves for load cells, with error limits shown.

APPENDIX C

INDIVIDUAL DATA RECORDS

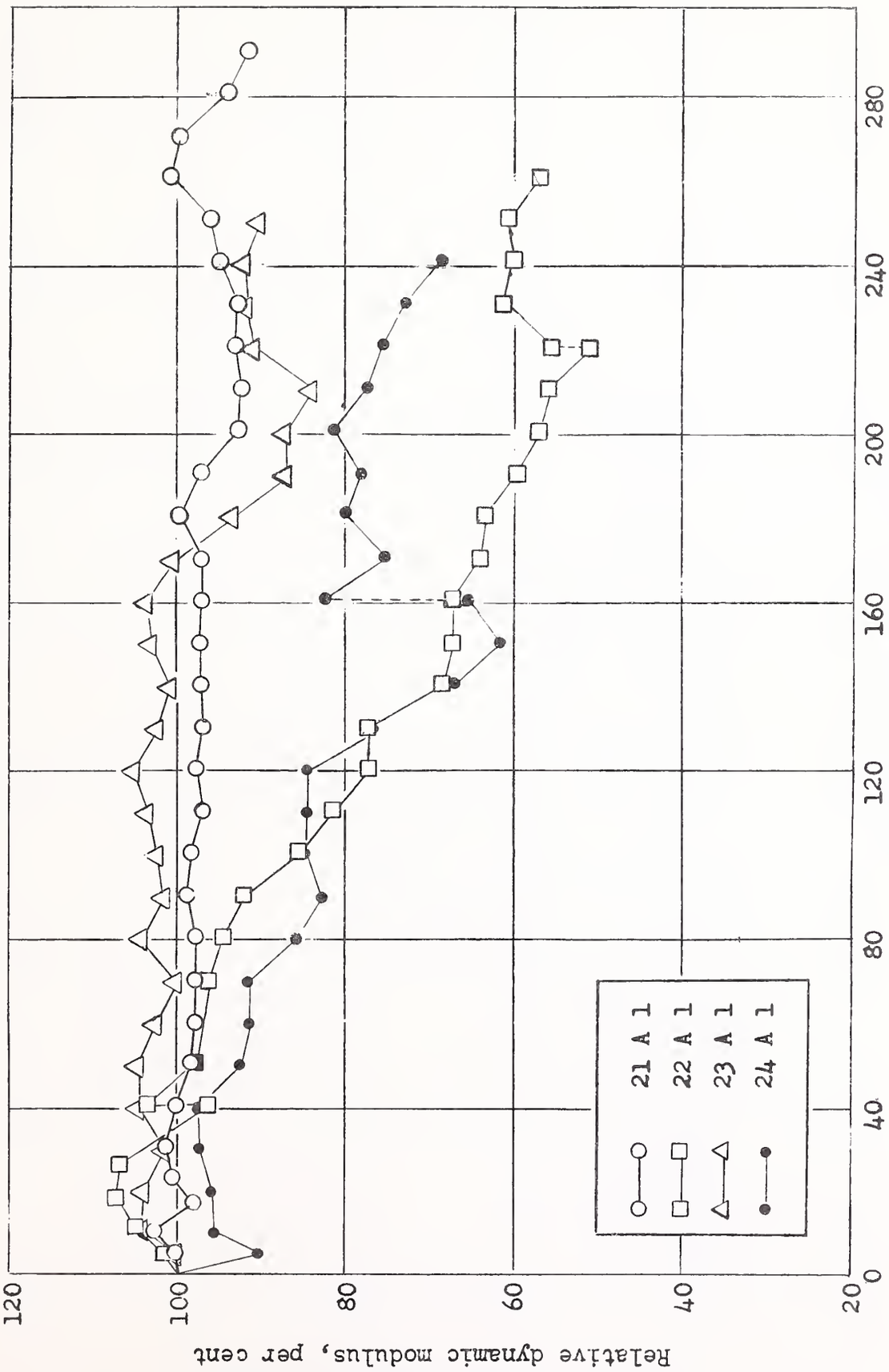

Fig. 45. Relative dynamic moduli of elasticity versus number of freeze-thaw cycles for non-stressed, normally cured, water ponded slabs.

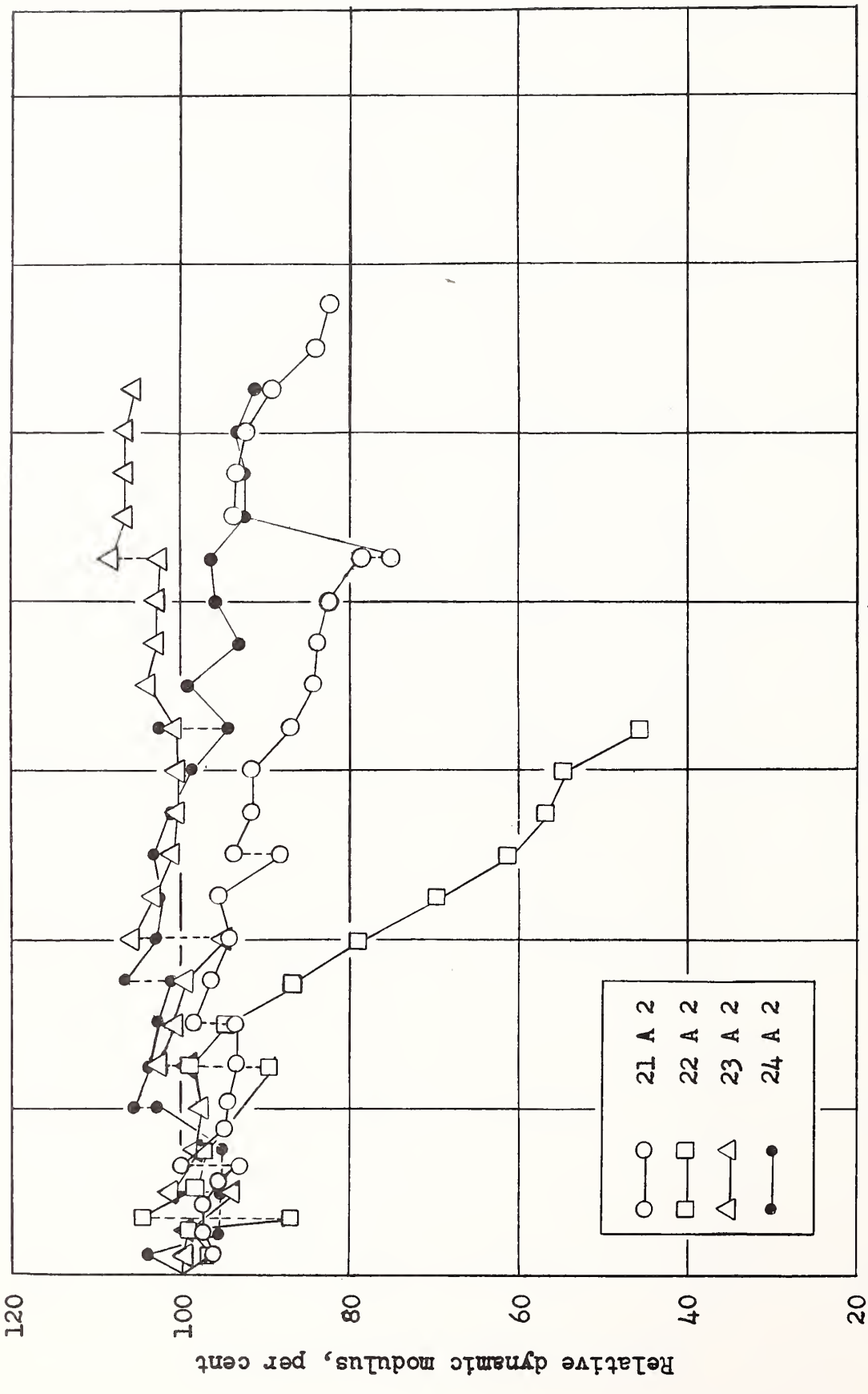

Fig. 46. Relative dynamic moduli of elasticity versus number of freeze-thaw cycles for non-stressed, normally cured, $CaCl_2$ solution ponded slabs.

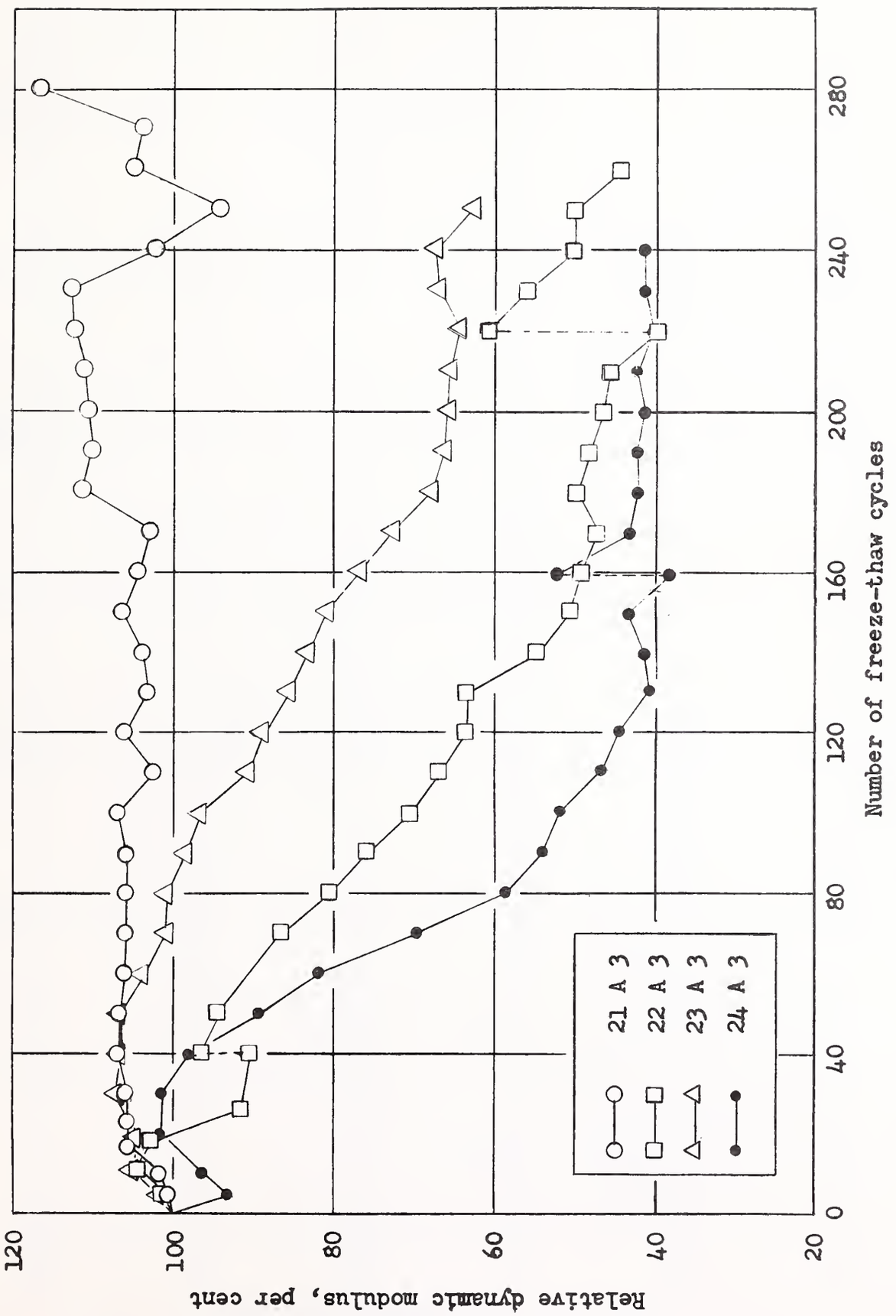

Fig. 47. Relative dynamic moduli of elasticity versus number of freeze-thaw cycles for non-stressed, steam cured, water ponded slabs.

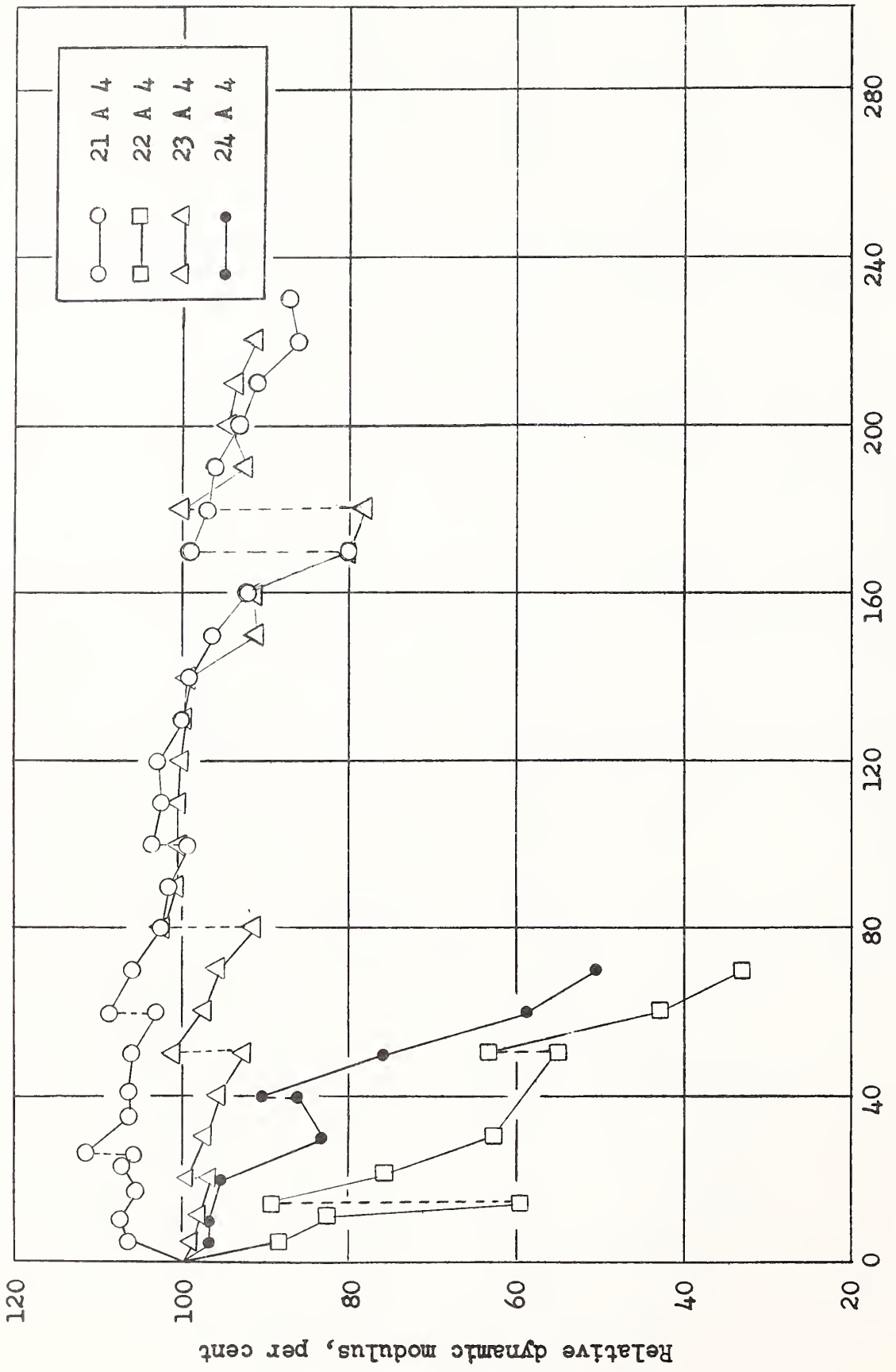

Fig. 48. Relative dynamic moduli of elasticity versus number of freeze-thaw cycles for non-stressed, steam cured, $CaCl_2$ solution ponded slabs.

Fig. 49. Relative dynamic moduli of elasticity versus number of freeze-thaw cycles for 500 psi., normally cured, water ponded slabs.

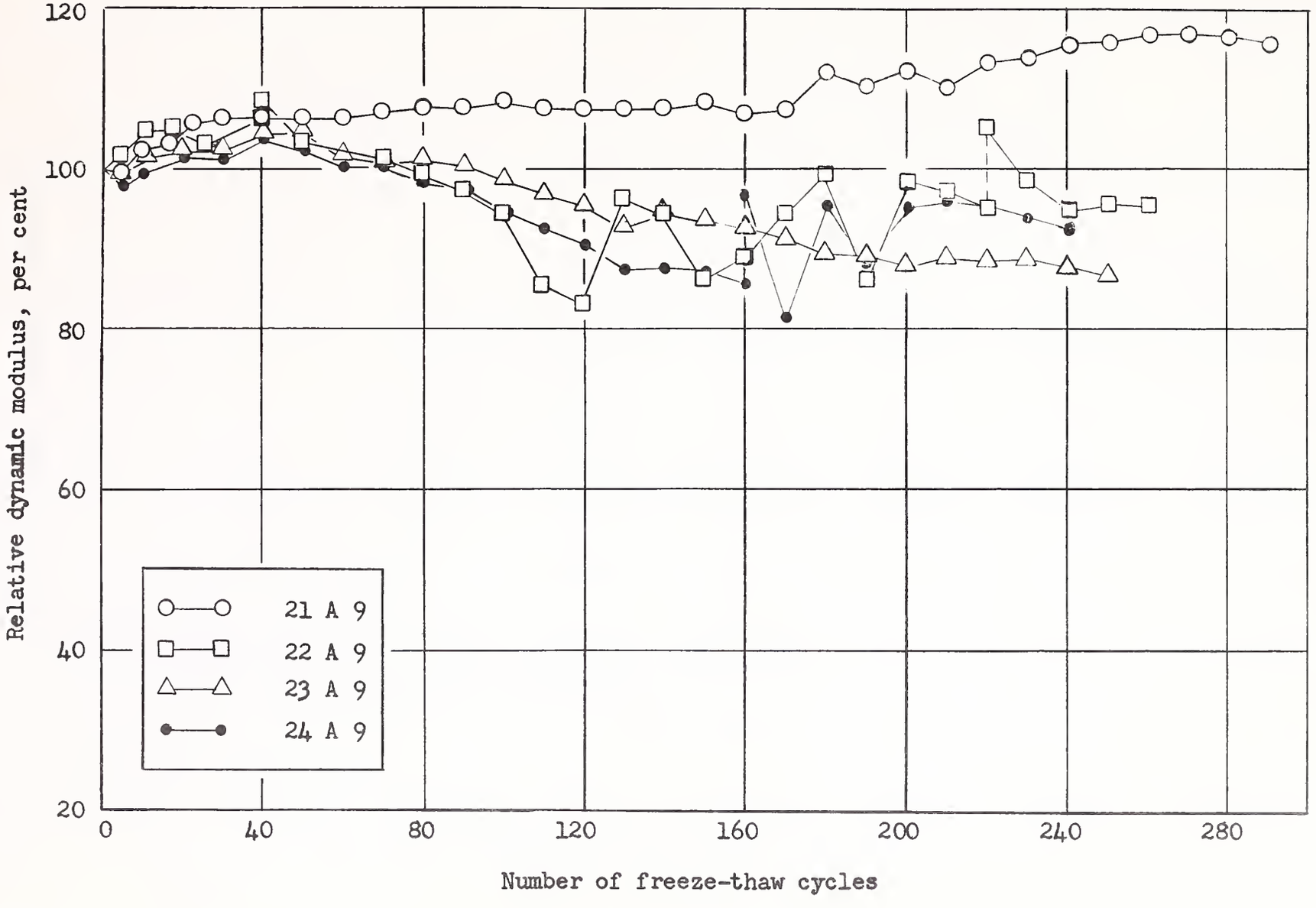

Fig. 50. Relative dynamic moduli of elasticity versus number of freeze-thaw cycles for 500 psi., normally cured, $CaCl_2$ solution ponded slabs.

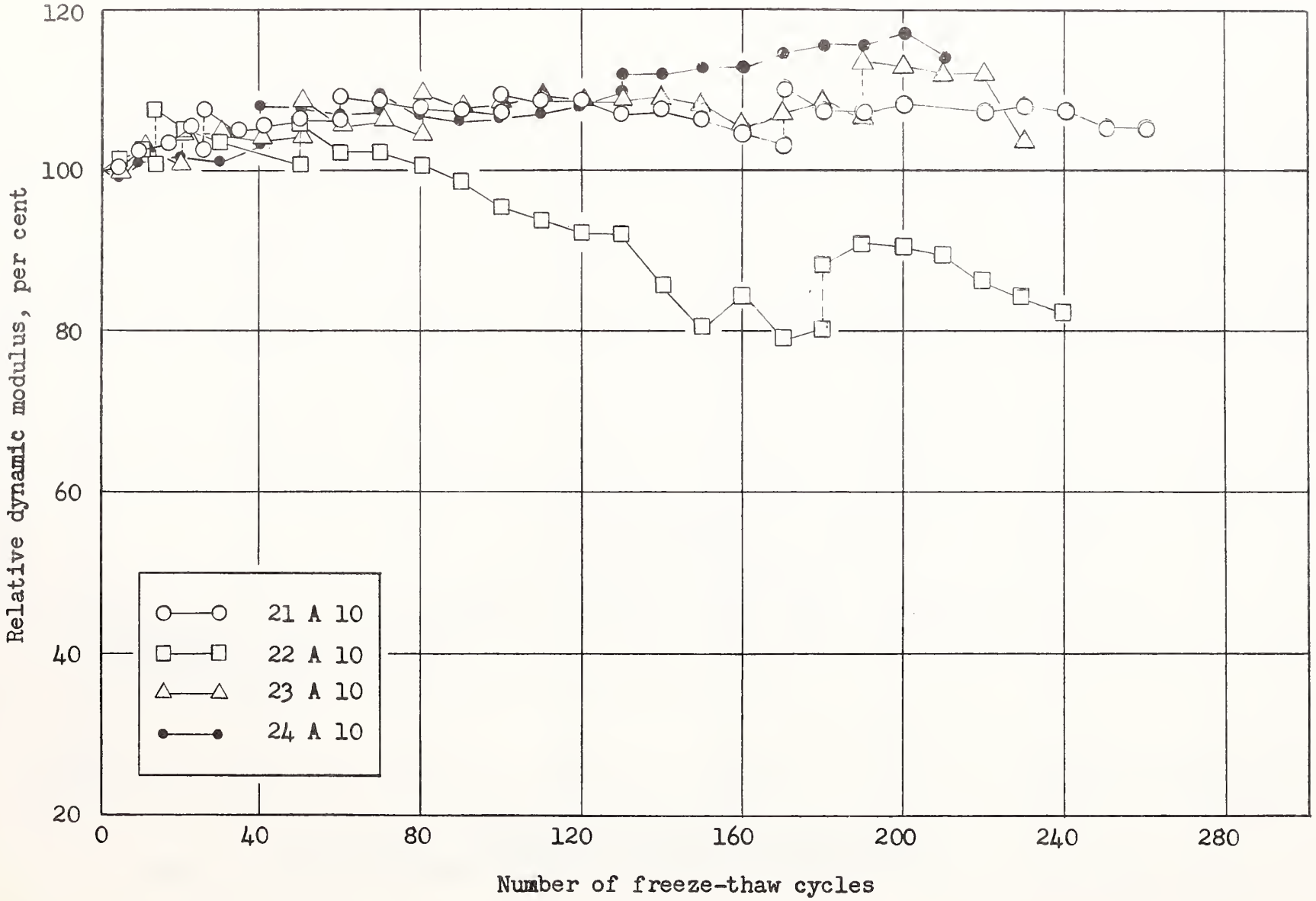

Fig. 51. Relative dynamic moduli of elasticity versus number of freeze-thaw cycles for 500 psi., steam cured, water ponded slabs.

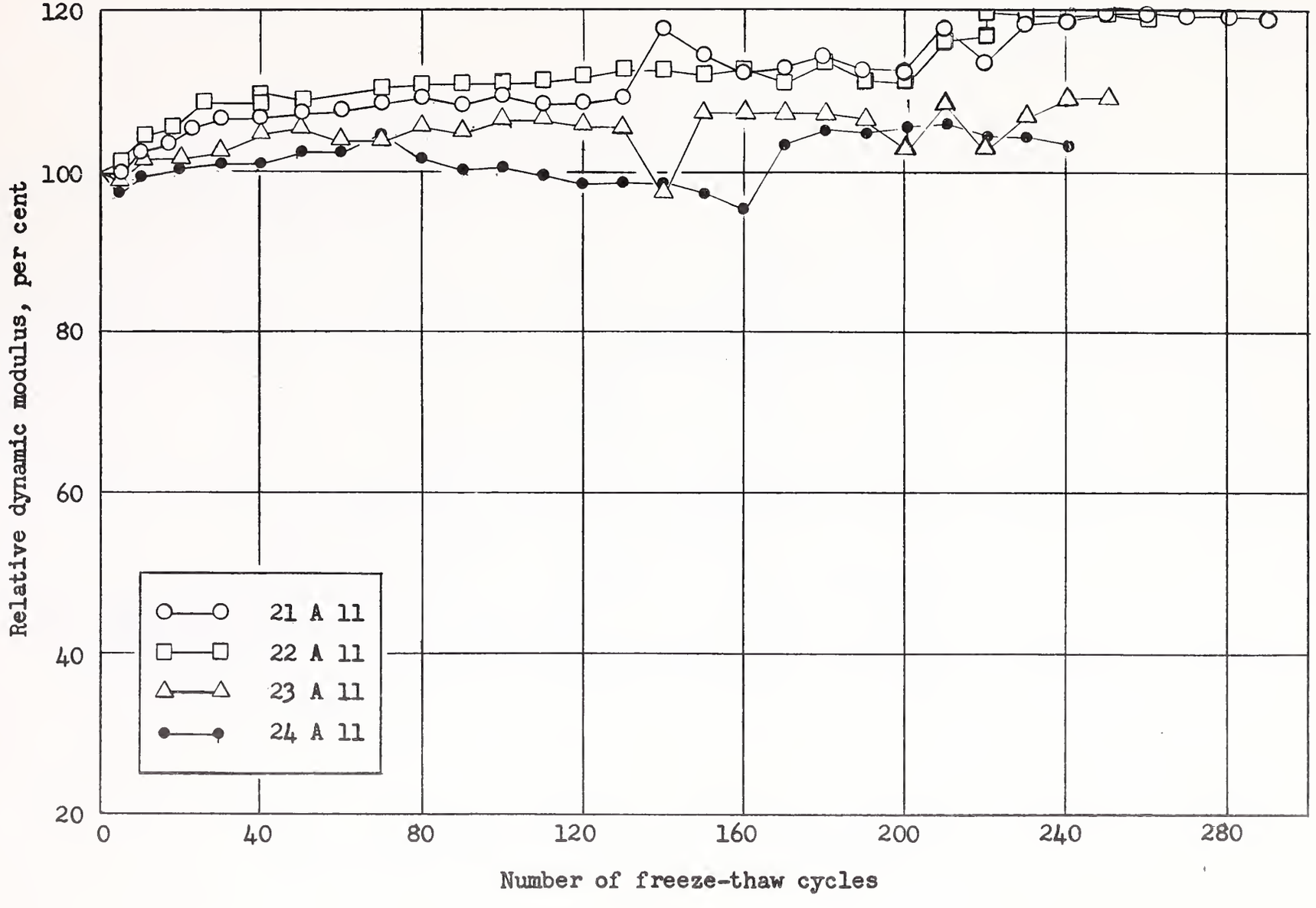

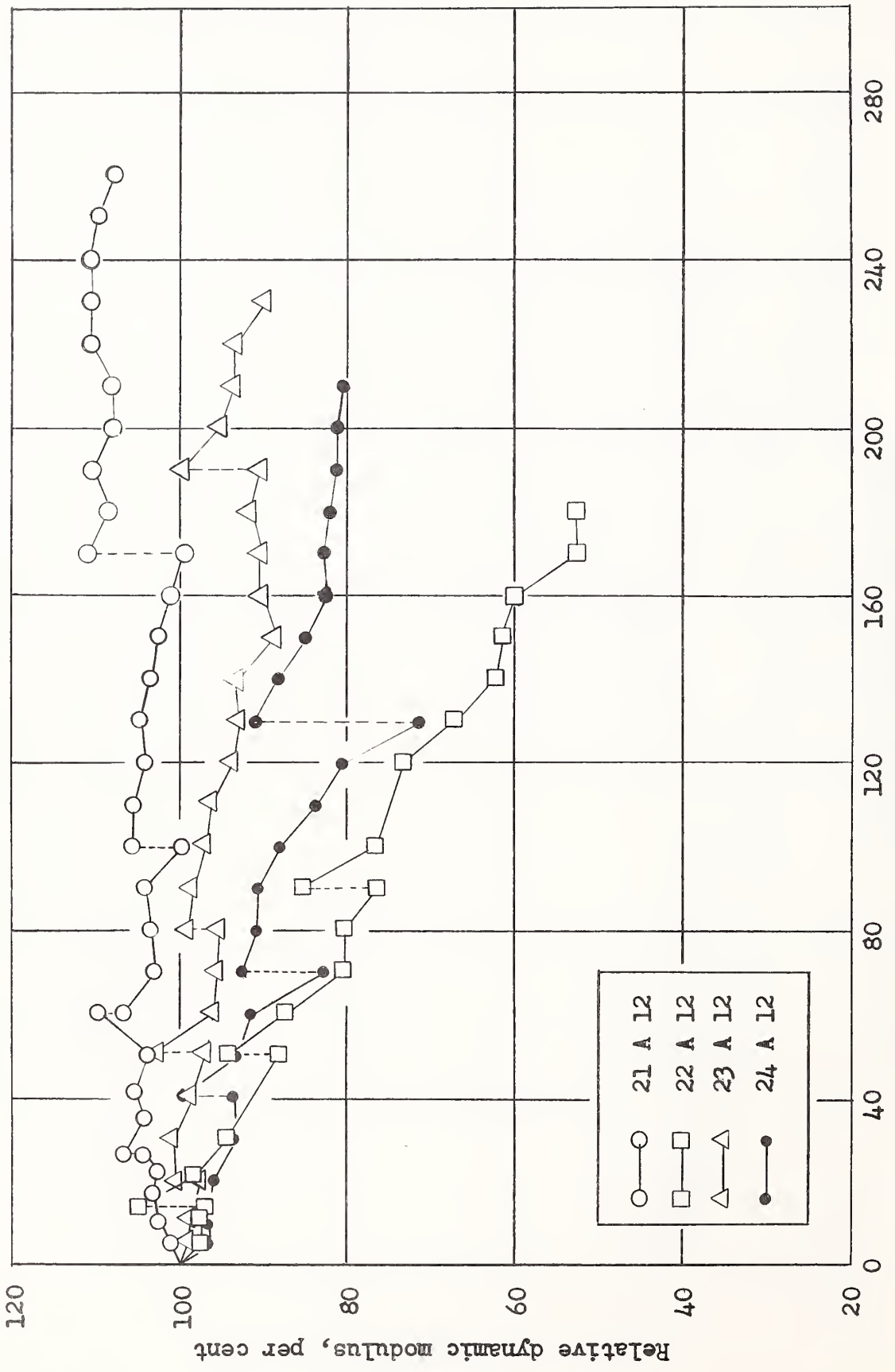

Fig. 52. Relative dynamic moduli of elasticity versus number of freeze-thaw cycles for 500 psi., steam cured, $CaCl_2$ solution ponded slabs.

Fig. 53. Relative dynamic moduli of elasticity versus number of freeze-thaw cycles for 1200 psi., normally cured, water ponded slabs.

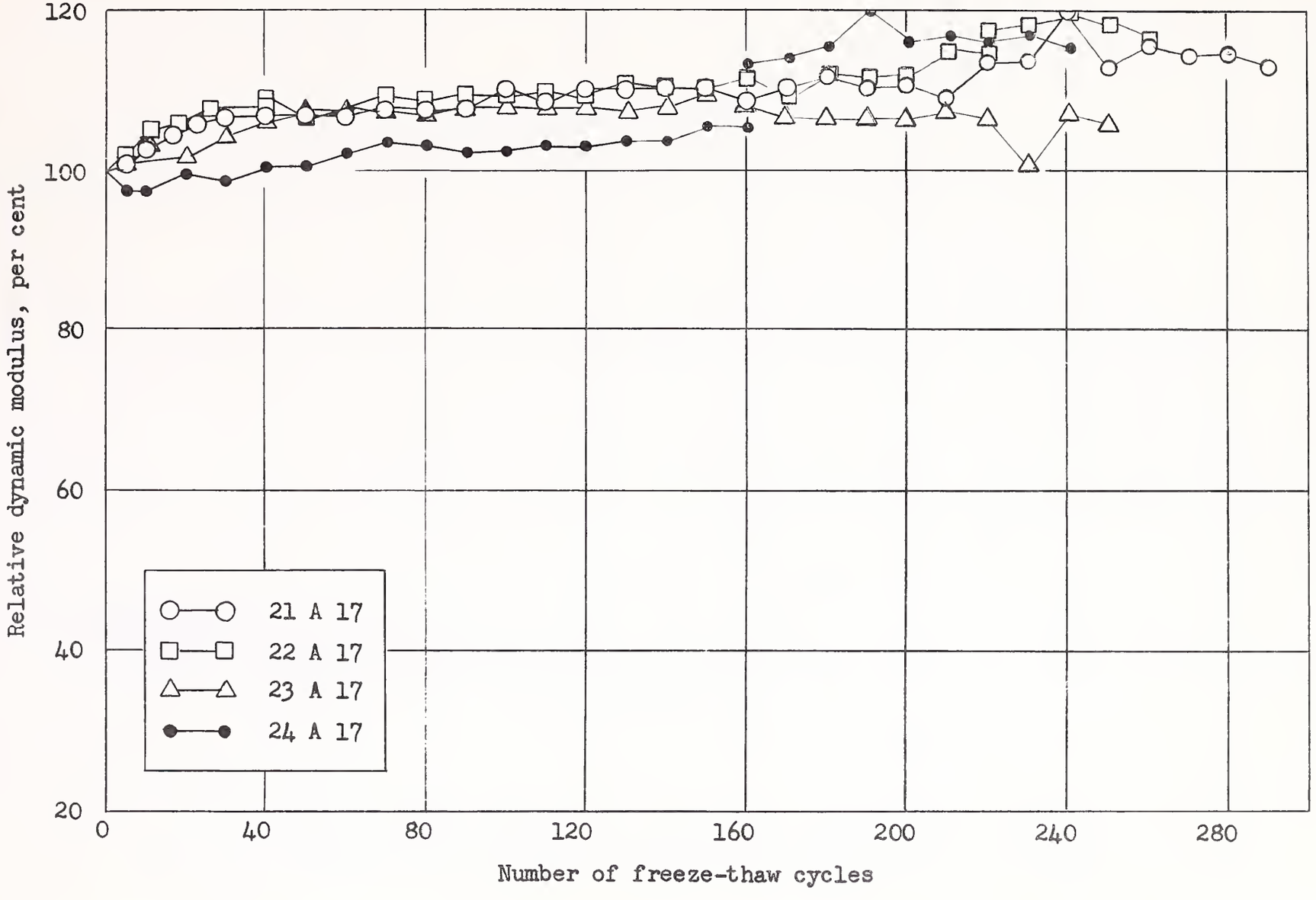

Fig. 54. Relative dynamic moduli of elasticity versus number of freeze-thaw cycles for 1200 psi., normally cured, $CaCl_2$ solution ponded slabs.

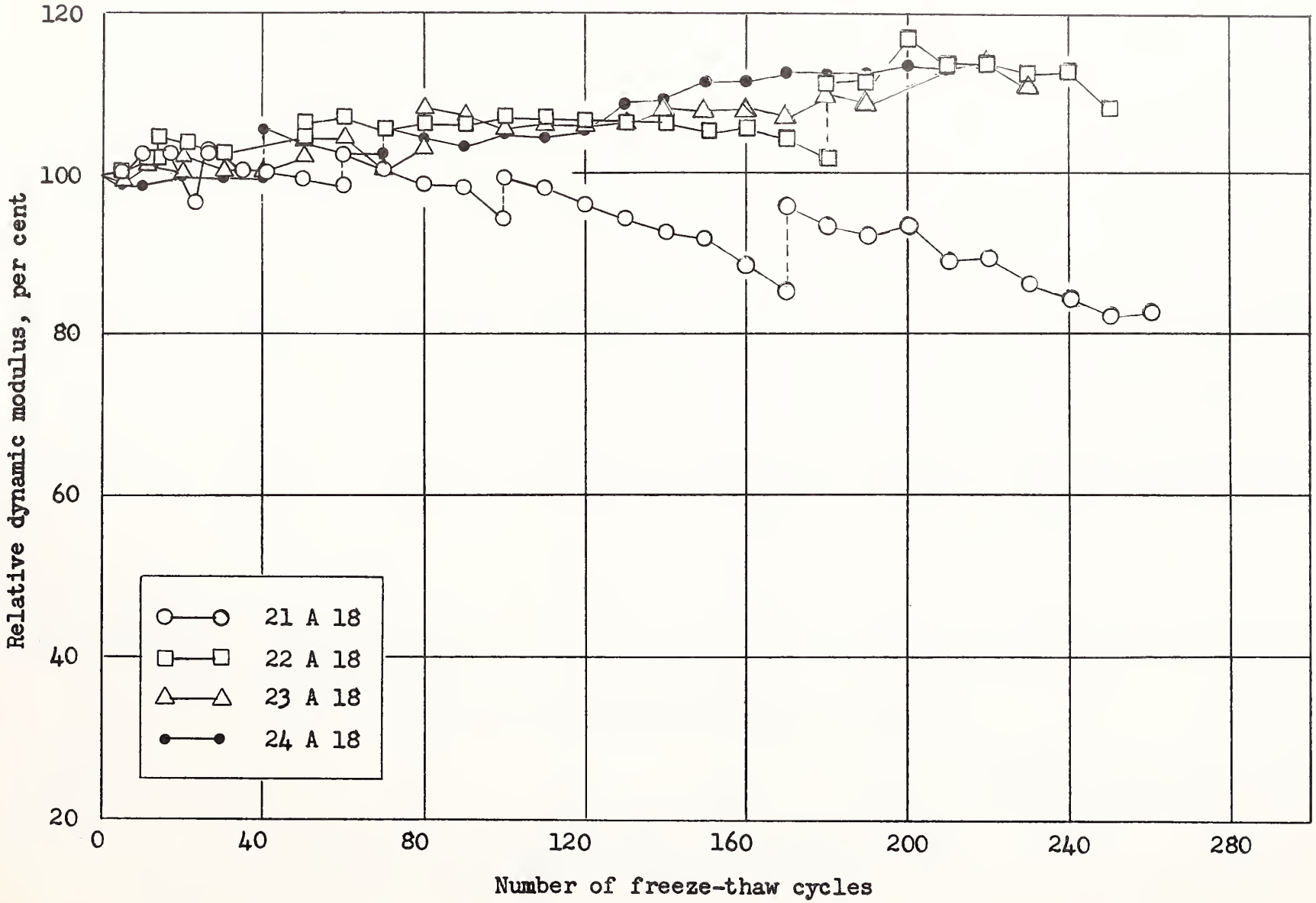

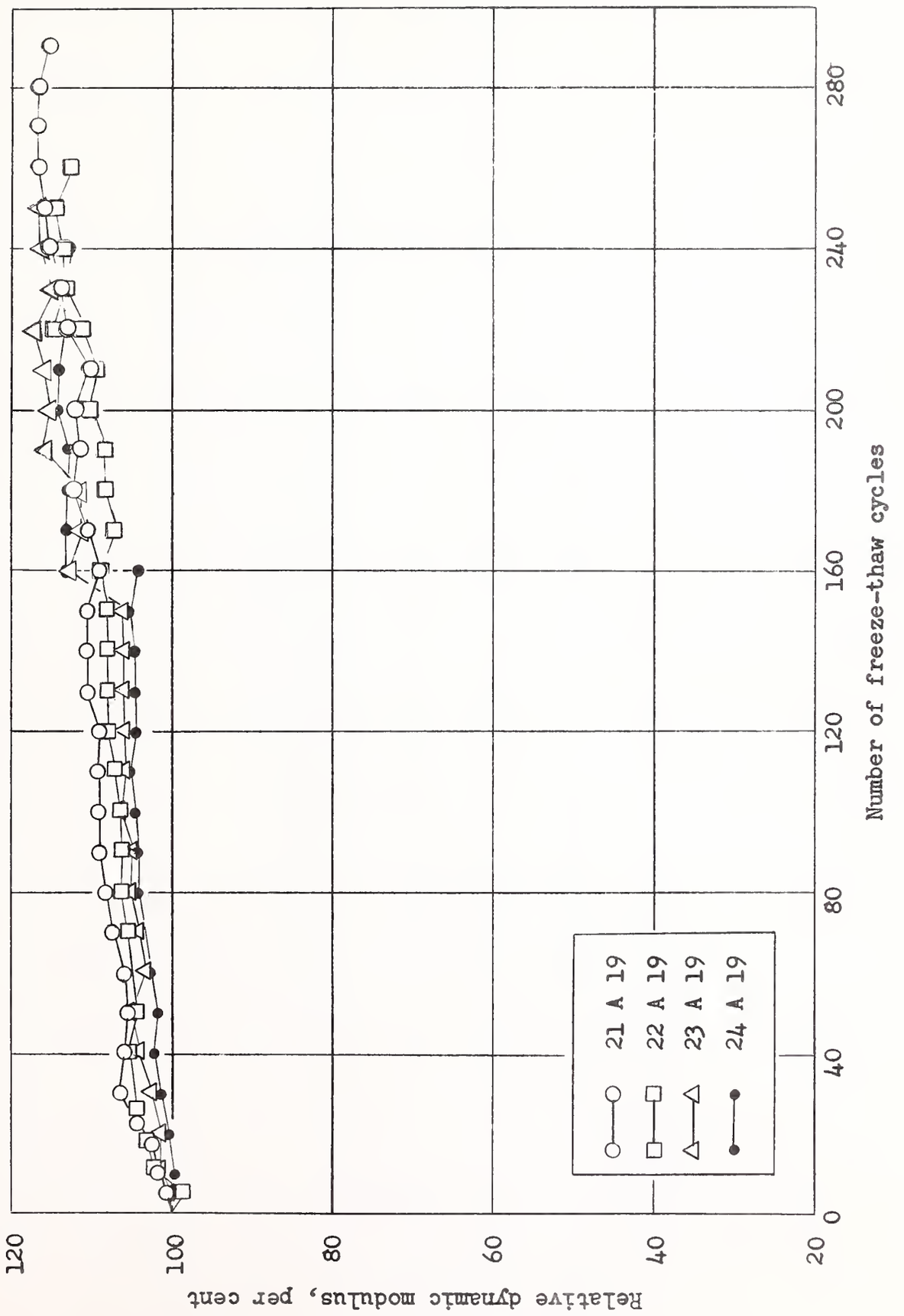

Fig. 55. Relative dynamic moduli of elasticity versus number of freeze-thaw cycles for 1200 psi., steam cured, water ponded slabs.

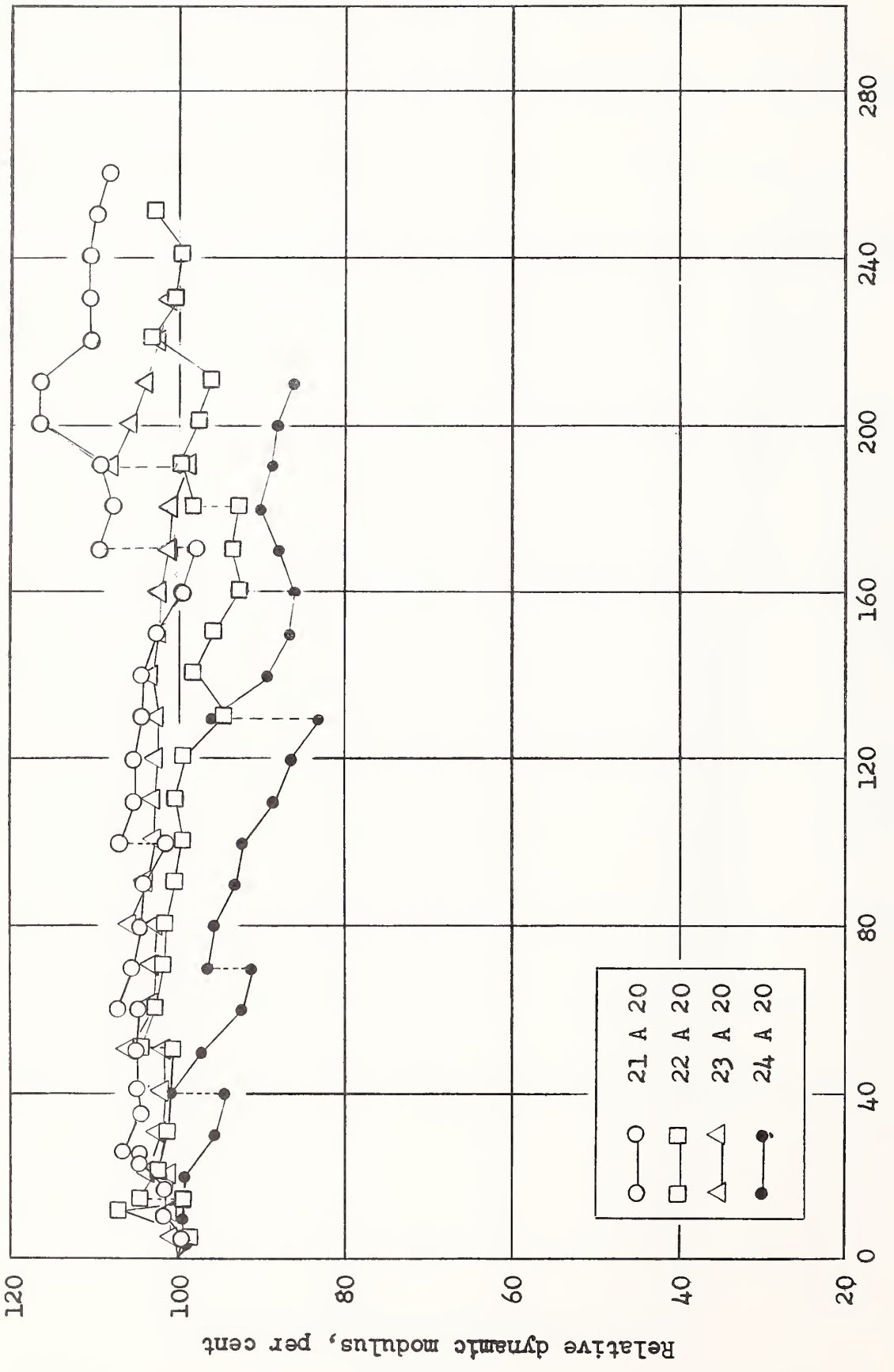

Fig. 56. Relative dynamic moduli of elasticity versus number of freeze-thaw cycles for 1200 psi., steam cured, $CaCl_2$ solution ponded slabs.

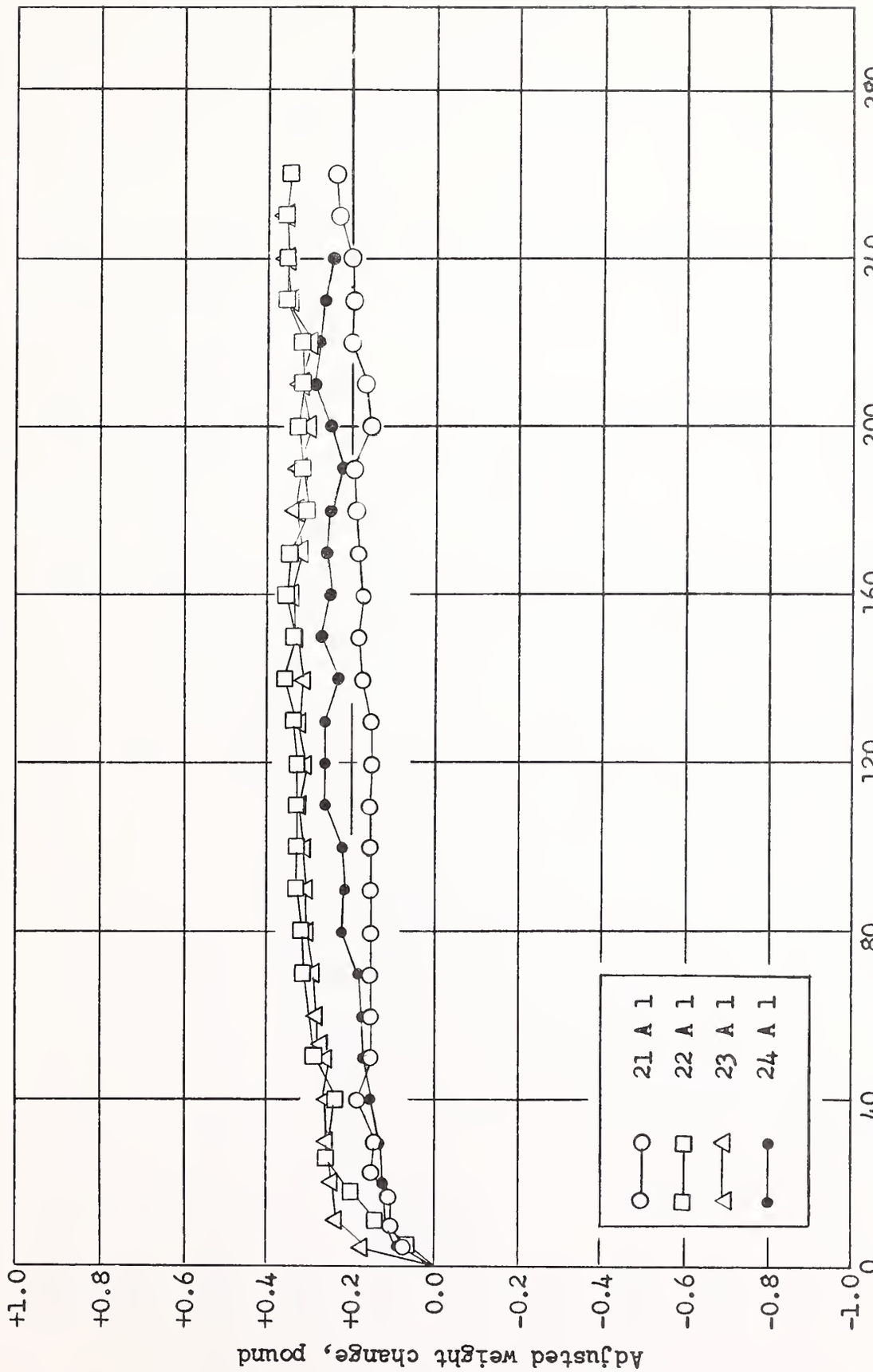

Fig. 57. Adjusted weight changes versus number of freeze-thaw cycles for non-stressed, normally cured, water ponded slabs.

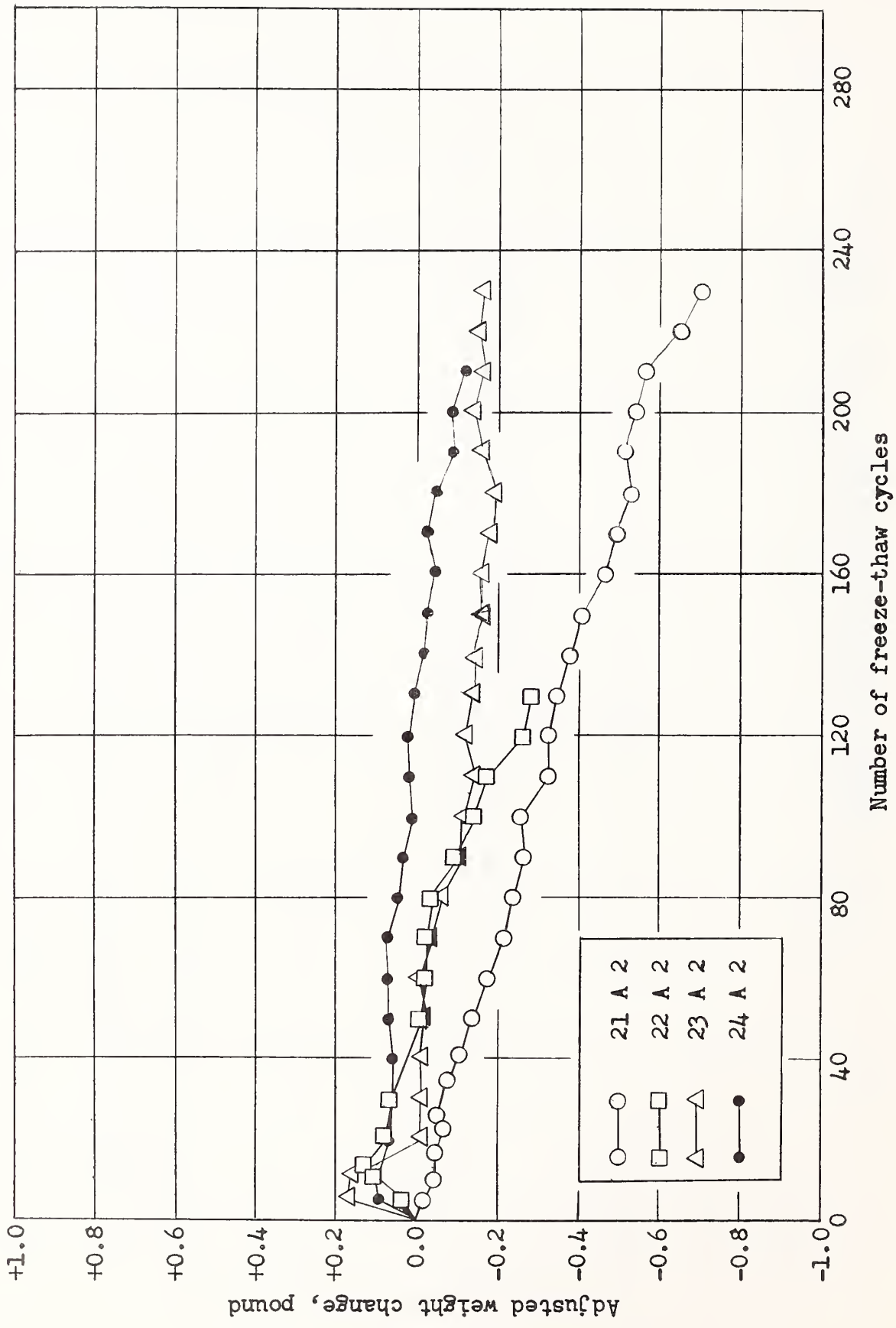

Fig. 58. Adjusted weight changes versus number of freeze-thaw cycles for non-stressed, normally cured, $CaCl_2$ solution ponded slabs.

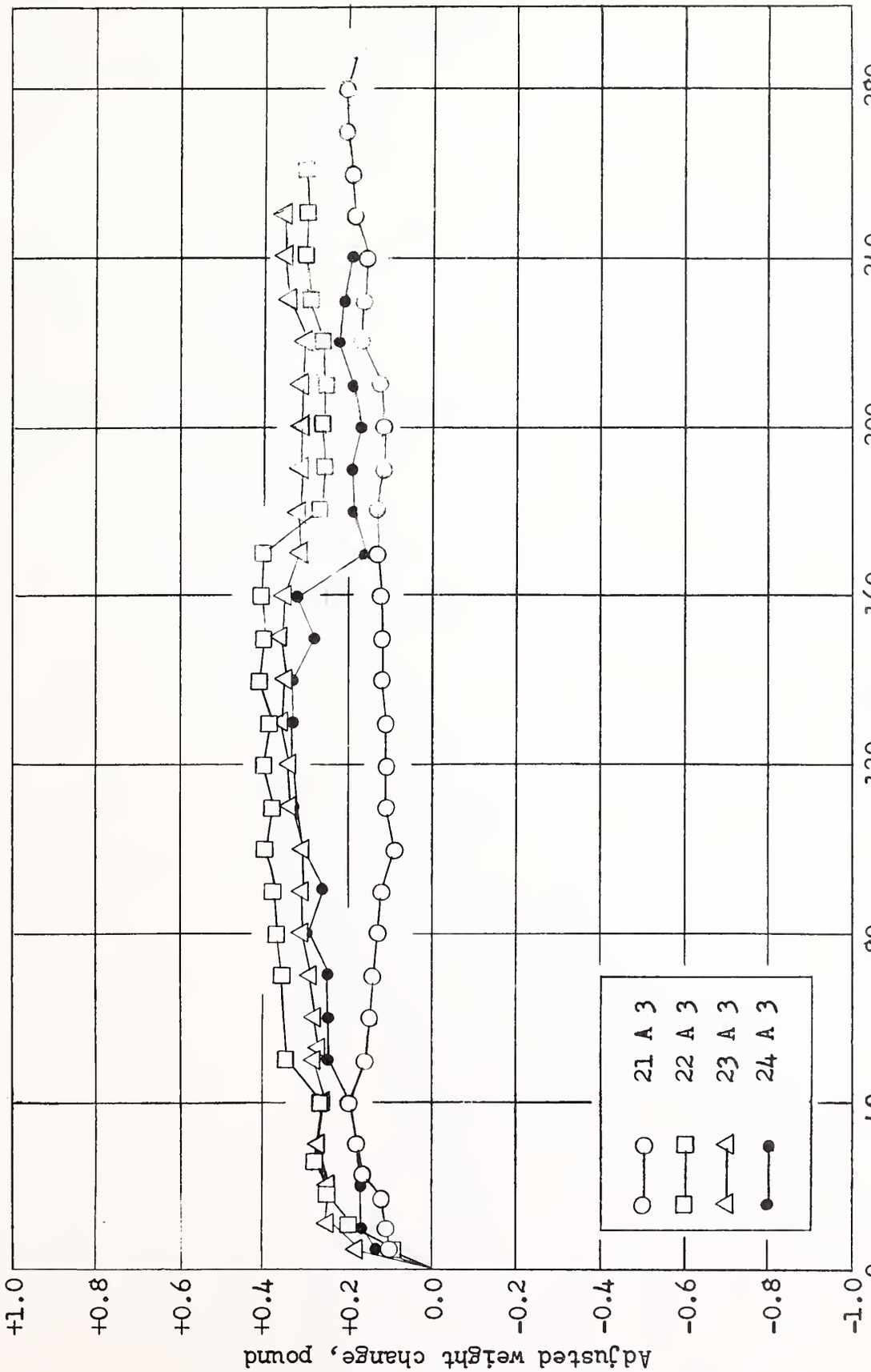

Fig. 59. Adjusted weight changes versus number of freeze-thaw cycles for non-stressed, steam cured, water ponded slabs.

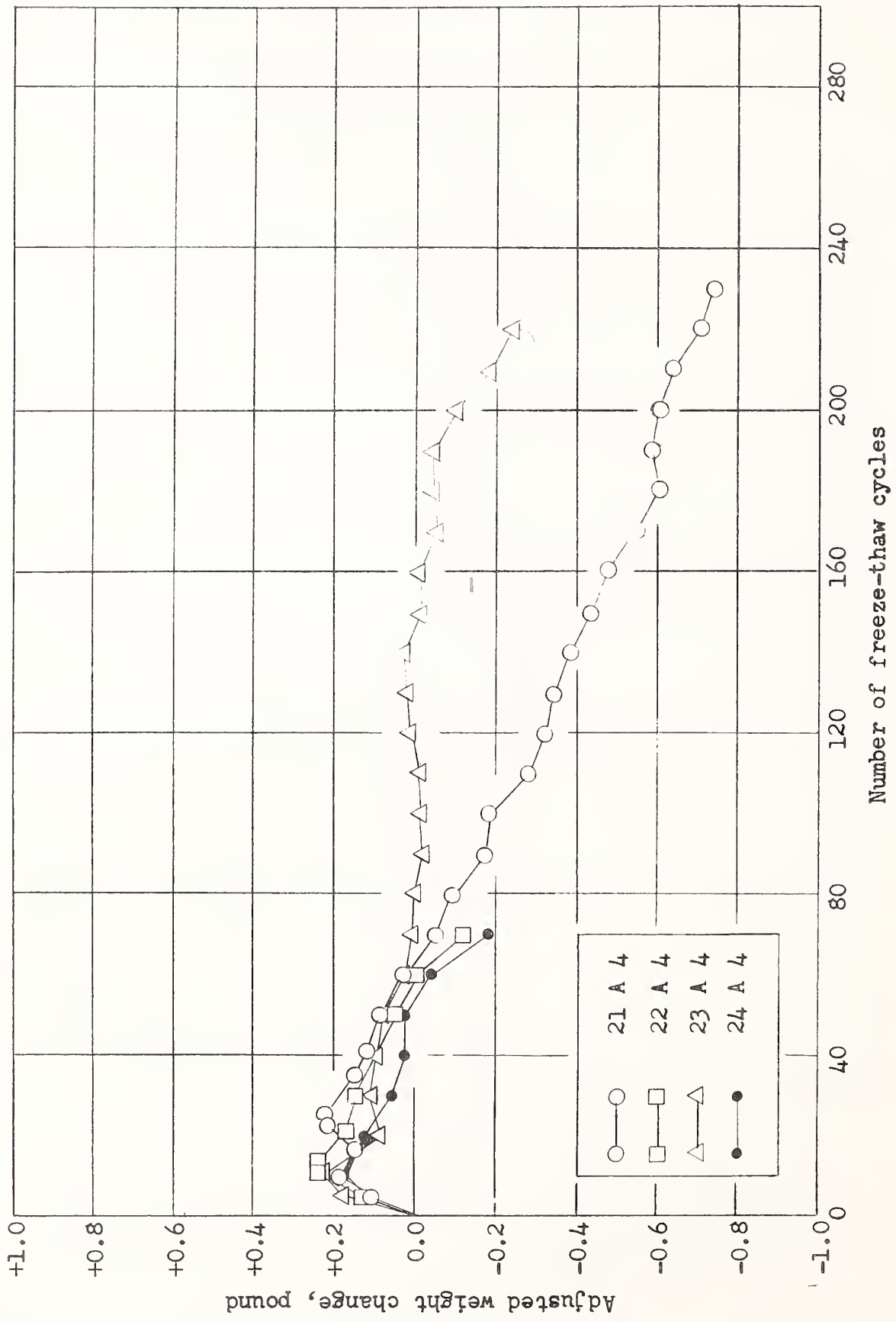

Fig. 60. Adjusted weight changes versus number of freeze-thaw cycles for non-stressed, steam cured, $CaCl_2$ solution ponded slabs.

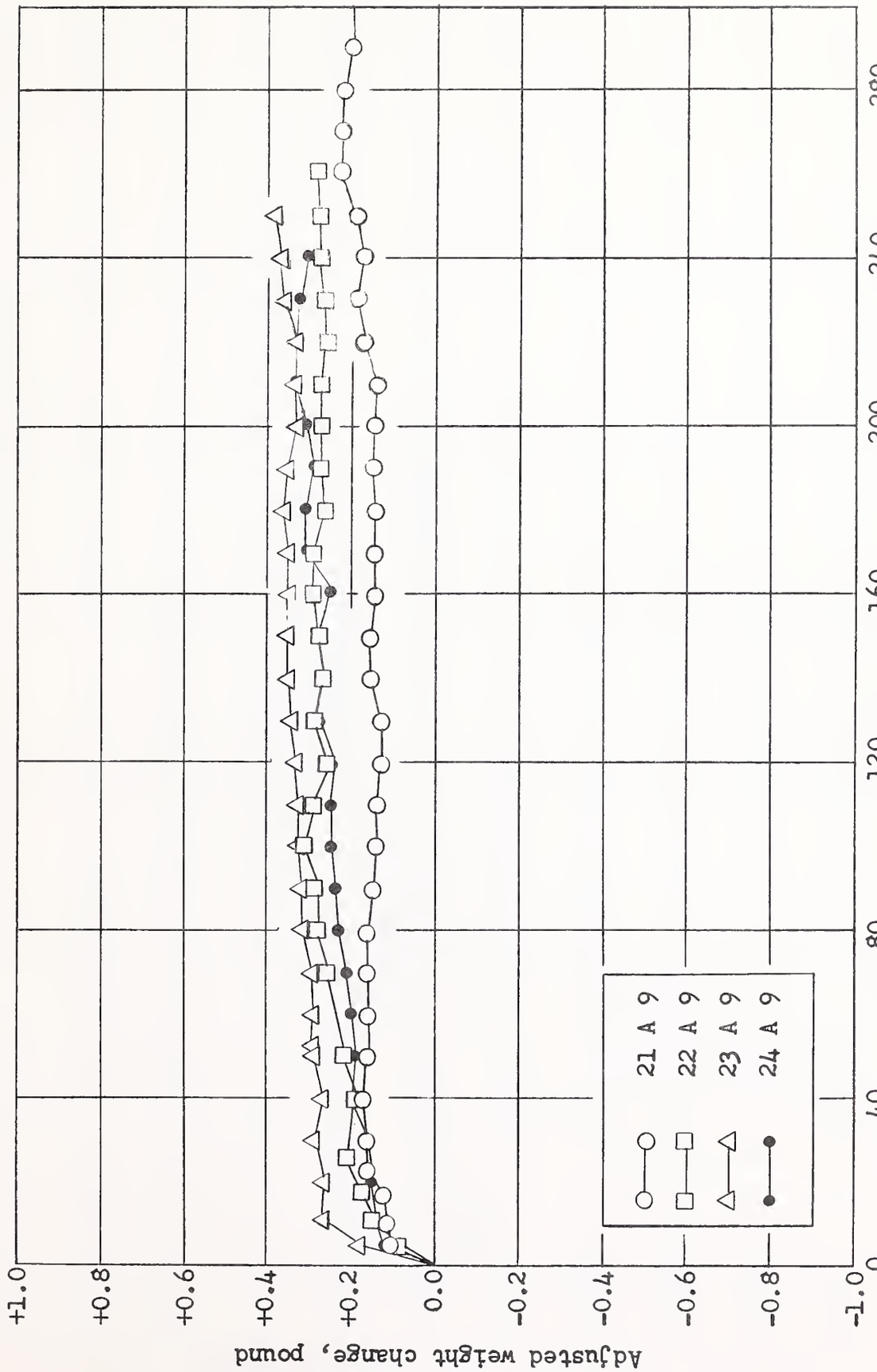

Fig. 61. Adjusted weight changes versus number of freeze-thaw cycles for 500 psi., normally cured, water ponded slabs.

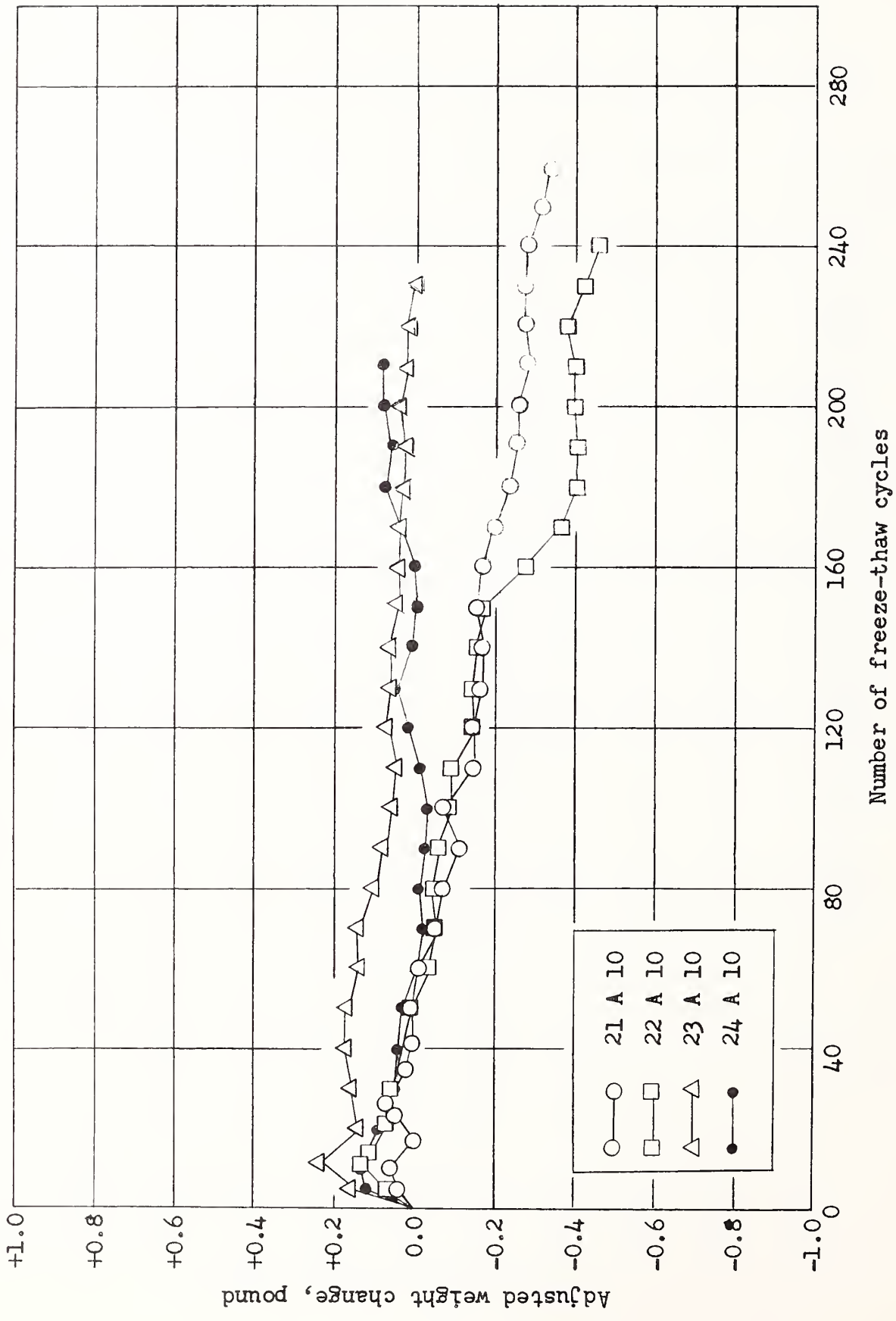

Fig. 62. Adjusted weight changes versus number of freeze-thaw cycles for 500 psi., normally cured, $CaCl_2$ solution ponded slabs.

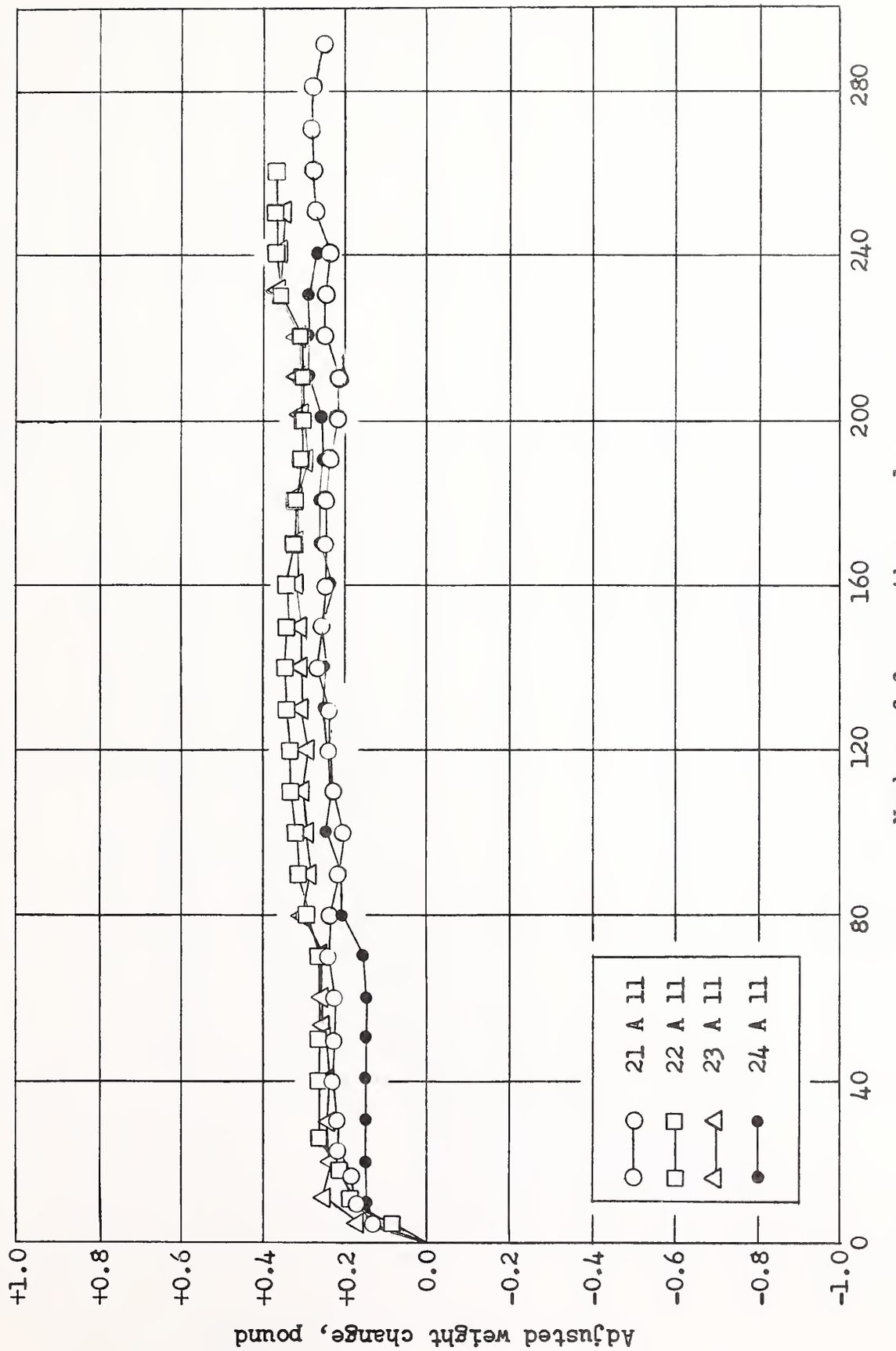

Fig. 63. Adjusted weight changes versus number of freeze-thaw cycles for 500 psi., steam cured, water ponded slabs.

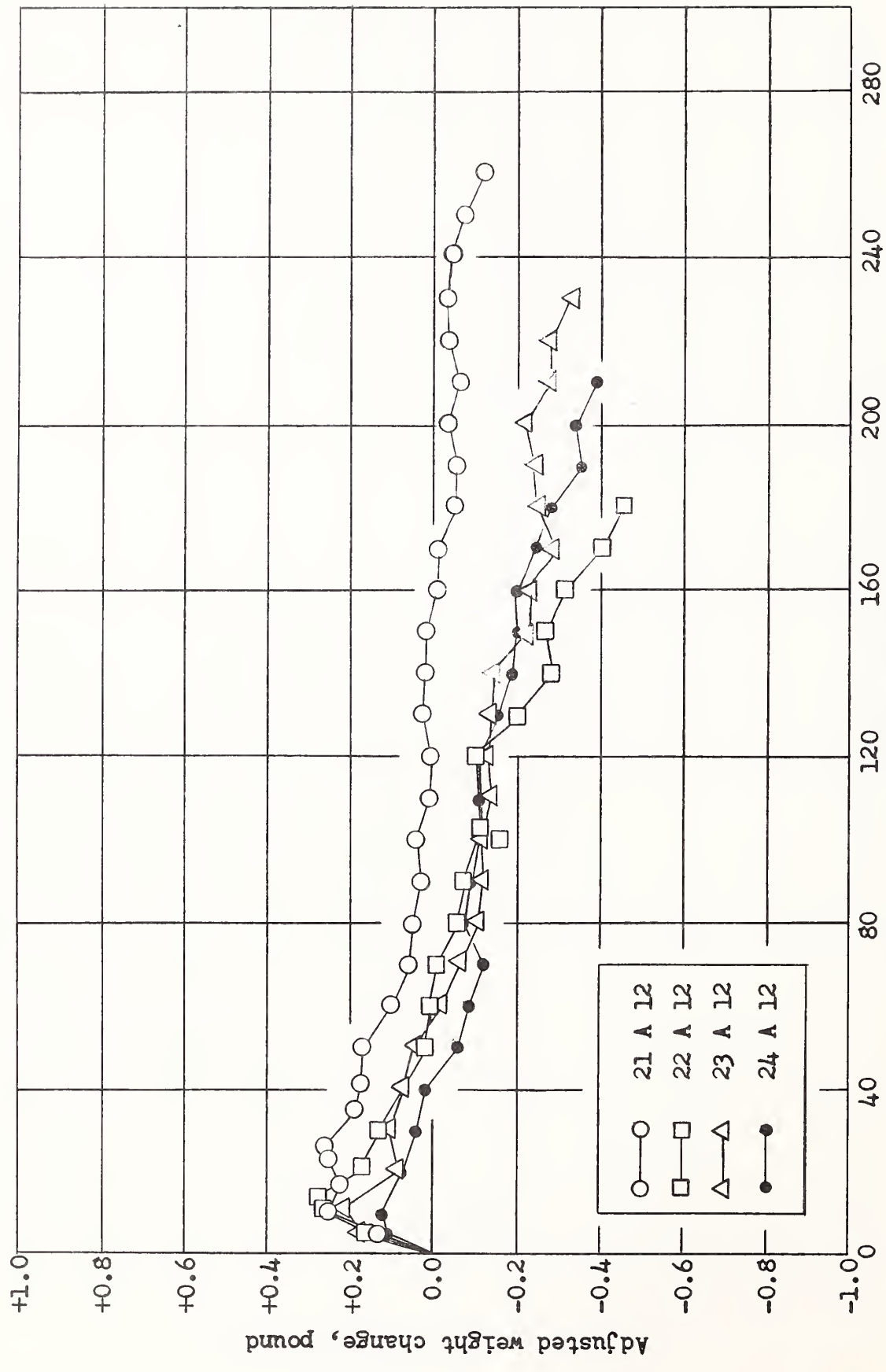

Fig. 64. Adjusted weight changes versus number of freeze-thaw cycles for 500 psi., steam cured, $CaCl_2$ solution ponded slabs.

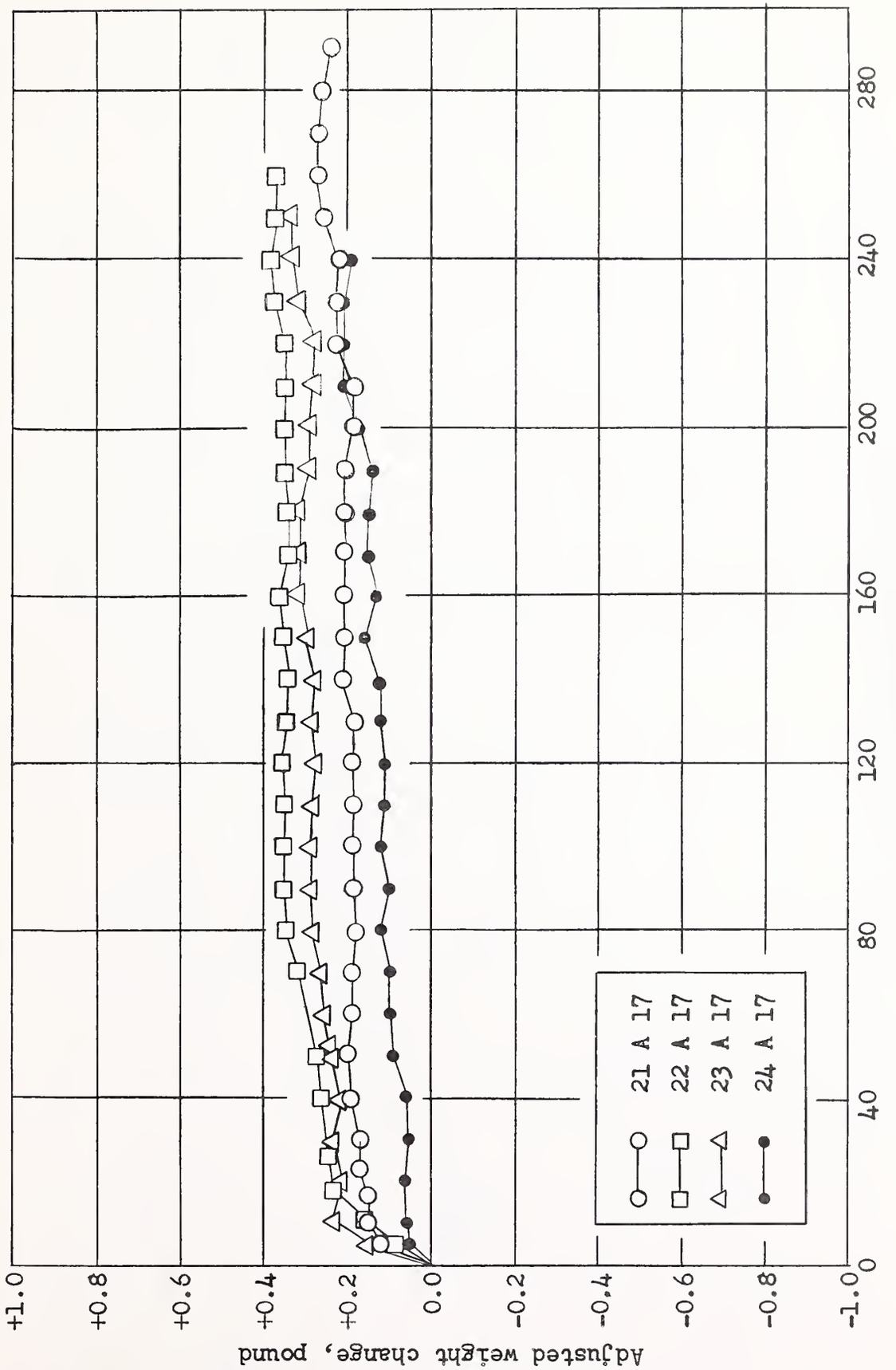

Fig. 65. Adjusted weight changes versus number of freeze-thaw cycles for 1200 psi., normally cured, water ponded slabs.

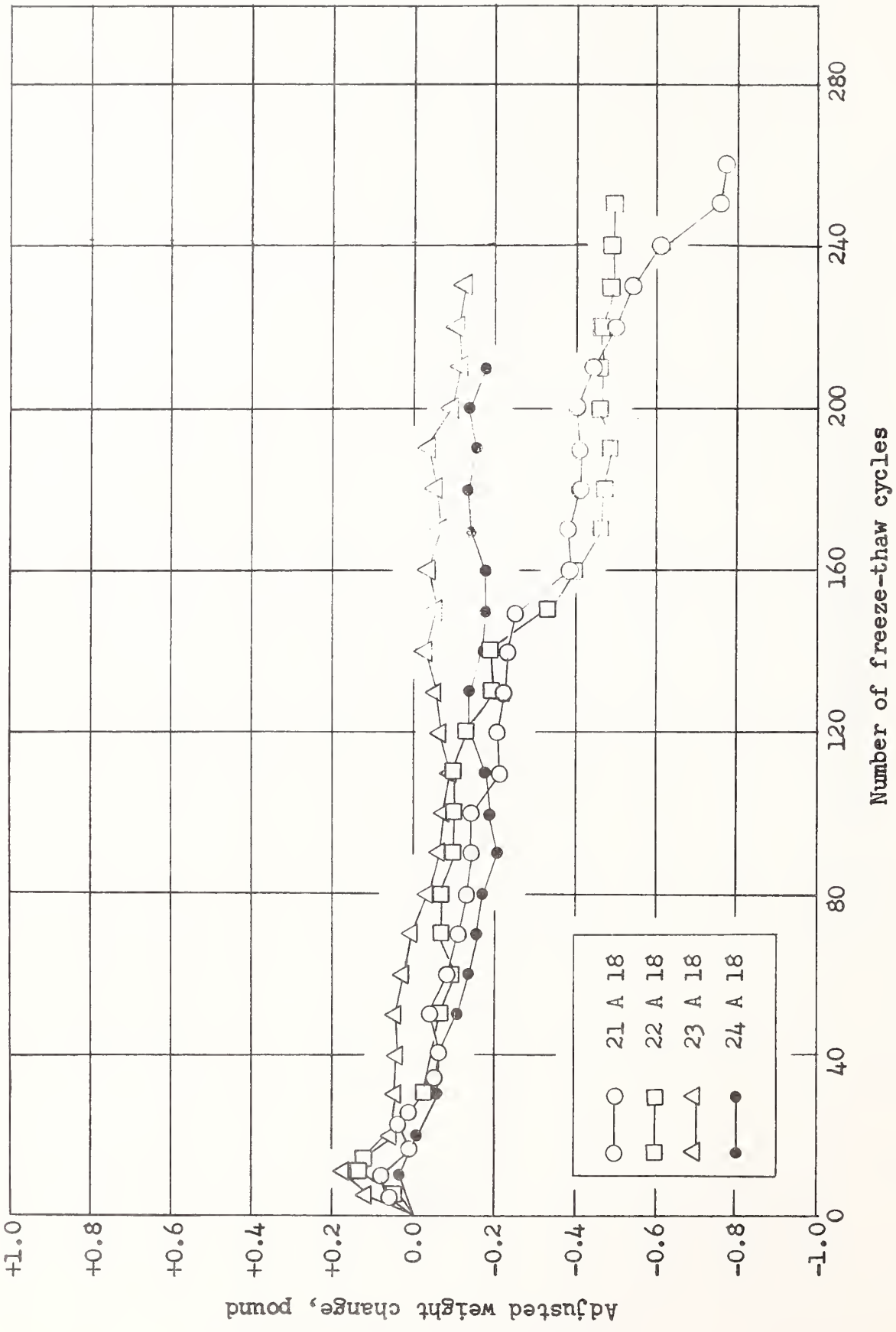

Fig. 66. Adjusted weight changes versus number of freeze-thaw cycles for 1200 psi., normally cured, $CaCl_2$ solution ponded slabs.

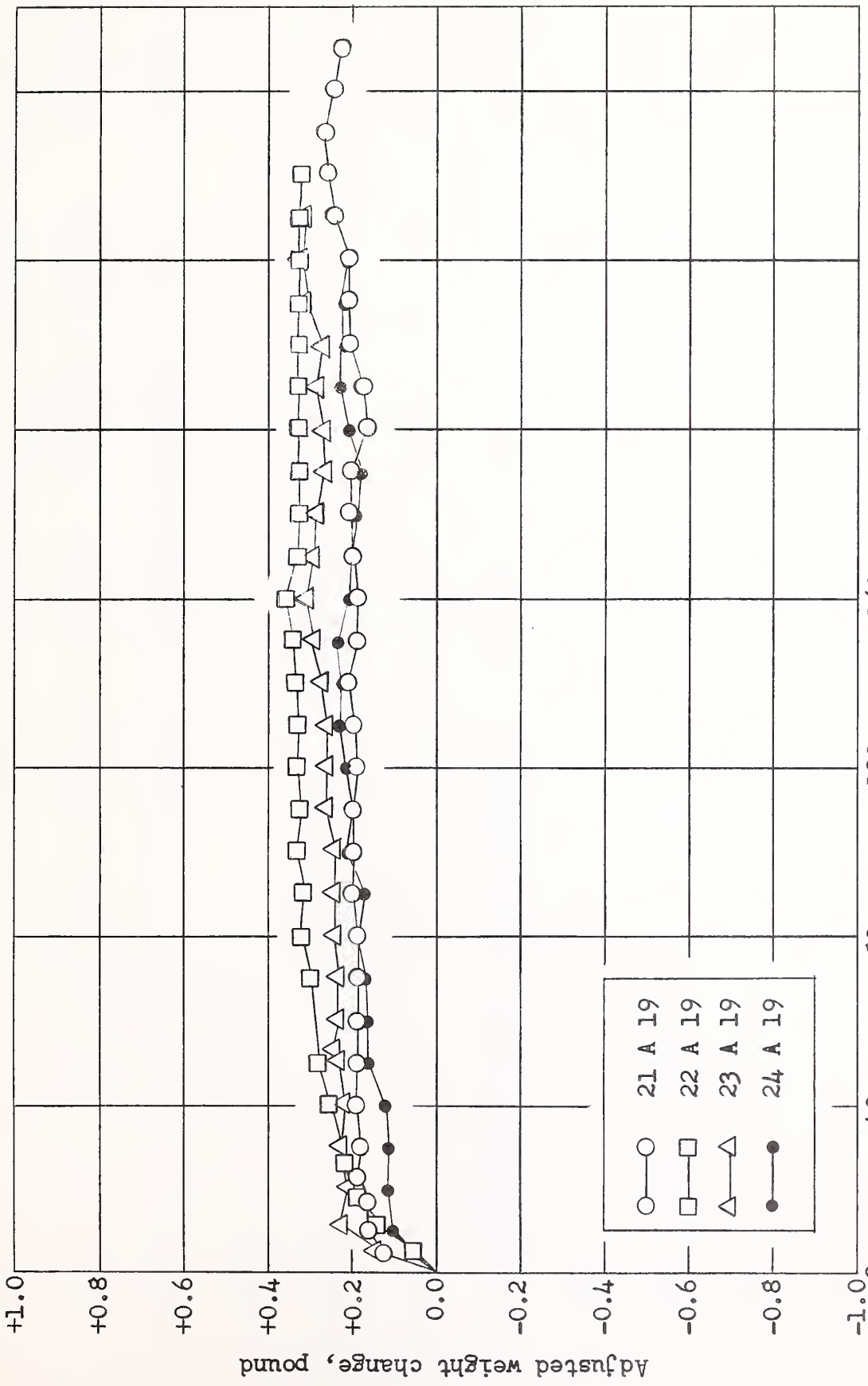

Fig. 67. Adjusted weight changes versus number of freeze-thaw cycles for 1200 psi., steam cured, water ponded slabs

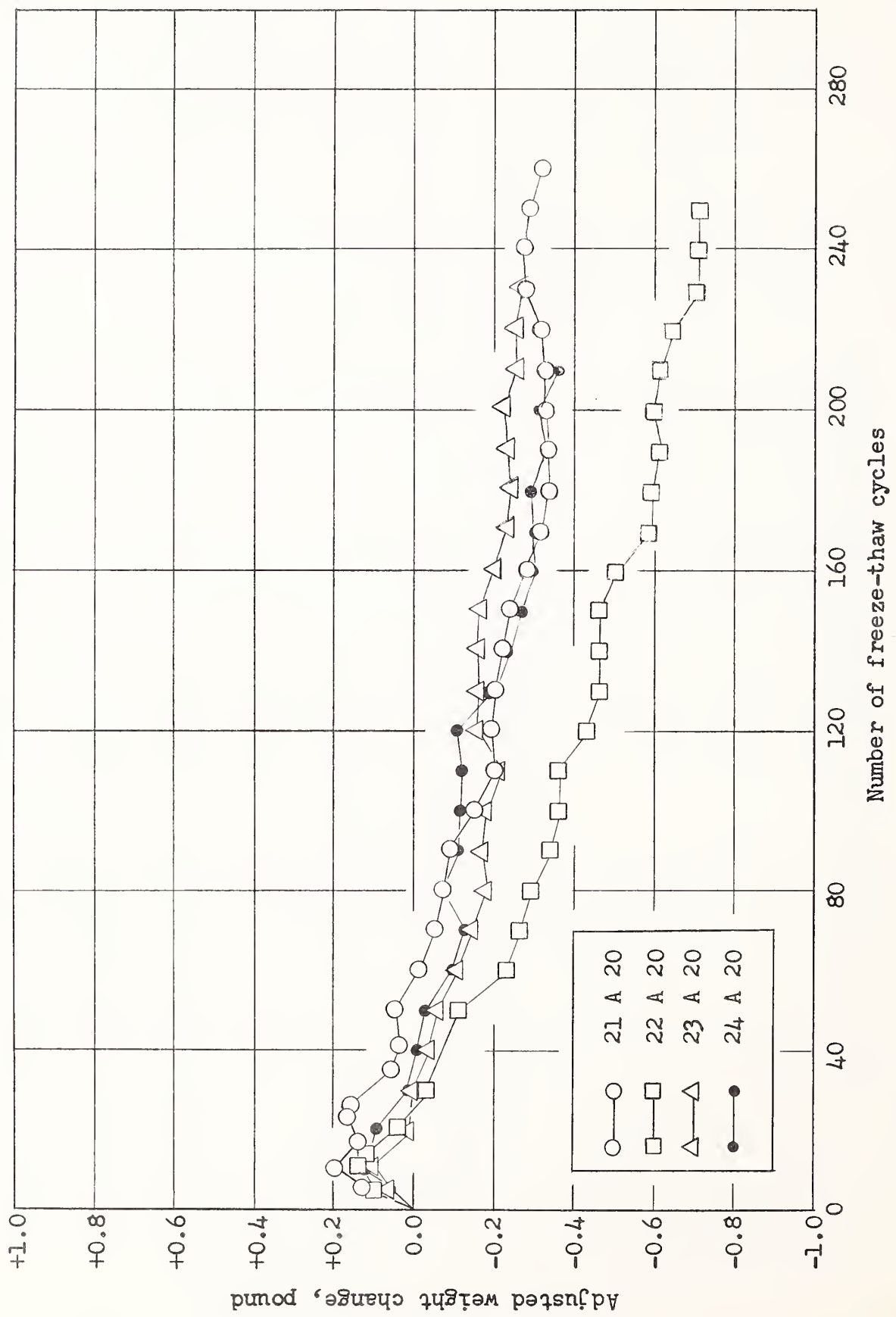

Fig. 68. Adjusted weight changes versus number of freeze-thaw cycles for 1200 psi., steam cured, $CaCl_2$ solution ponded slabs.

Fig. 69. Length changes versus number of freeze-thaw cycles for non-stressed, normally cured, water ponded slabs.

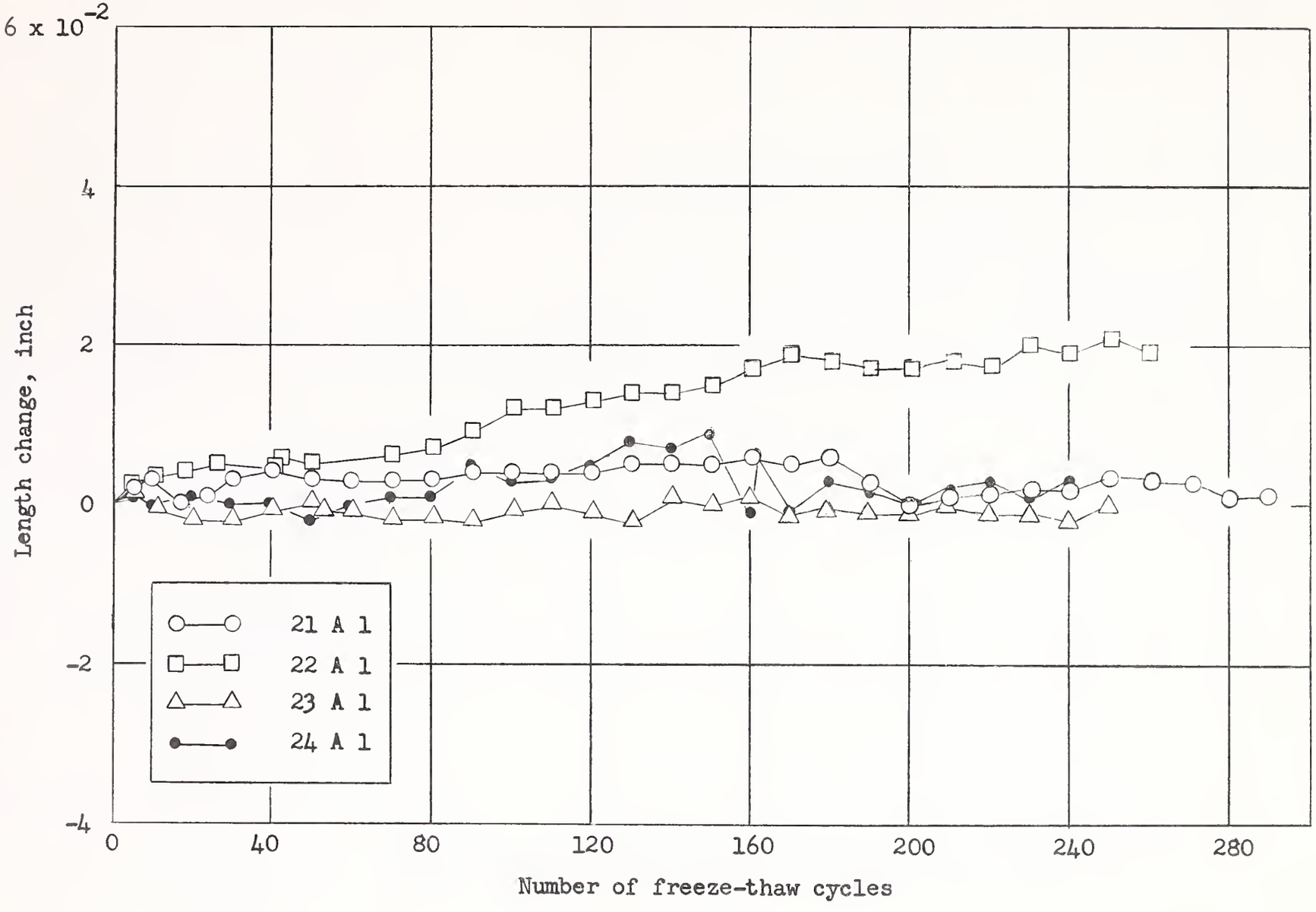

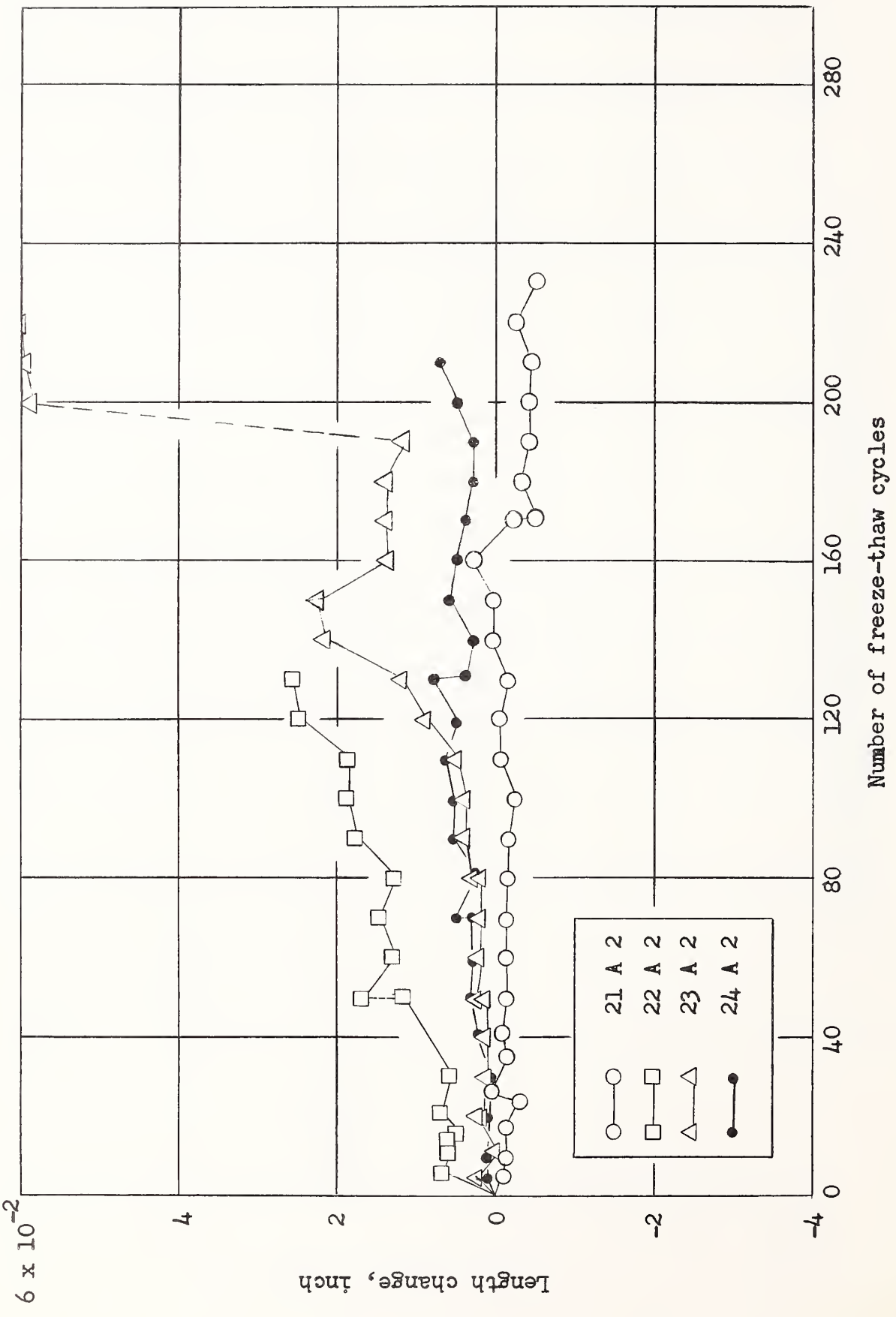

Fig. 70. Length changes versus number of freeze-thaw cycles for non-stressed, normally cured, $CaCl_2$ solution ponded slabs.

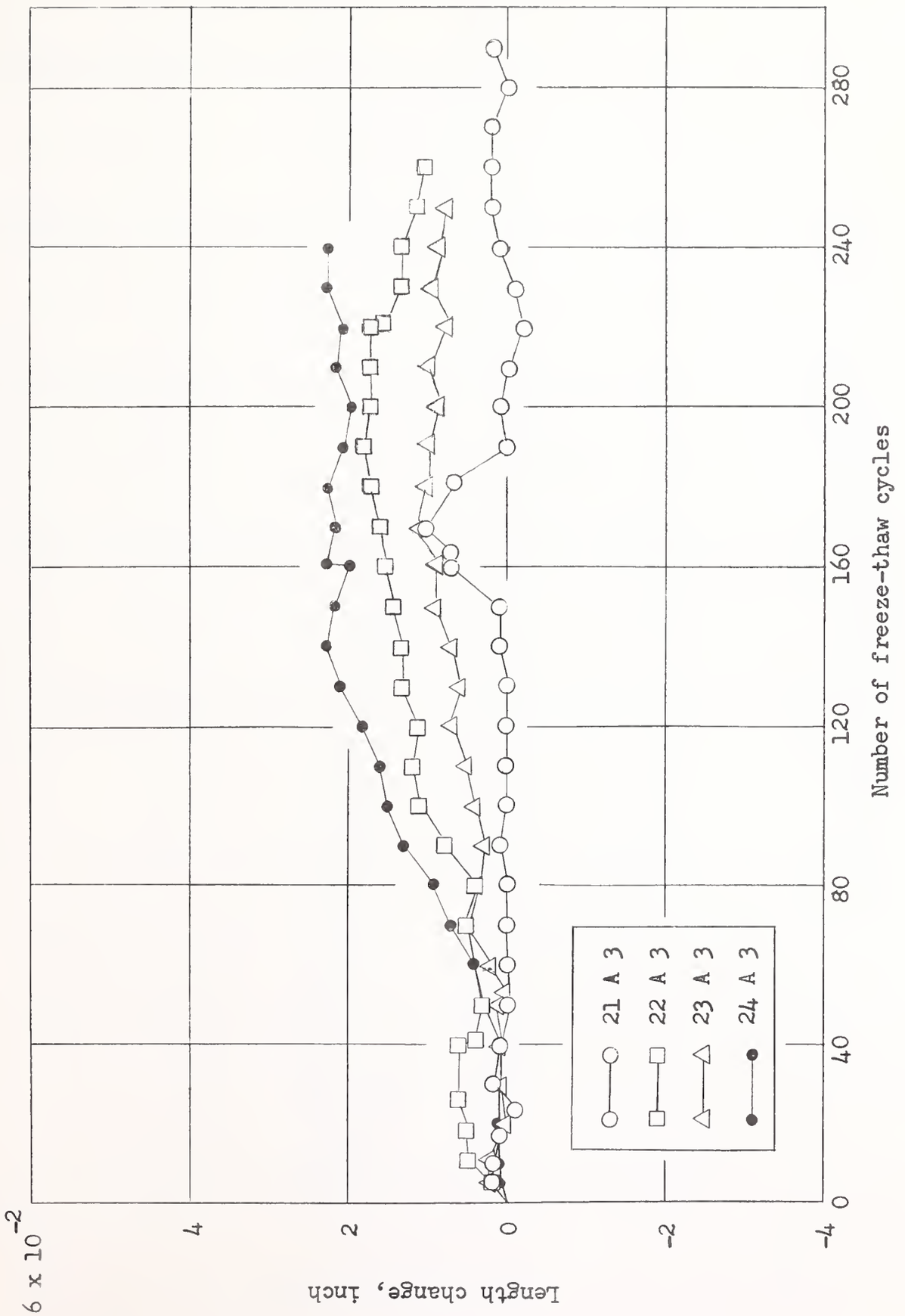

Fig. 71. Length changes versus number of freeze-thaw cycles for non-stressed, steam cured, water ponded slabs.

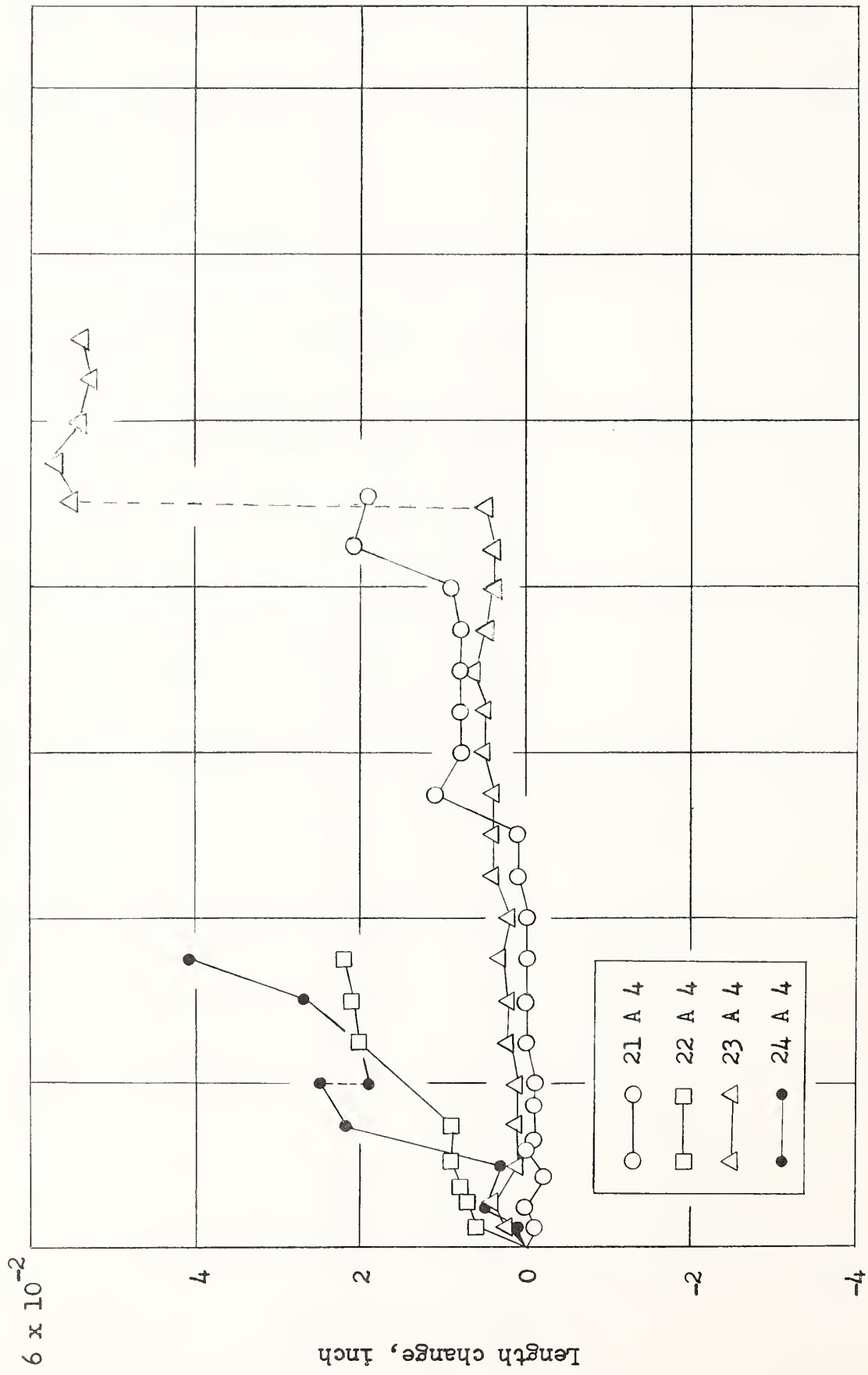

Fig. 72. Length changes versus number of freeze-thaw cycles for non-stressed, steam cured, $CaCl_2$ solution ponded slabs.

Fig. 73. Length changes versus number of freeze-thaw cycles for 500 psi., normally cured, water ponded slabs.

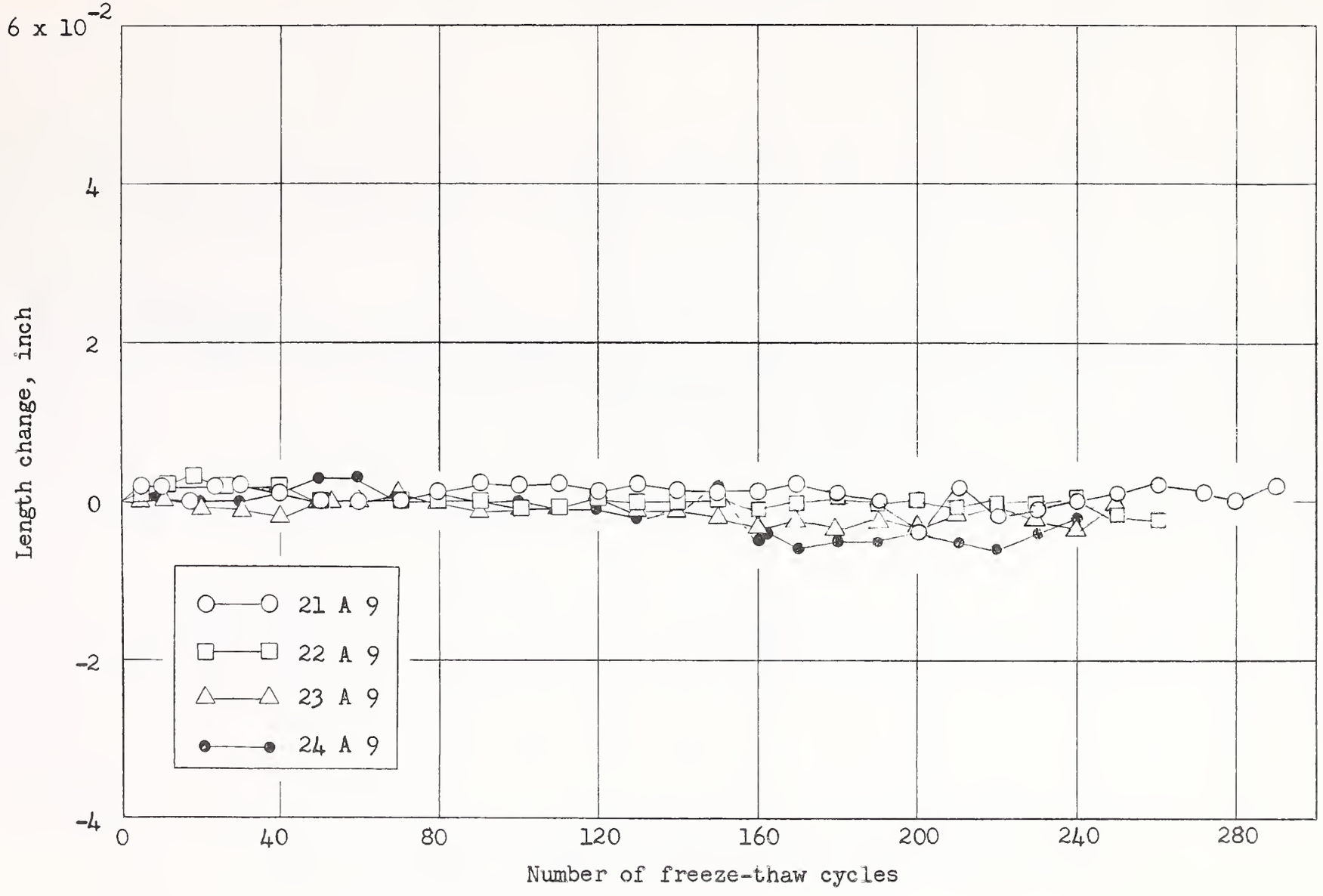

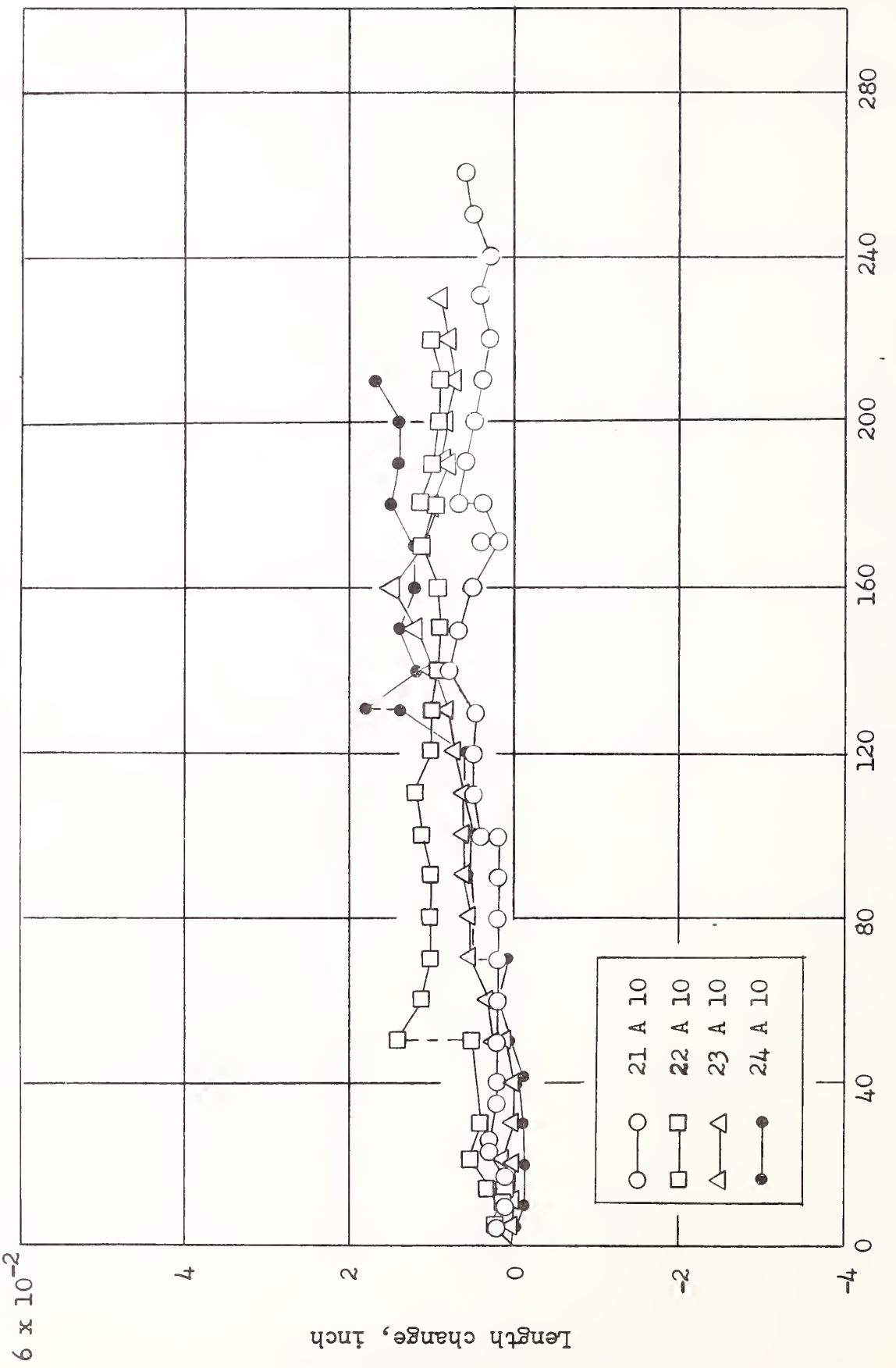

Fig. 74. Length changes versus number of freeze-thaw cycles for 500 psi., normally cured, $CaCl_2$ solution ponded slabs.

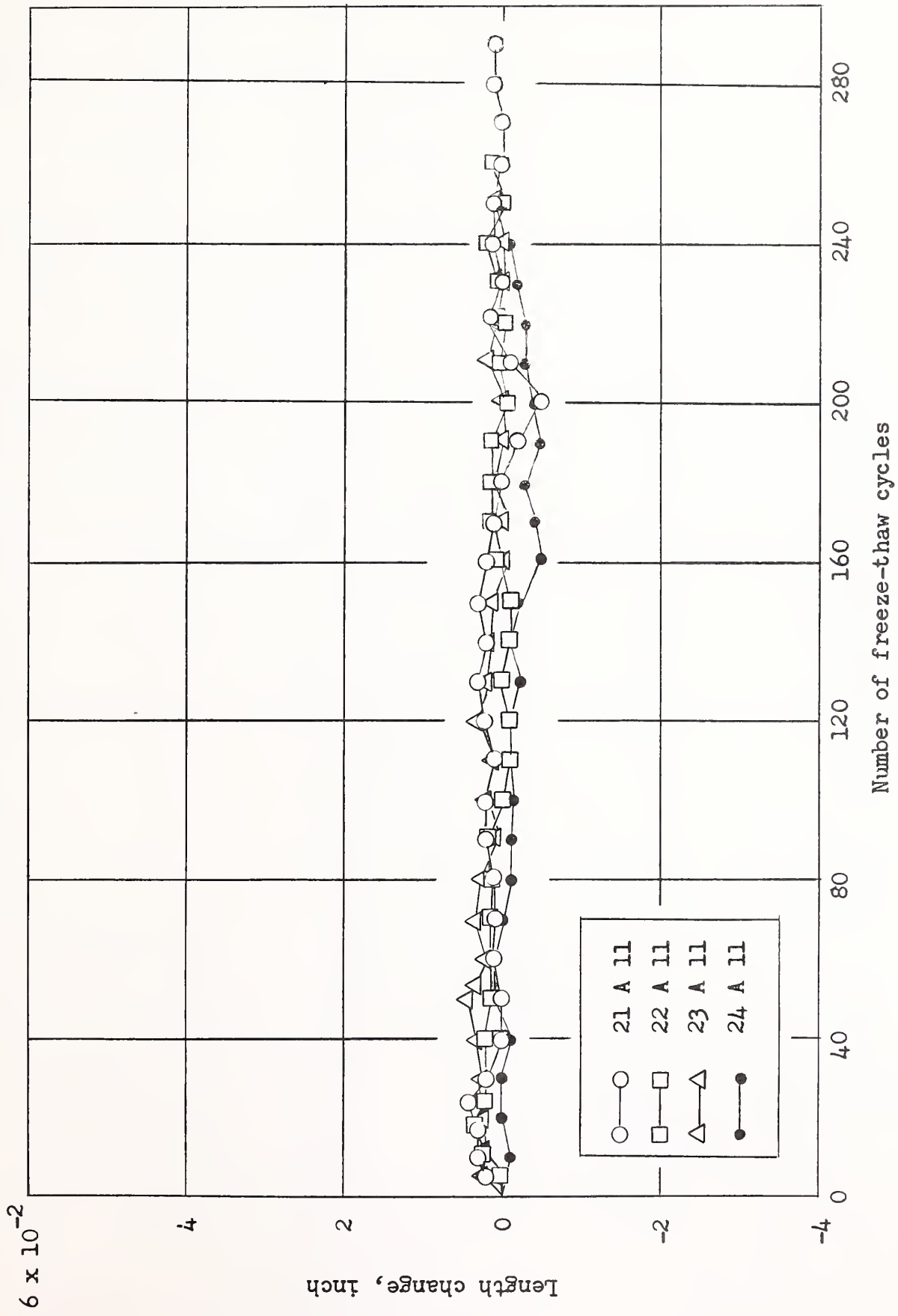

Fig. 75. Length changes versus number of freeze-thaw cycles for 500 psi., steam cured, water ponded slabs.

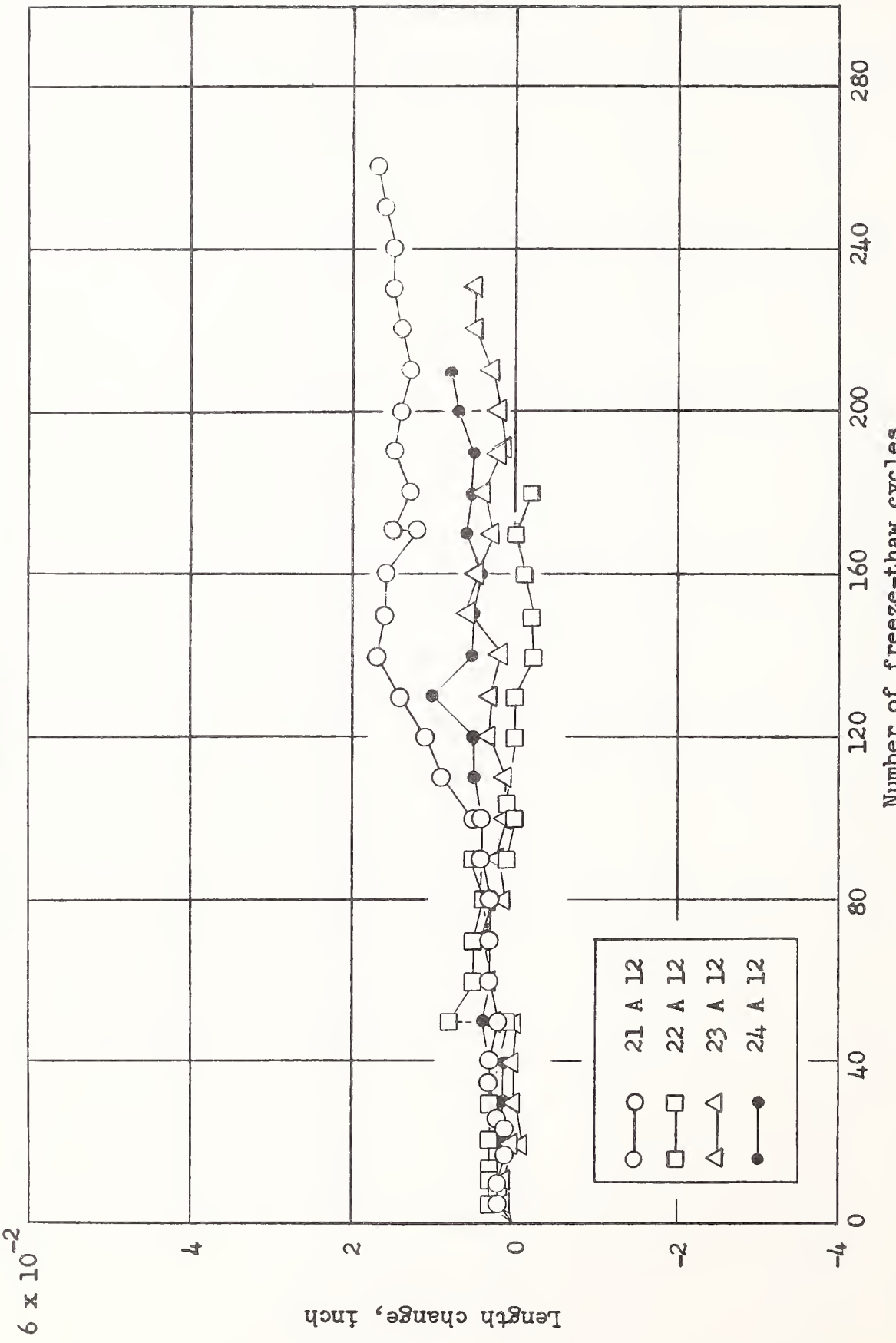

Fig. 76. Length changes versus number of freeze-thaw cycles for 500 psi., steam cured, $CaCl_2$ solution ponded slabs.

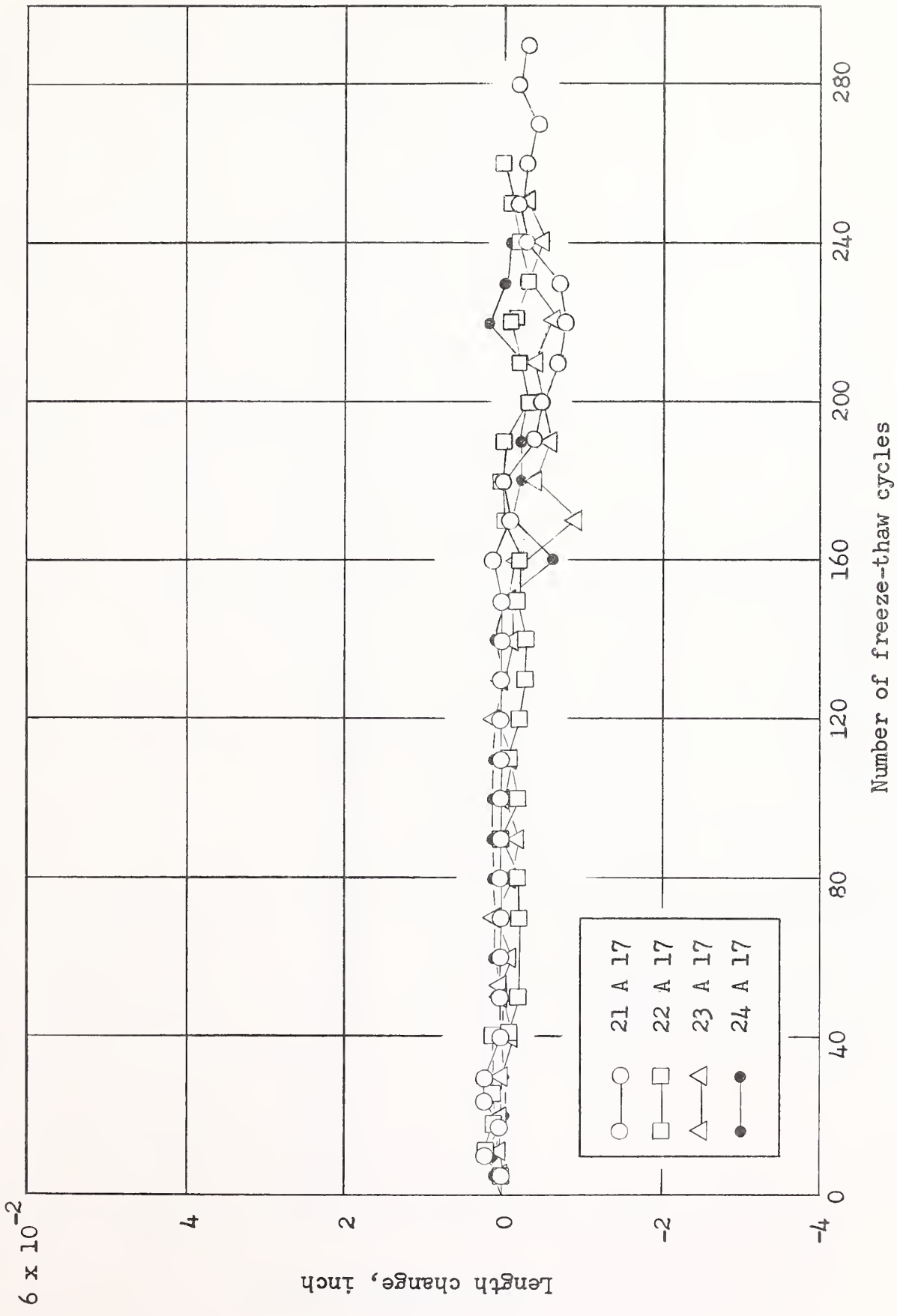

Fig. 77. Length changes versus number of freeze-thaw cycles for 1200 psi., normally cured, water ponded slabs.

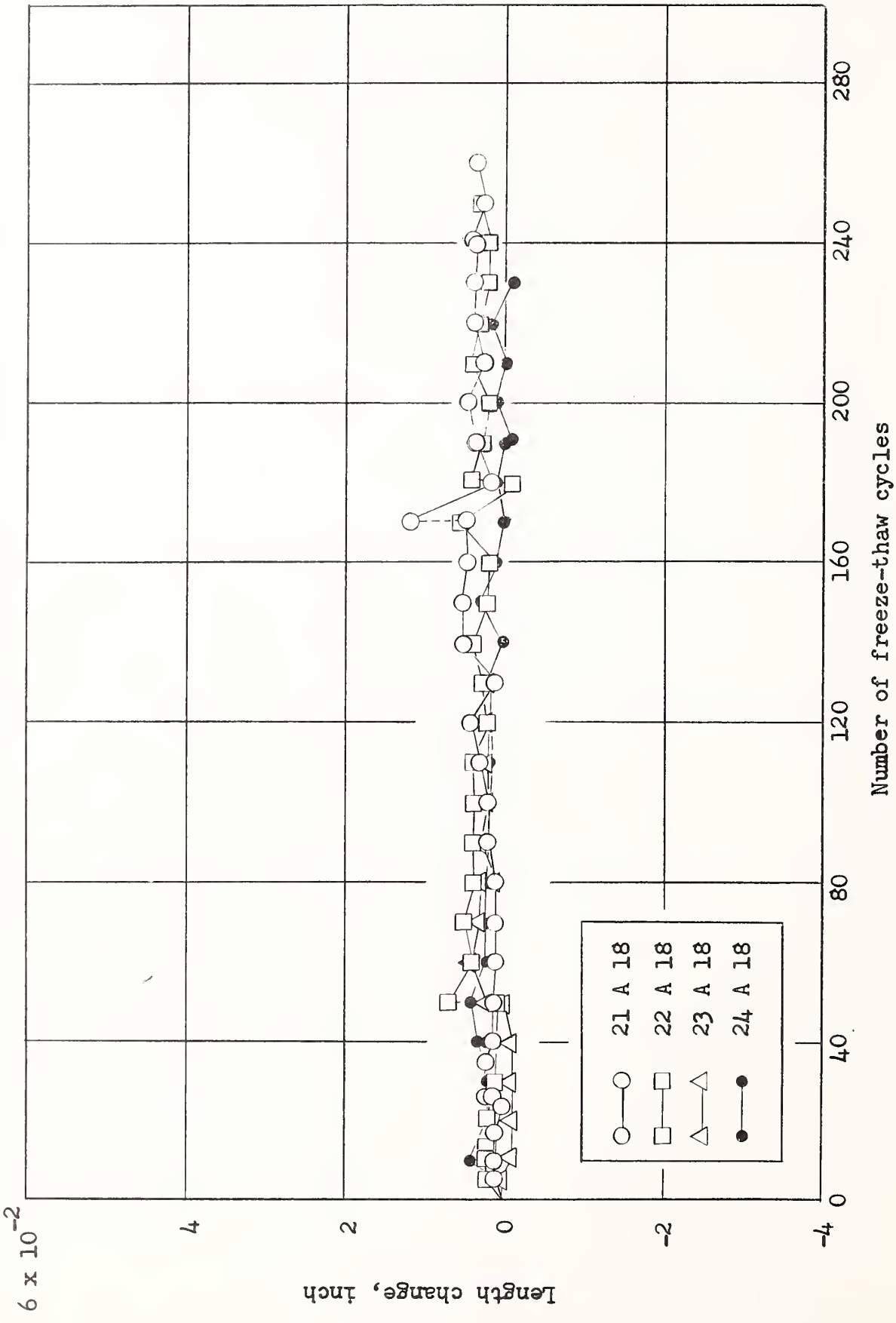

Fig. 78. Length changes versus number of freeze-thaw cycles for 1200 psi., normally cured, $CaCl_2$ solution ponded slabs.

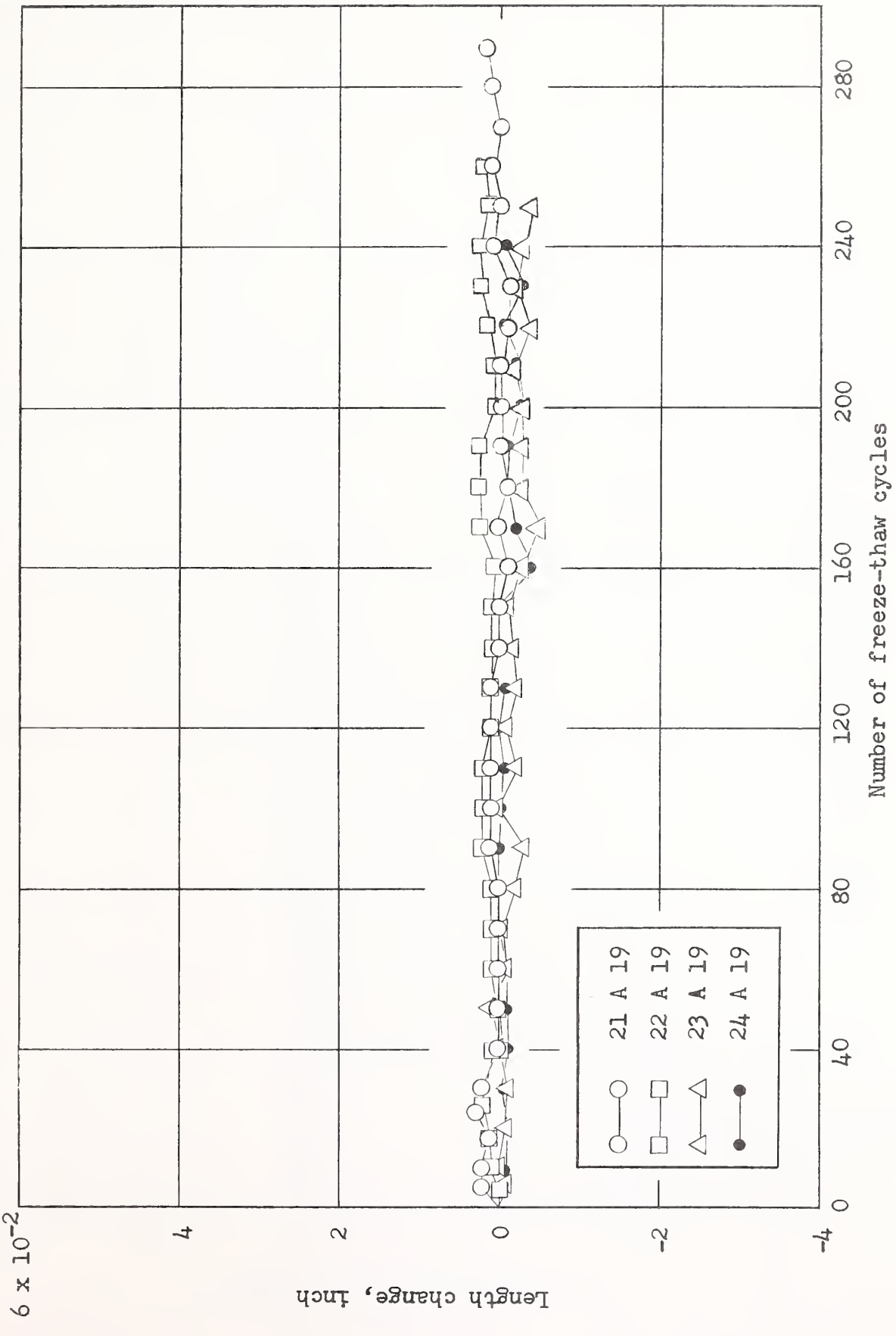

Fig. 79. Length changes versus number of freeze-thaw cycles for 1200 psi., steam cured, water ponded slabs.

Fig. 80. Length changes versus number of freeze-thaw cycles for 1200 psi., steam cured, $CaCl_2$ solution ponded slabs.

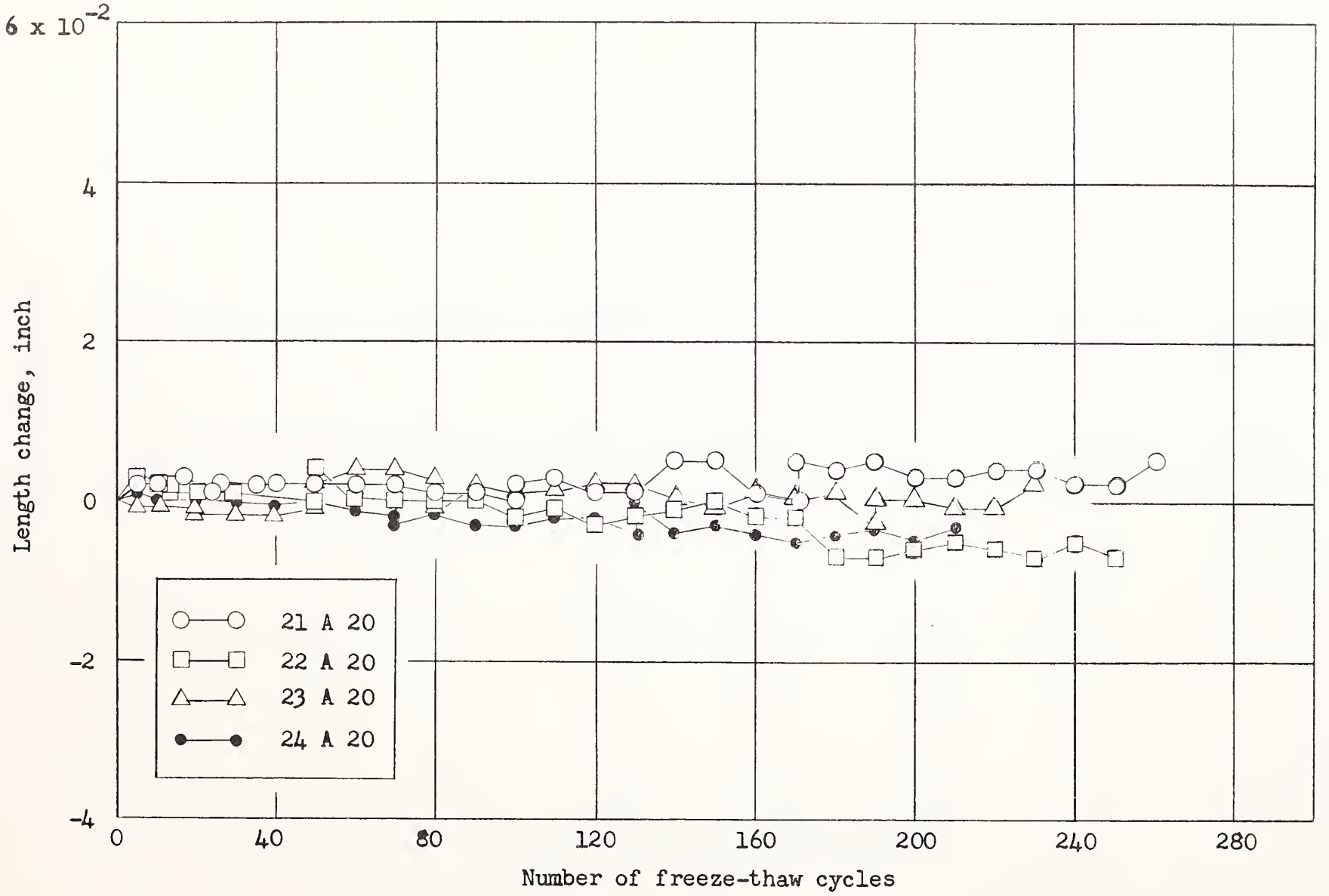

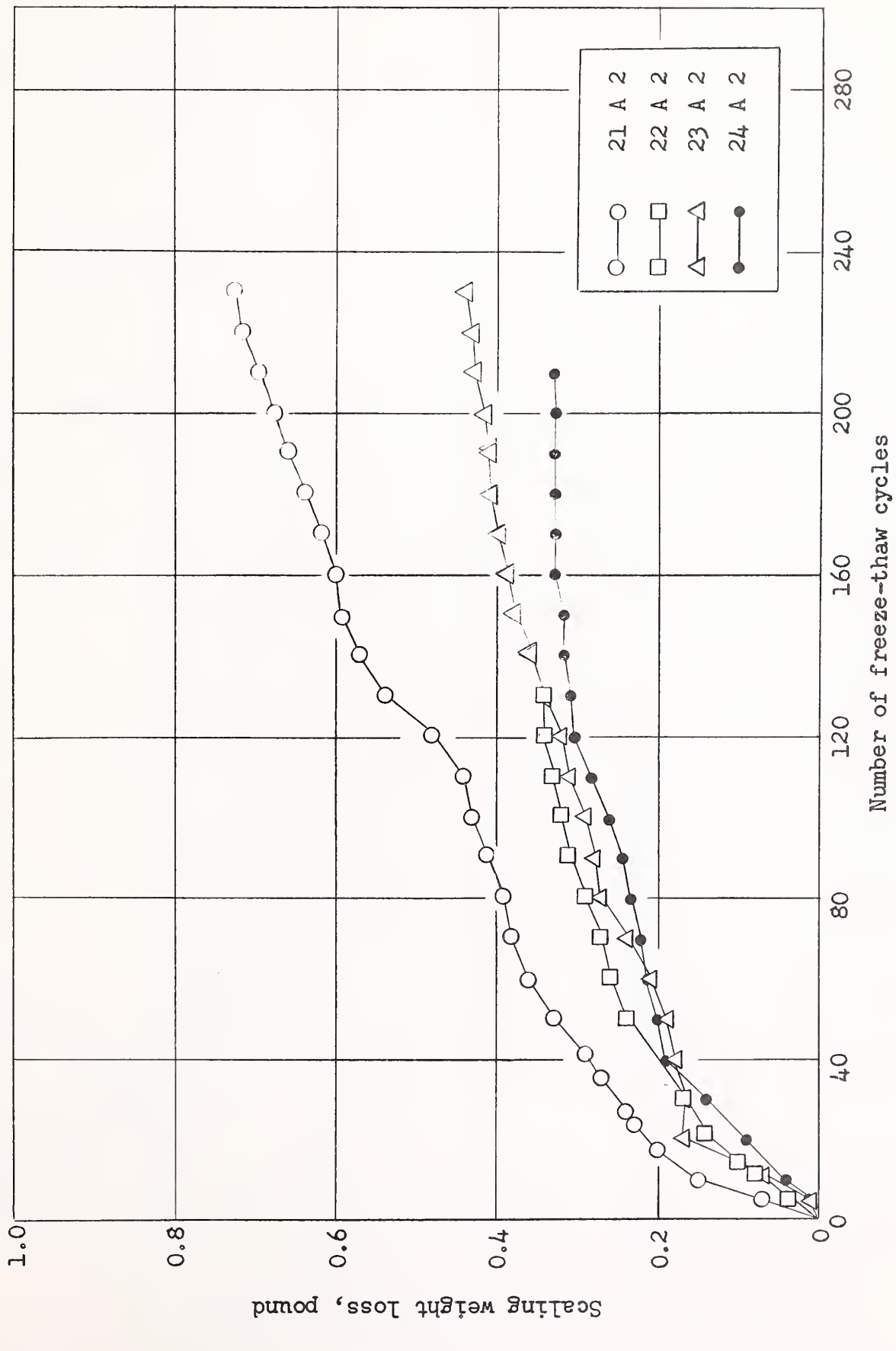

Fig. 81. Scaling weight losses versus number of freeze-thaw cycles for non-stressed, normally cured, $CaCl_2$ solution ponded slabs.

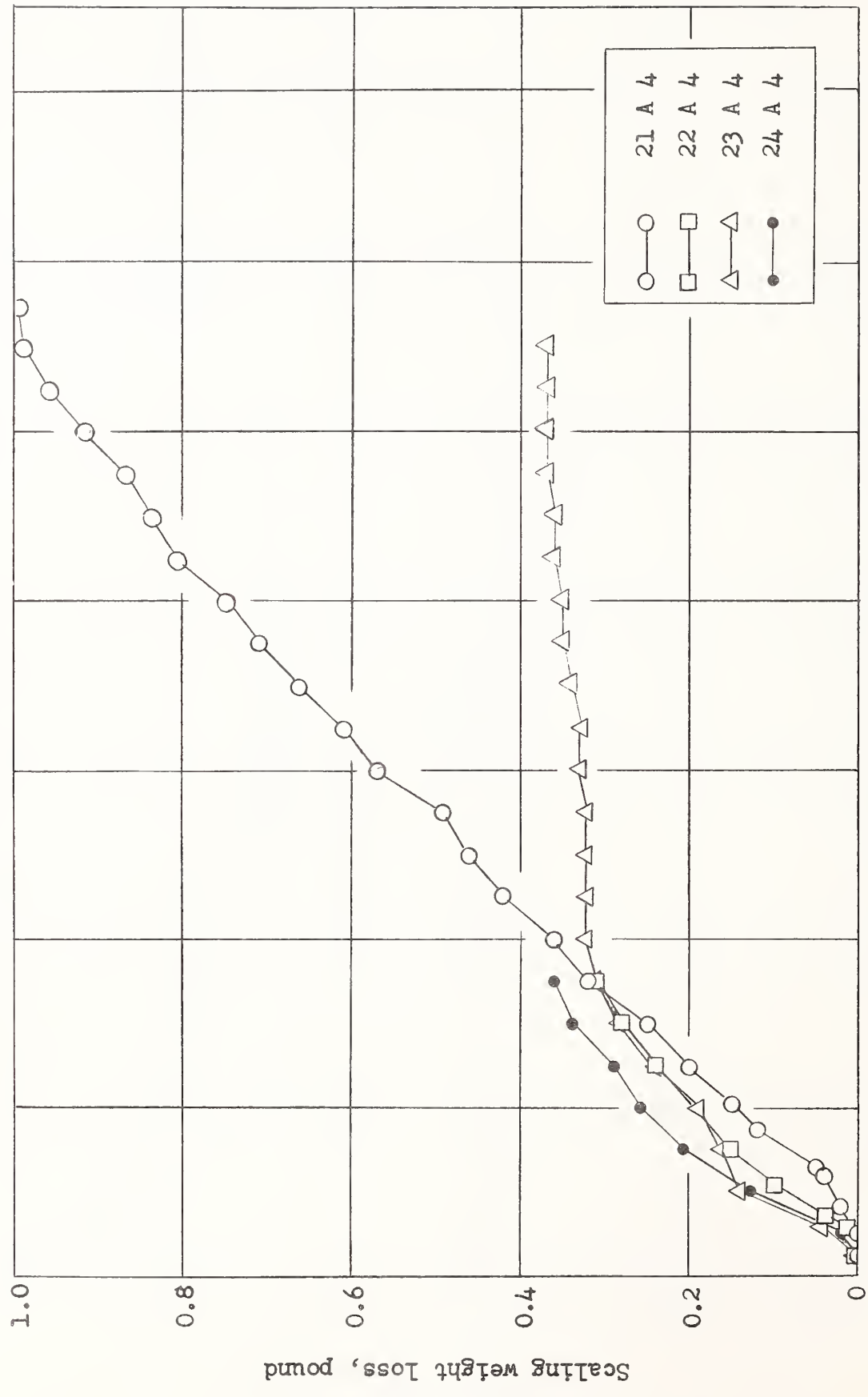

Fig. 82. Scaling weight losses versus number of freeze-thaw cycles for non-stressed, steam cured, $CaCl_2$ solution ponded slabs.

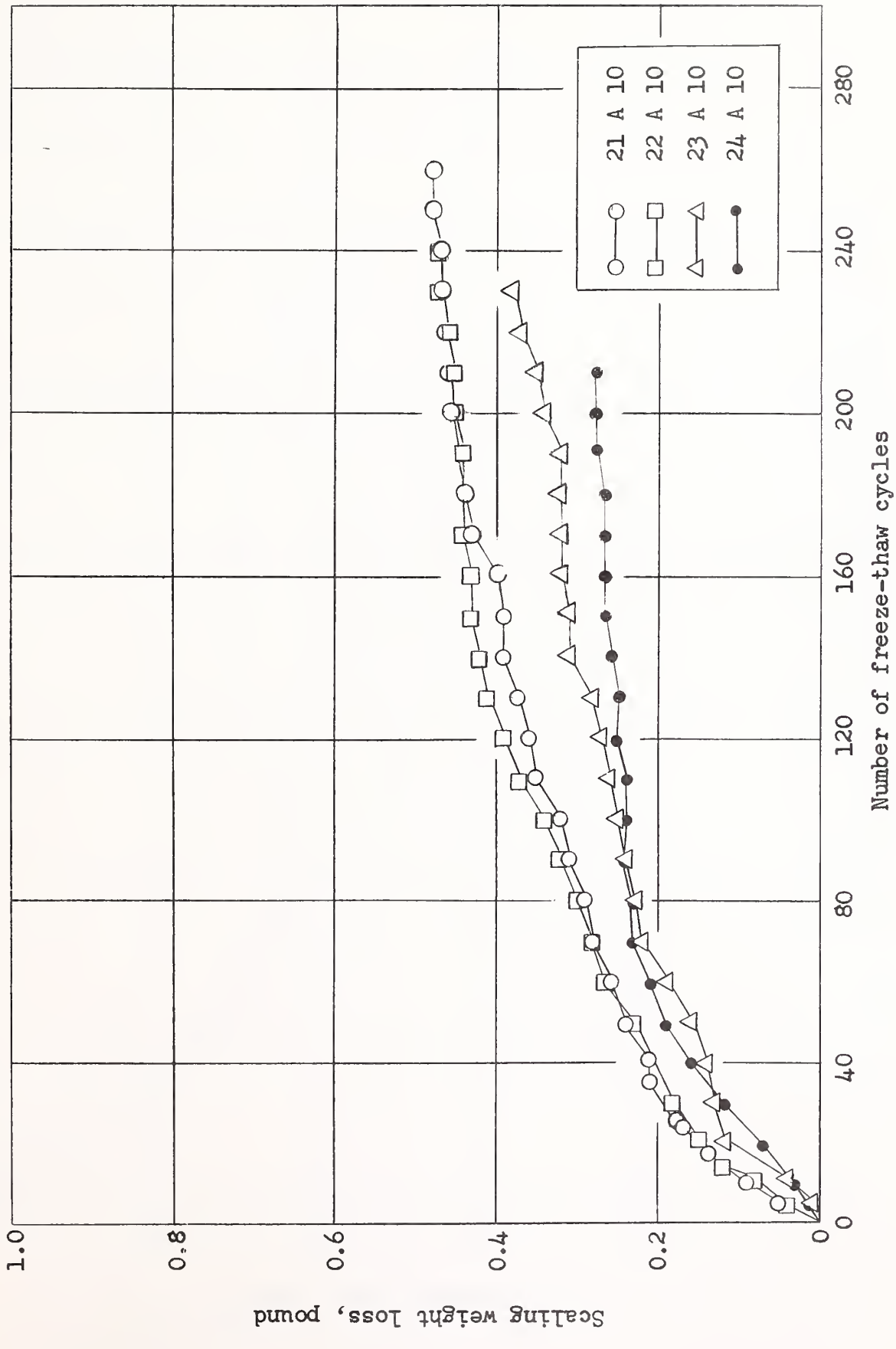

Fig. 83. Scaling weight losses versus number of freeze-thaw cycles for 500 psi., normally cured, $CaCl_2$ solution ponded slabs.

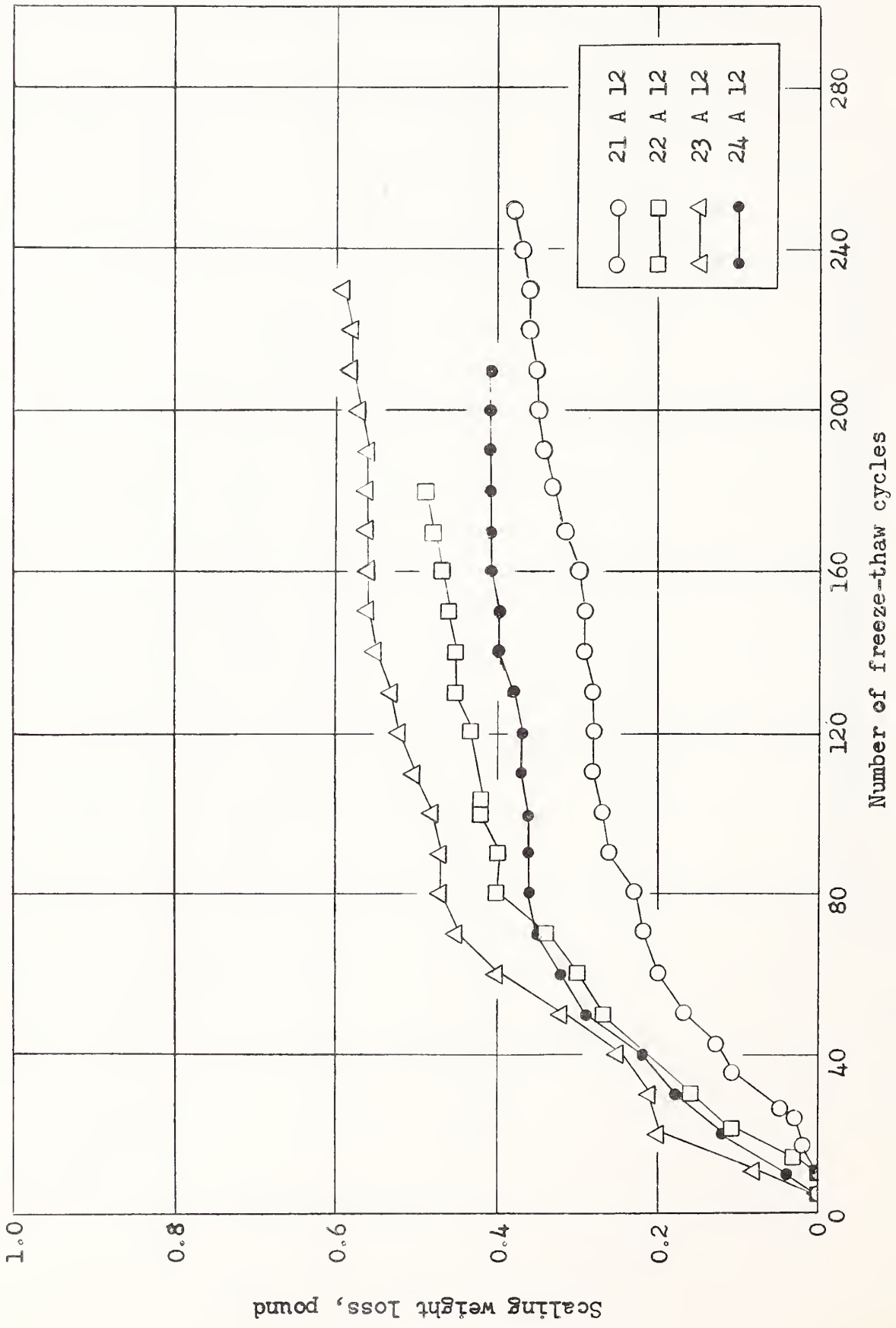

Fig. 84. Scaling weight losses versus number of freeze-thaw cycles for 500 psi., steam cured, $CaCl_2$ solution ponded slabs.

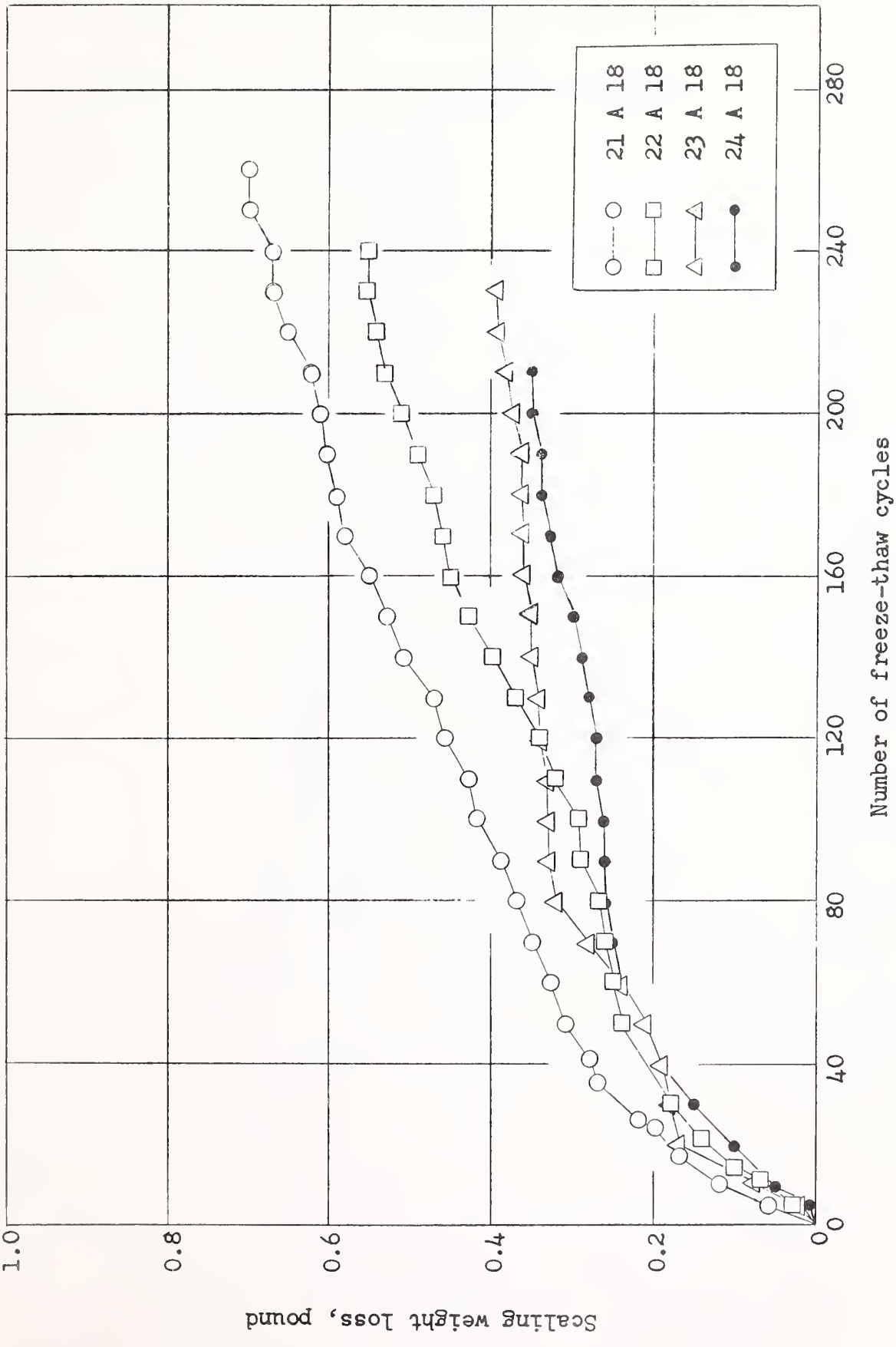

Fig. 85. Scaling weight losses versus number of freeze-thaw cycles for 1200 psi., normally cured, $CaCl_2$ solution ponded slabs.

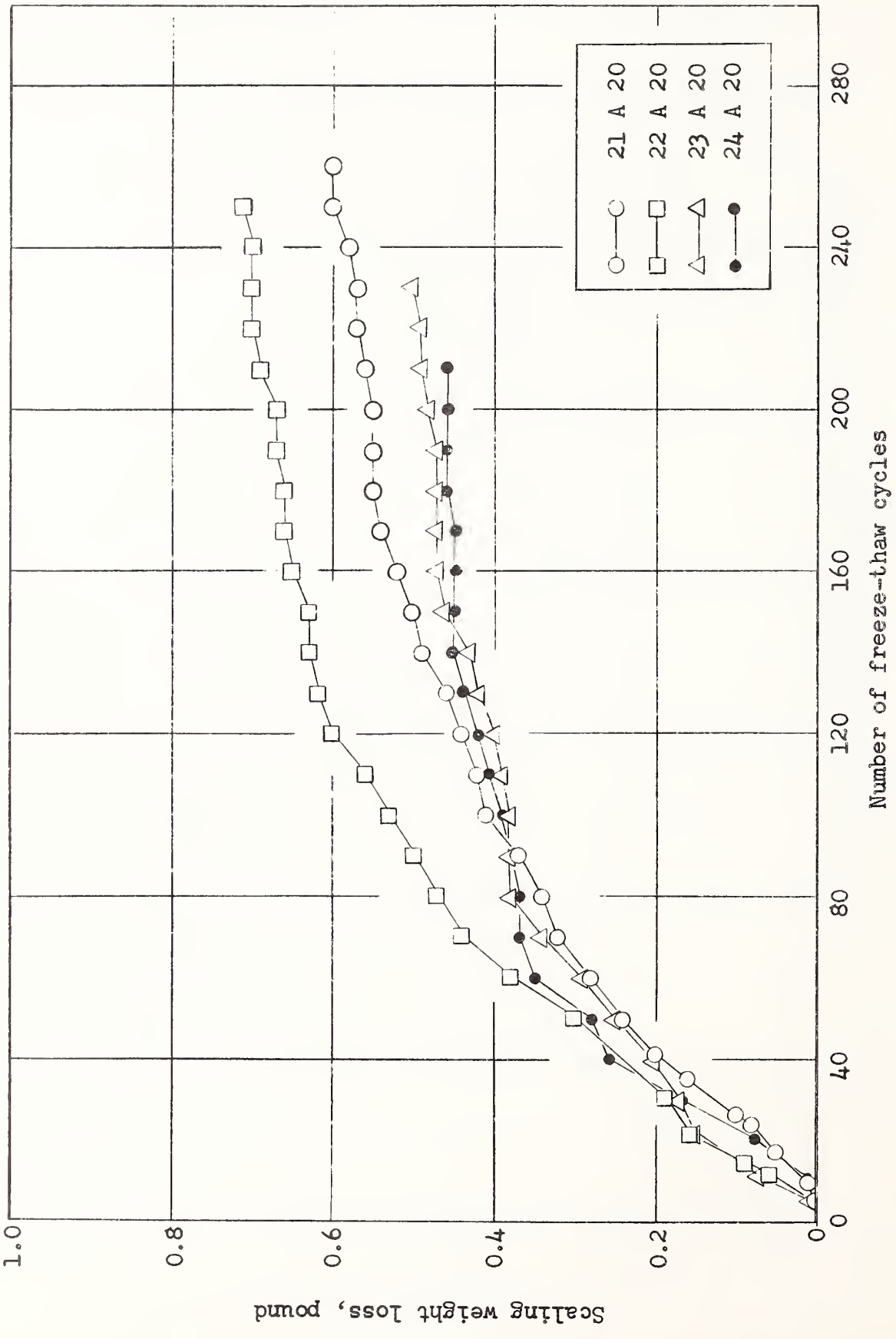

Fig. 86. Scaling weight losses versus number of freeze-thaw cycles for 1200 psi., steam cured, $CaCl_2$ solution ponded slabs.

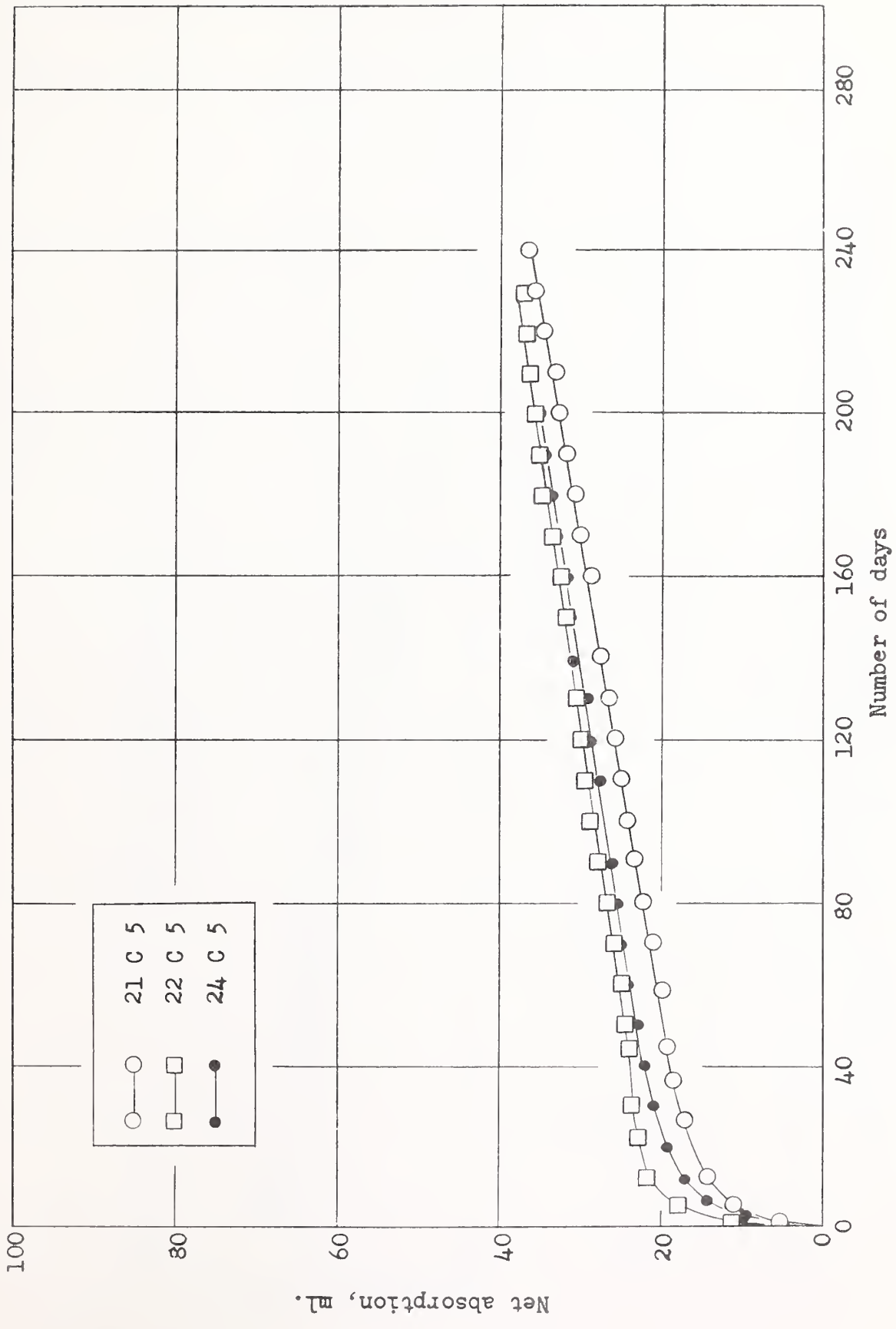

Fig. 87. Net absorptions versus number of days for non-stressed, normally cured slabs under two-foot head of water.

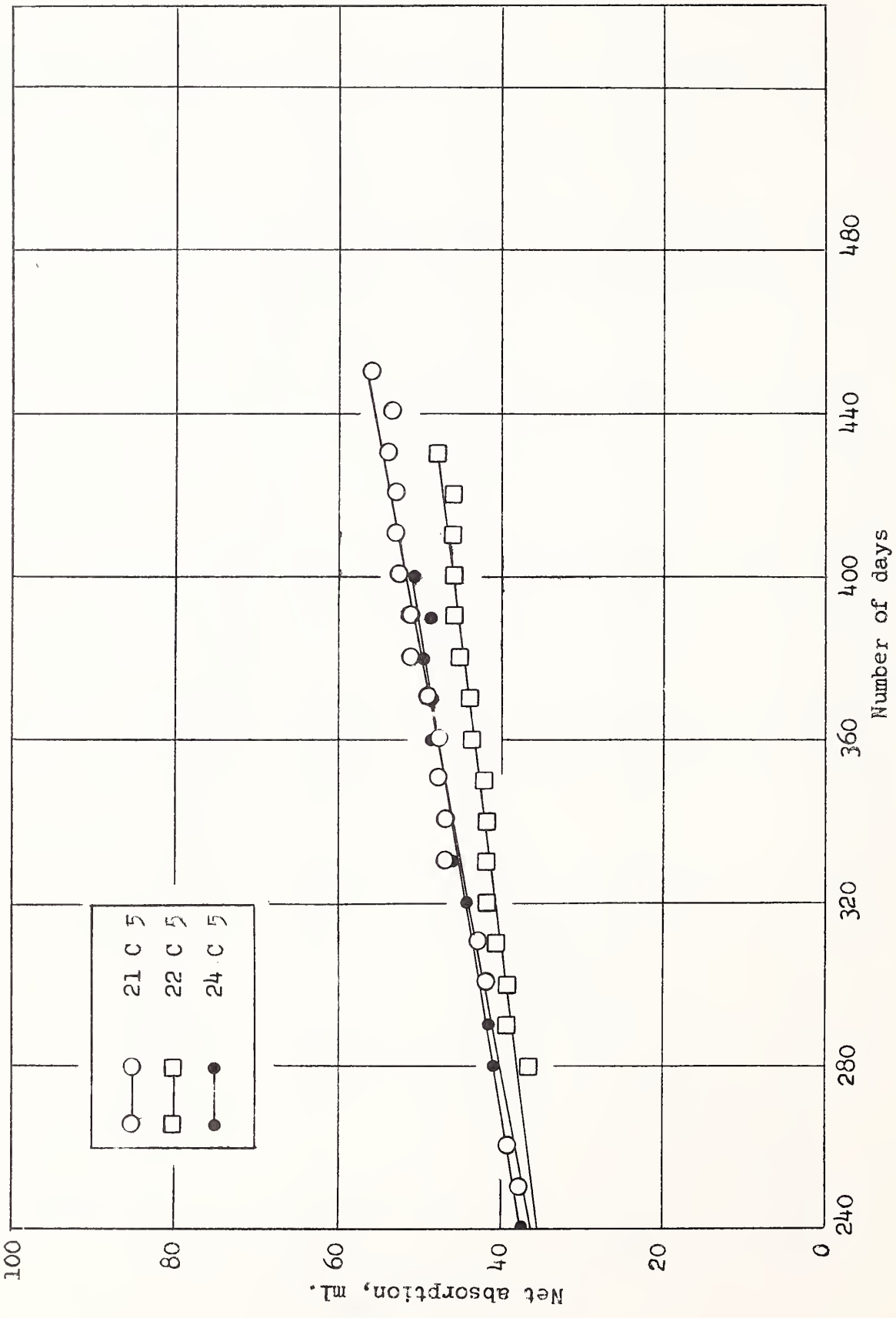

Fig. 87. (Cont.) Net absorptions versus number of days for non-stressed, normally cured slabs under two-foot head of water.

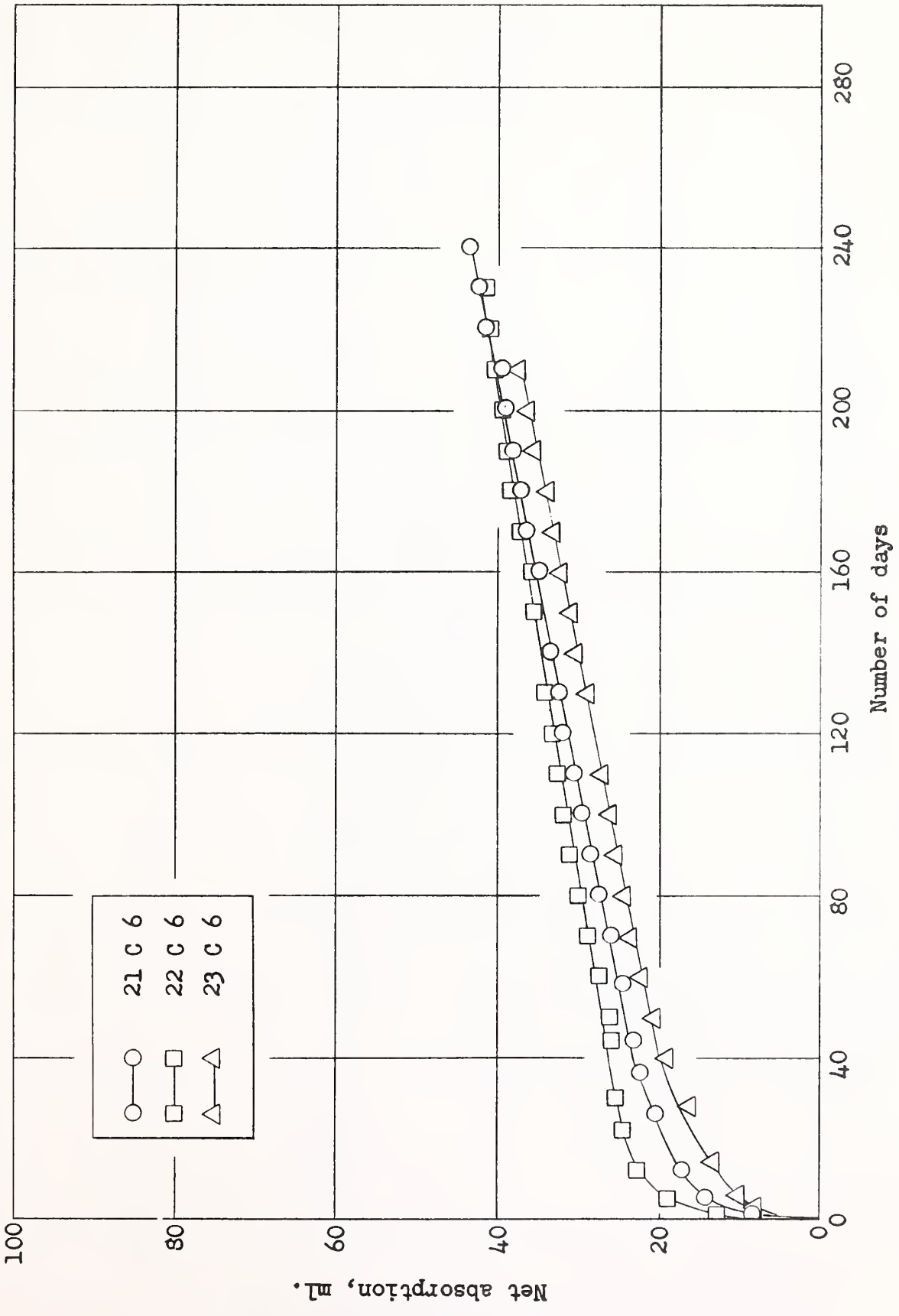

Fig. 88. Net absorptions versus number of days for non-stressed, normally cured slabs under two-foot head of $CaCl_2$ solution.

Fig. 88. (Cont.) Net absorptions versus number of days fornon-stressed, normally cured slabs under two-foot head of $CaCl_2$ solution.

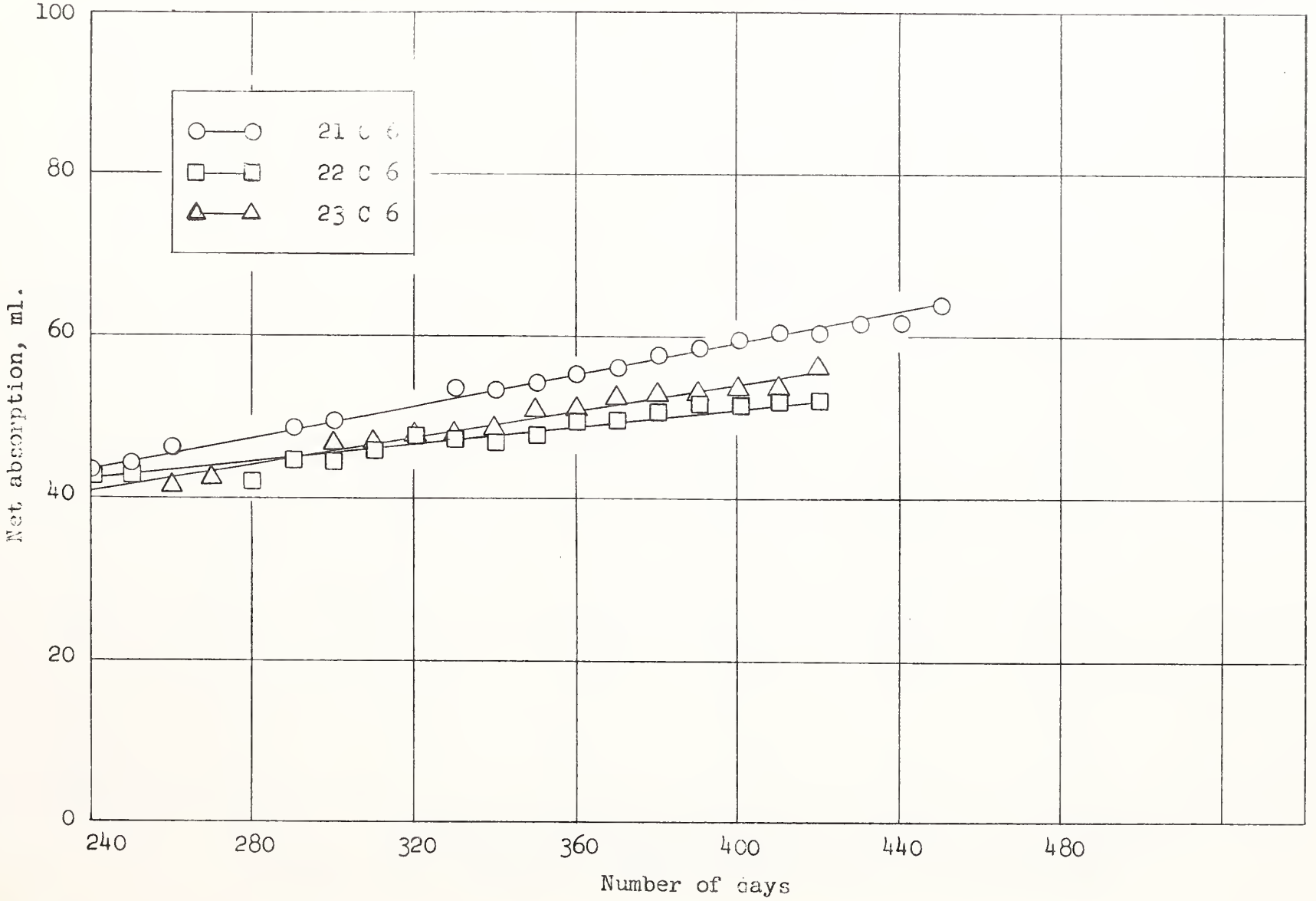

Fig. 89. Net absorptions versus number of days for non-stressed, steam cured slabs under two-foot head of water.

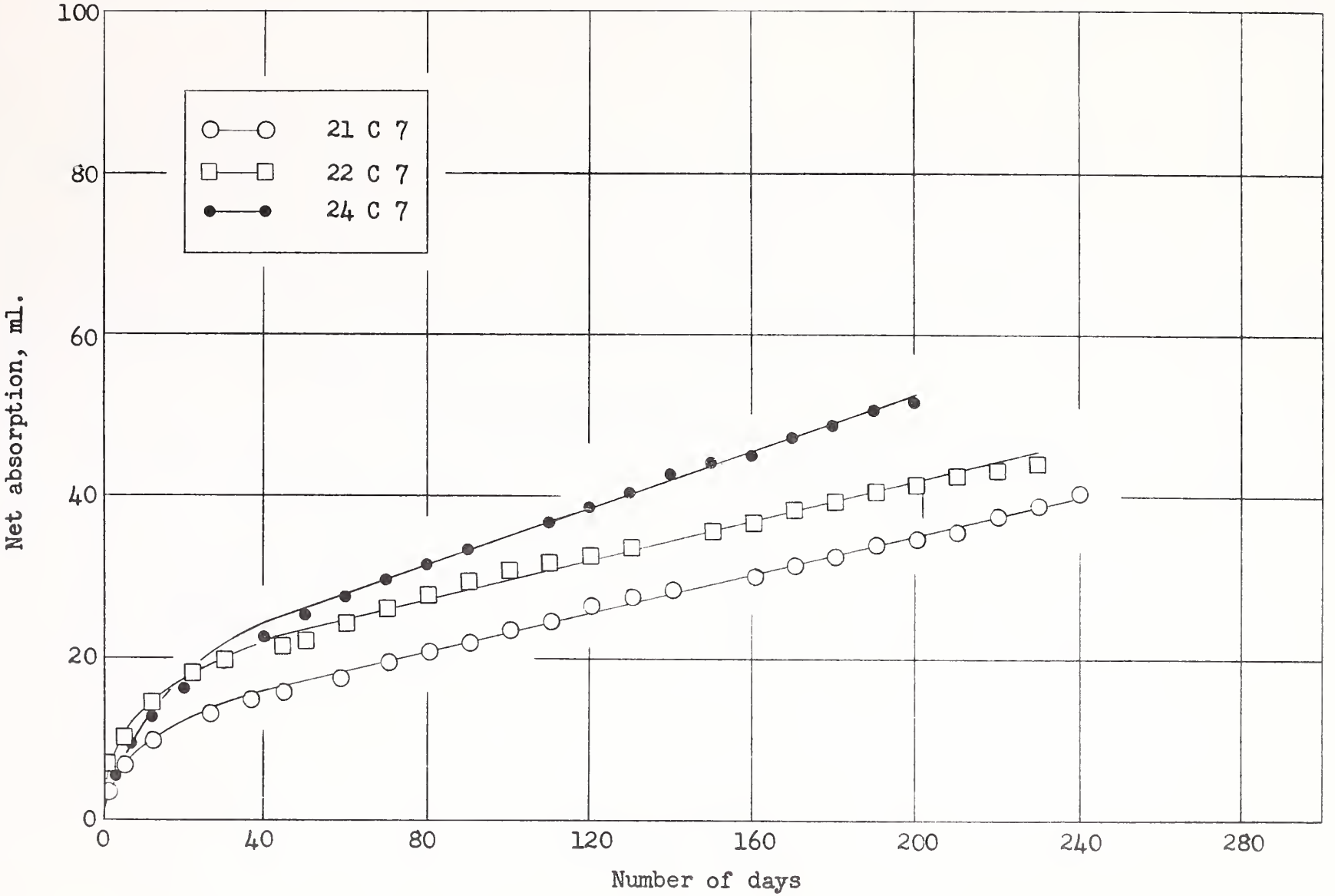

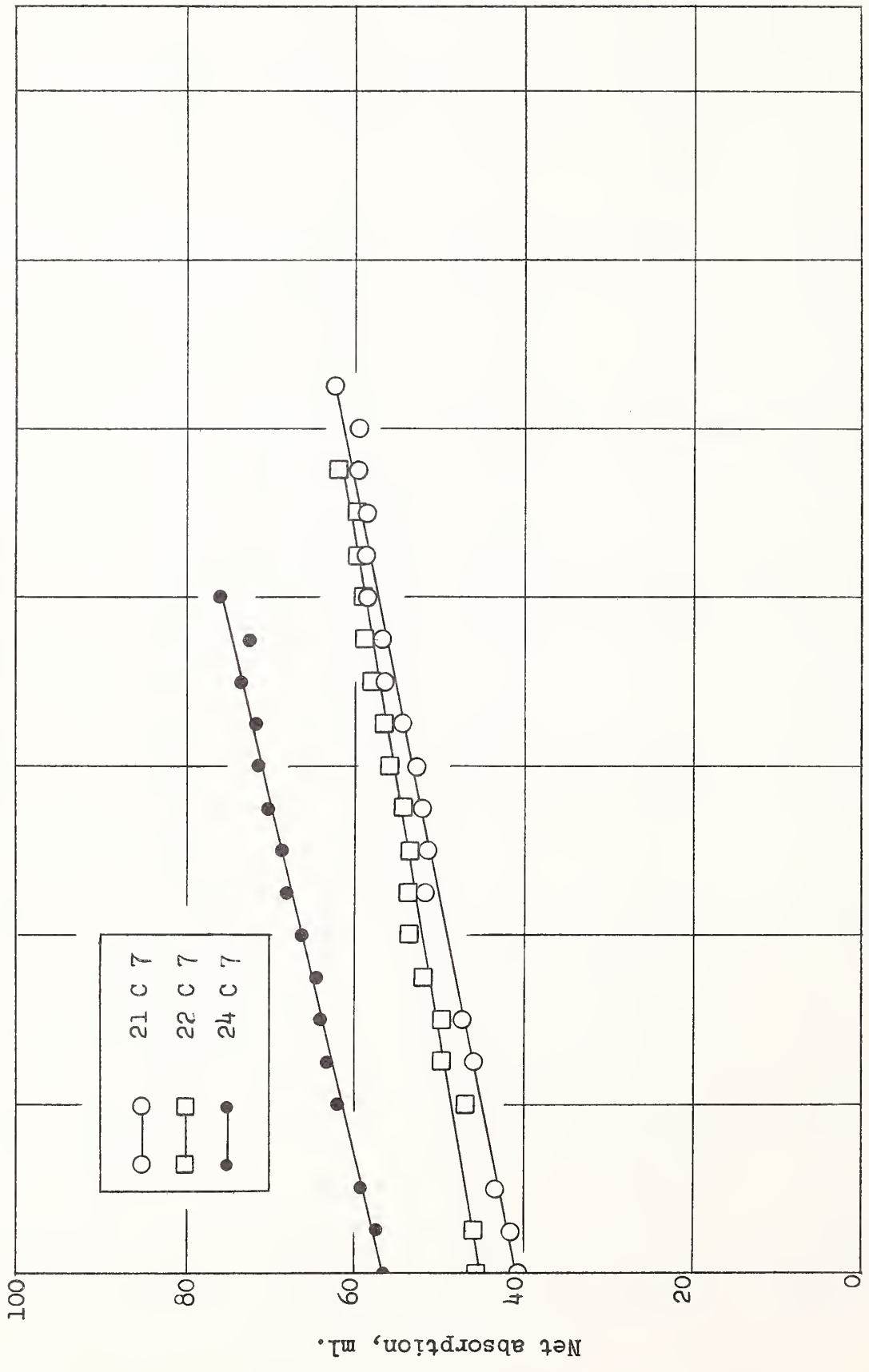

Fig. 89. (Cont.) Net absorptions versus number of days for non-stressed steam cured slabs under two-foot head of water.

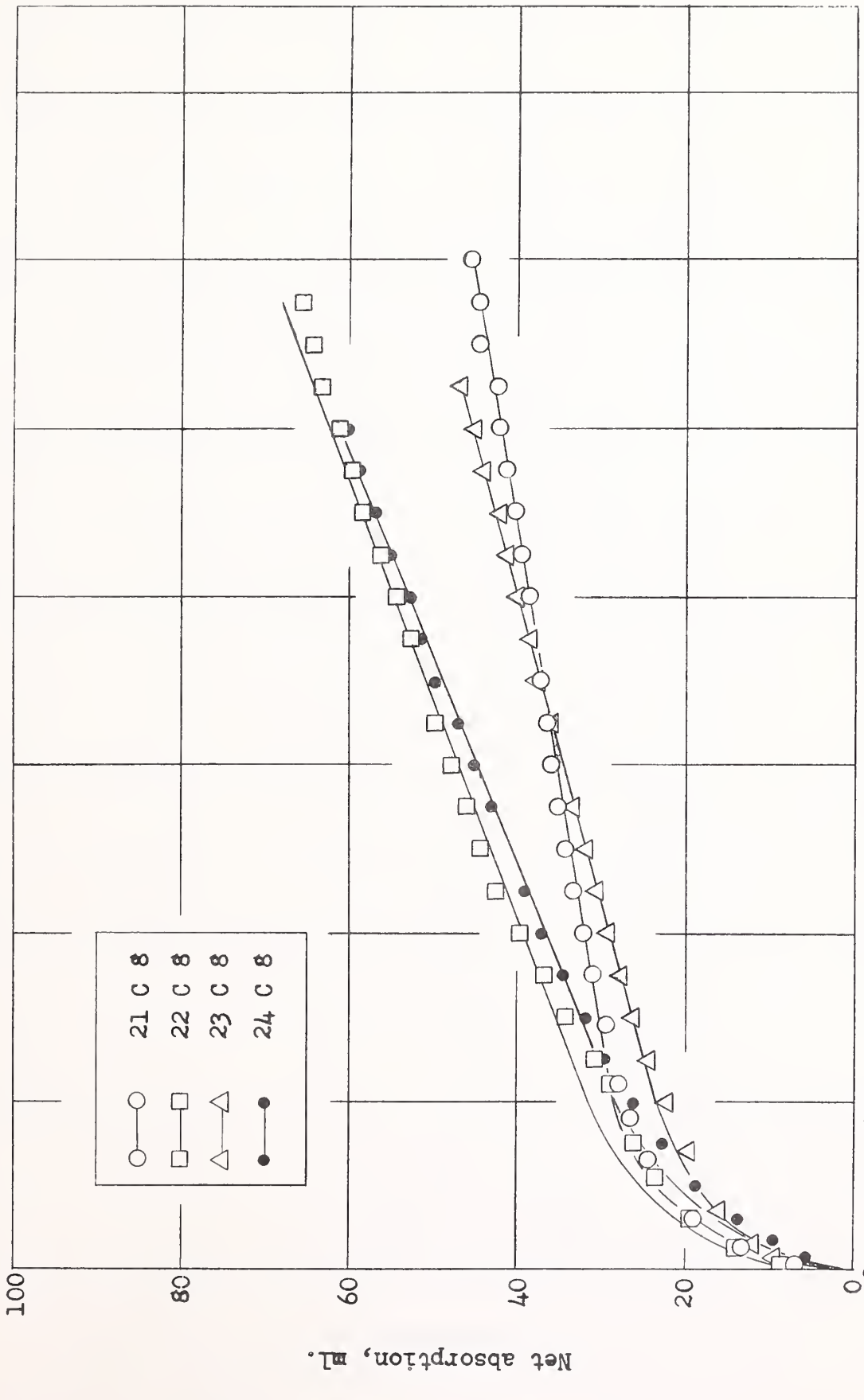

Fig. 90. Net absorptions versus number of days for non-stressed, steam cured slabs under two-foot head of $CaCl_2$ solution.

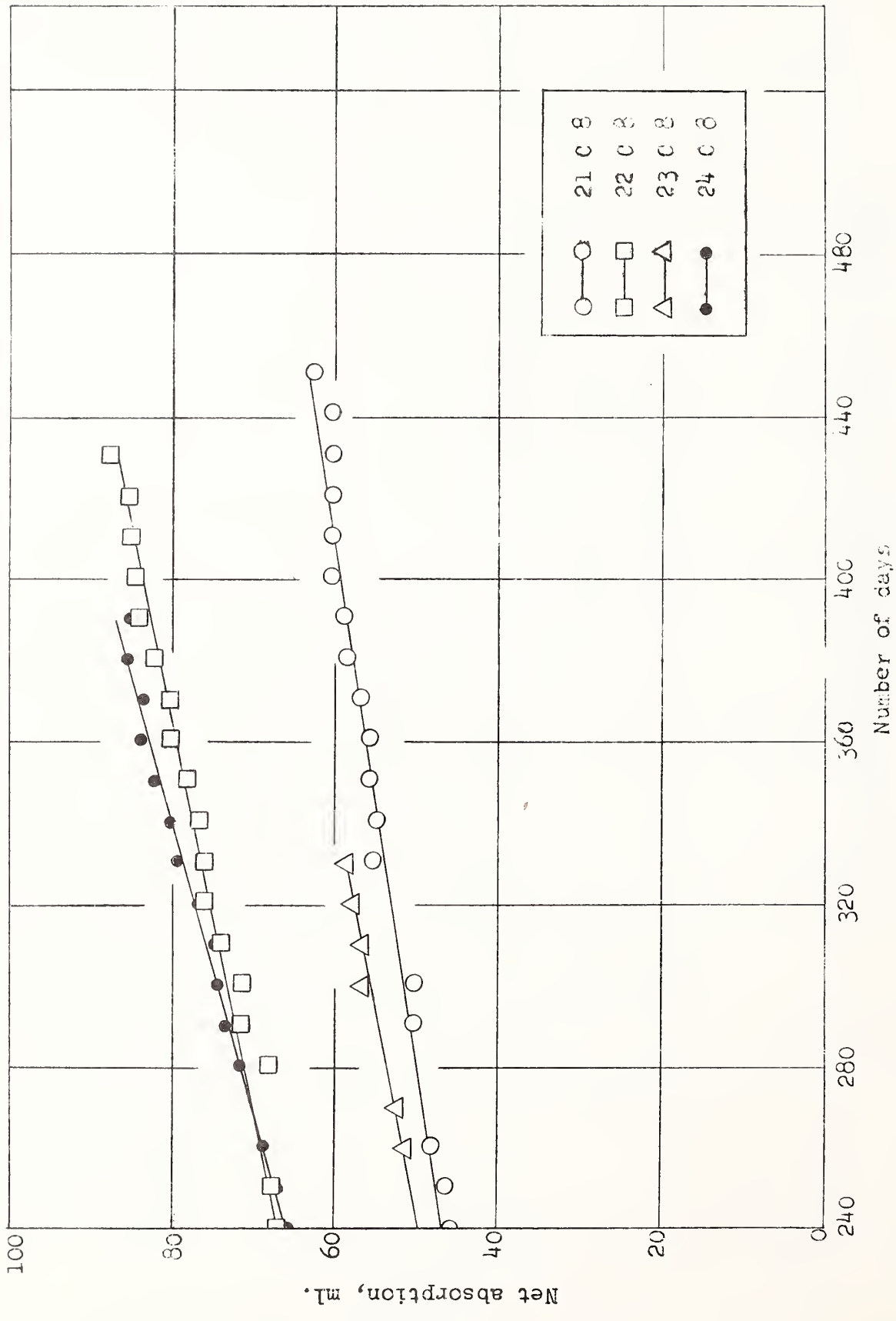

Fig. 90. (Cont.) Net absorptions versus number of days for non-stressed, steam cured slabs under two-foot head of $CaCl_2$ solution.

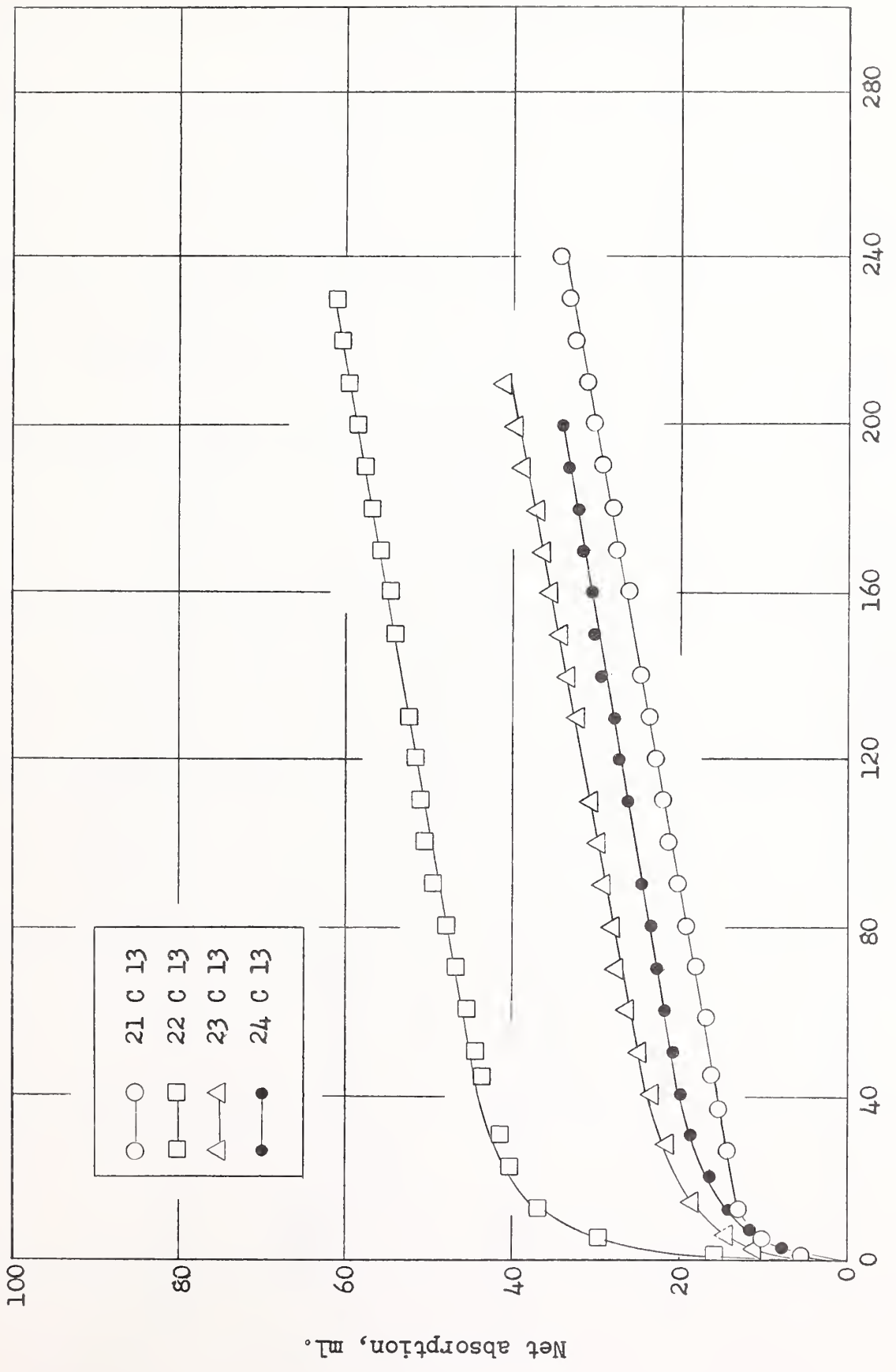

Fig. 91. Net absorptions versus number of days for 500 psi., normally cured slabs under two-foot head of water.

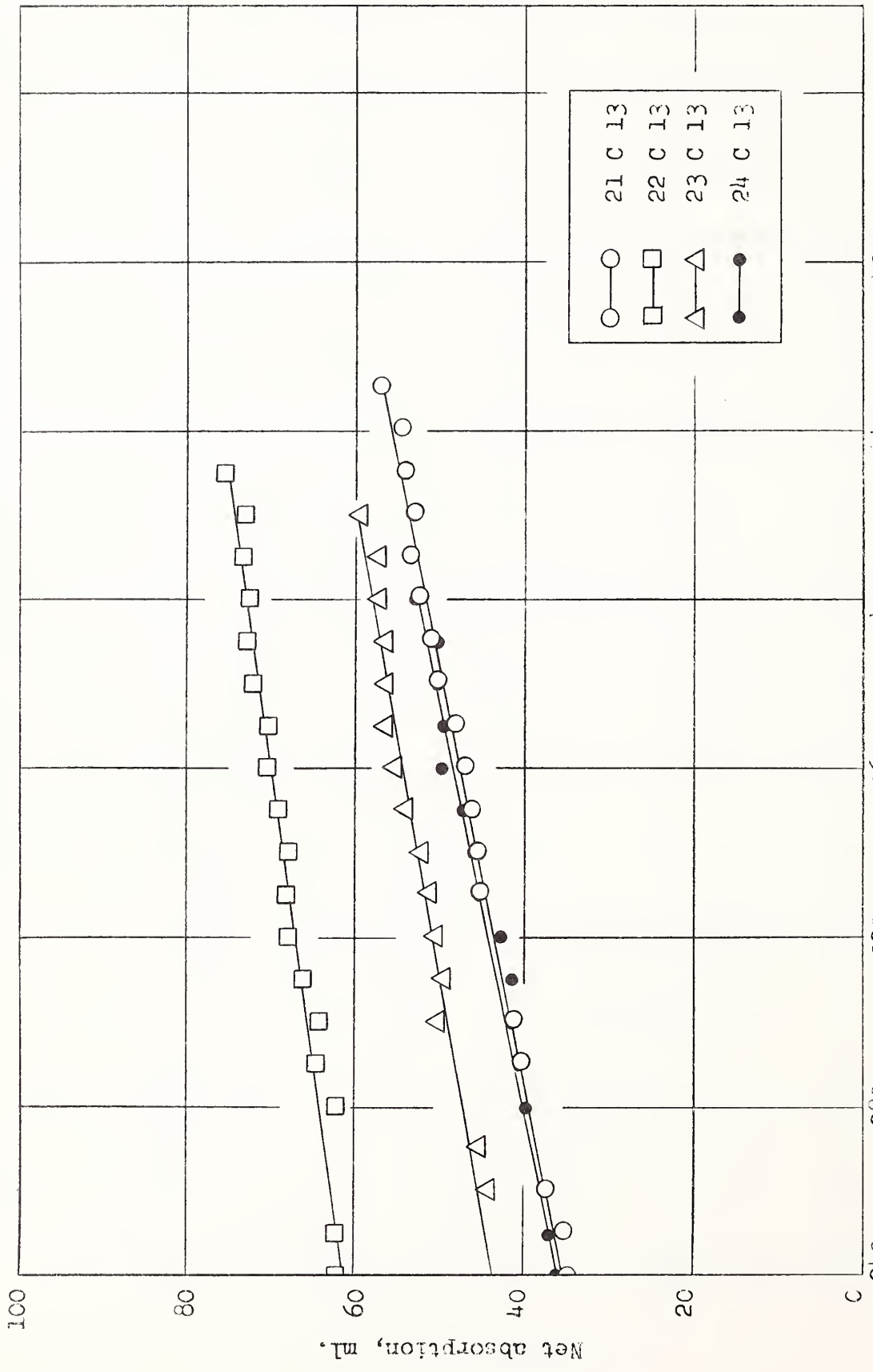

Fig. 91. (Cont.) Net absorptions versus number of days for 500 psi., normally cured slabs under two-foot head of water.

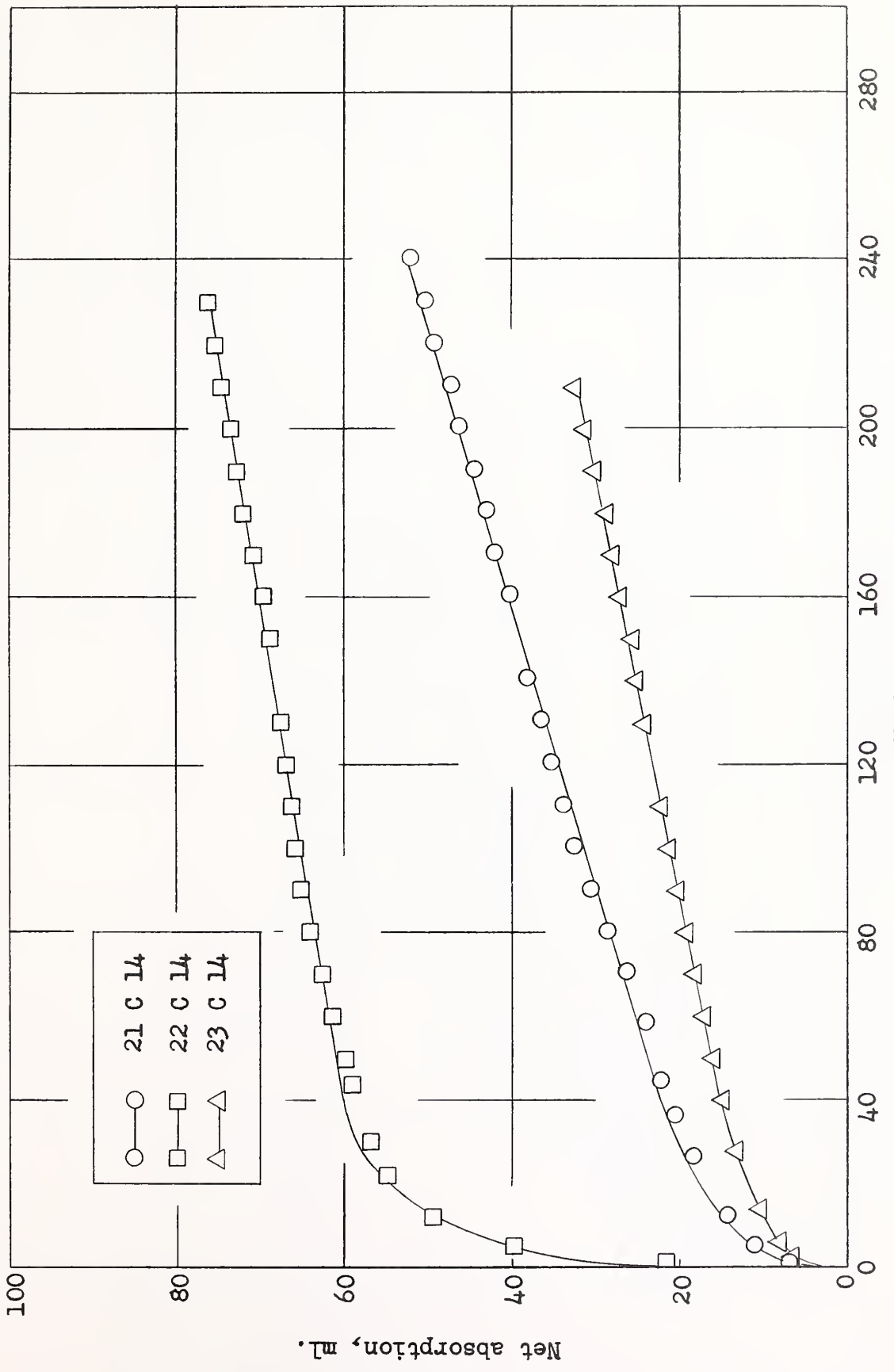

Fig. 92. Net absorptions versus number of days for 500 psi., normally cured slabs under two-foot head of $CaCl_2$ solution.

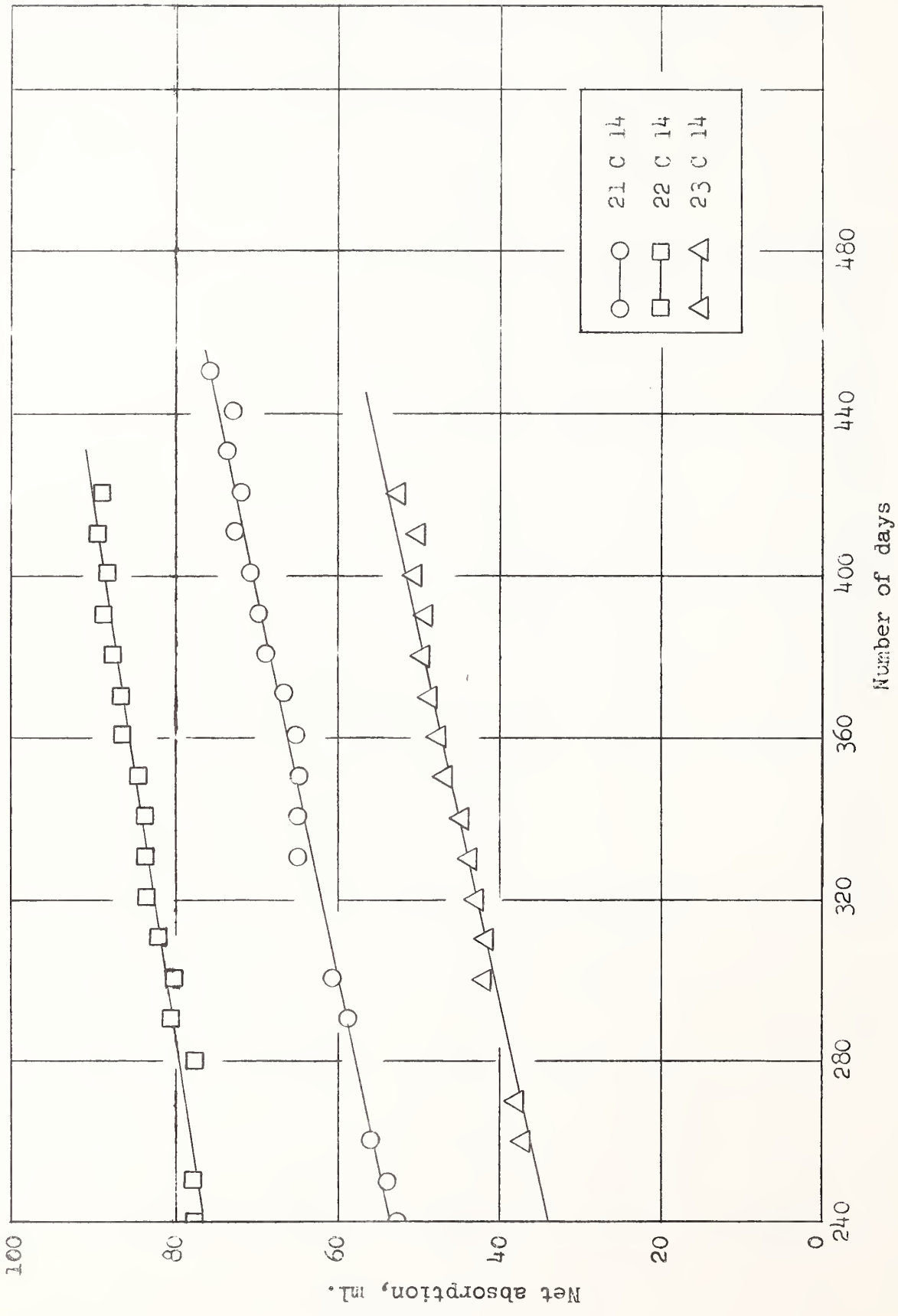

Fig. 92. (Cont.) Net absorptions versus number of days for 500 psi., normally cured slabs under two-foot head of $CaCl_2$ solution.

Fig. 93. Net absorptions versus number of days for 500 psi., steam cured slabs under two-foot head of water.

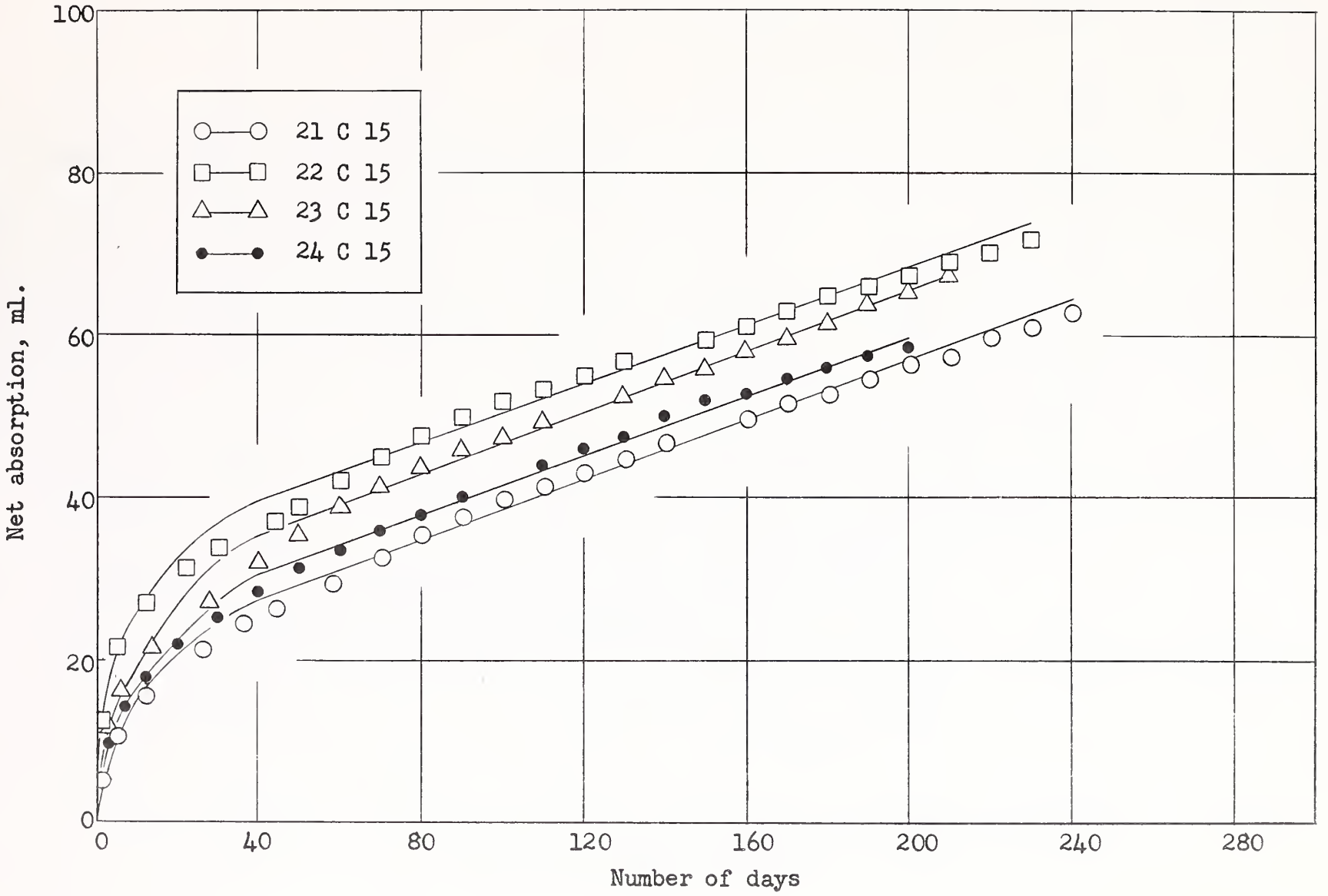

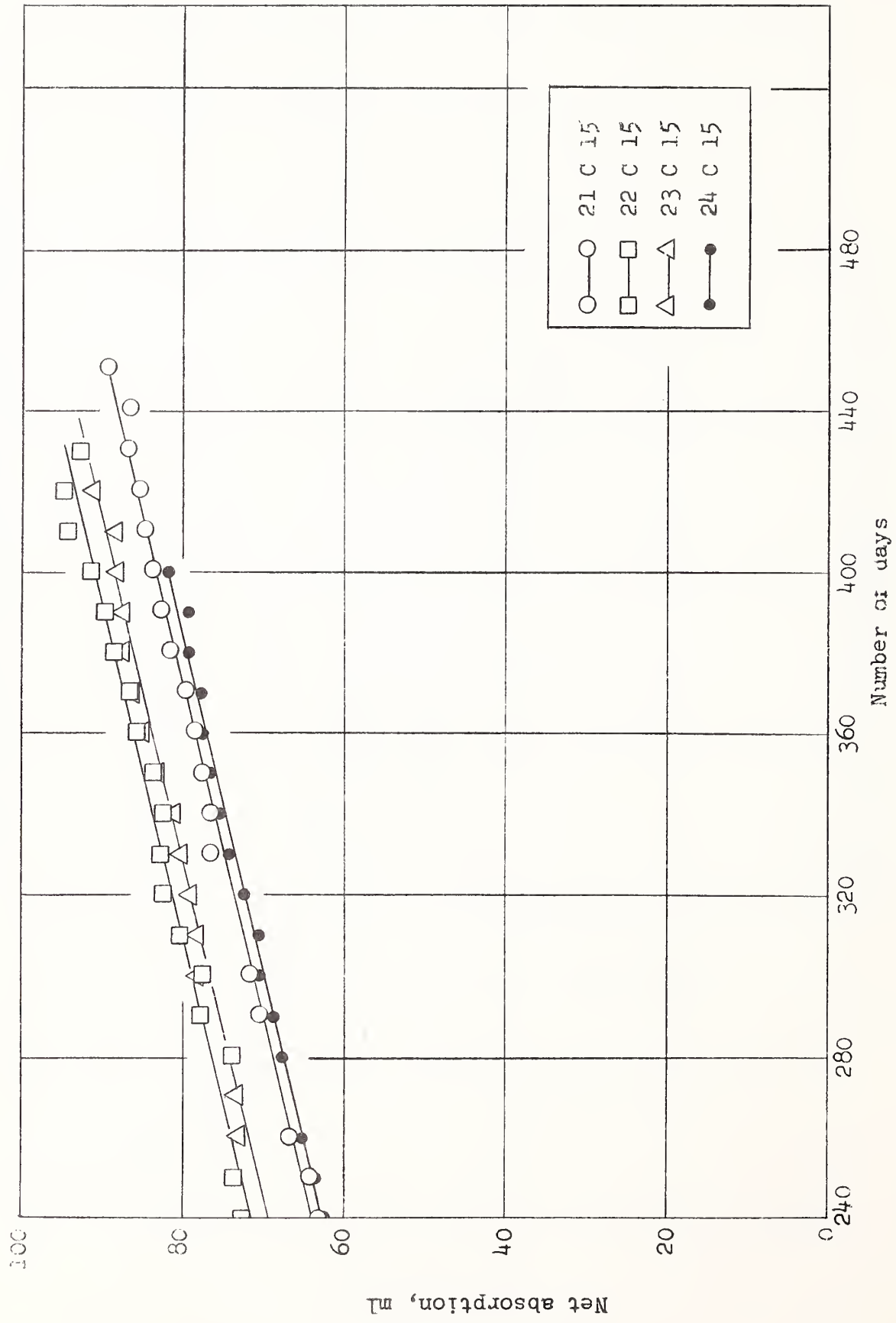

Fig. 93. (Cont.) Net absorptions versus number of days for 500 psi., steam cured slabs under two-foot head of water.

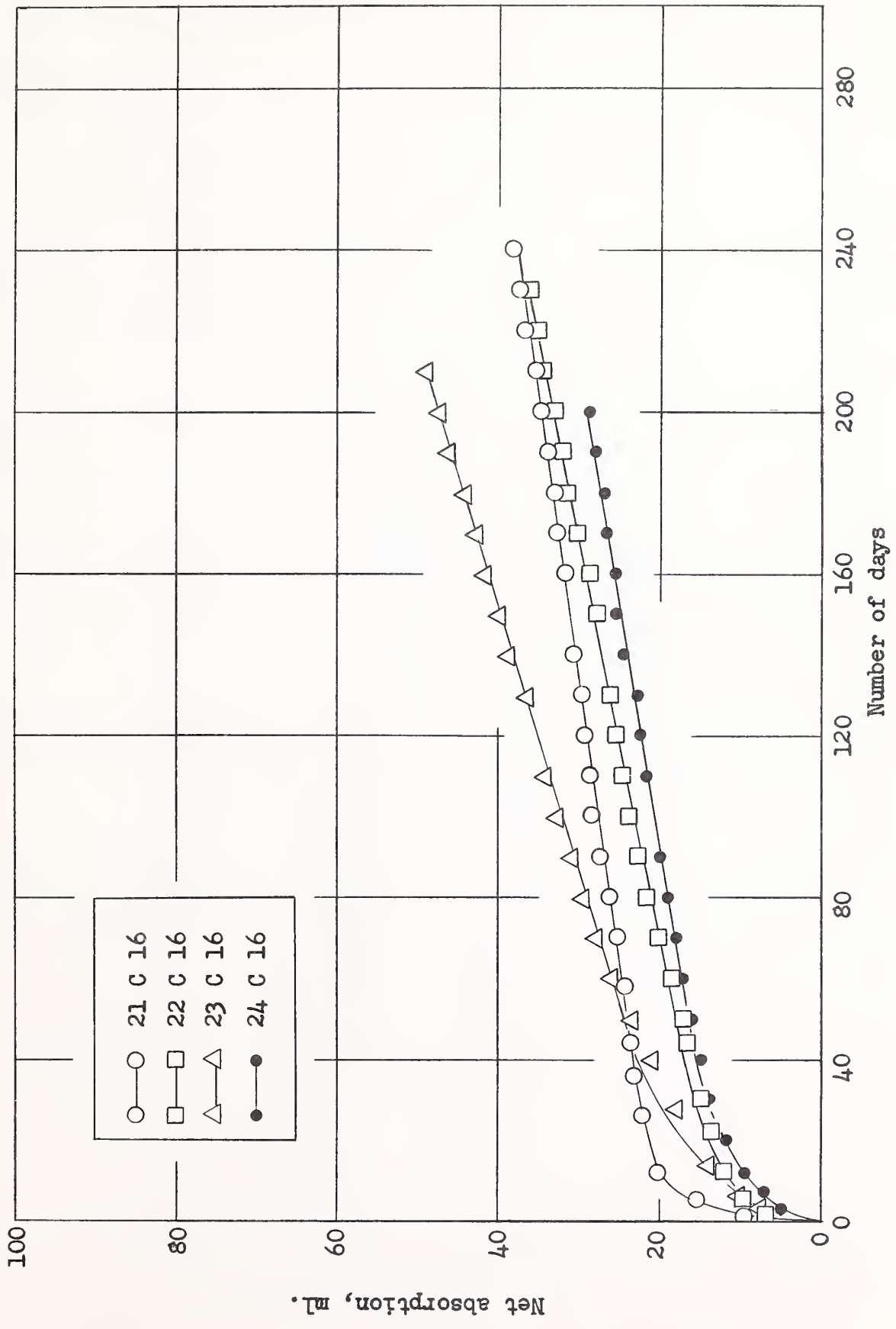

Fig. 94. Net absorptions versus number of days for 500 psi., steam cured slabs under two-foot head of $CaCl_2$ solution.

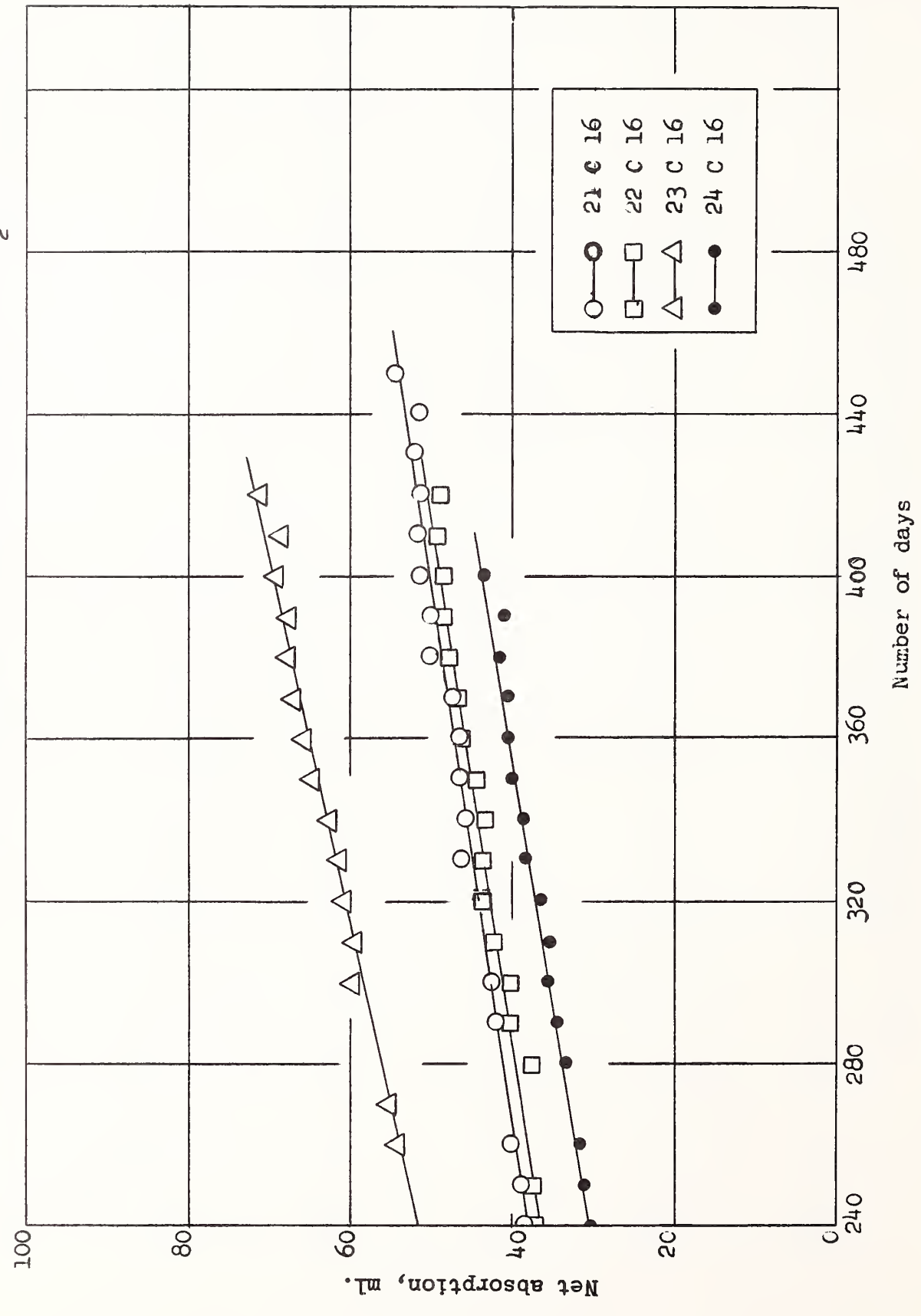

Fig. 94. (Cont.) Net absorptions versus number of days for 500 psi., steam cured slabs under two-foot head of $CaCl_2$ solution.

Fig. 95. Net absorptions versus number of days for 1200 psi., normally cured slabs under two-foot head of water.

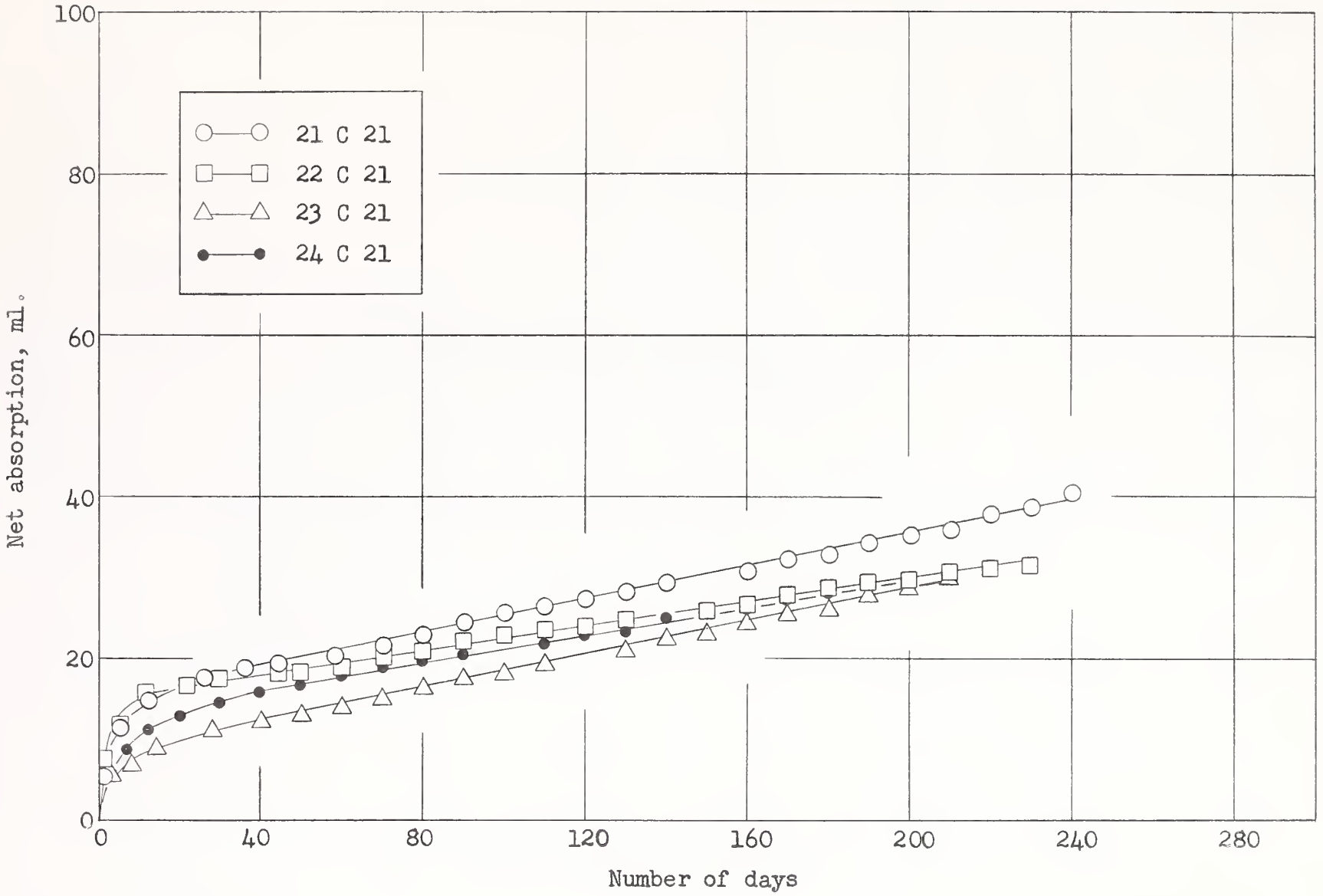

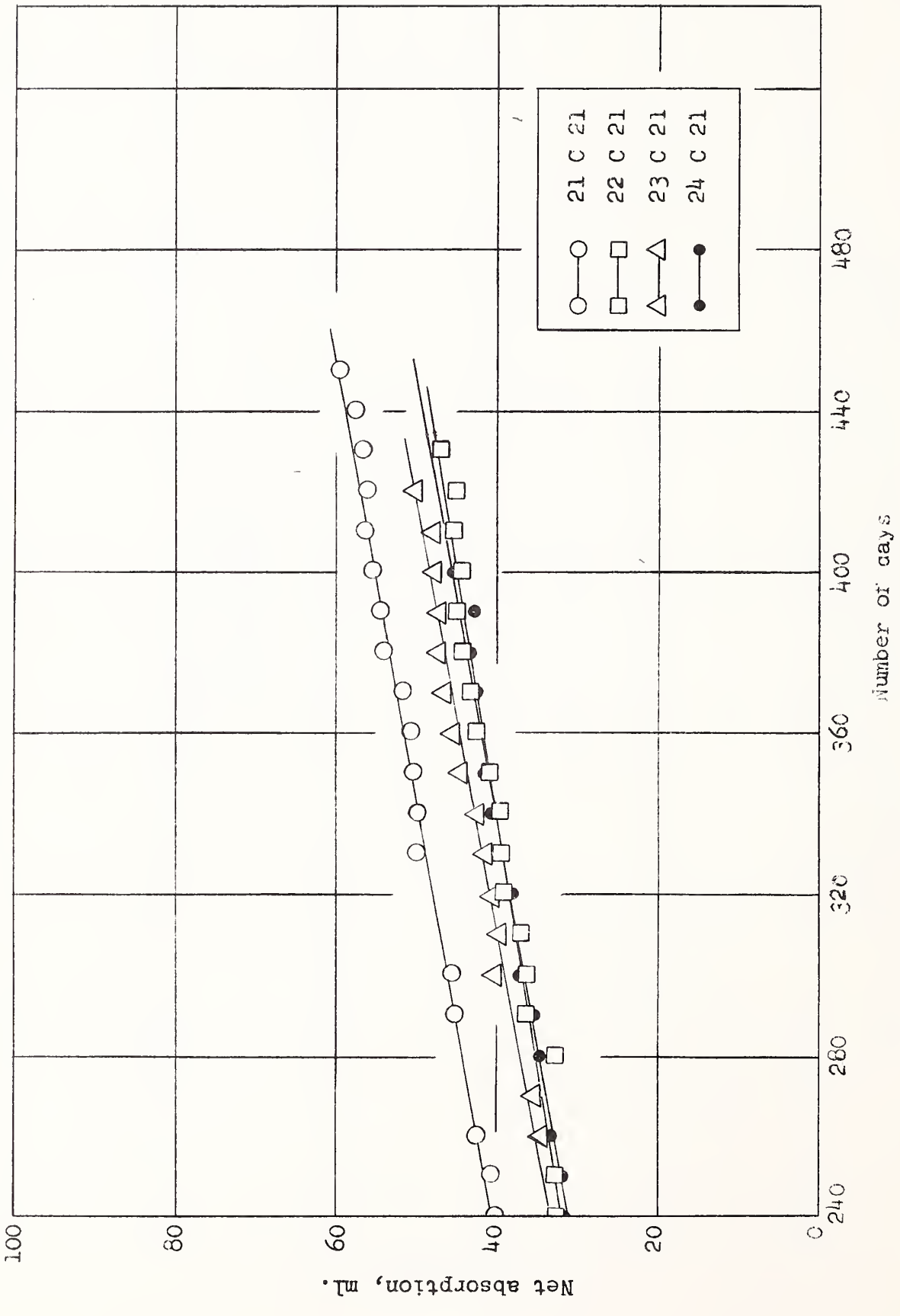

Fig. 95. (Cont.) Net absorptions versus number of days for 1200 psi., normally cured slabs under two-foot head of water.

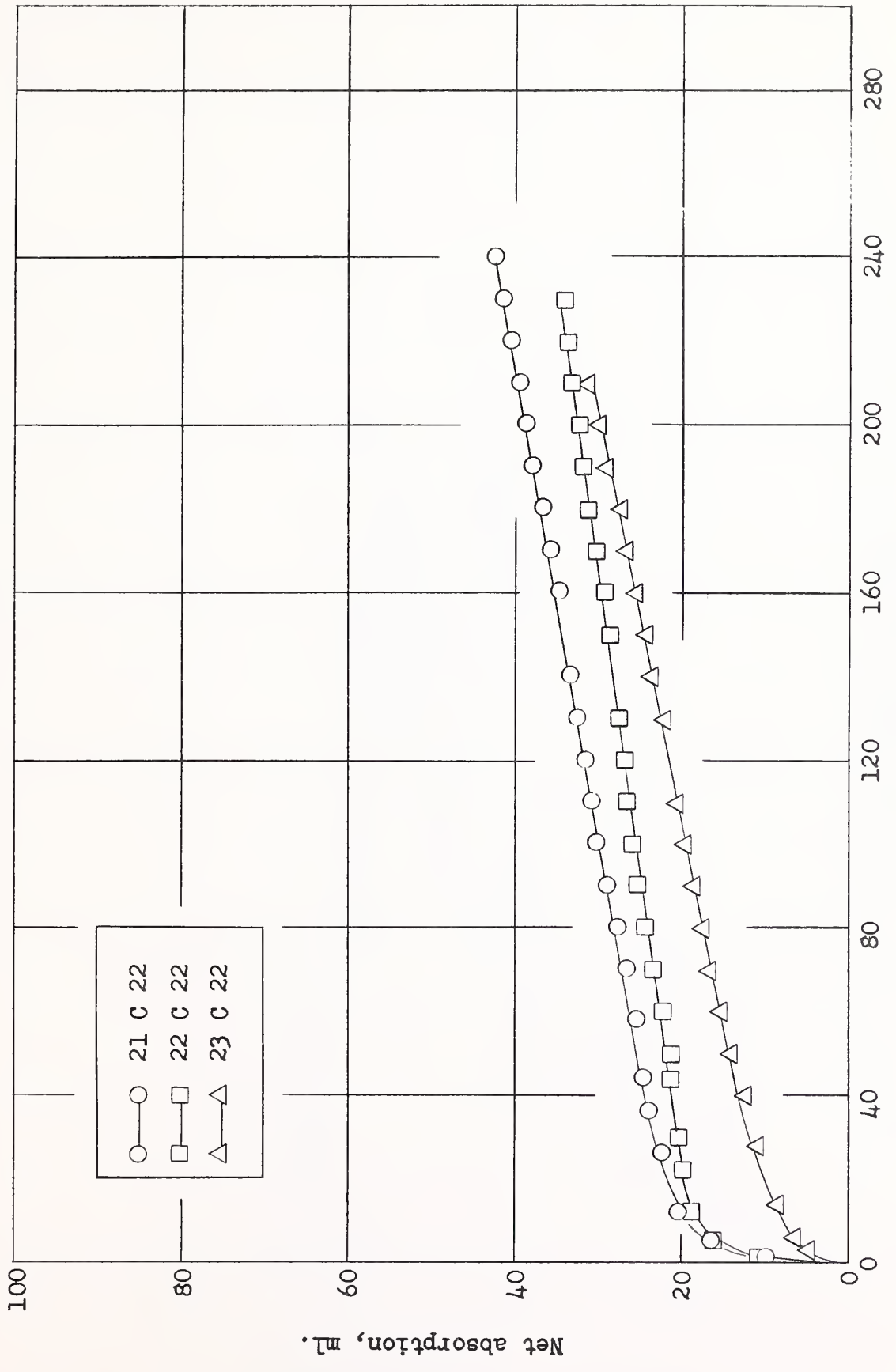

Fig. 96. Net absorptions versus number of days for 1200 psi., normally cured slabs under two-foot head of $CaCl_2$ solution.

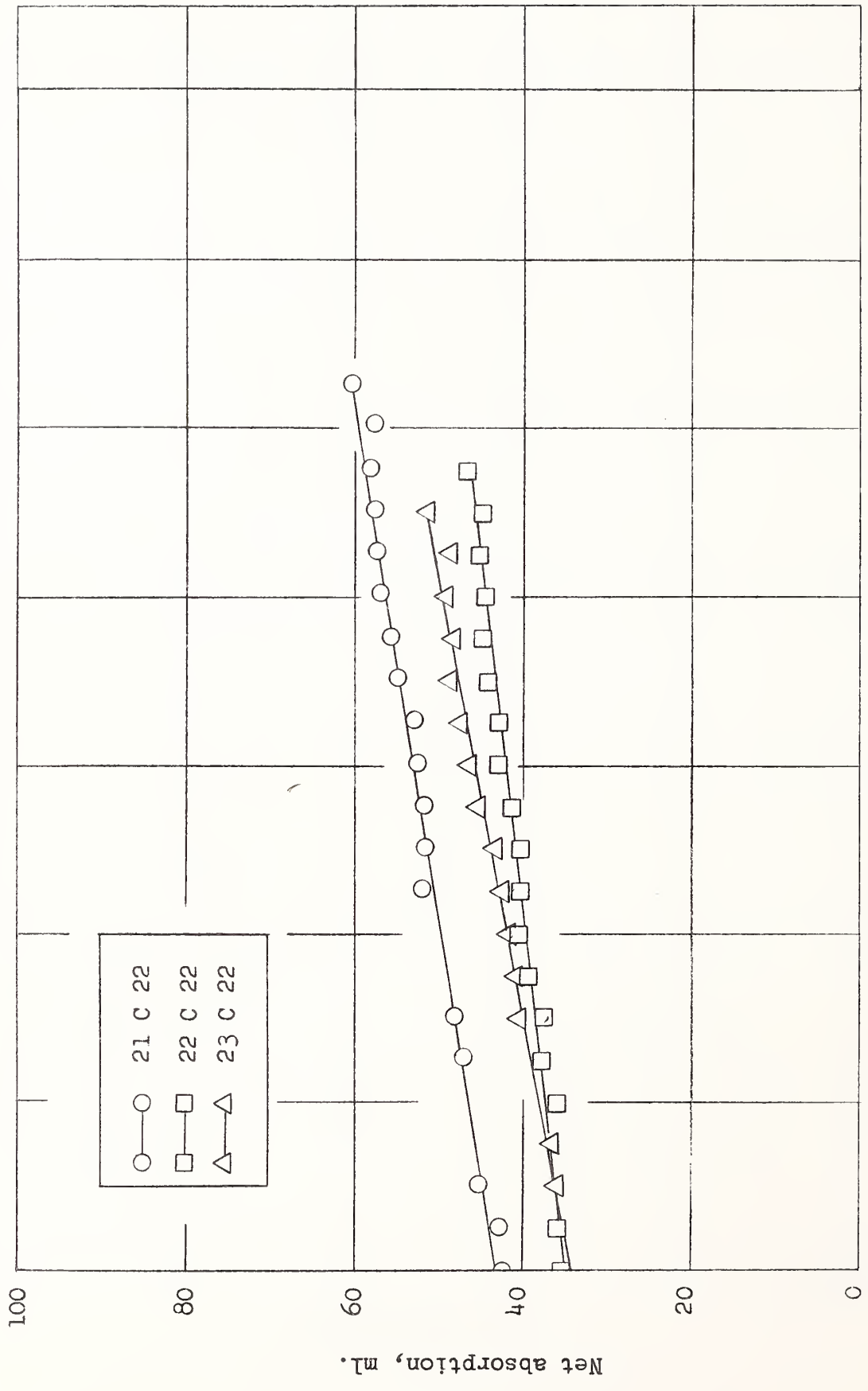

Fig. 96. (Cont.) Net absorptions versus number of days for 1200 psi., normally cured slabs under two-foot head of $CaCl_2$ solution.

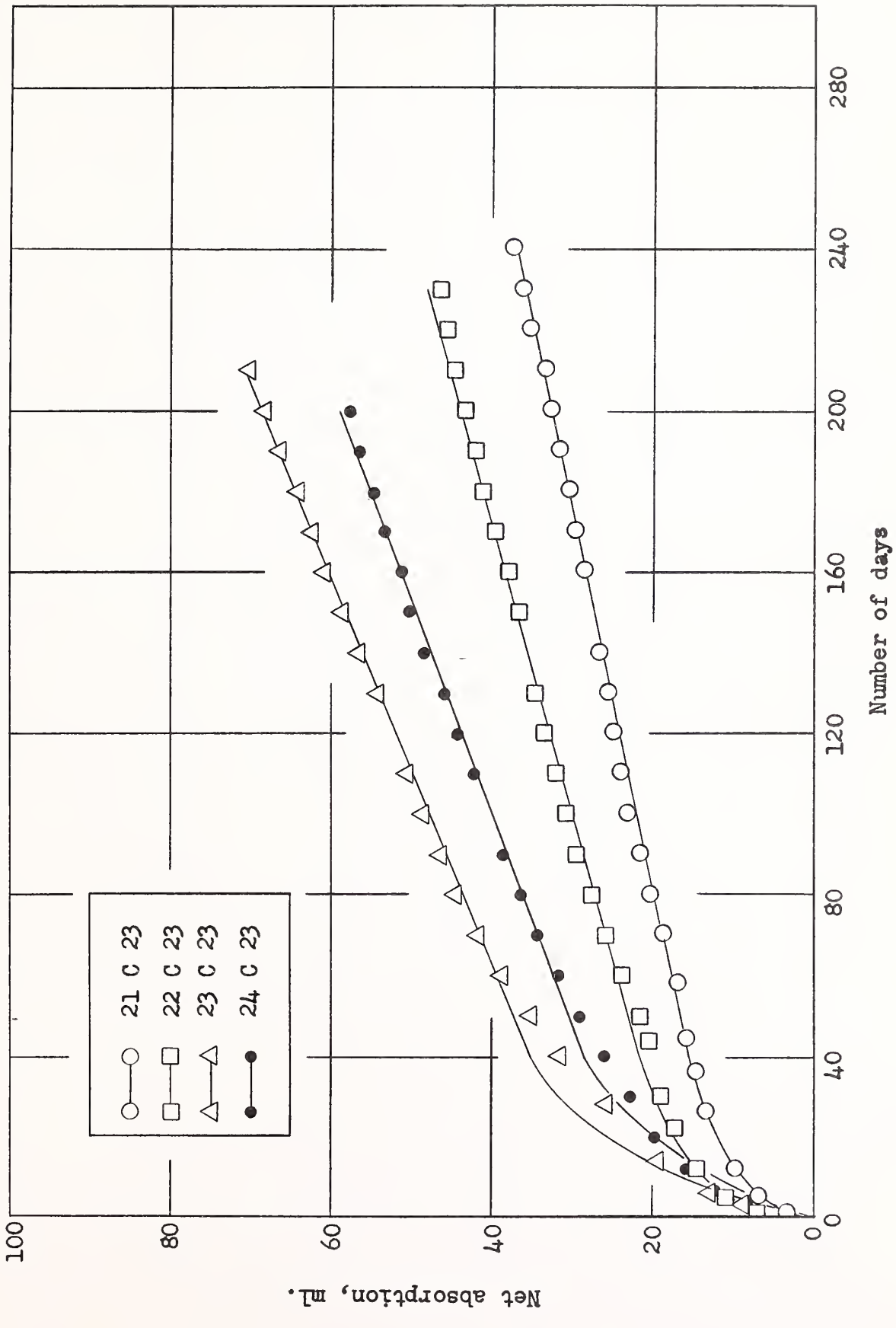

Fig. 97. Net absorptions versus number of days for 1200 psi., steam cured slabs under two-foot head of water.

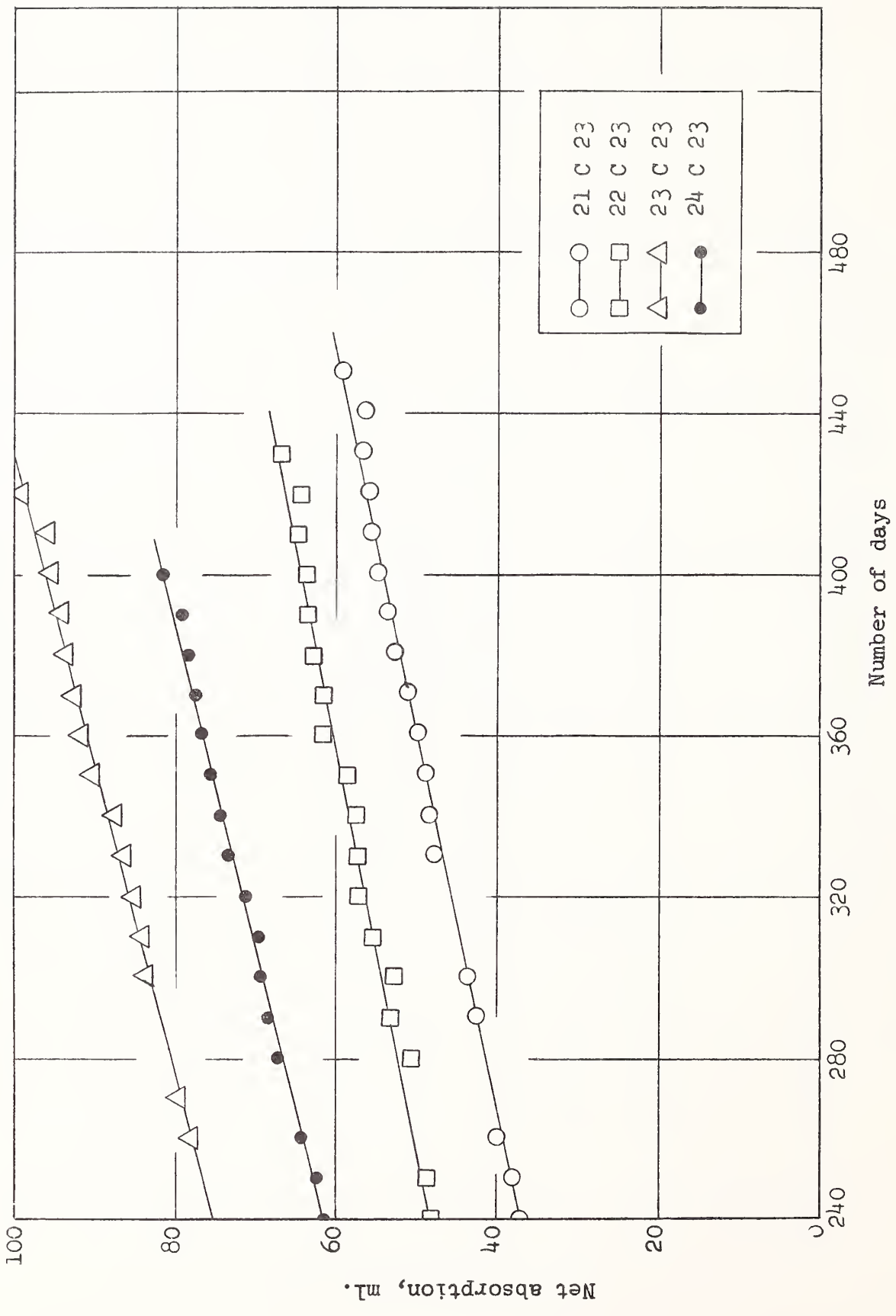

Fig. 97. (Cont.) Net absorptions versus number of days for 1200 psi., steam cured slabs under two-foot head of water.

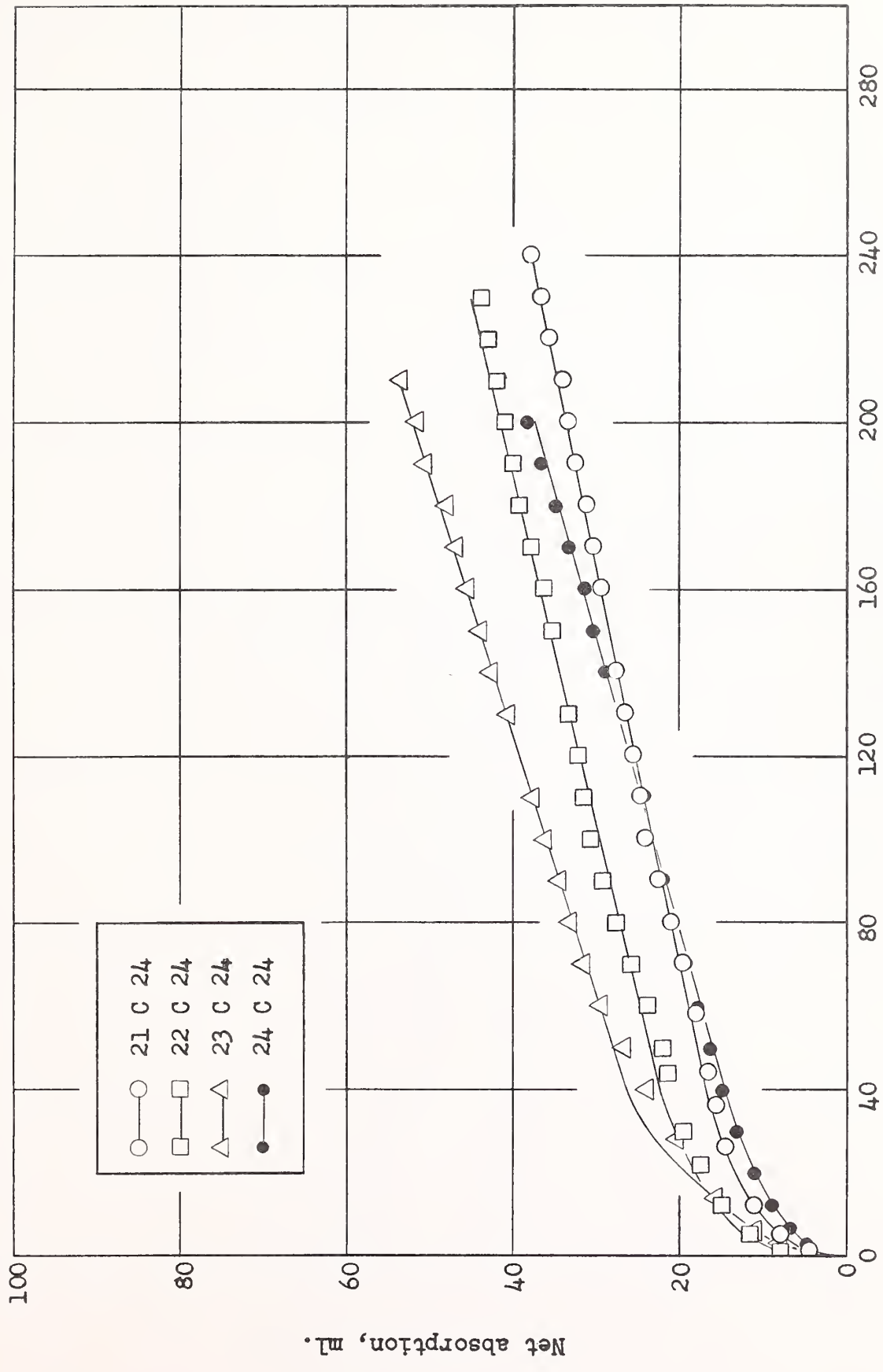

Fig. 98. Net absorptions versus number of days for 1200 psi., steam cured slabs under two-foot head of $CaCl_2$ solution.

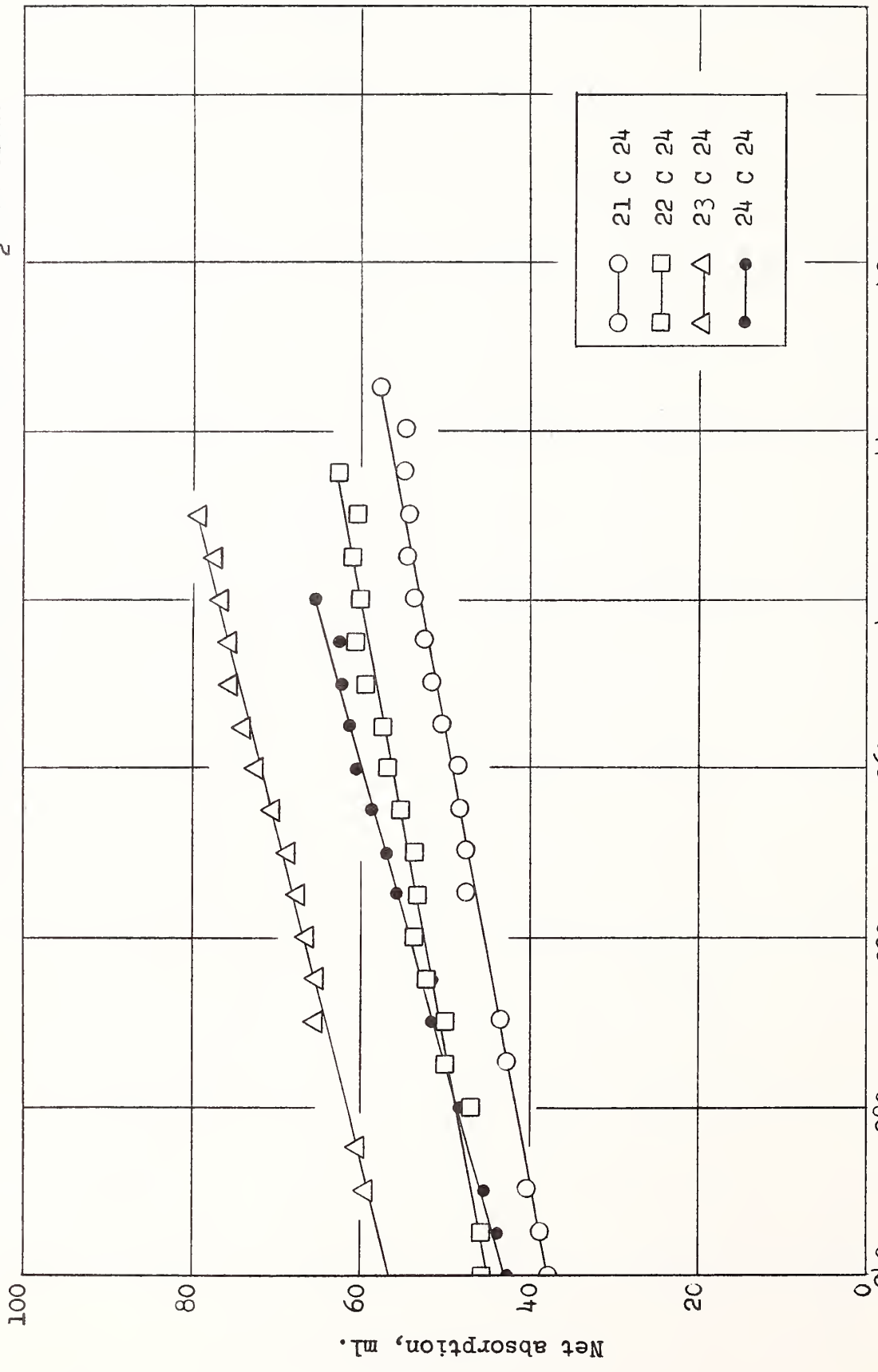

Fig. 98. (Cont.) Net absorptions versus number of days for 1200 psi., steam cured slabs under two-foot head of $CaCl_2$ solution.

APPENDIX D

STATISTICAL METHODS (23)

An example of the output obtained from the computer programs is given in Figure 99 for treatment comparison I (all stresses, steam cured, both solutions) of the adjusted weight change values at 70 freeze-thaw cycles.

Treatment number	Mean adjusted weight change (lbs.)	Variance ($lbs.^2$)	Standard deviation (lbs.)
3	0.260	0.00*	0.09
4	-0.085	0.00	0.08
11	0.230	0.00	0.04
12	-0.035	0.00	0.07
19	0.222	0.00	0.05
20	-0.147	0.00	0.08

Bartlett test for homogeneity of variance:

computed	corrected	tabulated	tabulated
χ^2	χ^2	$\chi^2_{(0.05)}$	$\chi^2_{(0.01)}$
1.78	1.58	11.1	15.1

Duncan multiple-range test:

P	$SSR_{(0.05)}$	$LSR_{(0.05)}$
2	2.97	0.111
3	3.12	0.117
4	3.21	0.120
5	3.27	0.122
6	3.32	0.124

Fig. 99 Example of Bartlett and Duncan test results

* Since the computer was instructed to truncate these values after two decimal places, these values are misleading.

In Figure 99 χ^2 (chi-squared) is the test statistic used in the Bartlett test for determining whether the variances are homogeneous or non-homogeneous. χ^2 is defined as the sum of squares of independent, normally distributed variables with zero means and unit variances. The distribution of χ^2 depends on the number of independent deviates, that is, on the degrees of freedom. Thus, there is a χ^2 distribution for each number of degrees of freedom, where the number of degrees of freedom is one less than the number of samples. Tables of these χ^2 distributions appear in many texts relating to statistics. Homogeneity or non-homogeneity of variance is declared on the basis of comparisons of computed χ^2 values with these tabulated values, at the chosen significance levels.

For the Duncan test, P refers to the number of ranked means across which a comparison is being made; and SSR is an abbreviation for "significant studentized range." SSR values are tabulated in many statistics texts for various numbers of degrees of freedom, at both the 5 per cent and 1 per cent protection levels. Presumably they are computed for means of sample characteristics which are normally distributed with unit variances. The LSR (least significant range) values are obtained by multiplying the SSR values by the "pooled" estimate of variance for all treatments.

The procedures and equations for these tests, including those for finding the "computed χ^2", "correct χ^2", and "pooled" estimate of variance, are standard and may be found in most statistics texts;

however, they will not be presented in this discussion for the sake of brevity. (See reference 20 for a complete description of these tests.)

The interpretation of the output of Figure 99 would be as presented in the following discussion:

Since the value of χ^2 is less than the appropriate tabulated values of χ^2 at both the 5 per cent and 1 per cent levels, the hypothesis that the variances are homogeneous is accepted. If χ^2 had been greater than 11.1 but less than 15.1, this hypothesis would also have been accepted. However, had χ^2 exceeded or equalled 15.1, the value of the "corrected" χ^2 would have been similarly tested. Acceptance or rejection of the hypothesis of homogeneous variances would then have been decided according to the tests of the "corrected" χ^2 value.

Since the variances have been declared homogeneous the Duncan test may be applied. To facilitate the test, the mean values are ranked.

Treatment number	Mean adjusted weight change
20	-0.147
4	-0.085
12	-0.035
19	0.222
11	0.230
3	0.260

Differences between mean values are then computed, and compared with the appropriate LSR (least significant range) values. These comparisons are presented on the following page; the treatment numbers are underlined, and in parentheses, indicating the means being compared.

Treatment mean difference calculations:

(3 - 20): 0.260 - (-0.147) = 0.407 >0.124 **

(3 - 4): 0.260 - (-0.085) = 0.345 >0.122 **

(3 - 12): 0.260 - (-0.035) = 0.295 >0.120 **

(3 - 19): 0.260 - (-0.222) = 0.038 ≥0.117 n.s.

Comparison of the mean values for treatments 3 and 11 is unnecessary, since the mean values for treatments 3 and 19 are declared insignificantly different.

Conclusions thus far would be that the average adjusted weight increases of slabs subjected to treatment 3 (non-stressed, steam cured, water ponded) are greater than those of slabs subjected to treatments 20, 4, and 12 (all stresses, steam cured, ponded with $CaCl_2$ solution), but not different from those of slabs subjected to treatments 19 and 11 (1200 psi. and 500 psi., resp., steam cured, water ponded), at the 5 per cent protection level, after 70 freeze-thaw cycles.

To continue:

(11 - 20): 0.230 - (-0.147) = 0.377 > 0.122 **

(11 - 4): 0.230 - (-0.085) = 0.315 > 0.120 **

(11 - 12): 0.230 - (-0.035) = 0.265 > 0.117 **

(11 - 19): declared insignificantly different above

(19 - 20): 0.222 - (-0.147) = 0.369 > 0.120 **

(19 - 4): 0.222 - (-0.085) = 0.307 > 0.117 **

(19 - 12): 0.222 - (-0.035) = 0.257 > 0.111 **

(12 - 20): -0.035 - (-0.147) = 0.112 ≥ 0.117 n.s.

Similarly, the comparison of the mean values for treatments 4 and 20 is unnecessary.

The symbols used are in keeping with common statistical notation, in that "n.s.", "*", and "**", designate test statistics which are non-significant, significant at the 1 per cent protection level, and signicant at the 5 per cent protection level, respectively.

To summarize the results of this example, it is declared that the average mean adjusted weight increases of slabs subjected to treatments 3, 11, and 19 (all stresses, steam cured, water ponded) are greater than those of slabs subjected to treatments 4, 12, and 20 (all stresses, steam cured, ponded with $CaCl_2$ solution), but not different from each other at the 5 per cent protection level, after 70 freeze-thaw cycles. Nor are the average mean adjusted weight losses of slabs subjected to treatments 4, 12, and 20 different from each other after 70 freeze-thaw cycles.

The accepted method for presenting the results of the example above would be as follows,

$$\underline{20 \quad 4 \quad 12} \qquad \underline{19 \quad 11 \quad 3} \ ,$$

where the treatment identification numbers are arranged from left to right in order of ascending treatment mean values. Lines are then drawn beneath those treatment numbers which have mean values that are declared insignificantly different at the chosen protection level.

In an attempt to reduce the number of statistically invalid applications of the Duncan test to comparisons of the mean relative dynamic

moduli, an arcsin transformation of their coded values was made before applying the Bartlett and Duncan tests. The coded values were obtained by subtracting 20 per cent from each value, and then dividing by 100, to assure that all values would be in the range: 0 to 1.0. These diminished values were further modified by extracting their square roots. Thus, the transformation used was

$$\arcsin\sqrt{\frac{P_c - 20}{100}}$$

This trigonometric transformation is recommended (20) for percentage values which lie within the range of values observed in this study in order to stabilize the variances. Accordingly, the Bartlett test results presented in Table XII and the Duncan test results presented in Figures 8 through 19 were performed on the transformed values. However, the plotted mean values are in the original scale.

LITERATURE CITED

1. Tallamy Associates, Bertram D., "Evaluation of Methods of Replacement of Deteriorated Concrete in Structures," National Cooperative Highway Research Program, Report 1. Highway Research Board. 1964.

2. Klieger, Paul, "Some Aspects of Durability and Volume Change of Concrete for Prestressing," Research & Development Laboratories of the Portland Cement Association, Bulletin 118, Nov. 1960.

3. Grieb, W. E., Werner, George, Woolf, D. O., "Resistance of Concrete Surfaces to Scaling by De-Icing Agents," Highway Research Board, Bulletin 323, 1962.

4. Gutzwiller, M. J., and Musleh, F. E., "Freezing and Thawing Effects on Prestressed Concrete," American Society of Civil Engineers, Proceedings, Journal of the Structural Division, Vol. 86, No. ST10,

5. Rieb, Stanley Lee, "Preparation and Durability Testing of Pretensioned Prestressed Concrete," Journal of the Prestressed Concrete Institute, Vol. 4, No. 3, December 1959.

6. Monfore, G. E., and Verbeck, G. J., "Corrosion of Prestressed Wire in Concrete," Research and Development Laboratories of the Portland Cement Association, Bulletin 120, December 1960.

7. Godfrey, Howard J., "Corrosion Tests on Prestressed Concrete Wire and Strand," Journal of the Prestressed Concrete Institute, Vol. 5, No. 1, March 1960.

8. Roberts, M. H., "Effect of Calcium Chloride on the Durability of Pretensioned Wire in Prestressed Concrete," Cement and Concrete Association, Magazine of Concrete Research, Vol. 14, No. 42, Nov. 1962, London.

9. Tyler, I. L., "Long-Time Study of Cement Performance in Concrete, Chapter 12," Research and Development Laboratories of the Portland Cement Association, Bulletin 114, May 1960.

10. Klieger, Paul, "Extensions to the Long-Time Study of Cement Performance in Concrete," Journal of the PCA Research and Development Laboratories, Vol. 5 No.1, January 1963.

11. Ost, B., and Monfore, G. E.,"Corrodibility of Prestressing Wire in Concrete made with Type 1 and Type 1S Cements," Journal of the PCA Research and Development Laboratories, May 1963.

12. Abeles, P. W., "Partial Prestressing in England," Journal of the Prestressed Concrete Institute, Vol. 8, No. 1, February 1963.

13. Moskvin, V. M., "Corrosion in Hydrotechnic Structures," Corrosion of Concrete and its Prevention. Published for the National Science Foundation, Washington, D. C., and Department of the Interior, U.S.A. by Israel Program for Scientific Translations (translated from Russian conference held in 1953).

14. Hansen, W. C., "Crystal Growth as a Source of Expansion in Portland-Cement Concrete," American Society for Testing Materials, Preprint 84, 1963.

15. Neville, A. M., Properties of Concrete, John Wiley and Sons, Inc. New York, 1963.

16. "Effects of De-Icing Chemicals on Structures," A Symposium, Highway Research Board, Bulletin 323, 1962.

17. Neville, A. M., Discussion of Paper by O. Ishai, "Influence of Sand Concentration on Deformation of Mortar Beams Under Low Stress," Journal of the American Concrete Institute, Proceedings Vol. 59, No. 6, Part 2, June 1962.

18. Troxell, George E. and Davis, Harmer E., Composition and Properties of Concrete, McGraw-Hill Book Co., Inc., New York, 1956.

19. Glucklich, Joseph and Ishai, Ori, "Creep Mechanism in Cement Mortar," Journal of the American Concrete Institute, Proceedings, Vol. 59, No. 7, July 1962.

20. Steel, Robert G. D. and Torrie, James H., Principles and Proceedures of Statistics, McGraw-Hill Book Co., Inc., New York, 1960.

21. Synder, M. J., "Protective Coatings to Prevent Deterioration of Concrete by Deicing Chemicals," National Cooperative Highway Research Program, Report 16. Highway Research Board. 1965.

22. Ost, B., and Monfore, G. E., "Penetration of Chloride into Concrete," Journal of the PCA Research and Development Laboratories, Vol.8, No. 1, January 1966.

23. Gonsior, M. J., "The Effect of Prestress on Concrete Durability," M. S. Thesis, Montana State University, Department of Civil Engineering and Engineering Mechanics, June, 1965.

24. Lin, T. Y., Design of Prestressed Concrete Structures, John Wiley and Sons, Inc., New York, 1955.

25. "Design and Control of Concrete Mixtures," Portland Cement Association, Tenth Edition.

26. Newlon, Howard H., Jr., "A Field Investigation of the AE-55 Air Indicator," Highway Research Board Bulletin 305, National Academy of Sciences, National Research Council Publication 934, Washington, D.C. 1961.